

STRATIGRAPHY, STRUCTURE AND METAMORPHISM OF THE
RENIA BASEMENT GNEISS BODY AND THE ADJACENT COVER
SUCCESSION IN THE WESTERN HINTERLAND ZONE OF THE
NORTHERN LABRADOR TROUGH, WEST OF KUJJUAQ,
NORTHERN QUEBEC

by

James Moorhead

Department of Geological Sciences
McGill University, Montréal, Québec

A thesis submitted in partial fulfillment
of the requirements of the degree of
Master of Science

August, 1989

© James Moorhead, 1989

ABSTRACT

The western portion of the hinterland zone in the northern Labrador Trough is characterized by four NW trending en échelon Archean basement bodies. From south to north the bodies are: the Scattered, the Moyer, the Renia and the Boulder. The Scattered and Renia have synformal geometries whereas the Moyer and Boulder have antiformal ones.

These bodies are overlain by a cover sequence consisting, from the base upwards, of: various calcareous units, pelitic and semi-pelitic schists, an iron formation, a basalt horizon and a thick assemblage of coarse siliciclastic rocks. The sequence up to the basalt horizon can be correlated with the Kaniapiskau Supergroup of the Labrador Trough. The overlying sediments, the Thévenet Formation, are thought to correlate with the more extensive Laporte Group found in the hinterland of the central trough. Facies changes indicate an eastern provenance for the Thévenet Formation and the upper portion of the sediments underlying the basalts. The uplifted source region would include siliciclastic sediments, minor mafic volcanics and granitoid basement rocks.

Four distinct phases of deformation were recognized. The first deformation event (D_1) is responsible for the development of a basal décollement surface, westerly vergent thrust faults and fault associated folds. The next deformation event (D_1') is restricted to this portion of the hinterland zone. It is characterized by two large WNW vergent basement-cored nappe structures. The next deformation episode (D_2) formed E to NE trending shallowly plunging large-wavelength open cross-folds. The area was then subjected to large amplitude NNW trending, E to SE plunging, upright folds. These folds are responsible for the sequential arrangement of antiformal and synformal basement bodies and the large amount of structural thickness (up to 23 km) visible in oblique section at the surface. The synform-cored basement gneisses, the Renia and Scattered, probably represent F_3 refolds of the earlier basement cored (F_1') nappes. The antiformal-cored basement gneisses, the Boulder and Moyer, represent interference between two upright folding phases; F_2 and F_3 .

The isograds trend N-S clearly cross-cutting the traces of the F_3 folds indicating the metamorphic climax was post-kinematic. Metamorphic grade increases west to east from the garnet isograd near the Lac Rachel fault where conditions attained 510-550 °C and 4.0 to 5.0 kb through the nearly overlapping staurolite and kyanite isograds up to the northern closure of the Renia Gneiss where temperatures of 570-630 °C and pressures of 8.1-8.4 kb have been recorded.

In the final event the N trending late to post-metamorphic Lac Rachel reverse fault unroofed the folded and metamorphosed basement-cover complex.

RESUME

La portion occidentale de l'arrière pays de la Fosse du Labrador se caractérise par la présence de quatre corps de socle gneissique Archéen. Du sud vers le nord, ils sont: le Scattered, le Moyer, le Renia et le Boulder. Le Scattered et le Renia sont des synformes tandis que le Moyer et le Boulder sont des antiformes.

Les corps gneissiques sont cernés par une séquence supracrustale qui est constituée de la base au sommet de: diverses unités calcaireuses, schistes pélitiques et semi-pélitiques, une formation de fer, un horizon de basalte et une épaisse séquence de roches siliciclastiques à grains-grossiers. Jusqu'à l'horizon de basalte la séquence peut se corréler au Supergroupe de Kaniapiskau de la Fosse du Labrador. Les sédiments sus-jacent aux basaltes, la Formation de Thévenet, sont considérés comme corrélatifs au Groupe de Laporte qui forme la plus grande partie de l'arrière pays de la partie centrale de la Fosse du Labrador. Les changements de faciès indiquent une provenance orientale pour la Formation de Thévenet et la partie supérieure des sédiments sous-jacent aux basaltes. La région source devrait inclure des sédiments siliciclastiques, des laves mafiques et un socle granitique.

Quatre phases de déformation distinctes furent reconnues. La première phase (D_1) est responsable de la formation d'un décollement de base, des failles de chevauchement déversées vers l'ouest et de plis associés à ces failles. La prochaine phase (D_1') est confinée à la partie ouest de l'arrière pays. Elle se caractérise par deux grandes nappes à coeur gneissique déversées vers le ONO. La prochaine phase de déformation (D_2) a formé des plis transversaux ouverts orientés E-NE à faible plongé et à grande longueur d'onde. La région a ensuite été reprise par des plis droits orientés NNO à grande amplitude plongeants soit vers l'E ou le SE. Ces plis sont responsables de la disposition séquentielle des gneiss antiformes et synformes ainsi que la grande épaisseur structurale visible sur la surface d'érosion. Les deux corps gneissiques synformes représentent probablement des nappes (F_1') replissées par F_3 . Les gneiss antiformes semblent être le produit de l'interférence de deux phases de plissement droits, soit F_2 et F_3 .

Les isogrades s'orientent N-S recoupant la trace des plis F_3 , indiquant que les conditions métamorphiques maximales furent atteintes de manière post-cinématique. Le grade métamorphique augmente d'ouest en est de l'isograde du grenat où les conditions ont atteintes 510 à 550 °C et 4.0 à 5.0 kb, en passant par les isogrades très rapprochées de la staurotide et de la kyanite, jusqu'à la fermeture NO du Gneiss de Renia où des températures de 570 à 630 °C et des pressions de 8.1 à 8.4 kb ont été enregistrées.

Un mouvement inverse, tardi à post-métamorphique, le long de la faille N-S du Lac Rachel marque le dernier événement tectonique qui remonta le complexe socle-couverture, plissé et métamorphisé, vers la surface.

ACKNOWLEDGEMENTS

This project owes much to the support and encouragement of many people that I have come to know and appreciate over the length of this project. The foremost is the supervisor of this study Dr. Andrew Hynes who set the framework, provided key insights and brought much needed rigor to certain aspects of the thesis. He is above all thanked for his patience in accepting my habit of taking on additional commitments. The fieldwork was supported by the Ministère de l'Energie et des Ressources du Québec grant to Dr. Normand Goulet and is gratefully acknowledged. Financial support for my stay at McGill University was provided for by an F.C.A.R. scholarship, the Max Bell award and an F.C.A.R. operating grant to Dr. Andrew Hynes.

This study has been helped by discussions with Tom Clark, Normand Goulet, Marc Bélanger and Réjean Girard concerning various aspects of the Labrador Trough geology. Tom Clark is also thanked for kindly providing unpublished compilation maps.

I would like to warmly thank the following persons that were involved in studies of the Labrador Trough during the same period: Serge Perreault and Glenn Poirier for helping me with the metamorphic and computer aspects of this study, Erica Boone for accepting to share a confined office space. The following people made my stay at McGill the most enjoyable: Marlène Charland, Bruce Mountain, Roland Deschesne, Richard Forest, James Gebert, Gerald Panneton and Tom Skulski. Moira MacKinnon is thanked for her help and introduction to the sometimes temperamental ion microprobe.

Charles Roy helped with the running of the stereonet program. Marc Ducharme drafted several of the figures in this thesis.

Table of contents

Abstract.....	i
Resumé.....	ii
Acknowledgements.....	iii
Table of contents.....	iv
List of Figures.....	vii
List of Tables.....	viii
Chapter 1. Introduction	
1.1 General geology.....	2
1.1.1 Geological setting.....	2
1.1.2 General stratigraphy.....	5
1.2 Previous work.....	6
1.3 Dates.....	8
1.4 Evolution models.....	13
1.4.1 Ensialic basins.....	13
1.4.2 Passive margins.....	15
1.4.3 Passive margin in addition to a foredeep origin for the upper part of the Kaniapiskau Supergroup.....	18
Chapter 2. Stratigraphy	
2.1 General stratigraphy.....	19
2.1.1 Cycle I.....	19
2.1.1.1 Central Labrador Trough.....	19
i) Shelf phase.....	19
ii) Basin phase.....	20
2.1.1.2 Northern Labrador Trough.....	23
2.1.2 Cycle II.....	24
2.1.2.1 Shelf phase (Ferriman Subgroup).....	25
2.1.2.1A Autochthonous shelf sequence.....	25
2.1.2.1B Para-autochthonous & allochthonous shelf sequence.....	26
2.1.2.2 Basin phase.....	28
2.2 Stratigraphic succession in study area.....	31
2.2.1 Basement gneisses.....	32
2.2.2 Cover sequence.....	35
i) Calcareous rocks.....	35
Dolomitic marbles.....	35
Calc-silicate rocks, calcareous schists and heterogeneous amphibolites.....	36
ii) Lower Iron Formation.....	38
iii) Lower micaceous schist.....	39
A) The West zone.....	39
B) The East zone.....	39
iv) Upper Iron Formation.....	40
v) Upper micaceous schists.....	40
vi) Mafic volcanics.....	41
vii) Volcanic-rich conglomerate.....	41
viii) Siltstones, sandstones and conglomerates	

(siliciclastic assemblage).....	42
ix) Intrusives.....	44
Gabbros.....	44
Glomeroporphyritic gabbros.....	44
Ultramafics.....	44
2.3 Correlations.....	46
2.4 Summary.....	53
2.5 Discussion.....	56
1) Marginal basins.....	57
2) Foredeep basin.....	58
 Chapter 3. Structure	
3.1 Introduction.....	61
3.2 Structures west of the Lac Rachel fault.....	63
3.2.1 The first deformation event (D_1).....	63
3.2.2 The second deformation event (D_2).....	64
3.2.3 The third deformation event (D_3).....	65
3.2.4 Transverse faults.....	67
3.2.5 The Lac Rachel fault.....	69
3.3 Structures east of the Lac Rachel fault.....	72
3.3.1 Basement Gneiss exposures.....	72
3.3.1.1 Antiformal basement bodies.....	72
3.3.1.1A) The Moyer Dome.....	72
3.3.1.1B) The Boulder Dome.....	72
3.3.1.2 Synformal basement bodies.....	76
3.3.1.2A) The Renia Synform.....	76
3.3.1.2B) The Scattered Synform.....	78
3.3.2 Down plunge section.....	78
3.3.3 Origin of basement gneiss bodies.....	85
3.3.3.1 Introduction.....	85
3.3.3.2 Diapirism.....	87
3.3.3.3 Sheath folding.....	90
3.3.3.4 Interference between early basement cored Pennine style nappes (F_1') and a later more upright folding phase (F_3).....	93
3.3.3.5 Analogies with some other basement- cover complexes.....	94
3.3.4 Deformation events.....	96
3.3.4.1 The first phase of deformation (D_1)..	96
3.3.4.1A F_1 folds.....	96
3.3.4.1B Faults.....	98
i) The basal décollement.....	98
ii) Thrust faults.....	99
3.3.4.2 The late first phase of deformation (D_1').....	100
3.3.4.2A Introduction.....	100
3.3.4.2B Folds.....	101
3.3.4.3 The second phase of deformation (D_2)..	103
3.3.4.4 The third phase of deformation (D_3)..	104
3.3.4.5 Late tectonic features.....	105
3.3.4.5A Brittle failure on the SW margin of the Boulder Dome.....	105
3.3.4.5B Transverse faults.....	106

3.4 Summary.....	106
Chapter 4. Metamorphism	
4.1 Setting and previous work.....	109
4.2 General petrography.....	113
4.2.1 Introduction.....	113
4.3 Mineral petrographic observation.....	114
4.3.1 Garnet.....	114
4.3.2 Biotite.....	115
4.3.3 Muscovite.....	115
4.3.4 Staurolite.....	115
4.3.5 Kyanite.....	116
4.3.6 Chlorite.....	116
4.3.7 Hornblende.....	116
4.3.8 Tremolite-Actinolite.....	117
4.3.9 Plagioclase.....	117
4.3.10 Epidote.....	117
4.3.11 Accessory minerals.....	117
4.4 Quantitative petrology.....	118
4.4.1 Introduction.....	118
4.4.2 Geothermometry.....	118
4.4.3 Geobarometry.....	119
4.4.4 Approach and assumptions.....	122
4.4.5 Sources of error.....	125
4.4.6 Results.....	127
4.4.6.1 Geothermometry.....	127
4.4.6.2 Geobarometry.....	133
4.4.6.2A) Chlorite-biotite-muscovite assemblage.....	133
4.4.6.2B) Plagioclase-biotite-garnet- muscovite assemblage.....	133
4.4.6.2C) Kyanite bearing assemblage.....	133
4.5 Burial history.....	136
Chapter 5. Summary	
5.1 Stratigraphy.....	140
5.2 Structure.....	141
5.2.1 Basement gneiss bodies.....	141
5.2.1.1 Diapirism.....	141
5.2.1.2 Sheath folding.....	142
5.2.1.3 Refolding of early Pennine type nappe structures.....	142
5.2.2 Tectonic history.....	143
5.3 Metamorphism.....	144
Chapter 6. Conclusions and suggestions for further work	
6.1) Conclusions.....	145
6.2) Suggestions for further work.....	146
References.....	148
Plates.....	166
Appendix I. Probe analyses of minerals.....	182

LIST OF FIGURES

Figure 1. Generalized map of the Proterozoic terranes surrounding the Archean Superior craton.....	3
Figure 2. Major subdivisions of the Labrador Trough.....	4
Figure 3. Features of the first deposition cycle in north-central Labrador Trough.....	7
Figure 4. Simplified geology of the northern Labrador Trough.....	9
Figure 5. Outline of previous studies in the northern Labrador Trough...	10
Figure 6. Features of the second deposition cycle in the northern Labrador Trough.....	23
Figure 7. Stratigraphic correlations in the northern Labrador Trough....	24
Figure 8. Litho-stratigraphic correlations between the hinterland zone, the central and western zones of the northern Labrador Trough.	46
Figure 9. Schematic stratigraphy and "correlations" between the Belcher Group and the Kaniapiskau Group.....	52
Figure 10. Simplified map of the northernmost Labrador Trough.....	66
Figure 11. Simplified map of the northern extension of the Labrador Trough, from 57°30' to 60°00'.....	68
Figure 12. Structural domains of the Boulder, the Renia and the Moyer basement bodies.....	73
Figure 13. Stereographic projections of the S ₁ schistosity present within the Moyer basement dome.....	74
Figure 14. Stereographic projections of the S ₁ schistosity present within the Boulder basement dome.....	75
Figure 15. Stereographic projections of the S ₁ schistosity present within the Renia basement synform.....	77
Figure 16. Traces and plunges of the major folds used to construct the down plunge section.....	80
Figure 17. Composite down plunge section.....	83
Figure 18. Down plunge projections of the NW closures of the Boulder and Moyer domes.....	84

Figure 19. Schematic representation of outwardly cascading folds on the margins of an ascending diapir.....	89
Figure 20. Schematic representation of radially arranged vertical folds around the "neck" of a rising diapir.....	89
Figure 21. Metamorphic zones of the Labrador Trough, its eastern hinterland and of the adjacent Superior craton.....	110
Figure 22. Prograde chemical zonation patterns in garnet sections.....	123
Figure 23. Prograde chemical profiles of garnets coupled with small retrograde zonations along their rims.....	124
Figure 24. Grossular versus spessartine content of garnet retrograde rims.....	137
Figure 25. Pressure-temperature diagram of the different metamorphic zones of the study area compared with the results of Gélinais & Perreault (1985).....	139

LIST OF TABLES

Table I. Temperature determinations from the different metamorphic zones of the study area.....	128
Table II. Pressure determinations using the chlorite-biotite-muscovite assemblage.....	134
Table III. Pressure determinations using the garnet-plagioclase-biotite-muscovite assemblage.....	137

1.0) INTRODUCTION

The foreland or external portions of orogens have been studied for many decades whereas their internal or core zones have come under intense scrutiny only more recently. The characterization of tectonic features in these zones has brought added understanding of the structural and metamorphic processes that were operative during the tectonic collapse and closure of sedimentary basins.

The foreland zone of the Labrador Trough, which represents an early Proterozoic thrust and fold belt on the eastern edge of the Archean Superior Province, has been the subject of numerous stratigraphic and structural studies, most notably by Dimroth (1970, 1971, 1972, 1978, 1981, 1985; Dimroth *et al.*, 1970; Wardle & Bailey 1981; Le Gallais & Lavoie 1982 and Clark 1988). Its adjacent eastern metamorphic hinterland or core zone has been relatively less well studied.

This study focuses on the stratigraphic, structural and metamorphic aspects of deformed cover and basement rocks in a 120 km² area in the westernmost, lowest grade hinterland of the Northern Labrador Trough.

At this latitude the westernmost hinterland is characterized by four en échelon Archean basement bodies overlain by metamorphosed metasediments and metavolcanics. Two of the basement bodies have synformal geometries while the other two can be characterized as doubly plunging antiforms.

The remobilized Archean basement and metamorphic imbricates are juxtaposed to the less deformed and metamorphosed central zone of the Trough along a late post-metamorphic reverse fault.

A correlation of the observed stratigraphic succession overlying the basement culminations with the better understood western foreland succession is presented. Several models are presented to account for the presence of

basement bodies of contrasting styles, these include large-scale sheath folds, fold interference patterns and refolded Penninic nappe structures. Most structural features can be reconciled, albeit not exclusively, with refolded Penninic nappe structures.

Finally, pressure and temperature determinations bracket the burial depth under which the tectonic evolution took place.

The features observed and deduced in this area are comparable with features of other overthrust core zones of more recent orogens.

1.1) General geology

1.1.1) Geological setting

The Labrador Trough, situated in NE Quebec, forms an elongate belt stretching 900 km from the northernmost western edge of Ungava Bay to the E trending Grenville Front (Fig. 1). It is an integral part of the more widespread Trans-Hudsonian orogen (Hoffman, 1988) bounding the Superior and Churchill Structural Provinces. The Labrador Trough consists of early Proterozoic imbricated and folded volcano-sedimentary rocks bounded to the west by the Archean gneisses of the Superior Province (Stockwell, 1964, 1982; Douglas, 1973), Minto subprovince (Card & Ciesielski, 1986), and to the east by an enigmatic hinterland consisting of Archean and Hudsonian gneisses (Dimroth & Dressler, 1978; Taylor, 1979). This hinterland is itself flanked to the east by the early Archean Nain Province (Taylor, 1971).

The Labrador Trough has been subdivided into three major lithotectonic domains (Dimroth 1970, 1972; Dimroth et al., 1970, Fig. 2) that are from west to east:

- 1) The western autochthonous to para-autochthonous zone resting unconformably on the Superior craton. This zone varies from undeformed

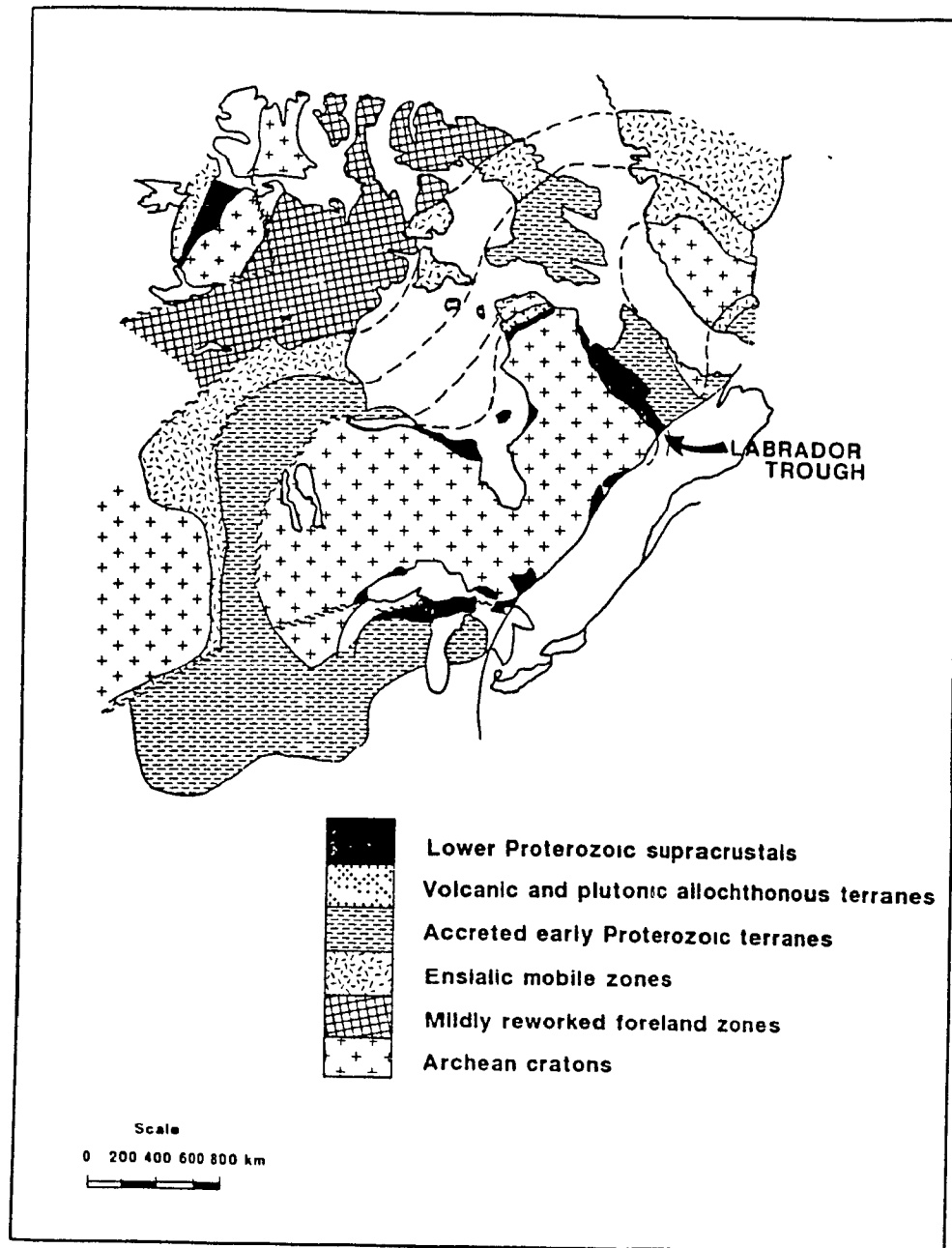


Figure 1 : Map showing the generalized elements of the Trans-Hudsonian Orogen and of other Proterozoic and Archean terranes, simplified after Van Schmus et al. (1987)

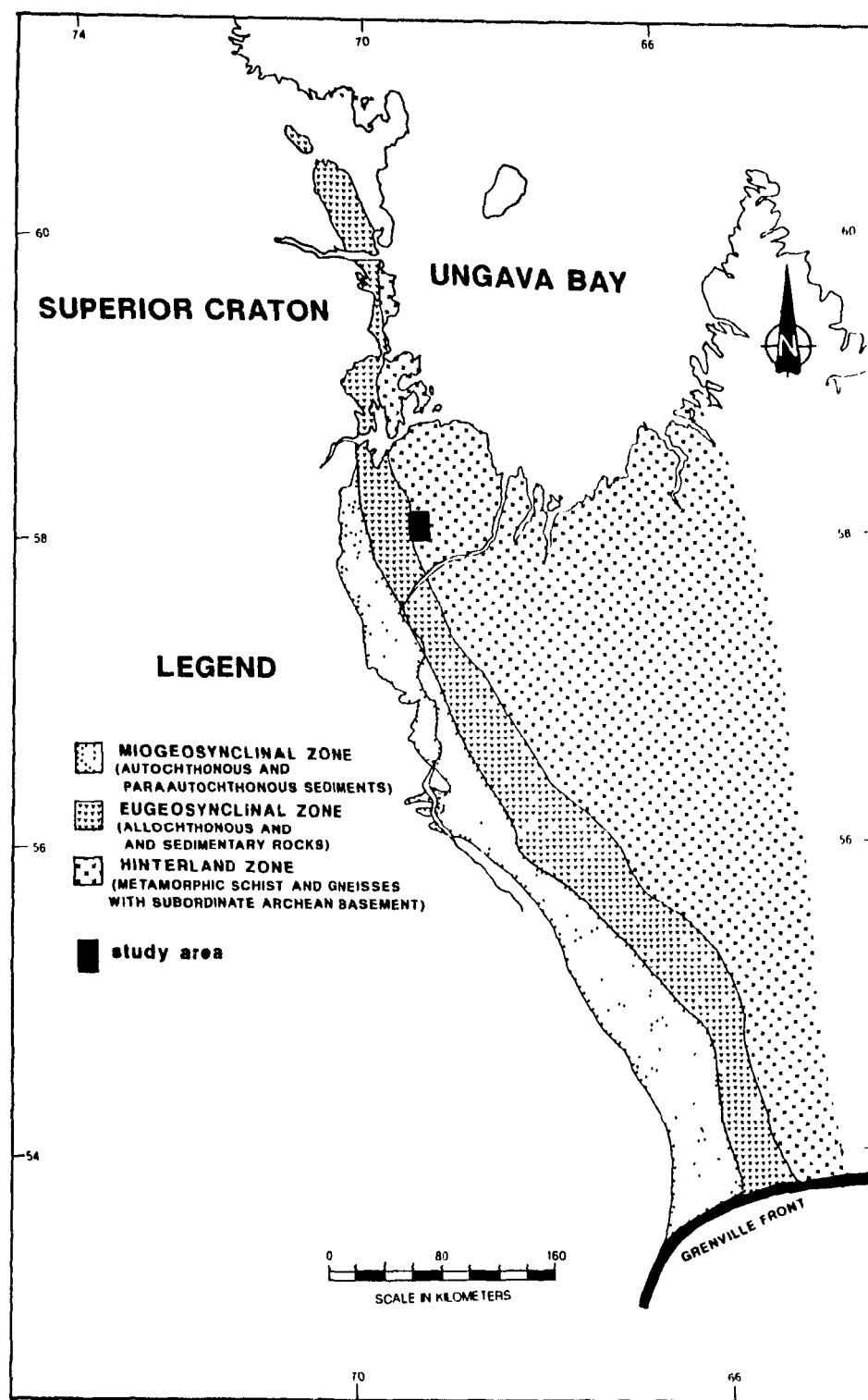


Figure 2 : Major subdivisions of the Labrador Trough, with study area outlined. Modified after Dimroth & Dressler (1978).

to thrust imbricated. It comprises an easterly facing sedimentary prism made up of platformal sediments overlain by deeper-water rocks and locally by coarse fluviatile deposits. This corresponds to Dimroth's (1970) miogeosynclinal zone;

- 2) **A central allochthonous thrust and folded zone.** It is made up predominantly of basinal sediments (siltstones and shales) intruded by numerous subvolcanic mafic sills, mostly gabbros, and capped by cogenetic (Sauvé & Bergeron, 1965; Wares *et al.*, 1988) basalts. This zone corresponds to Dimroth's (1970) eugeosynclinal zone;
- 3) **An eastern enigmatic gneissic hinterland zone** consisting of metamorphosed Aphebian metasedimentary rocks, interlayered with metavolcanic amphibolites, with local Archean basement culminations. This assemblage grades eastwards into higher grade rocks, attaining local granulite grade (Perreault *et al.*, 1987; Bélanger *et al.*, 1987), intruded by calc-alkaline granodiorite plutons (Bélanger *et al.*, 1987; van der Leeden *et al.*, in press; Poirier *et al.*, in press). The term "Labrador Trough" is commonly used to describe the first two zones.

1.1.2) General stratigraphy *

The volcano-sedimentary assemblage of the Labrador Trough is termed the Kaniapiskau Supergroup (Dimroth, 1970). The southern and central portions of the Labrador Trough contain two cycles of sedimentation and intrusive-extrusive activity. Both are characterized by an easterly facing, generally fining upwards, sedimentary assemblage. The more basinwards sediments are host to numerous mafic sills and are capped by basalts. The following summary is taken largely from Dimroth (1970 & 1978).

* A more detailed description of the sedimentation cycles is presented in the chapter dealing with stratigraphy.

Cycle I is the most voluminous and internally complex. Figure 3 gives a synopsis of its stratigraphy. This cycle comprises a lower shelf phase (Le Gallais & Lavoie, 1982) subdivided into two shallowing upwards subgroups; a lower Seward Subgroup and an upper Pistolet Subgroup. Both are characterized by a lower siliciclastic portion grading upwards through mixed siliciclastic-carbonate rocks to a carbonate platform margin sequence. In addition, the Seward Subgroup contains immature fluvial clastics at the base and alkaline mafic volcanics. The Pistolet Subgroup is overlain by the fine-grained sediments of the Swampy Bay Subgroup in the west and by the fine-grained sediments of the Attikamagen Subgroup in the east (Dimroth *et al.*, 1970; Dimroth, 1978). The Attikamagen Subgroup contains voluminous submarine basaltic lavas and associated gabbroic intrusives. Both subgroups form the basin phase of sedimentation of cycle I (Le Gallais & Lavoie, 1982). The lower portion of the Attikamagen correlates with the Swampy Bay Subgroup. The upper portion of the Attikamagen shoals upwards to a shallow water carbonate platform assemblage that blankets the first cycle of sedimentation.

Cycle I sediments are unconformably overlain by those of cycle II. They consist of shelf phase sediments, the Ferriman Subgroup, comprising quartzites and an iron formation and finer grained basinal sediments including an iron formation. The second cycle represents an easterly and northerly directed transgressive episode that involved rock units essentially similar to those of the first cycle. Cycle II rocks predominate in the northern segment of the Labrador Trough, i.e. north of the Koksoak River.

1.2) Previous work

The Labrador Trough has been the subject of numerous studies over the

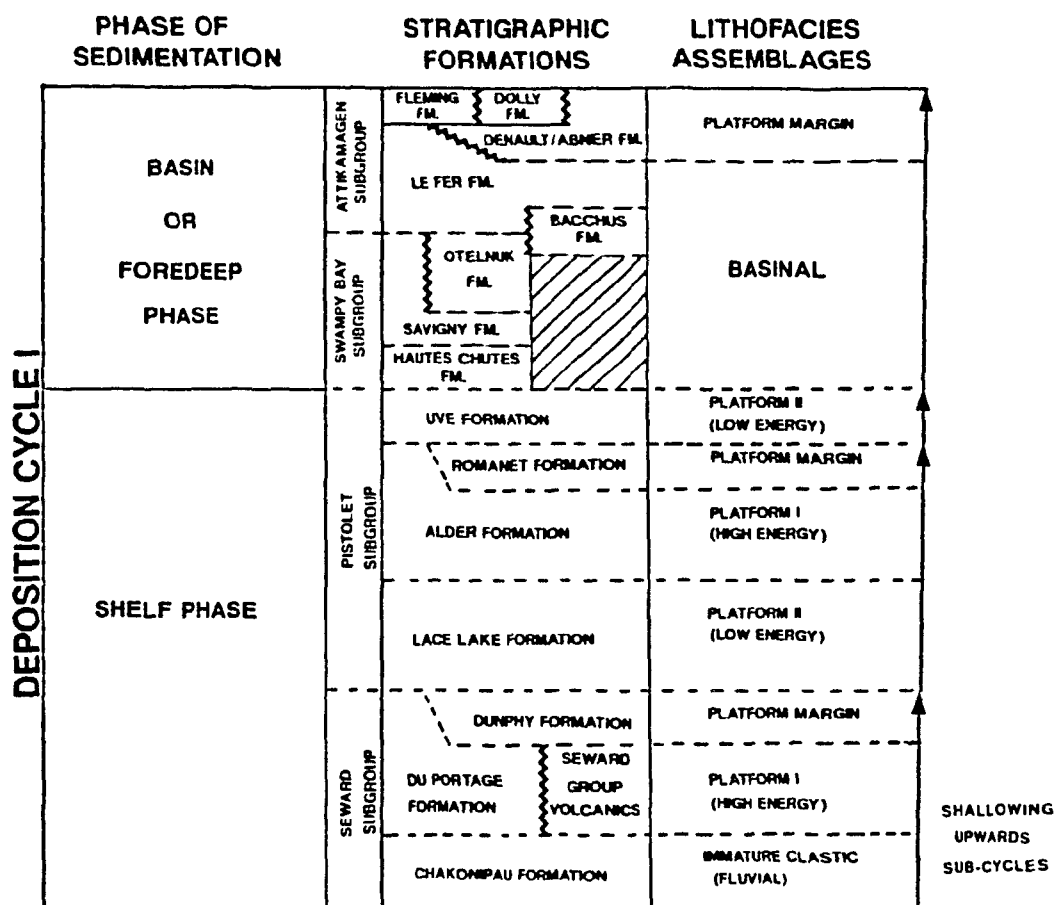


Figure 3 : Phases of sedimentation, stratigraphic formations and lithofacies assemblages of the first depositional cycle of the Kaniapiskau Supergroup, north-central Labrador Trough. Modified after Dimroth (1978) and Le Gallais & Lavoie (1982).

last two decades, dealing mostly with structural and stratigraphic aspects (Séguin, 1969; Harrison *et al.*, 1970; Dimroth, 1970, 1971, 1972, 1978, 1981, 1985; Dimroth *et al.*, 1970; Dimroth & Chauvel, 1973; Dimroth & Dressler, 1978; Dressler, 1979; Baragar & Scoates, 1981; Le Gallais & Lavoie, 1982; Simonson, 1985; Goulet, 1986, 1987; Hoffman, 1987; Wares *et al.*, 1988; Barret *et al.*, 1988; Clark, 1988).

The Labrador Trough has been subdivided into three geographic domains (Dimroth *et al.*, 1970); the south, central and north zones. The southern is formed by metamorphosed equivalents of the Labrador Trough contained within the Grenville province (Dimroth *et al.*, 1970). The central portion extends from 57°N southwards to the Grenville metamorphic front. It has been subdivided into a north central and a south central zone, approximately along 55°15'N. The south central zone has been studied by Wynne-Edwards (1960, 1961), Frarey (1961), Baragar (1967), Fahrig (1967), Evans (1978), Wardle (1979) and Ware & Wardle (1979). The north central zone has been extensively studied by Dimroth (1978) and to a lesser extent by Dressler (1979).

The northern zone extends from 57° to the NW edge of Ungava Bay at 60°45'N. Although most of the region has been mapped on a scale of 1 inch to 1 mile there is no regional synthesis or map currently available, except for the recently published 1:1 500 000 scale map of Quebec (Avramtchev 1985; Fig. 4). Figure 5 illustrates the locations of most of the previous mapping projects done in this zone. 1:250,000 scale maps are currently in preparation (Clark, in press). The area studied by this project straddles the boundary between the work of Gélinas (1958a) and Sauvé & Bergeron (1965).

1.3) Dates

The Superior craton has been dated by the K/Ar whole rock method, giving

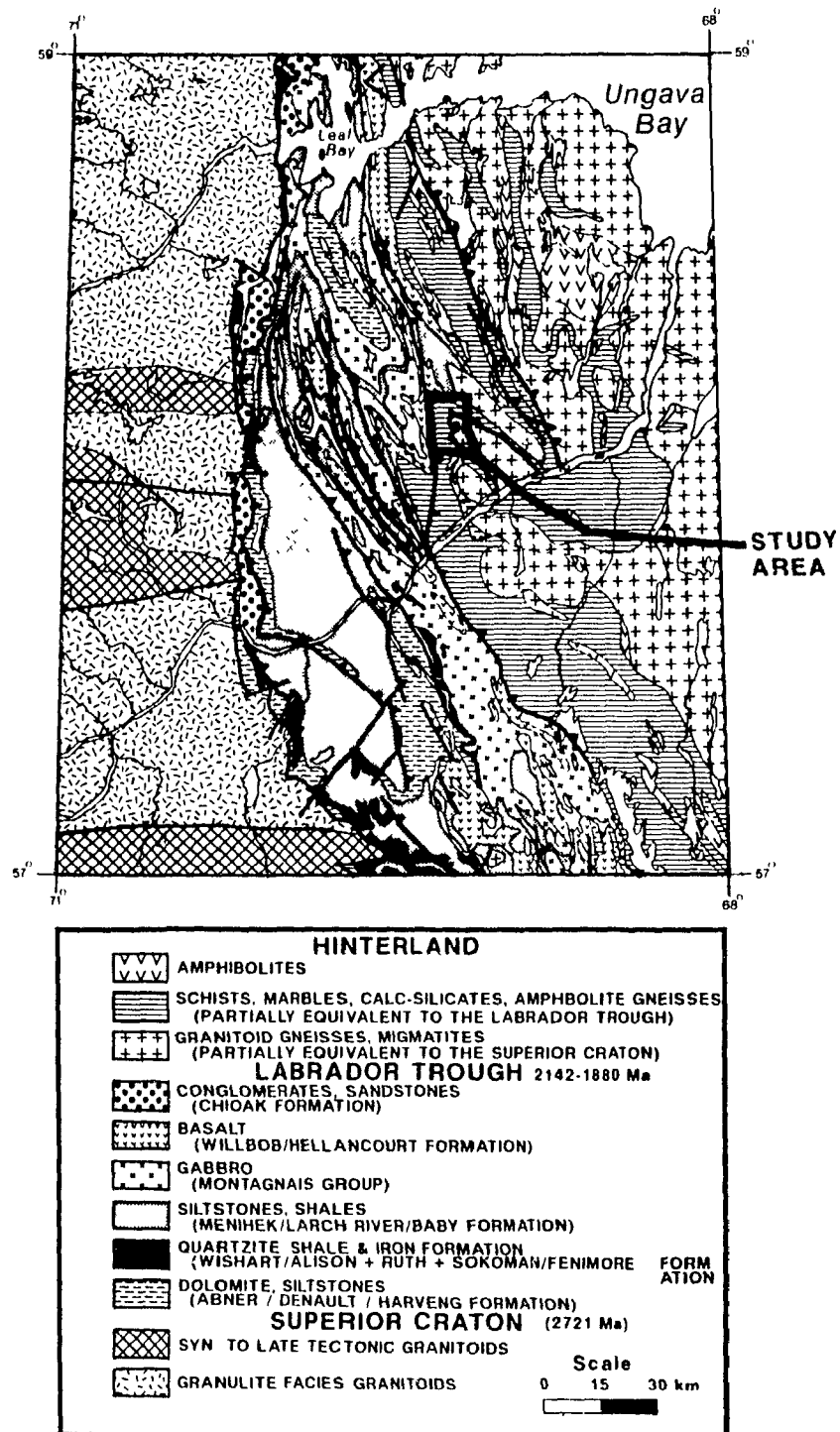


Figure 4 : Simplified geology of the Northern Labrador Trough, with study area outlined. Modified from Avramtchev (1985), Clark (1988, in press), Goulet (1987), Boone (1987).

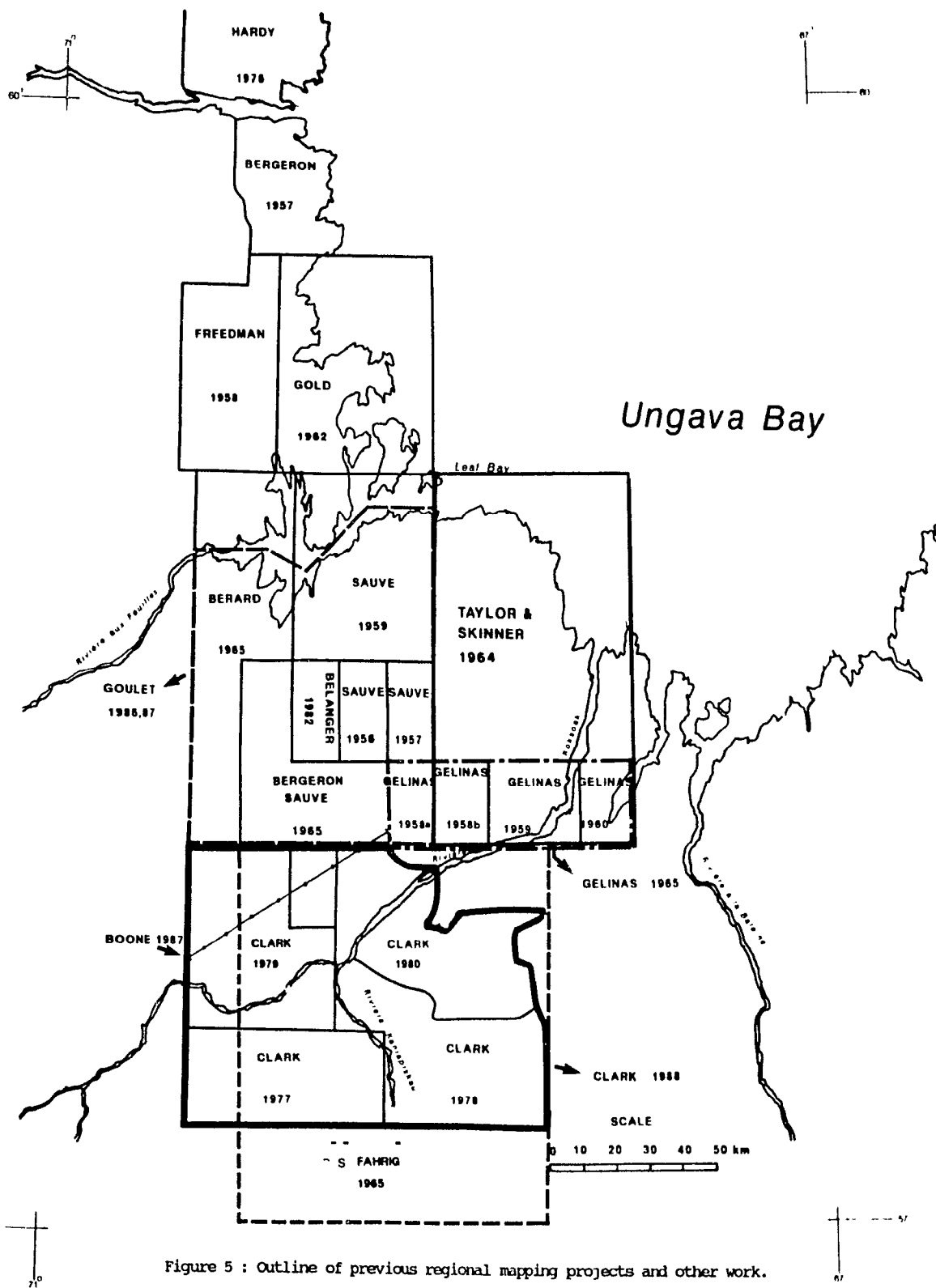


Figure 5 : Outline of previous regional mapping projects and other work.

ages between 2450 & 1770 Ma (Beall et al., 1963). An Rb-Sr errorchron yielded an age of 2685 Ma (Taylor & Loveridge, 1981). Wanless (1970) reports K/Ar biotite ages from 2510 to 1690 Ma. More recently Machado et al., 1987 obtained an U/Pb zircon age of $2721 \pm 5/-3$ Ma for the gneisses adjacent to the unconformity in the vicinity of Leaf Bay. The diabase dykes cutting large portions of the northwest Superior province yielded K/Ar ages of 1790 to 1995 Ma (Wanless, 1970) and 2150 Ma (Fahrig & Wanless, 1963).

In the Labrador Trough "sensu stricto" the following dates have been found:

The earliest values were K/Ar whole rock ages from biotite schists, ranging from 1400 to 2060 Ma with an average of 1600 Ma (Beall et al., 1963). Lowden et al. (1963) obtained a K/Ar mica age of 1560 Ma. Wanless (1970) reports K/Ar ages from 1800 to 1410 Ma. Most of these dates are probably related to late metamorphic effects of the Hudsonian orogeny.

In Fryer (1972), a composite isochron for shale samples from both sedimentation cycles gave an age of 1879 ± 43 Ma. Samples from the uppermost cycle II gave an age of 1855 ± 74 Ma, the lower cycle gave a reference isochron of 1900 Ma.

Dressler (1975) found a K/Ar whole rock age of 1873 ± 53 Ma for a mafic dyke related to alkaline volcanics present within the Sokoman iron formation, at the base of the second cycle of sedimentation. The same volcanic unit was dated by Chevé & Machado (1988) who reported a zircon U/Pb age of 1880 ± 2 Ma. These ages bracket the start of the second cycle of sedimentation.

R. Parrish (pers. comm. 1987; cited in Hoffman, 1988) reports zircon U/Pb ages of 1.88 Ga for the Sokoman iron formation and a differentiated gabbro sill intruding the Menihek Formation of the second cycle of sedimentation.

Dressler & Krogh (cited in Clark, 1984) obtained a zircon U/Pb age of 2142 ± 2 Ma for the Mistamisk Formation which Clark & Thorpe (in press) consider correlative with the mafic volcanics, the Bacchus Formation, situated at the top of the first cycle. Thus there seems to be a 260 Ma hiatus recorded in the unconformity between cycle I and cycle II.

Clark and Thorpe (in press) found model lead ages, taken from galena occurrences, of 2309 ± 5 Ma for the base of the Kaniapiskau Supergroup and 1793 ± 5 Ma near the top. One of the conclusions of their study was that the two sedimentation cycles encompassed as much as 450 Ma, in comparison with 260 Ma dictated by the zircon dates. This latter value is however only a minimum since the basal units of cycle I and the uppermost units of cycle II have not been dated by zircon U/Pb methods. Clark & Thorpe (in press) also found a time gap of 110 Ma between cycles I and II.

Within the hinterland the following dates have been obtained:

2850 Ma, 2868 and 2878 ± 5 Ma from three basement gneiss domes (Machado et al., 1987);

1769 ± 15 Ma and 1793 to 1783 Ma for the main Hudsonian metamorphism (Machado et al., 1987; Goulet et al., 1987) and (Machado et al., 1988) respectively;

1829, 1840 and 1845 ± 2 Ma for syntectonic granitoid intrusives (Machado et al., 1988; Perreault et al., 1988);

1840 Ma from rocks similar to the above mentioned in the hinterland of the central Labrador Trough (S. Bowring pers. comm. 1987, cited in van der Leeden et al., in press).

2320 Ma for intrusive rocks on the east side of the above mentioned intrusive rocks (S. Bowring pers. comm. 1987, cited in van der Leeden, in press).

1.4) Evolution models

Models proposed by different authors for the tectonic evolution of the Labrador Trough fall into three categories:

1) **ENSIALIC BASIN** of variable original width that was asymmetrically deformed and metamorphosed (Dimroth, 1970, 1972, 1981; Dimroth et al., 1970; Dimroth & Dressler, 1978; Baragar and Scoates, 1981).

2) **PASSIVE MARGINS** for both cycles of sedimentation that included platform, slope-rise and basin sedimentary facies, the latter facies being host to intrusions and volcanism, that was folded, imbricated and translated onto the Superior craton (Gibb & Walcott, 1971; Hynes, 1978; Thomas & Keary, 1980; Hamilton, 1980; Wardle & Bailey, 1981; Le Gallais & Lavoie, 1982; Simonson, 1985; Boone, 1987; Boone & Hynes, in press; Bélanger et al., 1987; Poirier et al., in press; van der Leeden et al., in press).

3) **PASSIVE MARGIN** for the first cycle of sedimentation and a **FOREDEEP ORIGIN** for the second cycle (Hoffman, 1987, 1988).

1.4.1) Ensialic basins

Dimroth (1970, 1972) and Dimroth et al. (1970) originally argued an ensialic origin for the Labrador Trough on the basis of:

- 1) Provenance studies indicating both a westerly and an easterly source for the sediments;
- 2) An essentially "mirror image" of sedimentary facies onlapping the Superior craton to the west and the remobilized basement culminations, in the westernmost hinterland, to the east.
- 3) The lack of any true remnant of ocean crust or products of destructive plate margins (calc-alkaline volcanics or batholiths).

The asymmetry in deformation and metamorphic grade between the eastern

and western flanks of the trough, which is not characteristic of more modern ensialic failed rifts (e.g. the Keweenaw rift; McSwiggen et al., 1987; Berg & Kewin, 1988) was accounted for in later papers (Dimroth & Dressler, 1978; Dimroth, 1981). The model involved overthrusting of the eastern margin by large, recumbent, basement cored, nappes and concurrent easterly directed delamination of the sialic crust, underneath the westerly telescoping cover rocks. This type "A" subduction (Bally, 1981) was deemed responsible for 100 to 200 km of crustal shortening, the lost crustal material being interpreted to have underplated and buoyantly uplifted the eastern hinterland. This was necessary to produce the needed 20 to 30 km of tectonic unroofing dictated by the mineral assemblages present in the hinterland (Dimroth & Dressler, 1978; Gélinas & Perreault, 1985; Moorhead & Hynes, 1986; Perreault et al., 1987).

This model, although increasing the original width of the basin, did not allow for the creation of oceanic crust. The intracratonic rift was interpreted to have underlain the present central igneous volcanic zone of the Labrador Trough. This is not compatible with the palinspastic reconstruction of Boone (1987) and Boone & Hynes (in press) in the northern Labrador Trough that places the first occurrence of mafic volcanics well eastwards of the Archean basement culminations along the western edge of the hinterland zone. The cross-section of Dimroth & Dressler (1978) shows the basal décollement to terminate in the central zone. Since it is not present for the whole length of the basement the amount of shortening in the cover rocks is difficult to account for. A basal décollement present in the foreland zone but absent in the higher grade internal zones is not compatible with observations from other exhumed orogens (Read & Brown, 1983; Okulitch, 1984; Hynes & Francis, 1982; St-Onge et al., 1986; King, 1986).

1.4.2) Passive margins

The similarity between the eastern and western flank sediments (Dimroth, 1970, 1972) was questioned by Le Gallais & Lavoie (1982) who reinterpreted the Trough as part of a platform/shelf-basin sequence with two main fining upwards sedimentation cycles and four shallowing upwards subcycles. Provenance for the sediments was thought to be mostly westerly. These authors also disagreed with Dimroth's (1970) interpretation of basement exposures within the parautochthonous zone as part of a central geanticline emergent during the deposition of the sediments. Le Gallais & Lavoie (1982) noted that the absence of onlap or local facies changes near the basement exposures is more compatible with basement involved thrusting or post-orogenic vertical movements. Small basement thrust slices are found in the same zone elsewhere in the Trough (Dressler 1978). Basement allochthons similar to these are found in other thrust imbricated passive margin sequences, such as the Canadian Cordillera (Price & Mountjoy, 1970; Okulitch, 1984; McDonough & Simony, 1988).

In the south-central Labrador Trough, Wardle and Bailey (1981) interpreted the Kaniapiskau Supergroup to have formed as a continent shelf and slope-rise system on the western edge of a proto-oceanic rift system of unknown width.

Bélanger *et al.* (1987) and van der Leeden *et al.* (in press) studied the broad hinterland east of the central portion of the Labrador Trough. They interpreted the thrust fault separating the easternmost exposure of mafic volcanics, belonging to the central allochthonous igneous-sedimentary zone, from the metasedimentary schists of the hinterland to represent the cryptic surface expression of a suture. In this model the proto-oceanic crust, represented in part by the igneous-volcanic zone of the Trough, was subducted

below a westerly facing arc. The westernmost schists of the hinterland were interpreted as remnants of a fore-arc accretionary wedge that included mostly schists and greywackes interlayered with MORB-like low K tholeiites and mafic-ultramafic slivers. These latter rocks were interpreted as scraped off remnants of the easterly subducting ocean floor. The fore-arc is bounded to the east by an 1.84 Ga (S. Bowring pers. comm. 1987 cited in van der Leeden et al., in press) I-type calc-alkaline granitoid batholith.

The hinterland of the Northern Labrador Trough has also come under scrutiny. Gélinas (1965) studied the metamorphism of a large swath of metasediments, along an E-W traverse at the latitude of Kuujjuaq. From a complexly folded area in the same region as Gélinas's study, Hynes (1978) studied early refolded recumbent folds involving the metamorphosed cover rocks, which were interpreted to have been detached at an early stage from their underlying crystalline basement. The observed features, compatible with large scale horizontal displacements, were deemed inconsistent with a strictly ensialic model for the Labrador Trough.

Covering roughly the same area as Gélinas's (1965) work Poirier et al. (in press) presented a model similar in many respects to the one put forth by Bélanger et al., 1987 and van der Leeden (in press) in the southern hinterland. In this case an arc complex consisting of gneissic metasandstone and epiclastic amphibolites, intruded by granodioritic-tonalitic calc-alkaline plutons, was juxtaposed to metamorphosed and imbricated equivalents of the Trough's Kaniapiskau Supergroup.

Recent metamorphic studies in the northern hinterland (Gélinas & Perreault, 1985; Moorhead & Hynes, 1986; Perreault et al., 1987) confirmed the large amount of unroofing, up to 30 km, necessary for the westernmost metamorphic imbricates of the Labrador Trough. Such large uplifts are

characteristic of other orogenic belts (Journeay, 1983; St-Onge, 1984; Simony et al., 1980; St-Onge & Lucas, 1986) where convergent plate processes are thought to have occurred.

In summary, many attributes of the Labrador Trough can be adequately accounted for by a passive-margin type model, such as: a predominantly westerly source for the sediments, differences in the platform and basin phases of sedimentation and the voluminous outpouring of a MORB-like, low K tholeiitic sill-volcanic complex.

However, the passive margin model is hampered by the following features of the Labrador Trough:

- A) The recurrence of the fining upwards cycle of sedimentation;
- B) The lack of true remnants of ocean crust;
- C) The lack of destructive volcanism products;

Point A has been interpreted to reflect a two-stage rifting event (Dimroth 1970, 1972; Dimroth et al., 1970; Baragar & Scoates, 1981) related to renewed basement subsidence.

Although the problem of point B, the lack of true complete remnants of oceanic crust, remains, van der Leeden et al. (in press) interpreted the mafic-ultramafic bodies present in the westernmost metasedimentary hinterland as sliced off oceanic crust incorporated in an easterly translating and accreting fore-arc assemblage.

There is a lack of destructive volcanism products (point C) in the Labrador Trough "sensu stricto". Its hinterland, however, contains voluminous calc-alkaline batholiths along with immature sedimentary and volcanoclastic sequences similar to those of modern continental arcs (Poirier et al., in press; van der Leeden et al., in press). Thus the absence of related volcanism may simply be a byproduct of the deep erosion level observed in the

hinterland. Studies in the Cape Smith fold belt, the adjacent segment of the Circum-Superior belt (Baragar & Scoates, 1981), have brought to light the existence of true ocean floor volcanism (Hynes & Francis, 1982; Francis *et al.*, 1983), the dismembered remnants of an ophiolite succession (St-Onge *et al.*, 1987, 1988) and calc-alkaline volcanism (Baragar, 1974; Moore, 1977; Moorhead, unpublished data).

1.4.3) Passive margin in addition to a foredeep origin for the upper part (cycle II) of the Kaniapiskau Supergroup.

Hoffman (1987) interpreted the first sedimentation cycle in the same fashion as Wardle & Bailey (1981) and Le Gallais & Lavoie (1982), to represent the evolution of a passive margin sequence. Although he mentions that the Swampy Bay and Attikamagen Subgroups could also represent foredeep deposits. Chevé (1987) has described a westerly vergent folding and faulting event affecting the shales and greywackes of the Savigny Formation (cycle I) in the western zone of the north-central area of the Labrador Trough. This deformation event was not observed in the overlying cycle II sediments or in the cross-cutting carbonatite dykes associated with alkaline volcanism in the Sokoman iron Formation. The presence of a pre-cycle II westerly vergent compressional tectonic event would seem to corroborate the foredeep model.

The second sedimentation cycle is thought to be related to a westerly migrating foredeep, synchronous with easterly directed underthrusting of the products of the first cycle of sedimentation under the tectonically thickened hinterland. This model explains many of the sedimentation features of the trough but is less compelling in explaining the presence of voluminous and extensive MORB like basalts and subvolcanic sills in the central zone of the trough.

2.0) STRATIGRAPHY

In this chapter, the stratigraphy of the Kaniapiskau Supergroup in the western part of the Labrador Trough is briefly reviewed, and the stratigraphic succession in the study area is described in more detail. Finally, the stratigraphy of the study area is correlated to that of the Labrador Trough (*sensu stricto*) further west.

2.1) General stratigraphy

The Kaniapiskau Supergroup of the central Labrador Trough is disposed in an east facing sedimentary-volcanic prism containing two major cycles of shelf and basin style sedimentation (Dimroth, 1970, 1972, 1978; Dimroth, *et al.*, 1970; Wardle & Bailey, 1981; Le Gallais & Lavoie, 1982). Le Gallais & Lavoie (1982) subdivided the sediments of the first cycle into three shallowing-upward cycles (Figure 3). The following summary is taken largely from Dimroth (1970, 1978); Dimroth *et al.* (1970) and Le Gallais & Lavoie (1982).

2.1.1) Cycle I

Central Labrador Trough

i) Shelf phase

The Seward and Pistolet Subgroups form the shelf phase of sedimentation, the basin phase being represented by the Swampy Bay and Attikamagen Subgroups. The shelf phase begins with the deposition of the Du Portage Formation of the Seward Subgroup comprising shallow-water marine platform clastic sediments and subordinate carbonates. Immature fluvial clastics (the Chakonipau Formation) are present locally at this level. Cryptalgal laminated and stromatolitic carbonates of the Dunphy Formation overlie the Du Portage Formation, ending

the first shallowing-upward shelf subcycle of Le Gallais & Lavoie (1982). The overlying Pistolet Subgroup is characterized at the base by mudstones and siltstones grading upwards into carbonate-mudstone rhythmites (Lace Lake Formation) followed by mature high-energy quartzites grading up to cryptalgal and stromatolitic carbonates of the Alder Formation. Carbonate megabreccia horizons (Romanet Formation) occur locally basinwards east of the platform carbonates of the Alder Formation. This ends the second shallowing upward shelf subcycle of Le Gallais & Lavoie (1982).

The overlying Uvé Formation is the youngest member of the Pistolet Subgroup and is characterized by finely laminated shales and argillaceous siltstones capped by micritic carbonates. This represents the third shelf subcycle of Le Gallais & Lavoie (1982) that occurred under much deeper water conditions than the first two.

ii) Basin phase

The lower portion of the basin phase of sedimentation (Swampy Bay Subgroup) is characterized at the base by subgraphitic black shales of the Hautes Chutes Formation that are locally rich in pyrite. They are overlain by the grey shales of the Savigny Formation. Laterally eastwards and stratigraphically higher is the Otelnuik Formation. It contains a flysch like sequence of turbiditic greywackes interbedded with shale horizons. The lithological and stratigraphic characteristics of the Savigny and Otelnuik Formations indicate that they could represent a flysch sequence derived from an uplifted (upthrust?) eastern source underlain by coarse sandstones interbedded with shale horizons (Dimroth, 1970, 1978). The Savigny shales would represent a distal equivalent to the turbiditic quartz-wackes of the Otelnuik Formation. However the roundness of the quartz grains in the quartz-

wackes led Le Gallais & Lavoie (1982) to envisage a western cratonic source for the sediments of the Swampy Bay Subgroup.

In the west the Otelnuik and Savigny Formations are overlain by the Le Fer Formation. It consists of red shales in the west grading eastwards to green shales. A westerly source for these distal sediments was postulated by Dimroth (1978). To the west the Bacchus basaltic volcanism and magmatism occurs roughly at the same stratigraphic level as the Otelnuik and Le Fer Formations. The upper portion of the Le Fer Formation blankets the Bacchus basalts. The Le Fer Formation eventually grades up through a stromatolite reef complex to a supratidal dolomite platform, the Denault or Abner Formation (Clark, 1987; Hoffman, 1987). This could represent a fourth shallowing upwards subcycle similar to those described for the underlying units by Le Gallais & Lavoie (1982). Two laterally equivalent formations, the Dolly and Flemming, overlie the western portion of the Denault Formation. The Dolly Formation is composed of red, green and grey shales that were deposited in a low energy platform environment (Dimroth, 1978). The Flemming Formation is a chert breccia formed by evaporite solution collapse (Dimroth, 1978).

Chev  (1987) noted evidence for pre-cycle II compressional deformation in the north-central Labrador Trough. This information along with an easterly source for a large portion of the sediments in the Swampy Bay (Dimroth, 1970, 1978) and possibly the Attikamagen Subgroups, in addition to the presence of a westerly propagating stromatolite reef complex (Hoffman, 1987) indicates that the basinal phase of sedimentation of the first cycle could well have taken place in a foredeep environment (Hoffman, 1987, 1988).

Northern Labrador Trough

In the western part of the northern segment of the Labrador Trough the

Abner dolomite represents the oldest formation. Its thickness has been estimated at 30 to 122 m (Bérard, 1965). In the central allochthonous igneous-sedimentary zone the dolomitic Harveng Formation outcrops below the basinal sediments. It consists of massive arenaceous dolomite overlain by dolomitic schist (Sauvé & Bergeron, 1965; Bélanger, 1982). Sauvé & Bergeron (1965) estimated the total thickness at approximately 200 m. The Harveng possesses several lithological similarities to the Abner dolomite and has been correlated to it (Sauvé & Bergeron, 1965), probably representing an eastern, deeper water, distal equivalent to the shelf-platform facies of the Abner dolomite (Clark, 1988).

2.1.2) Cycle II

Cycle II sediments rest unconformably on those of cycle I, and on the Archean basement to the west. They form most of the stratigraphic succession in the northern segment of the Labrador Trough. The second cycle contains a shelf phase characterized by a siliciclastic-iron formation assemblage, and a basin phase marked by shales, turbiditic siltstones and sandstones intruded by numerous mafic sills (Fig. 6). The basin phase is capped by an extensive and uniform mafic volcanic sequence. The original stratigraphic column of cycle II proposed by Bérard (1965) and Sauvé & Bergeron (1965) for the northern segment of the Labrador Trough cannot readily be correlated with the one put forth further south by Dimroth (1970, 1972) (Fig. 7). However, Clark (1977, 1988), Budkewitsch (1986) and Goulet (1986) recognized a thrust fault that places the Abner dolomite onto the sandstones and conglomerates of the Chioak Formation. The dolomitic Abner Formation then becomes low in the original stratigraphic sequence, and can be correlated to the Denault Formation of the first cycle of sedimentation (Goulet, 1986; Clark, 1988; Fig. 7).

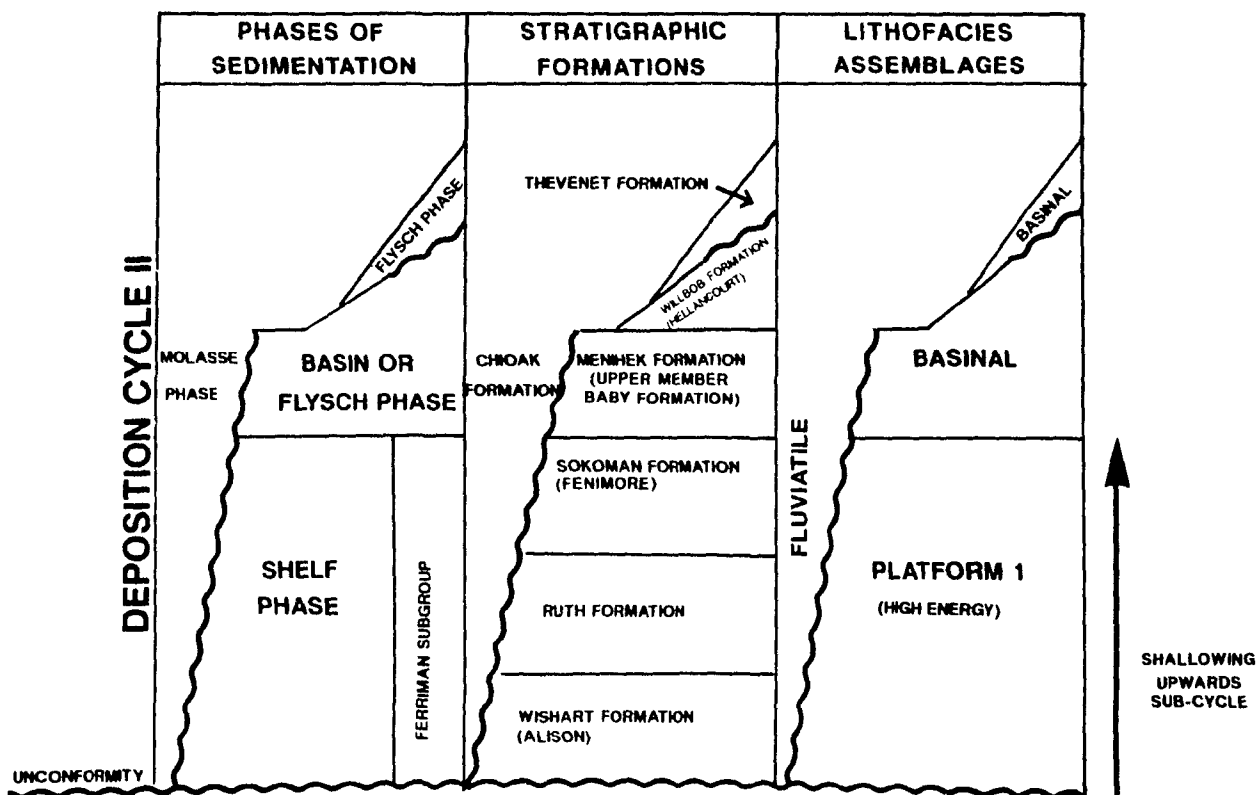


Figure 6 : Phases of sedimentation, stratigraphic formations and lithofacies assemblages of the second depositional cycle of the Kaniapiskau Supergroup, Northern Labrador Trough. Modified after Le Gallais & Lavoie (1982).

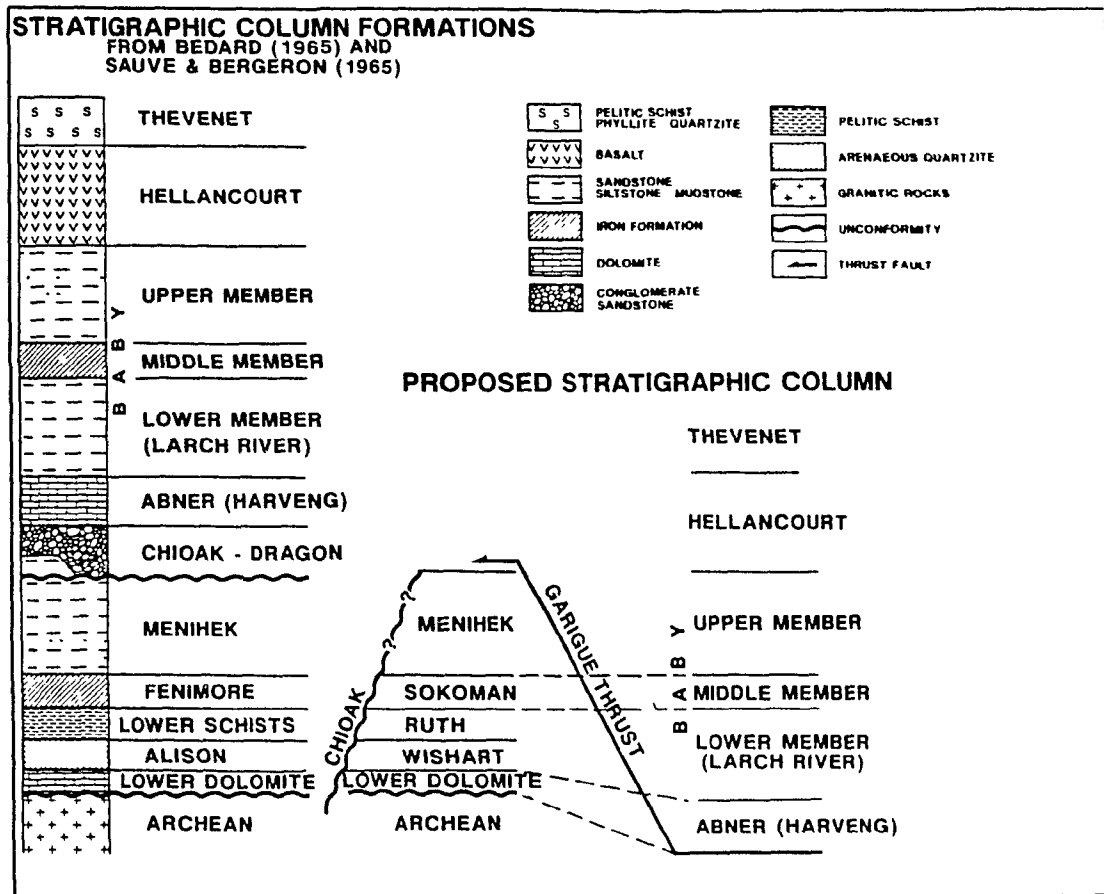


Figure 7 : Stratigraphic correlations in the northern Labrador Trough, modified from Clark (1988).

2.1.2.1) Shelf phase (Ferriman Subgroup)

2.1.2.1A) Autochthonous shelf sequence

The rocks directly overlying the Superior craton are the mature high energy quartzites, with argillaceous interlayers, of the Wishart (Alison) Formation (Bérard, 1965; Simonson, 1984). The stratigraphic thickness of this unit varies between 12 and 46 m in the Northern Labrador Trough (Bérard, 1965) and 100 to 300 m in the central zone (Le Gallais & Lavoie, 1982). Bérard (1965) mentions the presence of small dolomite exposures between the Superior craton and the Wishart quartzites. These could represent westerly representatives of the underlying Abner/Denault dolomite that caps the first cycle of sedimentation (Clark, 1988).

A ferruginous siltstone-sandstone unit, the Ruth Formation, overlies the quartzites. In the north-central Trough it attains 50-100 m thickness (Le Gallais & Lavoie, 1982) while in the north it is a thin unit of roughly 12 m (Clark, 1977). This formation is interpreted as a transitional facies between the underlying quartzites and overlying iron formation (Clark, 1977).

The overlying Sokoman (Fenimore) iron formation has been the subject of numerous studies (Gross, 1962; Bérard, 1965; Chauvel & Dimroth, 1973; Dimroth, 1977, 1985; Simonson, 1985). At this latitude of the Labrador Trough the Sokoman/Fenimore iron formation consists of a lower banded to massive iron oxide formation consisting of chert and iron oxides (magnetite, hematite) and an upper carbonate iron formation consisting of chert, iron carbonate and iron silicate (Clark, 1977). The carbonate member contains numerous and variably textured concentric ooids, peloids, pellets, pisolites and intraclastic conglomerates (Clark, 1977; Le Gallais & Lavoie, 1982). The thickness of the Sokoman in the northern segment of the Labrador Trough is quite variable; the

maximum thicknesses are 46 m (Bérard, 1965), 150 m (Le Gallais & Lavoie, 1982) and 113 m (Clark, 1988) in various different regions.

2.1.2.1B) Para-autochthonous & allochthonous shelf sequence

There are distal eastern equivalents to the formations that make up the autochthonous shelf sequence. The oldest unit is the Abner/Denault Formation and its eastern distal equivalent the Harveng Formation, both formations belonging to the last episode of the first cycle of sedimentation.

The Abner dolomite and Harveng dolomitic schists pass gradationally upwards into a shale and siltstone sequence. The sequence overlying the Abner dolomite has been called the Larch River Formation (Bérard, 1965), whereas the one overlying the Harveng Formation and capped by an iron formation has been termed the lower member of the Baby Formation (Sauvé & Bergeron, 1965). Clark (1988) correlates the Larch River and the lower member of the Baby Formation with the Wishart & Ruth Formations (Fig. 7).

Bérard (1965) estimates the thickness of the Larch River Formation to be between 10 & 80 meters. Boone (1987, & Hynes, in press) favours a much greater thickness, near 600 m, citing the large (several kilometers) apparent structural thickness, in part due to open upright F3 folds (Fahrig, 1965).

The thickness of the lower Member of the Baby Formation is quite variable and has been estimated at 15 to 35 m near the autochthonous sedimentary zone (Clark, 1988) in the west and 325 m or 600 m in the central volcanic zone by Clark (1988) and Sauvé & Bergeron (1965) respectively. The latter authors mention the presence of thick coarse-grained sandstone layers near the top of the member. These beds locally contain quartz-rich lithic fragments.

Bérard (1965) mentions the presence of fresh plagioclase in the Larch

River Formation which he attributes to a possible eastern volcanic source. Sauvé & Bergeron (1965) note the presence of volcanic fragments within the same formation, suggesting an eastern source. A western source cannot however be excluded. Although volcanics are rare at this stratigraphic level, a possible source rock would be uplifted (upthrust?) mafic volcanics of the Bacchus Formation in the first cycle of sedimentation or the rare occurrences of basalt within the lower Baby Formation (Bélanger, 1982; T. Clark, pers. comm. 1989). The first possibility would make the Larch River Formation an easterly derived syn-orogenic flysch deposit.

The stratigraphic position of the fault-bounded Larch River Formation is problematical to some degree. Clark (1988) correlated the Larch River Formation with the lower member of the Baby Formation and the Wishart-Ruth Formations based on structural and lateral facies relationships. However the Larch River's proximity and contact (gradational?) with the Chioak Formation (Bérard, 1965) could make it a correlative with the younger Menihek Formation.

The lower member of the Baby Formation / Larch River Formation is capped by an iron formation unit called the middle member of the Baby Formation (Sauvé & Bergeron, 1965).

Clark (1988) divided the Baby iron-rich member into four lithofacies: oxide, silicate-carbonate, carbonate and sulphide facies. As a general rule his lithostratigraphic sections show the sulphide and silicate-carbonate facies increasing basinwards (eastwards) at the expense of the carbonate facies. The oxide facies was found only locally in westernmost exposures of the Baby Formation (Clark, 1988). Thickness of this unit seems to be well constrained in spite of the presence of thrust faults, folds and the intrusion of gabbro sills; estimates vary from 46 m (Sauvé & Bergeron, 1965) through 50 m (Clark, 1988) to 53 m (Barrett et al., 1988).

Based on lithological similarities, Clark (1988) and Hoffman (1987) correlated the Sokoman/Fenimore and Baby iron formations, the latter being the distal more basinal equivalent of the former. The Baby iron formation has been the subject of recent studies (Clark, 1988; Barrett et al., 1988; Wares et al., 1988).

The studies of Clark (1988) and Barrett et al. (1988) focused on the origin of the iron formation. Using geochemical and stratigraphic evidence they concluded that the Baby iron formation was the product of hydrothermal activity on the ocean floor at the location of the gabbroic sill complex (Montagnais Group and Hellancourt volcanics). In the Southern Labrador Trough Simonson (1985), using sedimentological evidence, also postulated a basinward hydrothermal source for the iron of the Sokoman iron formation.

2.1.2.2) Basin phase

The autochthonous shelf sediments are unconformably overlain by the coarse-grained sediments of the Chioak Formation, consisting of siltstones, sandstones and polymictic conglomerates (Bérard, 1965; Clark, 1977, 1979, 1988). It is clear from the nature of the fragments - they all come from the underlying formations and basement rocks - that this formation is the result of uplift of the craton to the west. The unconformity between the Chioak and the underlying Ferriman Subgroup cuts stratigraphically downwards to the west (Hoffman, 1987), placing the Chioak in some instances directly over basement rocks (Bérard, 1965; Clark, 1979). The Chioak formation is interpreted to grade laterally eastward into the more distal turbidites of the Menihek Formation (Le Gallais & Lavoie, 1982; Clark, 1988) with local coarser conglomeratic channel deposits consisting of westerly derived fragments from the craton and Ferriman sediments. The Chioak Formation was deposited as a

result of late stage uplift of the Superior craton, that was caused either by (1) renewed basin subsidence and down-faulting (Dimroth 1970, 1972) or (2) flexural arching of the craton in response to subsidence in the basin induced by the weight of the advancing thrust sheets further eastwards (Hoffman, 1987, 1988). The first hypothesis makes the Chioak pre-Hudsonian compressional deformation, possibly as a prograding coarse clastic sequence that would represent a proximal lateral facies equivalent to the upper portion of the Menihek/Baby Formation. (Le Gallais & Lavoie, 1982). The second hypothesis would make the Chioak a syn-orogenic fluviatile molasse sequence developed in the last stages of infilling of the foredeep basin (Hoffman, 1987). Although this problem is beyond the scope of this study, our work in the western hinterland points to an eastern source for the sediments overlying, and possibly for the sediments underlying (T. Clark, pers. comm. 1989), the mafic volcanic unit. This interpretation, if correct, is easier to reconcile with Hoffman's (1987) interpretation of the Chioak formation as a late stage molasse sequence.

The eastern distal equivalents of the shelf sequence (Harveng Formation, lower and middle members of the Baby Formation) are overlain by the upper member of the Baby Formation (Sauvé & Bergeron, 1965; Clark, 1987). It consists of a shale sequence with local interlayers of turbiditic siltstone and sandstone. The thickness of this unit has been estimated at 460 m (Sauvé & Bergeron, 1965) and 400 m (Clark, 1980). The upper member (U.M.) of the Baby Formation is host to numerous gabbroic sills, locally with basal ultramafic portions (Sauvé & Bergeron, 1965). It can be readily correlated with the Menihek Fm. to the south (Clark, 1988).

Le Gallais & Lavoie (1982) report the presence of polymictic paraconglomerate horizons within the upper Menihek Formation. These include

some granite and granite-gneiss fragments. The authors interpret the horizons as resedimented conglomerates of the Chioak Formation in channel deposits within a submarine fan environment, clearly indicating a westerly source for the upper Menihek Formation.

In the eastern central zone the top of the Baby Formation is marked by the presence of coarse, locally conglomeratic, siliciclastic beds (Clark, 1978). The conglomerates contain mostly quartz pebble clasts with subordinate shale and dolomite fragments (Clark, 1978). Dimroth (1978) reports the presence of volcanic conglomerates in the uppermost eastern exposures of the Menihek Formation. The presence of basalt along with gabbro fragments seems to indicate that the conglomerates are the product of an uplifted source, not resedimented flow breccia horizons. The uplifted source could be either the product of local normal faulting, synchronous with the development of the mafic volcanic pile, or the result of upthrusting to the east.

To the west, at the same stratigraphical level, the coarse-grained beds are absent (Sauvé & Bergeron, 1965; Clark, 1977; Wares et al., 1988; Barrett et al., 1988). This facies change points to an eastern source for the clastics of the U.M. of the Baby Formation (T. Clark, pers. com., 1989).

The upper portions of the Baby and Menihek Formations show evidence of easterly and westerly sources respectively. If a foredeep model is accepted, the eastern source would represent an influx from the tectonically thickened and uplifted hinterland and the westerly source the start of the emergence of a flexural arch in the Superior craton.

The Baby Formation is capped by an extensive and uniform sequence of pillowed to massive basalts called the Hellancourt Formation (Sauvé & Bergeron, 1965). These basalts are low K tholeiites with geochemical characteristics transitional between P-type MORB and continental tholeiites

(Boone, 1987; Boone & Hynes, in press). The basalts are cogenetic extrusive equivalents of the underlying gabbro sills (Sauvé & Bergeron, 1965; Wares et al., 1988). This formation's thickness has been estimated at approximately 1370 m (Sauvé & Bergeron, 1965, between 200 & 1200 m (Boone, 1987) and 1000 m (Wares et al., 1988).

In the easternmost central zone of the Northern Labrador Trough the Hellancourt volcanics are overlain by a sequence of massive to interstratified argillites and quartzites, the Thévenet Formation. The minimum thickness of this unit is 610 m (Sauvé & Bergeron 1965). Correlation of this unit is problematic. Goulet (1987) interpreted a thrust contact with the underlying Hellancourt volcanics. Clark (1988), using the presence of this thrust fault, tentatively correlated the Thévenet Formation with the lower member of the Baby Formation.

This interpretation is however based on outcrops from the structurally attenuated short limb of a large fold. The observed shearing could possibly result from the local fold architecture and not from an early thrust fault as postulated by Goulet (1987). Based on the work of this study, we propose that the contact is conformable as originally stated by Sauvé & Bergeron (1965) and that the Thévenet Formation represents the westernmost toe of an easterly derived sedimentary apron, draped over the Hellancourt basalts. The eastern source would include uplifted sedimentary and volcanic strata of the Kaniapiskau Supergroup along with a crystalline source of uncertain nature.

2.2) Stratigraphic succession in study area

The study area is located within the westernmost metamorphic hinterland of the Northern Labrador Trough. The hinterland at this latitude is characterized by four NW trending en échelon Archean gneissic bodies

surrounded by a succession of amphibolite-grade metasediments and metavolcanics (map I). From south to north the gneissic exposures are the Scattered, the Moyer, the Renia and the Boulder. The Scattered and Renia exposures are SW plunging gneiss-cored synforms whereas the Moyer and Boulder exposures are doubly plunging gneiss-cored antiforms. This study focuses more specifically on the SW plunging northern closure of the Renia Synform.

The cover sequence adjacent to the Renia Synform comprises folded and imbricated metasediments and metavolcanic rocks. The first unit adjacent to the Renia gneisses is a succession of lithologically diverse calcareous rocks interbedded with pelitic schists. This assemblage grades stratigraphically upwards into semi-pelitic schist, with coarser-grained interlayers, capped by an iron rich sediment horizon. Mafic volcanics cap the siliciclastic sequence. The volcanics are themselves overlain by a coarse-grained assemblage comprising mostly siltstones and sandstones with several conglomeratic interlayers.

2.2.1) Renia gneisses

The Renia Gneiss exposure was originally thought to be intrusive into the cover rocks (De Romer, 1956). However, the presence of migmatitic segregations and pegmatite lenses, absent in the stratigraphically overlying kyanite bearing, amphibolite grade, cover rocks, indicates that the gneisses underwent a higher degree of metamorphism, more like that of the Archean Superior basement to the west (Sauvé, 1957; Gélinas, 1958a, 1958b, 1965).

Recently, Machado et al. (1987) have dated the adjacent northern Boulder Dome and southern Moyer Dome and found ages of 2868 ± 5 Ma and 2878 ± 5 Ma respectively. These were interpreted as metamorphic ages, but in any event are clearly indicative of an Archean origin for at least these gneisses. In

what follows, the Renia gneisses are assumed to represent Archean basement.

Since this study deals primarily with the structural features of the cover rocks and their relationship to the gneisses in the core of the Renia Synform, only a thin (1 km wide) band in the gneisses was inspected by the author. For a more detailed description of the lithological attributes of the Renia Synform, the Moyer Dome and the Boulder Dome, the work of Gélinas (1965) is recommended.

The western and northern end of the Renia Synform is composed of massive to banded, pink to grey gneisses of granitic to tonalitic composition (Plate Ia). Mineralogically the two compositional end members are characterized by a plagioclase-hornblende assemblage for the tonalitic gneisses and a microcline-biotite-muscovite one for the granitic gneisses. Mapping at the present scale has not allowed the delineation of separate gneissic units.

The principal mineral components of the gneisses are, in decreasing order of importance: quartz, microcline, plagioclase (oligoclase-andesine), biotite, muscovite, hornblende and epidote. Secondary minerals are calcite, sphene, chlorite, opaques and in two instances garnet.

The gneisses are usually well foliated and locally layered. The foliation is commonly characterized by 1-2 mm thick biotite-muscovite layers separating thicker, 2-8 mm thick layers consisting of granoblastic quartz with flattened crystals or aggregates of feldspar (usually microcline). In some localities good augen gneiss textures were observed. The gneissic layering is characterized by centimeter scale (0.5 to 50 cm) mafic and felsic layers. The felsic layers consist almost exclusively of quartz and feldspar, whereas the mafic layers contain these minerals as well as biotite, muscovite and locally hornblende. For the gneissic layering, the alignment of the micas is not as

pronounced as in the case of the foliation layers. The two planar fabrics, foliation and gneissic layering, are essentially parallel. Locally a strong axial planar schistosity cuts the two planar fabrics close to the fold closures.

Amphibolite layers, 0.1 to 2 m wide, commonly forming boudinaged or dismembered horizons, are found intercalated with the granitoid gneisses. The mafic minerals consist of varying proportions of hornblende and biotite. These mafic layers probably represent late stage mafic dykes, possibly contemporaneous with the ones present in the Superior craton to the west (Stevenson, 1968), dated at 2.5 Ga (Fahrig & Wanless, 1963).

Locally the quartzo-feldspathic layers coalesce to form pegmatite lenses. These are usually of centimetric scale, but locally can attain up to 3 m wide by 10 m long. They are composed chiefly of quartz and microcline.

The contact with the adjacent supracrustal rocks outcrops poorly even in areas of near continuous exposure; a narrow overburden covered trough often separates the two. The contact was observed only in two localities. Both sites contain a 1 m wide zone in which the gneisses become fine grained with a pronounced planar fabric defined by a very small amount of biotite and muscovite (Plate Ib). These textures are compatible with a zone of strain-induced grain size reduction formed in response to a décollement surface between the gneissic rocks and an overlying cover sequence. The postulated cover rocks also show good evidence of shearing, including asymmetrical and dismembered folds.

The southern flank of the Boulder Dome was briefly studied. It seems to be slightly different from the Renia synform, having a more pinkish color due to the preponderance of microcline, and displaying numerous well defined aplitic dykes. Gélinais (1958a) noted several map-scale bodies of augen gneiss

on the southern flank of the dome. The basement-cover contact was not observed. Near the contact with the overlying cover rocks the gneisses show evidence of brittle deformation with displaced aplitic dykes (Plate Ic) and a local 3 m wide tectonic breccia (Plate Id). This contrasts sharply with the meter wide zone of strain-induced grain size reduction, characteristic of a more plastic regime, at the assumed basement-cover interface on the Renia synform.

2.2.2) Cover sequence

Reliable facing criteria such as pillows and graded bedding are mostly confined to the lower grade portion of the study area, under the staurolite isograd, or in the coarse-grained sediments overlying the basalt horizon (Map III). No polarity determinations were made in the sediments between the basalt horizon and the Renia Gneiss. However the presence of a large N trending syncline west of Lac Raymond that folds most of the cover sequence onto itself would indicate that the sediments adjacent to the gneisses face outwards. This assumes that the sediments are contiguous around the fold closure, which they seem to be (Map III).

Given the synformal geometry of the Renia Gneiss (Map I, II, III) the cover sequence actually underlies the gneisses. In the following description of the stratigraphy terms such as overlying, underlying, higher and lower always refer to stratigraphic positions not geometrical ones.

The supracrustal rocks directly adjacent to the Renia gneisses are very variable in character. Transitional contacts were also observed in numerous localities. Map (II) shows some of the main lithological units but the scale of mapping did not permit the exact delineation of each lithological unit. Several different lithologies were found at or near the contact with the

adjacent gneissic rocks, including marbles, calc-silicates, pelites, semipelites and in one instance chert and an iron formation (rusty garnet - hornblende rocks). The most persistent and continuous units to drape the gneisses are marbles and to a lesser extent calc-silicate rocks.

i) Calcareous rocks

- Dolomitic marble

The marbles weather recessively to a pale grey or light orange-brown color, they vary from massive to layered on a centimetric scale. The bedding in this case is defined by tremolite rich layers or small semipelitic interlayers. The thin layers of tremolite are often characterized by strings of clustered crystals (Plate 1e). In sections parallel to bedding and the main schistosity the crystals are typically acicular and radial, with individual needles as much as 8 cm long.

The main mineral constituents are colorless tremolite, dolomite and phlogopite along with variable amounts of rounded to granoblastic quartz grains and in one locality plagioclase. In thin section tremolite varies from long acicular needles to prismatic crystal aggregates containing numerous inclusions of carbonate and quartz. The phlogopite is pleochroic, varying from clear to pale brown. De Romer (1956), using staining methods for distinguishing calcite from dolomite, subdivided the marbles into Fe-Mg rich limestones and dolomitic marbles, both being found at the same stratigraphic level. He noted many outcrops contained both calcite and dolomite. Marble layers also occur stratigraphically higher where they are interlayered with and grade transitionally into the marl units.

The dolomites are interlayered with many other units, rendering a thickness determination problematical; maximum thicknesses vary from 10 to 20

m, but actual thickness is often less than these values. Although lateral variations are also very common, the dolomites still form the most continuous unit over the basement. In many instances the marbles grade up into calc-silicate rocks.

- Calc-silicate rocks, calcareous schists and heterogeneous amphibolites

The **calc-silicate rocks** resemble the underlying marbles but are much richer in quartz and have pale green actinolite as the silicate phase instead of tremolite. The actinolite crystals have generally the same habit as the tremolite crystals in the marbles. Quartz, plagioclase, biotite and muscovite are much more common than in the marbles. This unit grades laterally and upwards into calcareous schists, micaceous schists or mafic marls. The thickness of this unit is difficult to estimate for the same reasons as the marbles. Single units vary between 1 m and 15 m thick.

The **calcareous schists** are generally characterized by regularly interlayered, 0.1 to 2 cm wide, calcite rich quartz layers (lime quartzites) with or without actinolite and semi-pelite layers (biotite-muscovite-quartz schist).

The **heterogeneous amphibolites** are characterized by the presence of centimeter to meter scale interlayers of dolomitic marble, calcareous schist, calcareous siltstone or semi-pelite. The amphibolite portion is composed of hornblende, quartz, calcite and plagioclase, locally with biotite, chlorite, garnet and opaques. The hornblende occurs typically as acicular or "feathery" crystals up to 4 cm long enclosing quartz and calcite aggregates between the individual crystal needles. Retrogressive chloritic alteration often occurs at the expense of hornblende and garnet. The persistent and often intricate interlayers and gradational contacts with sedimentary rocks indicate that the

heterogeneous amphibolites are of sedimentary origin. They probably were originally calcareous shale layers that were deposited in a mixed carbonate-siliciclastic environment.

Some of the amphibolites contain up to 25% garnet. They are typically more massive than the garnet-free amphibolites. Their main constituents are hornblende, garnet, quartz, plagioclase and to a lesser extent chlorite, biotite, calcite and opaques. Hornblende in the garnet rich amphibolites has a much more prismatic habit. On some outcrops garnets are concentrated in distinct layers <1 m thick, parallel to the adjoining bedding. Thus, although these garnet rich amphibolites lack distinct sedimentary interlayering they are still ascribed the same sedimentary origin as the other amphibolites described above. The observation that none of the demonstrably igneous amphibolites further west have garnet, even though the garnet isograd has been attained, supports this interpretation. The garnet rich amphibolites are also relatively poor in plagioclase compared with the igneous amphibolites further west. On many outcrops the sedimentary derived amphibolites have very rubbly surfaces contrasting sharply with the smooth rounded surfaces of the igneous amphibolites.

The thickness of all four members of this unit is difficult to estimate; single beds vary from 1 m to 10's of meters. A sequence of predominantly mixed calcareous members may attain 300 meters.

Within the study area the overall thickness of the mixed marble - calc-silicate - mafic marl sequence varies from a maximum of 250 m west of Renia Lake to less than 10 m on the northern flank of Renia Synform southeast of Fox Lake. This change in thickness does not seem to correspond to any observed faults or folds, precluding any structural repetition or thickening by thrusting or other means. The thickness variations are considered mostly

primary and may reflect local depositional controls on the ambient sedimentation.

ii) Lower iron formation

Only two occurrences of iron formation were noted near the contact with the gneisses of the Renia Synform. Both are meter scale elongated pods of rusty hornblende-garnet-quartz-rocks surrounded by semi-pelitic schist and underlain by marbles or calc-silicate rocks. Adjacent to the northern closure of the Boulder Dome, Sauv  (1956, 1957) mentions the presence of a layered iron formation a few tens of feet thick at the same stratigraphic level as the ones found near the Renia Gneiss. The iron formation is composed of ferruginous magnetic shales, grunerite schist and hornblende-garnet-quartz rocks locally interlayered with thin quartzite layers, possibly recrystallized chert (Sauv , 1957).

iii) Lower micaceous schists

Micaceous schists form the most extensive unit present in the study area. They occur from the garnet zone along the western shore of Rachel Lake to the staurolite-kyanite zone near the contact with the Renia Gneiss. This unit is quite variable in composition, ranging from semipelitic biotite - muscovite schist to pelitic kyanite-staurolite-garnet-biotite-muscovite schist. Coarser psammitic horizons were also observed. The micaceous schists grade into and are interlayered with the various calcareous units.

In view of the varying metamorphic grade and facies changes the micaceous schists are described in two sections.

A) The West zone

The West zone comprises the lowest-grade garnet zone between Lac Rachel

and the westernmost exposure of iron formation and/or mafic volcanics. The rocks are strikingly uniform, composed of generally dark, well-layered semi-pelitic schist. The beds are well graded on a few outcrops and resemble distal turbidite beds with only the lower portion of the Bouma sequence present (Plate If). All tops are easterly facing into the iron formation and mafic volcanics. The main mineral assemblage is, in decreasing order of importance: quartz-muscovite-garnet-chlorite-tourmaline.

B) The East zone

The East zone is located between the mafic volcanics, east of Rachel Lake, and the Renia gneiss synform. The following features distinguish the east zone rocks from those further west:

- 1) The rocks are generally much more pelitic, with kyanite - staurolite - garnet - biotite - muscovite assemblages. The pelitic horizons generally decrease in abundance away from the contact with the Renia Gneiss;
- 2) They are interlayered with and grade into the underlying calcareous rocks;
- 3) Primary sedimentological features are difficult to discern due to more intense deformation and higher metamorphic grade;
- 4) There are more numerous lenticular gabbro sills intruded into the east zone sequence; they are almost totally absent from the west zone;
- 5) At the top of the east zone sequence, near the iron formation and mafic volcanics, coarser psammitic layers are common. These sandstone beds vary from 0.1 to 1 m in thickness.

The thickness of the micaceous schist unit is variable. The thinnest section, approximately 30 m, between the Boulder Gneiss and the Renia Gneiss may have been affected by tectonic flattening. The greatest thickness,

approximately 500 m, was observed between the Renia Gneiss and the most southerly exposure of mafic volcanics. The gabbro sills have been excluded from the measured thicknesses.

iv) Upper iron formation

A second unit of iron-rich rocks is found mostly at or adjacent to the contact between the micaceous schists and the overlying mafic volcanics. This unit consists mostly of silicate iron facies and magnetic sulphide bearing ferruginous shales (Plate IIa). The most common lithology is a rusty garnet-hornblende rock with interlayers, often boudinaged, of white chert (Plate IIb). West of Lac Raymond the iron formation is host to several lenticular intrusions of blotchy gabbro.

v) Upper micaceous schists

Upper micaceous schists cap the upper iron formation and underlie the mafic volcanics. They outcrop poorly in this region and are even totally absent in some places where the iron formation is directly overlain by basalts. The unit is made up essentially of biotite-muscovite schists that are locally garnetiferous. The stratigraphic position of the unit is well constrained by the overlying and underlying lithologies.

vi) Mafic volcanics

Mafic volcanics outcrop in two structurally repeated bands west and north of Lac Rachel. They are composed of sheared, massive to pillowed, basaltic flows up to 10 m thick. They are generally aphanitic but at the base of the structurally highest volcanic band a basalt layer has up to 10% equant plagioclase phenocrysts. In low-strain areas good pillow forms were observed,

(Plate IIc) locally containing pillow shelves, providing reliable facing determinations.

vii) Volcanic-rich conglomerate

Three main bands of volcanic-rich conglomerates are found NW and N of the Renia Gneiss. The first directly overlies the mafic volcanics. The other two occur close together stratigraphically higher in the siltstone - sandstone - conglomerate sequence that overlies the volcanics in this area.

The lowest band overlies the mafic volcanics and is apparently restricted to this area. It has not been described in other areas of the northern Labrador Trough. It forms a roughly 25 m thick blanket on top of the structurally highest basaltic band.

The base of the conglomerate is characterized by angular to rounded basalt and gabbro fragments, varying in diameter from 0.2 to 14 cm, with a mode from 2 to 5 cm, set in a carbonate-chlorite matrix that weathers recessively (Plate IIId). Siltstone and quartz fragments occur rarely at the base, but become gradually more numerous near the top of the unit. The matrix also becomes much richer in quartz (Plate IIe). The volcanic-rich conglomerate eventually grades up into a sediment-dominated conglomerate or locally into sandstone and/or siltstone beds.

The two upper bands are clearly separated. They are interlayered with sedimentary conglomerates and siltstone-sandstone horizons, with individual beds varying from 1 to 10 m. Contacts vary from sharp to gradational with the enclosing sedimentary units. The fragments are mixed, including basalts, siltstones, sandstones, calcareous schist and quartz grains (Plate IIIf). The matrix is composed of hornblende, biotite, chlorite, epidote, calcite and quartz. The fragments are commonly strongly flattened (up to 10:1) and near

the fold closure they are stretched downdip subparallel to the fold axis of the syncline.

The origins of the volcanic conglomerates are discussed along with the sedimentary sequences they underlie and are interbedded with.

viii) Siltstones, sandstones and conglomerates (siliciclastic assemblage)

The siliciclastic assemblage unit occupies the heart of a large syncline north of Lac Raymond. It conformably overlies and contains interlayers of the volcanic conglomerates. It is characterized by a siltstone-sandstone succession interlayered with conglomerate beds. The thicknesses of individual beds vary from 1 cm to 1 m, the average being 10 cm. Numerous sedimentary textures such as trough and planar cross bedding (Plate IIIa), coarse graded bedding, scoured beds (Plate IIIb) and convolute bedding were noted. The siltstones and sandstones are composed predominantly of quartz with varying amounts of biotite and muscovite. Microcline rich arkose horizons were noted in some localities, but quartz is by far the predominant mineral in this unit.

The finer grained siltstone layers commonly contain calcareous nodules and locally thin (< 2 cm) beds, that are often boudinaged. These calcareous nodules are commonly rimmed by hornblende crystals (Plate IIIc) which are resistant to weathering compared with the siltstone and even more so compared with the calcite interiors, thus forming distinctive, flattened doughnut shaped structures on the outcrop surface (Plate VIId).

The conglomerates consist of fragments of siltstone, sandstone, quartz and locally plagioclase and basalt (Plate IIId). The matrix is made up of quartz and biotite. The fragments are commonly flattened (3:1 to 10:1; Plate IIIe). The quartz fragments tend to be rounder. As stated for the previous unit, the sedimentary sequence has gradational contacts with the volcanic

conglomerate layers.

Within the sediments several small discontinuous exposures of basalt were found. They appear identical to those underlying the unit. The presence of basalts within the sediments indicates that volcanic activity occurred sporadically after the main eruptive episode. There are also isolated gabbro, glomeroporphyritic gabbro and ultramafic intrusives within the siliciclastic sequence.

The unit as a whole appears to cut down stratigraphically to the southeast into the mafic volcanics, the underlying iron formation and micaceous schists. In the tight synclinal keel between the Boulder Dome and the Renia Synform this unit directly overlies the lower member of the Baby Formation, from which it is virtually indistinguishable. To the north of our study area, on the northern flank of the Boulder Dome, Sauvé (1956, 1957) shows a large zone of micaceous schist with several kilometers of structural thickness overlying the metamorphosed equivalent of the Hellancourt volcanics. These rocks could be correlatives of those described above.

ix) Intrusives

- Gabbros:

Gabbro sills are concentrated within the lower member of the Baby Formation where they form elongate discontinuous hills. They are composed essentially of hornblende and plagioclase, often completely saussuritized. They are found locally within the Harveng and Thévenet Formations.

- Glomeroporphyritic gabbros:

Glomeroporphyritic gabbros form laterally discontinuous, pod like sills which are found within or immediately underneath the iron formation of the

middle member Baby Formation. They have the same mineralogy as "normal" gabbro sills but have sub-idiomorphic plagioclase crystals which can attain 10 cm in diameter (Plate IIIIf). The sharp boundaries of the crystals is a metamorphic effect; the same intrusions within the lower greenschist grade central igneous zone have diffuse boundaries to the plagioclase porphyries, hence the term "blotchy gabbros" (Sauvé & Bergeron, 1965). Locally these sills contain lenses of normal gabbro.

- Ultramafics:

Ultramafic rocks form very elongate, generally thin, lenses within the gabbroic intrusives at the base of the mafic volcanic unit. Gradual transitions to the gabbroic portion of the intrusives were locally noted. The ultramafics probably represent cumulate horizons within differentiated sills. Similar relationships were observed in the allochthonous central zone (Sauvé & Bergeron, 1965). They weather to a pale green or brown color, typically with a pitted weathered surface (Plate IVa). Locally these sills grade up into pyroxenite and normal gabbro horizons, forming small layered intrusives. Their main constituents are tremolite, serpentine, chlorite, carbonates (ankerite) iron oxides, and there are local fresh pyroxenes. In places, chrysotile fibers fill fractures cutting the intrusives.

2.3) Correlations

An attempt has been made to correlate the informal units of the study area to the units found in the better studied central and western zones of the northern trough. The results are summarized in figure 8. The following section expands on some of the aspects of these correlations.

- 1) Two U/Pb zircon ages of 2868 and 2878 ± 5 Ma for the Boulder and Moyer

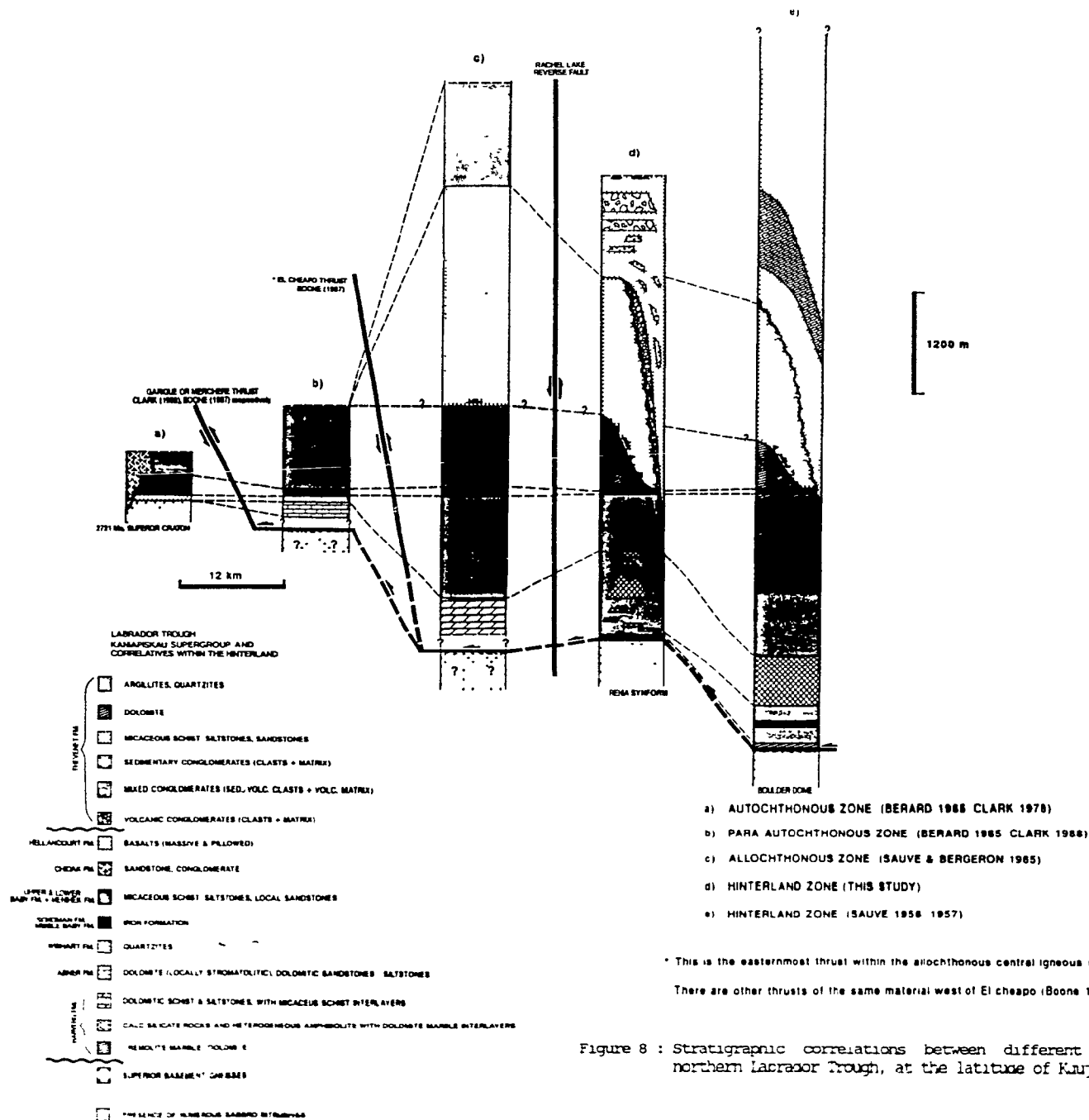


Figure 8 : Stratigraphic correlations between different segments of the northern Labrador Trough, at the latitude of Kuujuaq.

domes (Machado *et al.*, 1987) clearly show their Archean ages, and suggest an affinity to the Superior craton to the west.

2) The overlying calcareous rocks, although lithologically more complex, show interfingering and interlayering with semipelite similar to that of the basinal dolomitic assemblage of the Harveng Formation within the central allochthonous zone further west (Sauvé & Bergeron, 1965; Bélanger, 1982). The calcareous rocks show a gradual transition upwards to the semipelitic schist, which is also characteristic of the Harveng Formation and to a lesser degree its western platformal correlative, the Abner/Denault dolomite (Clark, 1988). The observed composite thickness of the calcareous assemblage west of Lac Renia exceeds the 200 m of Sauvé & Bergeron (1965), but since the base of the Harveng Formation was not observed in the type area this value represents only a minimum thickness.

3) The lower iron formation, adjacent to the basement gneisses, is neither thick nor extensive. Its stratigraphic position is well constrained by the presence of underlying dolomitic marbles and overlying calc-silicate rocks, both of which are probably correlative to the Harveng Formation further west. The most probable time correlative is the shale-siltstone assemblage that underlies the Abner/Denault Formation in the west or is interlayered with its eastern distal equivalent, the Harveng Formation. This fine-grained assemblage is part of the upper portion of the Attikamagen Subgroup. There are no iron rich rocks reported at this stratigraphic level, except for the red and green shales of the Le Fer Formation. Earlier in the basin phase of the first cycle of sedimentation there are pyrite shales at the base of the Swampy Bay Subgroup (Dimroth, 1978).

The iron formations of the second cycle of sedimentation (Sokoman and Baby Formations) are thought to be the result of magmatic related hydrothermal

activity in the central igneous-sedimentary allochthonous zone (Simonson, 1985; Clark, 1988; Barrett et al., 1988). A similar origin for the lower iron formation in the study area would imply that it is the product of hydrothermal activity related to the Bacchus Formation basaltic volcanism and/or their cogenetic gabbroic intrusions of the Attikamagen Subgroup. It would represent a rare example of iron formation associated with the first cycle of sedimentation.

4) The lower micaceous schist unit is composed chiefly of semipelite. Pelitic horizons are common at the base of the succession, but occur only sporadically in the upper portion. Coarse-grained siltstone and sandstone horizons are common in the upper portion of this unit. In the less metamorphosed western portion of this study area thin distal turbiditic beds were distinguished. The micaceous schists have strong lithological similarities to the lower member (L.M.) of the Baby Formation in the central allochthonous zone (Sauvé & Bergeron, 1965). The lower member (L.M.) of the Baby Formation is thought to correlate with the basal quartzites of the Wishart Formation and the ferruginous shales of the Ruth Fm. in the western autochthonous zone (Clark, 1988).

5) The upper iron formation consists of silicate-facies iron rich sediments interlayered with white chert beds and ferruginous shales. This strongly resembles the iron rich sediments of the middle member (M.M.) of the Baby Formation to the west (Sauvé & Bergeron, 1965). The iron rich rocks of the Baby Formation have been interpreted as distal correlatives of the platform (shelf type) Sokoman iron formation in the western autochthonous zone (Clark, 1988). However, the correlation of the two iron formations is not corroborated by model lead dates from the two iron formations (Clark & Thorpe, in press).

6) The upper micaceous schist forms a generally thin unit that varies markedly in thickness laterally. It is bounded by the underlying upper iron formation and the overlying mafic volcanics. They are mostly semipelitic in composition but do contain garnet-rich horizons. The bounding lithologies constrain this unit very well to represent the upper member of the Baby Formation.

7) The mafic volcanic unit strongly resembles the Hellancourt basalts in the central zone to the west (Sauvé & Bergeron, 1965; Boone, 1987; Wares et al., 1988). It contains roughly the same proportion of massive to pillowed flows as the Hellancourt Formation although the two flow types are harder to distinguish due to a higher degree of penetrative deformation. Underlying the mafic volcanic unit are laterally discontinuous differentiated sills and glomeroporphyritic gabbros. These types of intrusive also typically underlie the Hellancourt volcanics to the west (Sauvé & Bergeron, 1965).

8) The siltstone-sandstone-conglomerate unit overlying the mafic volcanics within this area has no widespread equivalent within the allochthonous central zone. The only described unit overlying the Hellancourt basalts is the Thévenet Formation southwest of Lac Thévenet (Sauvé & Bergeron, 1965; Clark, 1980), on the west side of the late stage Lac Rachel reverse fault (Sauvé, 1956; Moorhead & Hynes, 1986; Goulet, 1987). This formation occurs at the same general position as the unit described above. The Thévenet Formation is composed mostly of massive to interbedded argillites and quartzites with no coarse-grained fraction (Sauvé & Bergeron, 1965). The quartzites contain the same flattened calcareous concretions as those observed within the siltstones of the siliciclastic assemblage overlying the mafic volcanics (Sauvé & Bergeron, 1965 (plate VIa); Plate IIIc & VIId). The siliciclastic assemblage overlying the mafic volcanic unit in the study area

could represent a more proximal equivalent to the argillites and quartzites of the Thévenet Formation. The assemblage could possibly represent a mid- to upper-fan facies. In this model the Thévenet Formation would represent an outer fan facies in which turbiditic influxes of both siltstones and sandstones were deposited along with the finer-grained hemipelagic argillites.

To the north and east of our study area, on the NE flank of the Boulder Gneiss, Sauvé (1957) and Gélinas (1958) mapped a large zone of micaceous schist with several kilometers of structural thickness overlying the metamorphosed equivalents of the Hellancourt Formation. These rocks could represent an eastern equivalent to the siliciclastic unit of this study area. They lack the coarse-grained beds found in the study area (Sauvé, 1957).

In the western hinterland of the central Labrador Trough, metamorphosed sediments and subordinate metavolcanics and intrusives, termed the Laporte Group, are overthrust on the basalts of the central igneous-sedimentary zone (Baragar, 1967; Dimroth, 1970, 1972, 1978) and bounded to the east by the arc related calc-alkaline De Pas batholith (Bélanger & van der Leeden, 1987; van der Leeden *et al.*, in press). An arc related eastern provenance, distinct from the one for the Kaniapiskau Supergroup, has been postulated for the Laporte Group sediments (Bélanger & van der Leeden, 1987). The mafic volcanics and intrusives have been correlated with their counterparts from the second cycle of the Kaniapiskau Supergroup (Girard, 1989; van der Leeden *et al.*, in press). In the upper portion of the group, Girard (1989) mentions the presence of subareal gritty arkoses that could represent the final infilling of the basin from easterly derived sediments.

The Laporte Group is a plausible correlative to the Thévenet Formation present in the western hinterland of the northern Labrador Trough. The main difference between the northern and southern hinterland zones is that in the

northern hinterland a much greater proportion of recognizable units of the second cycle of sedimentation are found east of the hinterland/central zone boundary (Lac Rachel Fault or its southern extension).

A good analogue to the Thévenet Formation can also be found in another segment of the Circum-Superior belt (Baragar and Scoates, 1981); the Belcher islands fold belt located on the eastern side of Hudson Bay. The sedimentary succession in the Belcher Islands presents a near-identical stratigraphy to the second cycle of sedimentation in the Labrador Trough (Hoffman, 1987; Fig. 9). The following summary is taken from Dimroth et al. (1970) and Ricketts & Donaldson (1981).

Shallow marine quartz arenites (Mukpollo Formation) overlie karstic carbonate breccias (Rowatt Formation) and grade up into a fine-grained laminated iron formation (Kipalu Formation). Submarine basalts (Flaherty Formation) overlie the iron rich sediments. Paleocurrent and paleoflow determinations indicate that the site of extrusion for the basalts was to the west (Ricketts et al., 1982). The extrusion of the basalts marked a reversal in the dip of the paleoslope from W dipping to E dipping. The volcanics are disconformably overlain by shales and volcanic sandstones that grade up into a thick sequence of turbiditic greywackes (Omarolluk Formation), forming a flysch-like sequence. These sediments are rich in lithic and felspathic fragments. Volcanogenic fragments are common at the base of the Omarolluk Formation. They grade up into fluvial and marginal marine arkoses with interlayers of mudstones and conglomerates (Loaf Formation). This formation has been interpreted to represent a distal molasse sequence. Based on paleocurrent data and thickness variations the provenance for the sediments overlying the volcanics was to the NW, not the Superior craton to the east. There is a gradual upward decrease in volcanic fragments and plagioclase

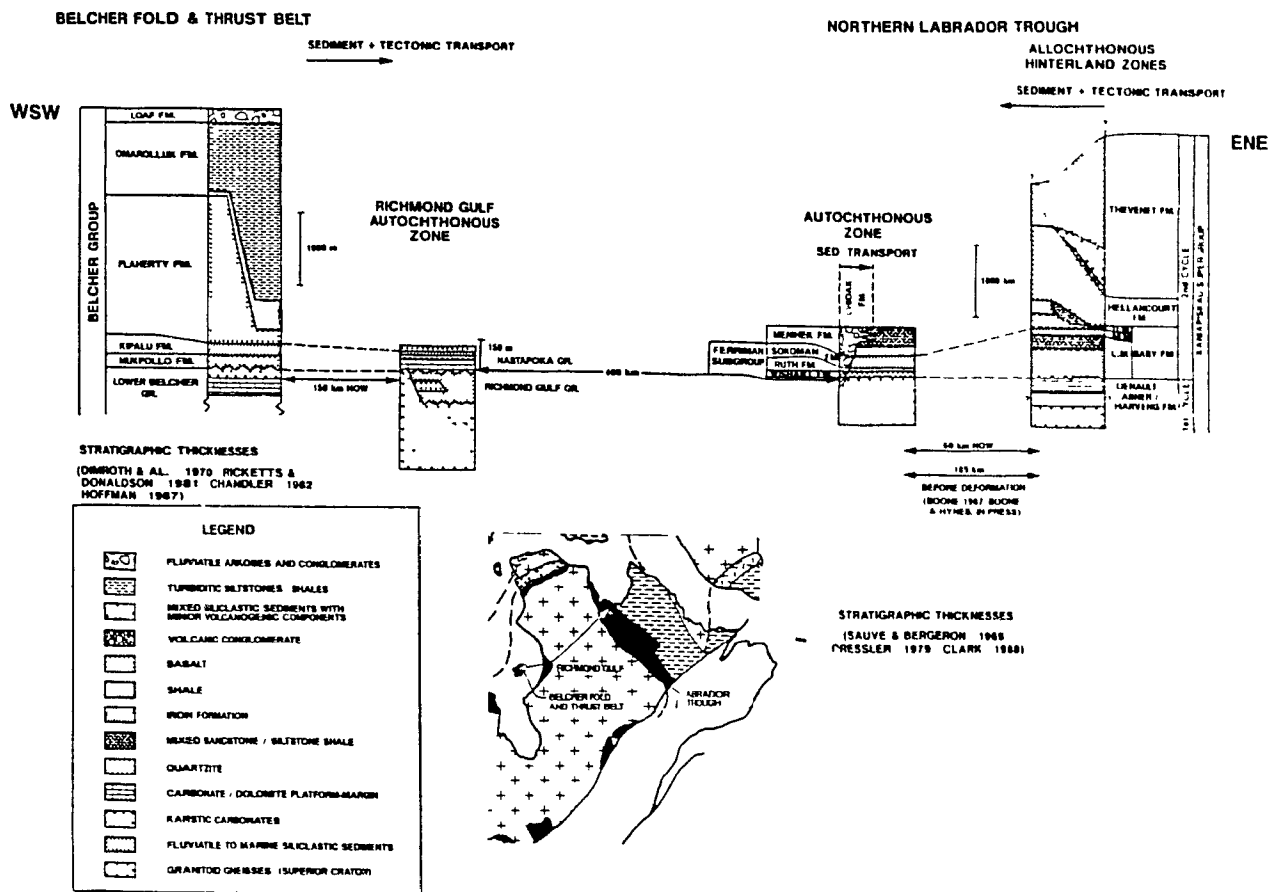


Figure 9 : Schematic stratigraphy and "correlations" between the Belcher Group and the Kaniapiskau Supergroup. (Belcher Group from Dimroth et al.(1970), Ricketts & Donaldson (1981), Hoffman (1987)- Kaniapiskau Supergroup from Dimroth (1978), Le Gallais & Lavoie (1982), Clark (1988).

content in the Omarolluk Formation towards the Loaf Formation and a concomitant increase in the amount of microcline. The NW source for the Omarolluk Formation includes the uplifted (upthrust?) underlying volcanics plus a cratonic source that gradually becomes the sole source for the sediments in the upper portion of the Omarolluk Formation and the Loaf Formation. Ricketts et al. (1982) interpreted the Nastapoka Group as an ensialic marginal basin on the E edge of the Superior craton, the mafic volcanics being either the product of rifting or representing the early stages of a nascent arc complex.

The main difference from the second cycle of the Kaniapiskau Supergroup is the absence of craton derived molasse-like fluviatile sediments overlying either the autochthonous equivalents of the Belcher Islands succession, the Nastapoka Group on the mainland to the east, or the underlying Richmond Gulf Group (Fig.9). This difference could indicate that either flexuring of the Superior craton during the eastwards imbrication and translation of the Belcher fold and thrust belt was absent or poorly developed or simply that the erosion level is deeper in the Richmond Gulf autochthonous zone than in the autochthonous zone of the northern Labrador Trough. This resulted in the molasse-like sediments being preserved in the western Labrador Trough and eroded in the Richmond Gulf autochthonous zone.

2.4) Summary

All the units found in this area have equivalents in the western, better studied, zone of the Labrador Trough. Figure 8 shows a composite stratigraphic column of this area compared with one from the adjacent zone to the west.

A few features of the study area deserve to be emphasized :

- The Harveng Formation equivalent in this area is lithologically complex and its thickness varies widely laterally. The thickness shown in the section is a representative one draping the gneiss domes.

- The lower iron formation is unique to this area.

- The lower member of the Baby Formation equivalent is essentially similar to the one to the west, including the presence of coarser beds near the top.

- The upper iron formation (M.M. Baby Formation equivalent) is essentially identical to its counterpart in the central allochthonous zone, although it occurs much closer to the overlying mafic volcanics.

- The upper member of the Baby Formation-equivalent is much thinner than its westerly equivalent and may even be absent from the easternmost correlatives.

- The Hellancourt Formation equivalent is thinner and more deformed than, but otherwise indistinguishable from, its counterpart further west.

- The Thévenet Formation equivalent in the study area appears to rest disconformably on the metamorphosed equivalents of the Hellancourt Formation. It forms a thick sequence of siltstones, sandstones and conglomerates. Many of its features are compatible with episodic influxes of coarse and fine sediments into the basin.

Two features of the sedimentary succession capping the Hellancourt basalts and eastern equivalents can be reconciled with an eastern provenance.

i) If the sedimentary sequence capping the Hellancourt basalts on either side of the Lac Rachel fault can be correlated, the general coarseness and thickness of the sequence decreases westward, pointing to an easterly source for the sediments (Fig. 8). A several kilometers thick (at least structurally), succession of biotite-muscovite schist blanketing the basalts

was noted to the north (Sauvé, 1956, 1957) that could also correlate with the Thévenet Formation.

ii) For most of the central zone of the trough the roof of the Hellancourt Formation is marked by a thrust fault. The Thévenet Formation could have originally extended west of its present position and have subsequently been removed by movement along the thrust surface. However the complete lack of any remnant of sediments overlying the basalts found in the central and western portions of the central zone is more easily, but not exclusively, reconciled with its never have been there initially. This would indicate that sediments overlying the basalts never extended much farther west than their present position. The sediments capping the Hellancourt basalts could possibly have been brought in from the west via some by-pass mechanism (i.e. a submarine canyon), but the local eastward increase in grain size across the Lac Rachel fault does not corroborate this.

The source rocks of the Thévenet Formation would comprise uplifted siliciclastic sediments and mafic volcanics, probably distal eastern correlatives of the Kaniapiskau Supergroup, in addition to crystalline rocks. There are arc-related granitoid intrusives to the east (Poirier, 1989; Poirier et al., in press) that are dated at 1829-1845 Ma (Machado et al. 1988). If these intrusives were the source for the Thévenet sediments, the Hellancourt-Thévenet Formation contact would mark a 35 Ma hiatus, given that the basalts are of the same age as a 1.88 Ga differentiated gabbro sill intruding the underlying sediments of the Menihek/Baby Formation (R. Parrish pers. comm. 1987, cited in Hoffman, 1988). In this setting the Thévenet Formation would represent a fore-arc deposit. Although there is evidence in the study area for truncation of the underlying succession by the Thévenet Formation, a 35 Ma hiatus at the Hellancourt-Thévenet contact is not consistent with the presence

of thin basalt horizons and gabbro intrusives, (correlative to the Hellancourt Formation ?) in the Thévenet Formation east of the Lac Rachel Reverse Fault (Sauvé, 1957; Gélinas, 1958a, 1958b; Sauvé & Bergeron, 1965). In addition, stratigraphic evidence points more to a continuum of sedimentation between the Baby Formation and Thévenet Formation. Volcanic activity is interpreted to have been swamped by the influx of easterly derived sediments in the more proximal eastern zone, but was unimpeded in the more distal area that now corresponds to the allochthonous central zone.

An equally likely crystalline source for the Thévenet siliciclastics is Archean rocks to the east. There is some geochronological evidence for the presence of Archean rocks east of the four basement exposures of the westernmost hinterland; 2850 Ma (Machado et al., 1987), 2783 Ma (Machado et al., 1988) for the Lac Olmstead and Turcotte granitoid gneisses respectively (map I). These Archean gneisses and other possible eastern occurrences may have shed sediments westwards prior to their intrusion by the Hudsonian (1845-1829 Ma, Machado et al., 1988) calc-alkaline I type volcanic arc granitoids (Poirier et al., in press). These Archean rocks could belong either to the Rae province (Hoffman, 1988) east of an interpreted paleo-suture (Bélanger et al. 1987; Perreault et al. 1988; Poirier, 1989; van der Leeden et al., in press; Poirier et al., in press) or could represent the uplifted easternmost margin of the distended Superior crust.

In the central hinterland zone of the southern Labrador Trough, east of the large calc-alkaline 1840 Ma De Pas Batholith there is also evidence for early Aphebian intrusives (2.32 Ga. S. Bowring pers. comm. cited in van der Leeden et al., in press) that could be possible source rocks for the sediments of the western southern hinterland zone.

2.5) Discussion

As mentioned previously the coarseness of the lower micaceous schist unit (Lower Member of the Baby Formation equivalent) increases upwards towards the upper iron formation and the basalts. These coarse-grained rocks are virtually indistinguishable from the overlying Thévenet Formation. This points to a continuum in the style of sedimentation between the sediments underlying and those overlying the basalts. The sediments underlying the basalts immediately west of the southern extension of the Lac Rachel fault are also characterized by coarse-grained facies (Clark, 1978), similar to the ones noted in the study area. Bérard (1965) and Sauvé and Bergeron (1965) mention the presence of volcanogenic clasts, presumably easterly derived, in the sediments underlying the basalts in the western central zone and the eastern portion of the autochthonous - para-autochthonous zone. The combination of all the above mentioned features seems to indicate that the influence of an easterly source of sedimentation extended far to the west of the hinterland/central zone boundary and that a large portion if not most of the second cycle of sedimentation in the central and eastern zones of the northern Labrador Trough is easterly derived. It is important to note that Le Gallais and Lavoie (1982) observed the presence of basement and platform facies sedimentary clasts in conglomerate beds within the Menihek Formation (Baby Formation equivalent) which they interpreted as westerly derived channel lag deposits. From the limited data listed above the line of convergent provenance for the sediments underlying the Hellancourt basalts may lie approximately at the boundary between the central igneous-sedimentary zone and the western sedimentary zone. Thus the basin seems to have been infilled by contemporaneous westerly and easterly derived clasts.

Two contrasting tectonic settings can be envisaged to account for an

easterly source of the sediments in the eastern portion of the northern Labrador Trough.

1) Marginal basins:

i) During the extension of the Archean Superior sialic crust, early in the Hudsonian Orogeny, sediments were shed westwards from eastern highs such as a marginal plateau, a continent ribbon, or an outer rise. The first two types of high are formed by the isolation of a relatively unstretched crustal block bounded by more attenuated (normal faulted) zones. The third type of high, the outer rise, is the result of isostatic uplift of the lower plate of a crustal scale detachment fault (Lister *et al.*, 1986). The required thinner sialic crust of this type of basin could have given the transitional characteristic of the Hellancourt basalts that were extruded on top of it (Boone, 1987; Boone & Hynes, in press).

ii) Another possibility is that the second cycle of sedimentation in the northern Labrador Trough was deposited in a nascent back-arc basin that developed behind a continental magmatic arc. However the calc-alkaline magmatic arc found in the central portion of the northern hinterland zone (Poirier, 1989; Poirier *et al.*, in press) and the southern hinterland zone (van der Leeden *et al.*, in press) is younger (1845-1829 Ma, Machado *et al.* (1988); Perreault *et al.* (1988)) than the products of the trough's second cycle of sedimentation (1888 Ma, Chevé and Machado (1988); R. Parrish pers. com. in Hoffman (1988)). These intrusives could possibly mask earlier intrusions that would be of the right age for the back-arc hypothesis. There are older intrusives (2.32 Ga, S. Bowring pers. com. in van der Leeden *et al.*, in press) spatially associated with the southern magmatic arc, but these are too old to be related to units of the Labrador Trough further west. They do however indicate that the magmatic arc in the hinterland zone, at least its

southern portion, may have had a long protracted history of intrusion.

The current status of the limited geochronological work in the hinterland zone of the Labrador Trough does not support a back-arc origin for any portion of the Labrador Trough (*sensu stricto*) succession further west. However the sparse data base cannot rule out entirely either the possible existence of older intrusives, slightly older than 1880 Ma which is the age of the Sokoman iron Formation (Chevé & Machado, 1988) and the Hellancourt basalts (R. Parrish pers. comm. (1987) cited in Hoffman (1988)), and thus the back-arc hypothesis.

2) Foredeep basin:

Hoffman (1987) has proposed that many of the early Aphebian basins bordering the Superior craton contain initial passive margin successions followed by foredeep deposits. In the Labrador Trough he suggested that the entire second cycle succession was deposited in a foredeep basin. This basin was initiated in response to flexural loading of the stretched Superior crust by a westerly advancing thrust thickened tectonic wedge. This wedge would incorporate products of the first cycle of sedimentation in addition to Archean Superior gneisses. This model explains quite well the eastern provenance for the eastern second cycle sediments but is less compelling in accounting for the voluminous MORB like basaltic magmatism (Boone, 1987; Wares *et al.*, 1988; Boone *et al.*, in press) as trench located volcanism.

In summary, the foredeep model (2) requires easterly directed subduction of the stretched Archean Superior crust and possibly laterally equivalent oceanic crust of which there are no remnants. In contrast the back-arc basin model (1ii) requires westerly directed subduction of an oceanic plate below the stretched margin of the Superior craton. The outer high model (1i) does

not require any particular subduction direction.

Geochronological dating of detrital zircons in the sediments underlying and overlying the Hellancourt Formation in the eastern half of the northern Labrador Trough may well bring much needed critical data with which to assess the validity of the three models listed above. From the nature of the clasts in the Thévenet and Baby Formation the zircons should include Archean ages (presence of microcline clasts) and 1880 Ma ages (presence of basalt and gabbro fragments). If the sediments contain no zircons slightly older than 1888 Ma, which is the age of the Sokoman and Hellancourt Formation then the back-arc model can be discounted. If they do not display any zircons related to the arc granitoids further east (1845-1829 Ma, Machado *et al.*, (1988); Perreault *et al.*, (1988)) then the foredeep model cannot be entirely discounted but would require the docking of another Archean terrane that shed sediments devoid of any signature of the Hudsonian subduction event taking place underneath it. The outer high model where a portion of the stretched Superior basement is uplifted and unroofed would seem more attractive in this case.

3.0) STRUCTURE

3.1) Introduction

Recent studies in the northern Labrador Trough (Moorhead & Hynes, 1986; Goulet, 1986, 1987; Perreault et al., 1987; Wares et al., 1988; Poirier, 1989; Poirier et al., in press) have distinguished 3 major folding/faulting events and late stage faults.

The first event (D_1) comprises NNW trending SW vergent thrusts, westerly vergent isoclinal folds (Goulet, 1986, 1987; Boone, 1987; Wares et al., 1988; Plate IVc & d) and a fault-associated NE directed stretching lineation (Hoffman, 1988). A cleavage or schistosity associated with D_1 usually lies parallel to the bedding surfaces. This deformation event is interpreted to be responsible for the imbrication and westward translation of the cover sequence onto the Superior Craton (Séguin, 1969; Harrison et al., 1970, Dimroth, 1970, 1972; Goulet 1986, 1987; Wares et al., 1988). In addition, in the western hinterland zone of the northern Labrador Trough, large scale westerly vergent basement-cored nappe structures are thought to have developed late in the D_1 event.

The second phase of deformation (D_2) produced E to NE trending upright, generally open cross-folds (Bosdachin, 1986; Goulet, 1987). A weak spaced cleavage is sometimes developed parallel to the axial planes of these folds.

The third phase of deformation (D_3) imparted the present structural grain of the trough. It forms large scale NNW trending, usually tight SW vergent folds with shallow to moderate SE plunges. A crenulation cleavage is usually associated with the folds.

Brittle deformation occurs in association with the late-stage N trending Lac Rachel reverse fault (Moorhead & Hynes, 1986) and minor transverse faults of limited extent and displacement.

Structures related to these deformation events are unevenly distributed within the trough. The western autochthonous - para-autochthonous zone is characterized by thrust faults & folds associated with the first event (D_1). The central allochthonous zone also contains D_1 thrusts but is characterized mostly by large-scale folds associated with the third event (D_3). Both these zones contain some examples of large-scale open F_2 cross-folds.

A late stage (post- D_3) reverse fault marks the boundary between the central zone and the eastern hinterland or "core zone" of the Labrador Trough. The hinterland zone is characterized by a much more pervasive and penetrative S_1 schistosity and a higher metamorphic grade. It contains several large (probably F_3) fold sets similar to the ones found in the central zone. There are also large-scale tight to isoclinal folds in the main schistosity (S_1) that have been refolded by the later (F_3) folds. Both fold sets involve basement and cover rocks. The relative age of the early folds is uncertain. In particular, it is unclear whether they are correlative to the F_2 folds present to the west. The resolution of this question is critically dependent on the interpretation of the structural evolution of the gneissic bodies that dominate the hinterland zone E of the Lac Rachel fault. These early basement-cored folds are referred to in this study as F_1' .

This study encompasses a portion of the westernmost hinterland zone that forms the hanging-wall of the Lac Rachel reverse fault. This portion of the hinterland zone is made up of a metamorphosed and imbricated volcano-sedimentary sequence and four NW trending, en échelon, exposures of Archean gneisses (map I). These gneissic bodies have commonly been referred to as "domes" and are from the NE to the SW: the Boulder, the Renia, the Moyer and the Scattered. Although the Boulder and the Moyer gneisses are exposed as doubly plunging antiforms, the Renia and Scattered ones are exposed as SE

plunging synforms.

The structural grain of the region is dominated by the NW-trending structures of these gneissic bodies, which are thought to be correlative to D_3 W of the Lac Rachel fault.

3.2) Structures west of the Lac Rachel Fault

3.2.1) The first deformation event (D_1)

In the western and central zones of the northern Labrador Trough the first phase of deformation is characterized by westerly vergent thrust faults and isoclinal folds (Goulet, 1986, 1987; Wares *et al.* 1988). Hoffman (1988) noted the presence of NE plunging sheath folds and stretching lineations, compatible with movement to the SW, on the sole thrust in the northern Labrador Trough. A cleavage or schistosity (S_1) associated with the first phase of deformation, commonly parallel to bedding, is visible on most non-igneous outcrops. The vergence of the folds is quite variable, from usually SW to NW in the western autochthonous and central allochthonous zones (Goulet, 1986; Wares *et al.*, 1988) to mostly W and NW in the eastern central zones (Goulet 1987). In the eastern hinterland zone Hynes (1978) interpreted a WNW vergence for the F_1 folding event. The F_1 folds are often small scale rootless intraformational folds (Plate IVb, IVc & IVd).

The extent of movement on individual thrust faults is quite variable, from under 100 meters in the imbricated para-autochthonous zone of the southern Labrador Trough (Dimroth, 1970) to up to 20 km in the central allochthonous zone of the northern trough.

The D_1 thrusts and to a lesser extent the F_1 folds have been interpreted to root down to a common décollement surface situated most probably at the basement-cover interface (Baragar, 1967; Séguin, 1969; Dimroth, 1970, 1972,

1981; Dimroth & Dressler, 1978; Boone, 1987; Boone & Hynes, in press). Séguin (1969), using various geophysical methods, estimates that the thrust faults do not cut down into the underlying basement but rather shallow down to a common plane at the basement-cover interface. There is however some local evidence in the central Labrador Trough for basement involvement in the D_1 thrusting event (Dressler, 1979; LeGallais & Lavoie, 1982).

Baragar (1967) and Dimroth & Dressler (1978) presented schematic cross-sections of the entire width of the Trough, but they did not project the basal décollement surface underneath the central allochthonous zone into the hinterland.

Recent studies in other orogens have shown that a basal decollement surface commonly caps basement exposures found in their exhumed core zones; Cape-Smith Fold Belt (Hynes and Francis, 1982; Lamothe *et al.*, 1984; St-Onge *et al.*, 1986), the Wopmay Orogen (St-Onge *et al.*, 1983; King, 1986), the Canadian Cordillera (Read & Brown, 1983; Okulitch, 1984).

3.2.2) The second deformation event (D_2)

In the western and central zone of the northern Labrador Trough, the second deformation episode is characterized by E trending upright, generally open, cross-folds (Goulet, 1987). These folds only seldom exhibit an axial planar cleavage. They are partially responsible for the change in plunge of the tighter, westerly vergent F_3 folds observed in the western regions of the northern Labrador Trough (Goulet, 1986, 1987; Wares *et al.*, 1988). Local reversal of plunge direction of the F_3 folds results in dome & basin patterns (type 1, (Ramsay, 1967)). A megascopic example of this pattern is the Lac Crochet basin in the westernmost portion of the central zone (Sauvé *et Bergeron*, 1965; Goulet, 1986; map I).

To the south in the western zone there is local evidence for basement involvement during F_2 , where the para-autochthonous sedimentary sequence and basement gneisses are folded into NE trending open upright folds that plunge shallowly to the NE (Dressler, 1979). The extreme northern synclinal (F_3) closure of the Labrador Trough shows roughly NE trending cross-folds, locally with fault-bounded northern limbs (Fig. 10). Hardy (1976) ascribed the cross-folds to a folding phase later than the tight NW trending southwesterly overturned F_3 syncline. However the cross-folds are much more flattened on the east side of the syncline than on its western limb. This may indicate that the E trending cross-folds were earlier and were subsequently preferentially flattened on the NE flank of the F_3 fold due to additional southwesterly directed shortening during the D_3 event. The F_2 folds in the northernmost portion of the Labrador Trough could possibly represent an extension of the E trending D_2 of deformation in the Cape-Smith foldbelt. St-Onge and Lucas (1988) have mapped large-scale E trending basement-involved folds in the southern isolated outliers of the Cape-Smith fold belt. These are situated roughly 35 km south of the Cape-Smith fold belt itself and 100 km north of the N termination of the Labrador Trough. The D_2 deformation of the Cape-Smith fold belt may possibly have been transmitted as far south as the northern tip of the trough.

3.2.3) The third deformation event (D_3)

Although the third deformation phase occurred relatively late in the tectonic history, it strongly affects the structural grain and morphology of the northern Labrador Trough.

Large NNW trending, westerly overturned F_3 folds with shallow to moderate SE plunging axes characterize the central allochthonous igneous-

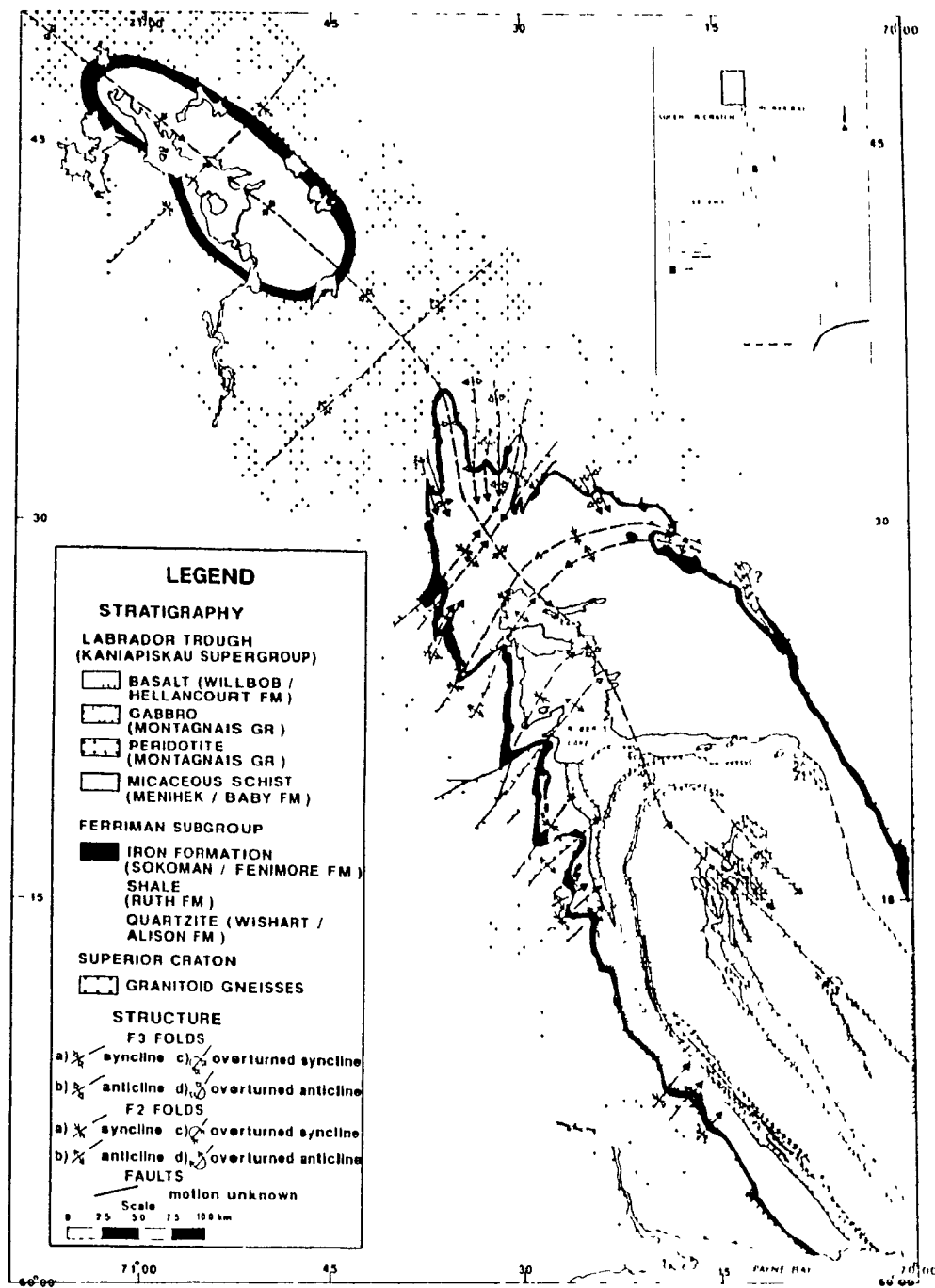


Figure 10: Map of the northernmost Labrador Trough, where early NE trending basement involved F_2 folds are refolded by the later NNW trending F_3 syncline. The F_2 folds on the NE limb of the F_3 syncline are more flattened than their counterparts on the SW limb. Simplified and modified from Hardy (1976) and Clark (in press).

sedimentary zone (Sauvé & Bergeron, 1965; Clark, 1978, 1980; Bélanger, 1982; Goulet, 1986, 1987; map I).

This folding phase only partially refolds features developed during the two previous deformation phases, the large-scale F_3 folds appear to be bounded by the early non folded thrust faults (Sauvé & Bergeron, 1965; Goulet, 1986; Boone, 1987; Boone & Hynes, in press). In the central allochthonous zone, these folds appear to have formed in the structurally highest levels and do not involve basement rocks (Boone & Hynes, in press).

In the higher grade amphibolite zone of the northernmost Labrador Trough the F_3 folds clearly involve the basement along with the cover rocks (Bergeron 1957; Freedman, 1958; Gold, 1962; Hardy, 1976; Clark, in press; Fig. 10 & 11).

3.2.4) Transverse faults

Transverse faults are oriented at a large angle to the main NNW tectonic grain of the northern Labrador Trough. Easily visible on the aerial photographs, they often form independent or conjugate sets oriented to the NE and SE, with the NE ones predominant. These types of fault seem to be better developed in the more competent gabbros and basalts. Sauvé and Bergeron (1965) mention displacements of 15 to 30 m on one of them. These faults cut limbs of F_3 folds in areas to the west (Sauvé and Bergeron, 1965). They could represent a late stage feature related to continuing, or late stage, westerly shortening during the F_3 folding event, with no significant displacements.

The roughly 90° angle between the two fault directions does not quite fit the classical model for conjugate shear fractures in which they form an acute angle towards the direction of maximum compression. Large scale rotations due to additional flattening could increase an initially acute angle to 90° . However this is unlikely given the small amounts of displacement

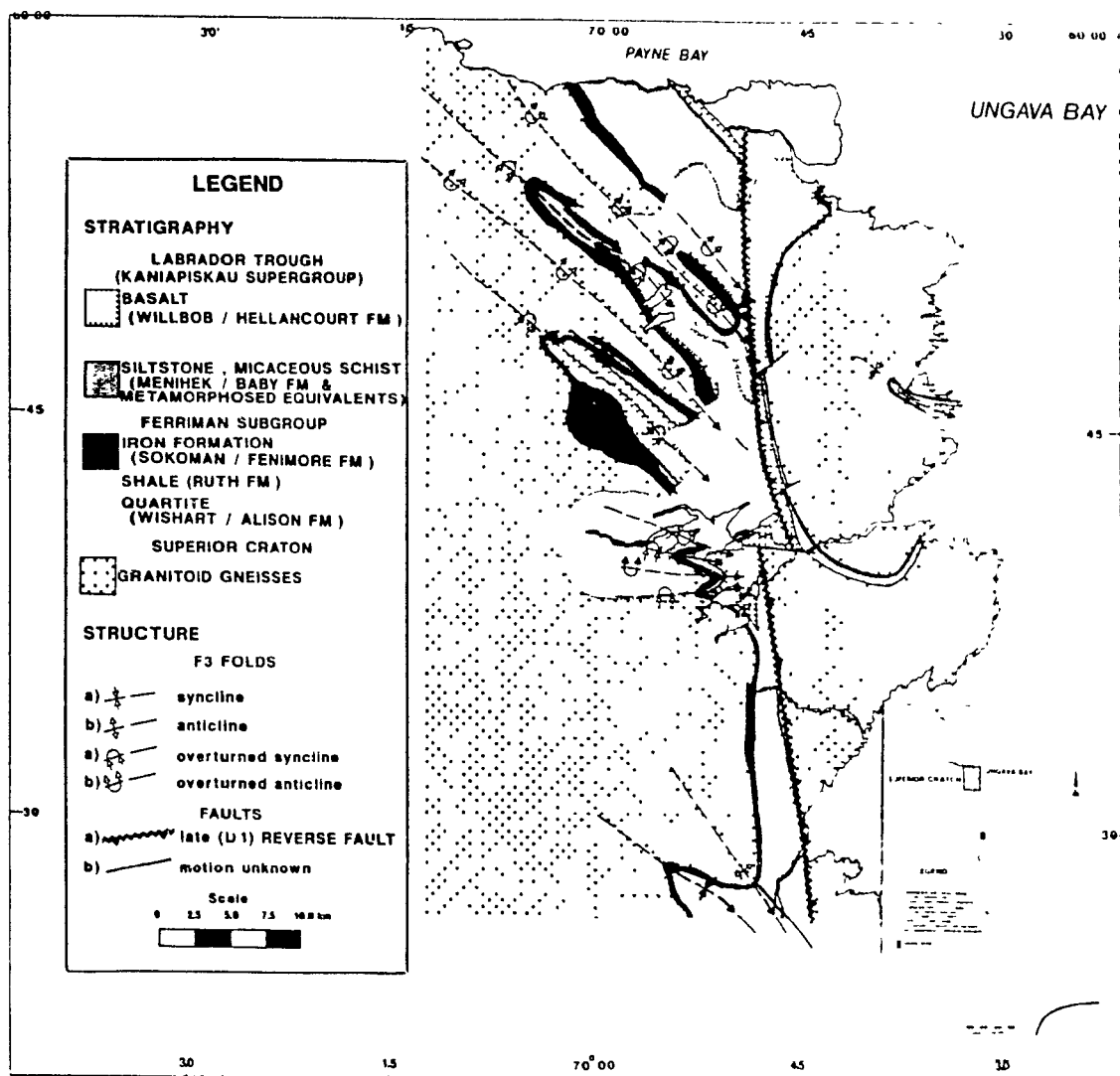


Figure 11: Schematic map of the northern extension of the Labrador Trough showing the traces of the NW trending F_3 folds being cut off against the N-S trending extension of the Lac Rachel fault. Simplified and modified after Bergeron (1957), Gold (1962), Freedman (1958) and Clark (in press).

and consequently rotation observed on the 1:50,000 scale maps and aerial photographs for these faults.

3.2.5) The Lac Rachel fault

This fault was originally designated as the Lac Phillips thrust fault in the region adjacent to the north (Sauvé, 1956; Fig. 5). It places the metamorphosed equivalents of the lower Baby Formation onto sheared Hellancourt basalts (map I). All along its length this fault juxtaposes metamorphic schists, partially equivalent to the Kaniapiskau sequence further west, along with remobilized Archean basement bodies, onto the uppermost units of the central allochthonous zone (map I).

In the study area the Lac Rachel fault is oriented N-S; further north Sauvé (1956, 1959) and south (Clark, 1978, 1980; Dimroth, 1978) its trace becomes parallel to the main NNW tectonic grain of the Labrador Trough (Fig. 4). The extension of the Lac Rachel Fault in the northernmost Labrador Trough is oriented N-S (Bergeron, 1957; Gold, 1962; Clark, in press; Fig. 11). At this latitude in the footwall of the fault the traces of NW trending, SW overturned, basement-involved F3 folds are cut off. West of the Renia Gneiss, the fault trace is occupied by Pleistocene cover or Lac Rachel, hence most of the information about this fault is indirect.

In the footwall of the fault, F₃ fold traces are either truncated or deflected into the fault plane (Sauvé, 1956; Sauvé & Bergeron, 1965). In the hanging-wall of the thrust, F₃ fold traces have a NW trend instead of the more prevalent NNW trend of other portions of the Labrador Trough; they curve gently into parallelism with the fault (Sauvé, 1956).

In our study area there is some evidence for a hanging-wall anticline structure on the Lac Rachel fault. A small exposure of iron formation,

presumably belonging to the Middle Member of the Baby Formation, is found on an island near the western shore of Lac Rachel. This implies that an anticlinal trace lies between this exposure and the more extensive horizon on the eastern shore of Lac Rachel. However no eastern facing outcrops have been observed on the western shore to confirm the fold trace.

The northerly extension of this fault was recently studied by Goulet (1986). He interpreted it as an oblique-slip fault with significant right lateral displacement of up to 10 to 15 km (N. Goulet, pers. comm., 1989). A mineral elongation measured in the fault plane has a pitch of 45° to the N (Goulet, pers. comm., 1989).

The vertical movement along the fault must have been substantial, because metamorphic imbricates and remobilized basement are juxtaposed against the upper part of the Kaniapiskau Supergroup in the northern Labrador Trough. Using stratigraphic thicknesses the minimum vertical movement is 600 to 1000 meters. In this area thermobarometric data are available only for the hanging-wall sedimentary schist; the volcanics being unsuitable for this type of study. To the south, in the area mapped by Clark (1980) (see Fig. 5), where metamorphosed sediments are found on both sides of the fault, a difference of barometric pressure of 200 MPa corresponding to vertical throw of 7.5 km was found between the hanging wall and footwall rocks (Poirier et al., in press).

The late nature of this fault is clear from the truncation of F_3 folds and the juxtaposition of two different metamorphic zones. Goulet (1986) noted the presence of pseudotachylite horizons in the northern extension of the fault, confirming the late to post metamorphic nature of the movement along the fault. Goulet (1987) considers this fault to have an early transcurrent motion. The dextral strike-slip movement along the fault plane

in conjunction with a similar type of motion on the Lac Olmstead Fault was interpreted to result in the formation of the large basement-cored F_3 folds that characterize this portion of the western hinterland zone (Goulet, 1987). In this scenario D_3 would be contemporaneous with the motion on the Lac Rachel Fault. Intersection of the F_3 fold traces with the Lac Rachel Fault yields ambiguous results; some of F_3 fold traces curve gently into parallelism with the fault planes (Sauvé, 1956; Fig. 12; map I & III) while others are clearly truncated by it (Bergeron, 1957; Fig. 11).

In summary, any early motion along the Lac Rachel Fault, has been largely obscured by late to post metamorphic movement and remains unknown. Most of the observed features are more compatible with a late to post metamorphic motion (Goulet, 1986; Poirier *et al.*, in press).

One way to in which to assess if any significant (pluri-kilometric) dextral strike-slip motion has occurred along the Lac Rachel Fault would be to map out the northern extensions of the isograds present in the area mapped by Gélinas (1965) (Perreault & Gélinas, 1985; Moorhead & Hynes, 1986; Perreault *et al.* 1987; Poirier, 1989). If there has been any significant dextral oblique motion on the fault the isograds present in the hanging-wall should eventually curve into and terminate at the fault plane. This is especially true if the stretching lineation that plunges 45° to the NE present in the fault plane (N. Goulet, pers. comm., 1988) is used as a bulk strain marker. From the 1:250,000 scale compilation map of Clark (in press) the two isograds depicted seem to extend northwards parallel to the fault. This may however be a too crude an approximation to allow the assertion that little late to post-metamorphic strike-slip motion has taken place.

3.3) Structures east of the Lac Rachel fault

3.3.1) Basement gneiss exposures

3.3.1.1) Antiformal basement bodies

3.3.1.1A) The Moyer Dome

The Moyer dome is ellipsoidal with a pinched southern zone. The southern extension of the dome is not well constrained. From information available from the maps of Fahrig (1965) and Clark (1980), the area south of the Koksoak river does not seem to contain any exposures of basement gneisses situated SE along strike of the Moyer Dome (Map I). There is however an unmapped zone on the southern shore of the Koksoak River situated SE along strike of the Moyer Dome. It lies in a critical area where it might be possible to establish whether the Moyer Dome is an isolated body or if it links up with the southern more extensive Scattered Gneiss. Extrapolating the information available from Fahrig (1965) and Clark (1980) the southern margin of the Moyer Gneiss probably corresponds to the area occupied by the Koksoak River. It does not seem to link up to the southern Scattered Dome (Map I).

The Moyer Dome has moderately dipping margins up to its pinched southern zone and a shallowly dipping core (Gélinas, 1958a; Clark, 1980; Fig. 12 & 13), features that are compatible with a shallow level of unroofing. The main structural features within the overlying cover rocks are synclines along the E and N margin of the dome.

3.3.1.1B) The Boulder Dome

The Boulder Dome is an elongated NW trending, doubly plunging, upright F_3 basement-cored anticline (Sauvé, 1956, 1957; Gélinas, 1958a, 1958b; Fig. 14). The north and south terminations seem to have moderate plunges, the flanks are

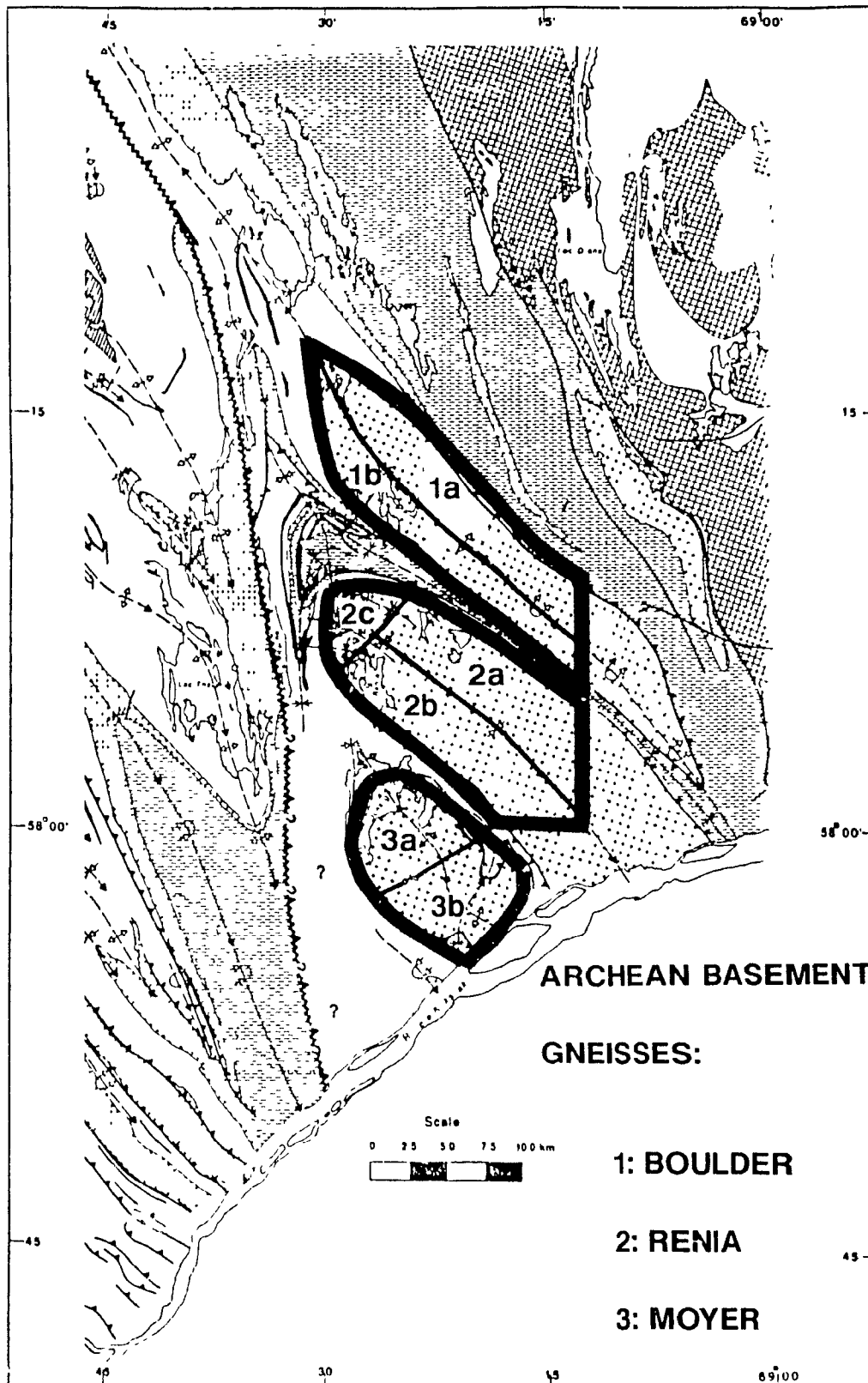


Figure 12: Domains of the 3 Archean basement gneisses north of the Koksoak River in the western hinterland zone.

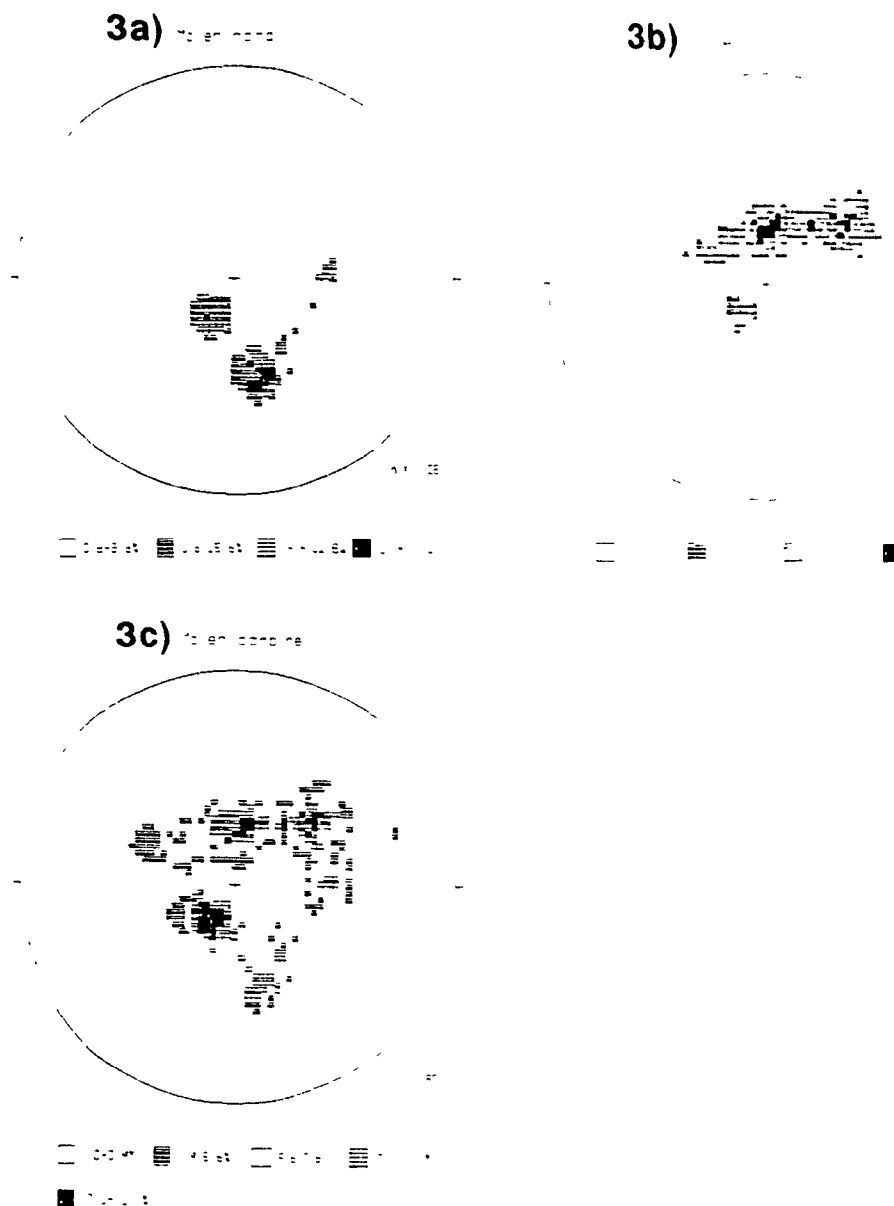


Figure 13: 3a: Shallow, northerly dipping N half of the Moyer dome
 3b: Shallow, southerly dipping S half of the Moyer dome.
 3c: Combined data from 3a and 3b.
 This data set is taken from Gelinas
 (unpublished maps) and Clark (1980).

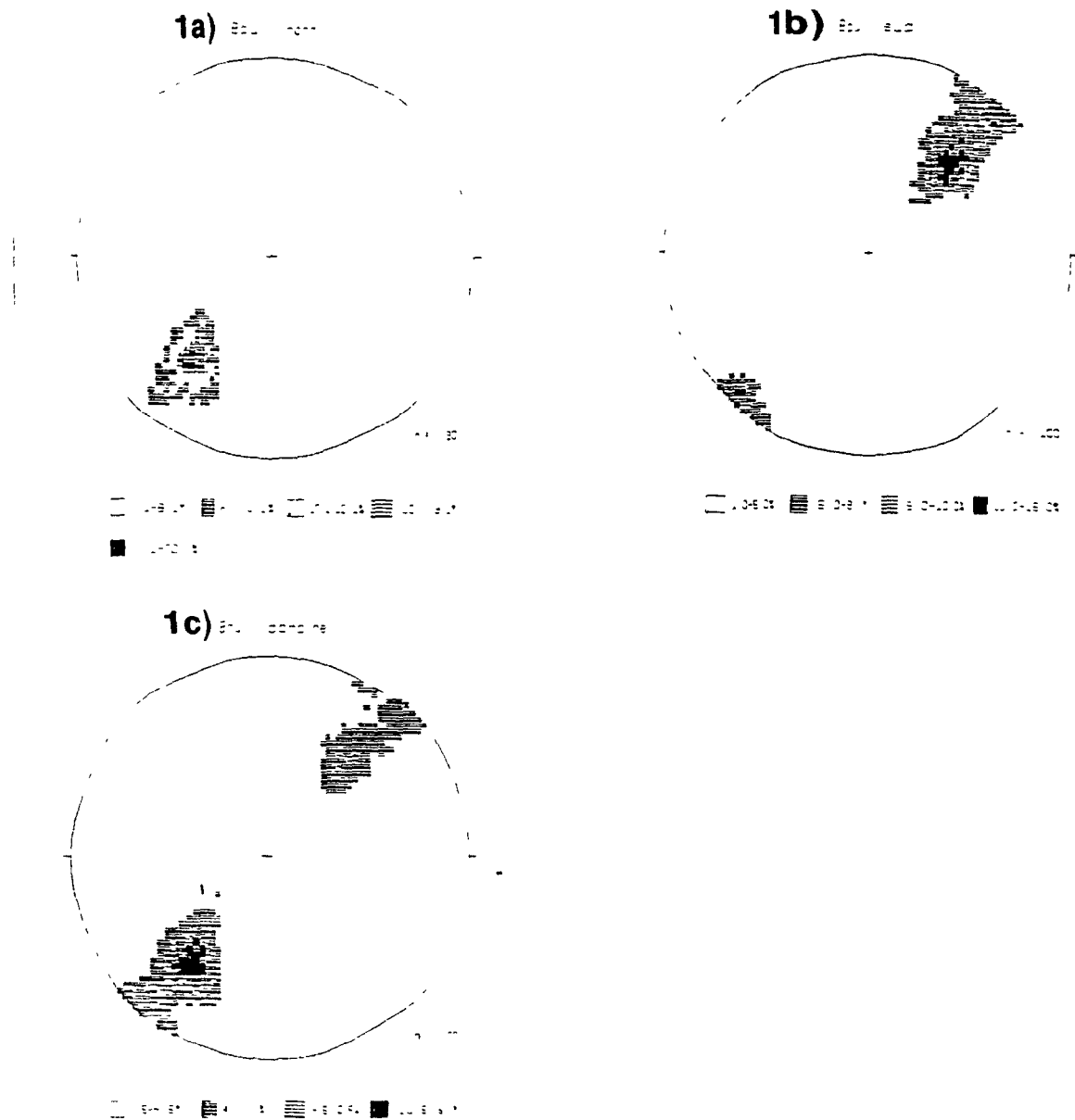


Figure 14: 1a: NE dipping NE half of the Boulder dome.
 1b: SW dipping to vertical SW half of the Boulder dome.
 1c: Combined data
 The data set is taken from Galinas (unpublished maps), Sauve (1956, 1957) and this study.

upright and steeply dipping, except in the southeastern end of the dome where both flanks are overturned to the SW (Gélinas, 1958b; Clark, in press; map I). The hinge line of zero plunge for the F_3 fold axis coring the dome is situated closer to the NW closure of the dome. This is clearly shown by the fold morphology of a large scale amphibolite dyke within the dome (Gélinas, 1958a; map I) and the sense of plunge of the associated folds within the cover sequence on the SW flank and NE flank of the dome (Goulet, 1986). There are no megascopic folds that repeat the stratigraphic units in the cover rocks overlying this dome. The cover sequence is however capped by a thrust fault on its SW margin.

3.3.1.2) Synformal basement bodies

3.3.1.2A) The Renia Synform

The Renia Gneiss has the most complicated structure of all four basement exposures. It is an elongated upright basement-cored F_3 synform, with a SE to E steeply plunging NW closure placing basement gneisses on top of the cover rocks (Fig. 15). The southern margin or extension of the Renia Gneiss is poorly constrained. It clearly lies to the SE of the area studied by Gélinas (1958a, 1958b, 1965 (see Fig. 5 & 12)). To the SE along strike, on the southern shore of the Koksoak River, Fahrig's (1965) study shows the presence of a large swath of biotite-muscovite schists and gneisses but no granitoid basement gneisses. The southern termination of the Renia Gneiss lies presumably between the southern limit of the area mapped by Gélinas (1958a, 1958b) and the first exposures on the south shore of the Koksoak River.

The NW closure of the Renia Gneiss body is also characterized by a tongue of sediments tightly infolded into the basement gneisses. The axial trace of the cover-cored syncline and its associated basement-cored anticline

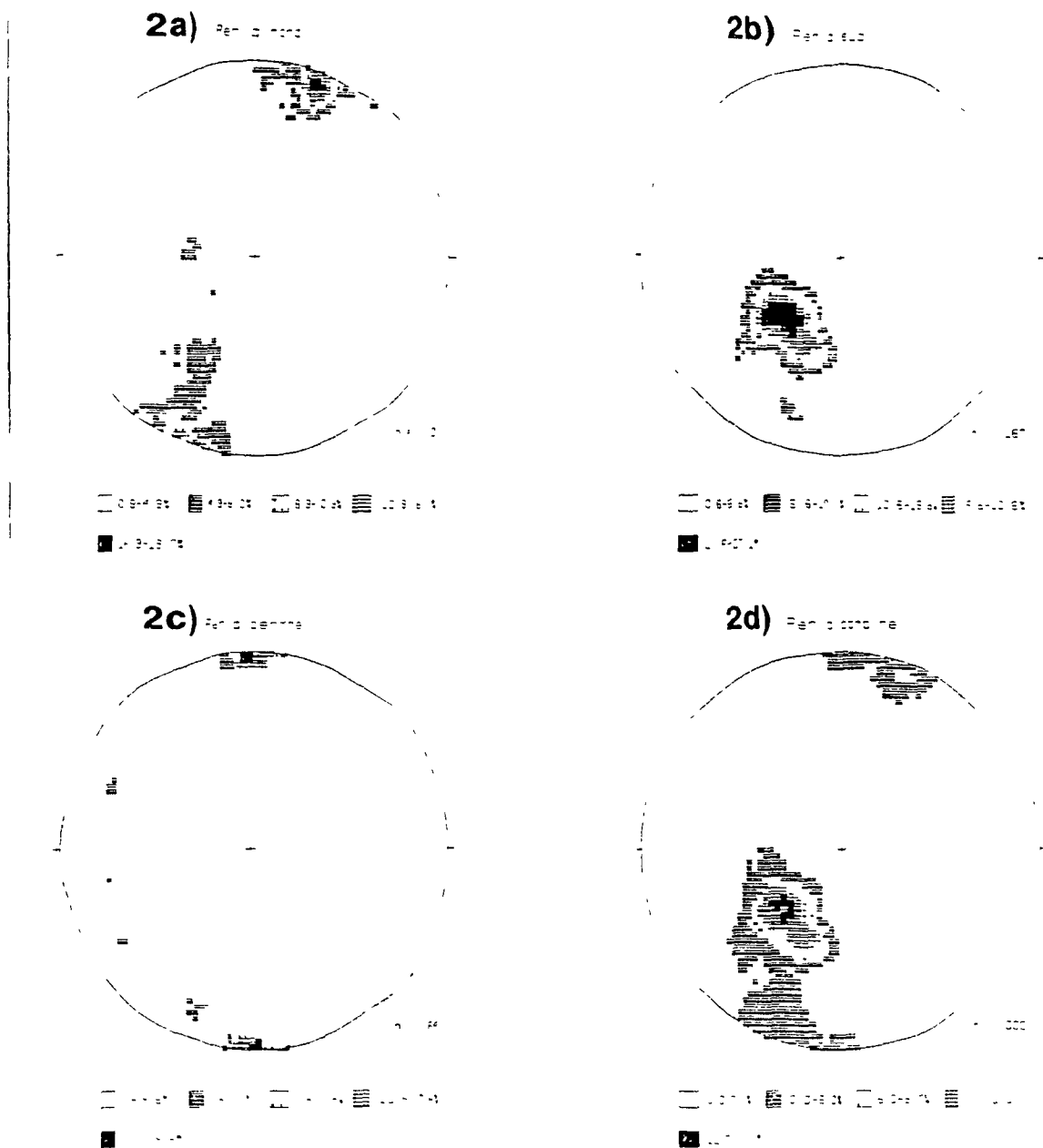


Figure 15: 2a: Steeply SSW to NNE dipping NE half of the Renia synform.
 2b: Moderately NE dipping SW half of the Renia synform.
 2c: Steeply E to SE plunging NW closure of the Renia synform.
 The stereonets include data from Gelinas (unpublished maps) and this study.
 2d: Combined data
 The data set is taken from this study and Gelinas (unpublished maps)

are clearly refolded by the NW trending F_3 folds. Structural information from the hinge zones of both of these folds is scant due to a lack of outcrops in strategic locations. From information derived from the symmetries of the parasitic folds on their limbs , they are likely to belong to the F_1' folding episode. Supporting this assigned chronology is the abundance of minor F_1' folds within the cover sequence adjacent to the NW end of the Renia Gneiss. The cover sequence NW of the Renia Gneiss is also folded by a regional scale F_1' fold.

3.3.1.2B) The Scattered Synform

The Scattered Gneiss found south of the Moyer Dome displays the same synform morphology as the Renia Gneiss. The NW termination of the Scattered Gneiss outcrops in a few localities north of the Koksoak River (Clark, 1980; map I). From data gleaned from Clark's (1980) study it appears that the NW closure of the Scattered Gneiss plunges shallowly to the SE. The synform becomes broader SE of the Koksoak River. It extends at least 50 km to the SE, where it seems to link up with a larger ill-defined mass of granitoid gneisses (Fahrig, 1965). SW of the main portion of the Scattered Gneiss there is a 30 km² elliptical body of granite of uncertain age (Clark, 1980; Fig. 4). NW of the gneiss lies a large area of paragneisses and schists of uncertain affinity (Fahrig, 1965).

3.3.2) Down plunge section

The structural grain of the region is dominated by the NW-trending structures of the gneiss bodies, which are thought to be correlative to F_3 folds west of the Lac Rachel fault. The straightforward structures associated with the gneiss bodies allow the construction of a section across the western

portion of the hinterland zone of the northern Labrador Trough (Fig. 16). The line of section approximately follows the Koksoak River which cuts the F_3 folds at an approximate right angle (Fig. 16). This section represents an offset extension of the down plunge section of Boone (1987) in the central and western portions of the northern Labrador Trough (Fig. 5). Although there is no vertical erosional relief in the northern Labrador Trough as in more recent mountain belts, the presence of large and continuous F_3 folds in this area results in considerable structural relief being exposed in oblique section at the surface.

The area covering the four basement gneiss exposures is much larger than the study area, which covers only the NW termination of the Renia Gneiss (Fig. 4). The section includes data from the following sources: G  linas (1958a, 1958b, unpublished maps), Sauv   (1956, 1957), Fahrig (1965), Clark (1980) and Goulet (1987). The small area covered by this study compared with the area covered by the section results in a higher level of uncertainty than usual for down plunge projections reported in other studies (King, 1986; St-Onge and Lucas, in press), the limiting factor here being the small amount of fold plunge data available from the studies listed above. Where appropriate, schistosity and bedding planes were plotted on stereonets to establish the plunge of the F_3 axes and complement the available fold data on the maps. The best constrained portion of the composite section is that for the lower portion of the Renia synform corresponding to the area covered by this study.

Construction of the section involves the down plunge projection of the surface geology north from the line of section and the up plunge projection of the surface data south of the line of section. The area north of the line of section contains four major F_3 fold sets, which are from S to N: the Scattered Synform, the Moyer Antiform, the Renia Synform and the Boulder Antiform. Data

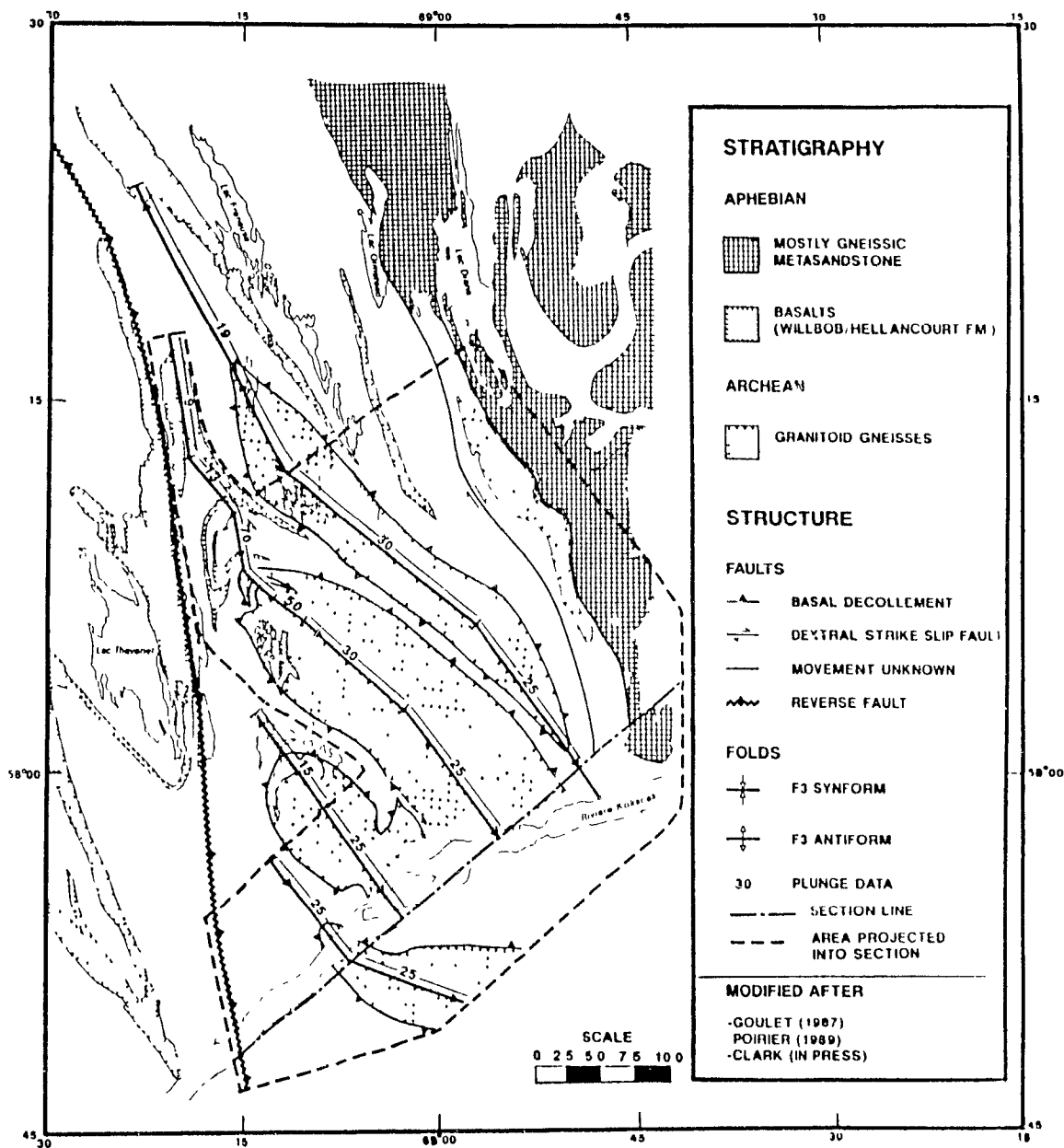


Figure 16: Traces and plunges of the major folds used to construct the down plunge section

from the SE portions of the Boulder, Renia and Moyer Gneisses along with the NW termination of the Scattered Gneiss were projected along a common F_3 axis plunging 25° to the SE (Fig. 16). This is an approximation given that variable plunges and to a lesser degree variable trends for the F_3 axes are reported in the Moyer Dome (Clark, 1980) and Boulder Dome (Goulet, 1987). The Renia Synform is the most complex of the four fold sets. Its NW portion, covered by this study, displays systematic variations in the plunges and trends of the F_3 folds (Fig. 16). Domains of constant trend and plunge were established. From these, individual down plunge sections were constructed, these were then stacked up one on top of each other to form a composite down plunge section for the Renia Synform. The section is thought to be only truly constrained down to 7 km. The lower portion of the section should be regarded as a more schematic representation if the surface geology is pulled through down onto the line of section using all changes in plunge data visible at the surface. Given the shallowing in plunge of the Renia Synform from NW to SE, it is not clear that stacking a section from the NW and central portions of the synform under the most SE part, near the Koksoak River, is justified. In addition it is not clear at all that the cover succession visible at the NW closure of the Renia Synform project all the way down plunge onto the line of section given the lithological variations visible along strike at the surface.

South of the line of section the Scattered Gneiss and its surrounding metasediments were projected up plunge along the F_3 synform axis that cores the gneiss body. Structural data south of the river are generally scant and inadequate from the point of view of this type of study. The area south of the river in the vicinity of the Scattered Synform was mapped by Clark (1980). The data set here allows for further SE down-plunge projection of the surface geology than the area adjacent to the N and NE of the Scattered Gneiss. The

composite section is shown in Figure 17.

Two features of the down plunge section merit comment:

1) The cover rocks surrounding the Boulder and Moyer Antiforms seen on the section were projected down dip onto the section and correspond to the ones present along the SW margin of the folds. Down plunge projections of the NW terminations of the basement antiforms are shown in Figure 18. It is clear from these sections and the maps of Gélinas (1958a, 1958b) and Clark (1980) that there is no simple correspondence between the cover rocks present on the NW margins and the ones present along the SE margins. This implies that there were pre-dome lithological variations across strike. These are thought to represent original stratigraphic variations across the basin, but unrecognized thrusts or other types of fault that disrupted the stratigraphic arrangement cannot be entirely discounted.

2) The area left blank on the west side of the section is due to the presence of the N trending post-D₃ Lac Rachel reverse fault (Moorhead & Hynes, 1986). Since it is at an angle to the trace of the lines of projections for the section it would appear to have an artificial shallow dip. The effect of this fault was essentially to remove "projectable" material in increasing amounts to the north.

The composite down plunge section may possibly display up to 24 km of structural thickness if all the surface data on the Renia Synform are projected down plunge onto the line of section. The striking features of the section are the highly flattened nature of the Boulder Antiform and Renia Synform and the recumbent morphology of the Scattered Gneiss.

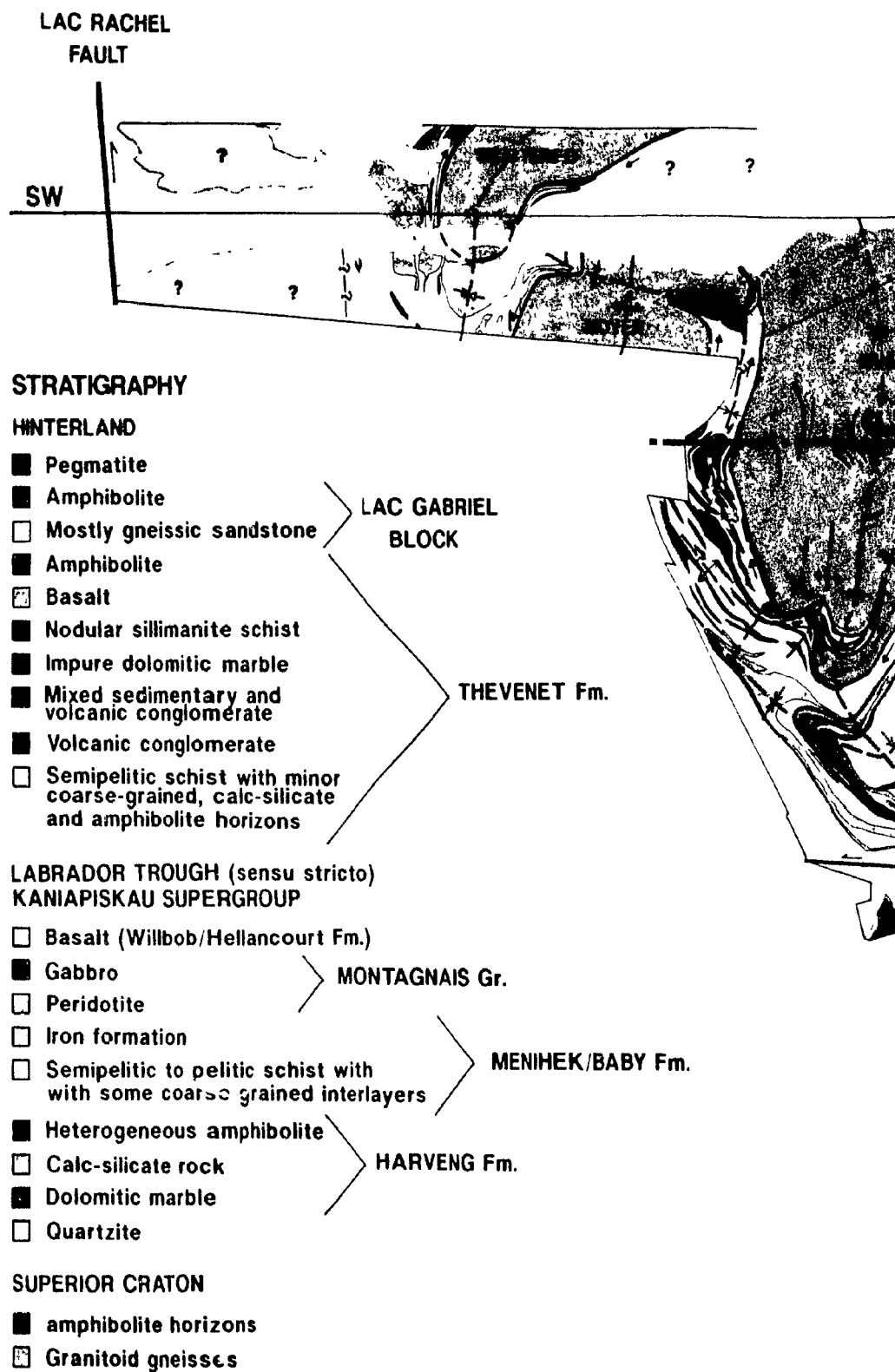
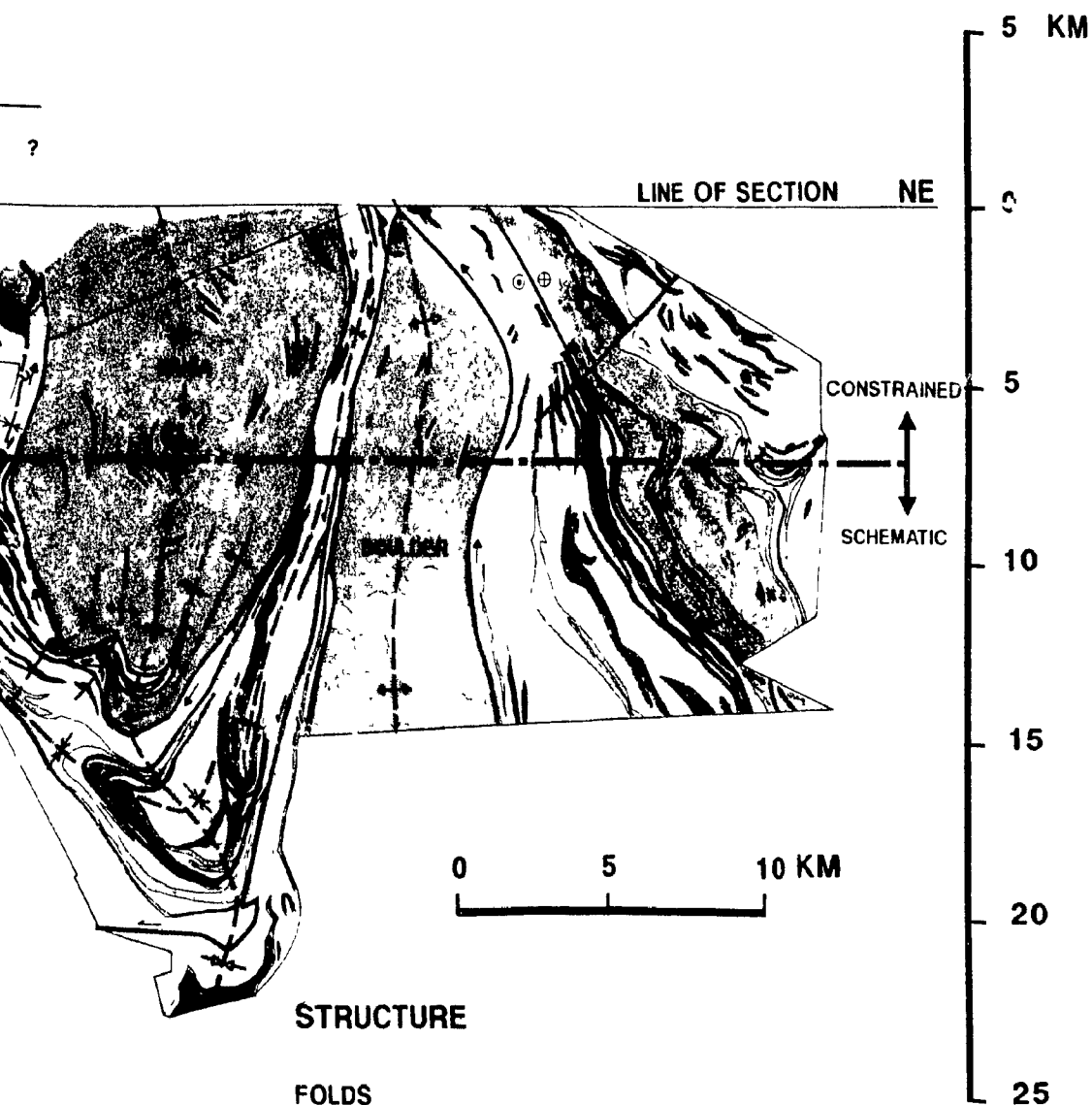


Figure 17 : Composite down plunge section



STRUCTURE

FOLDS

- ⊕ — F3 antiform
- ⊖ — F3 synform
- ⊕ — F1' anticline
- ⊖ — F1' syncline

FAULTS

- ↙ — Reverse fault
- ↘ — Thrust fault
- ← — Basal decollement
- ⊕ — Strike-slip fault ⊕ in ⊖ out
- ⊕ — Motion unknown

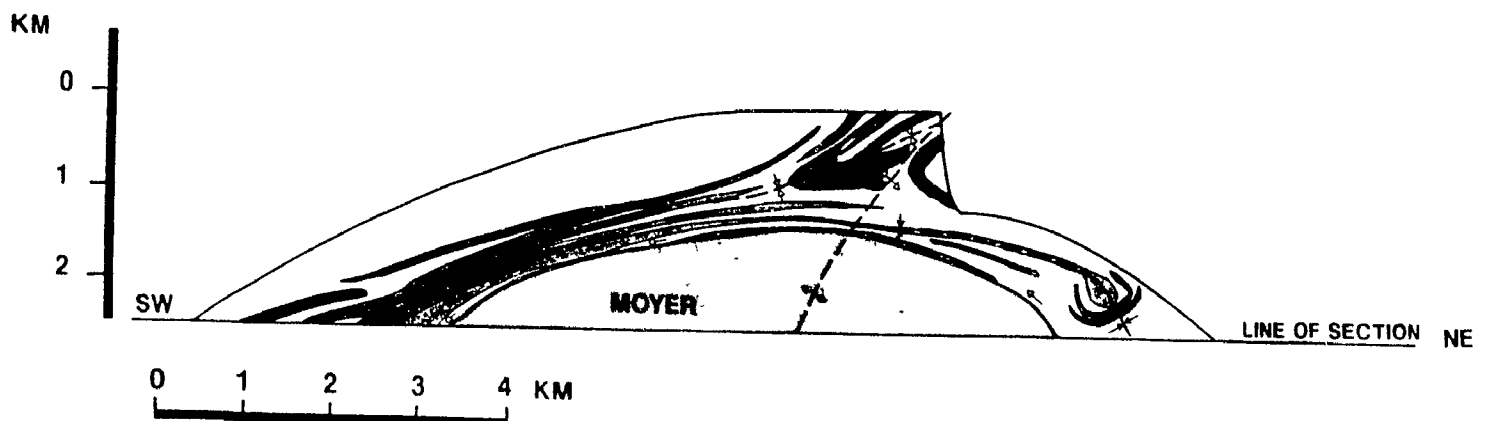
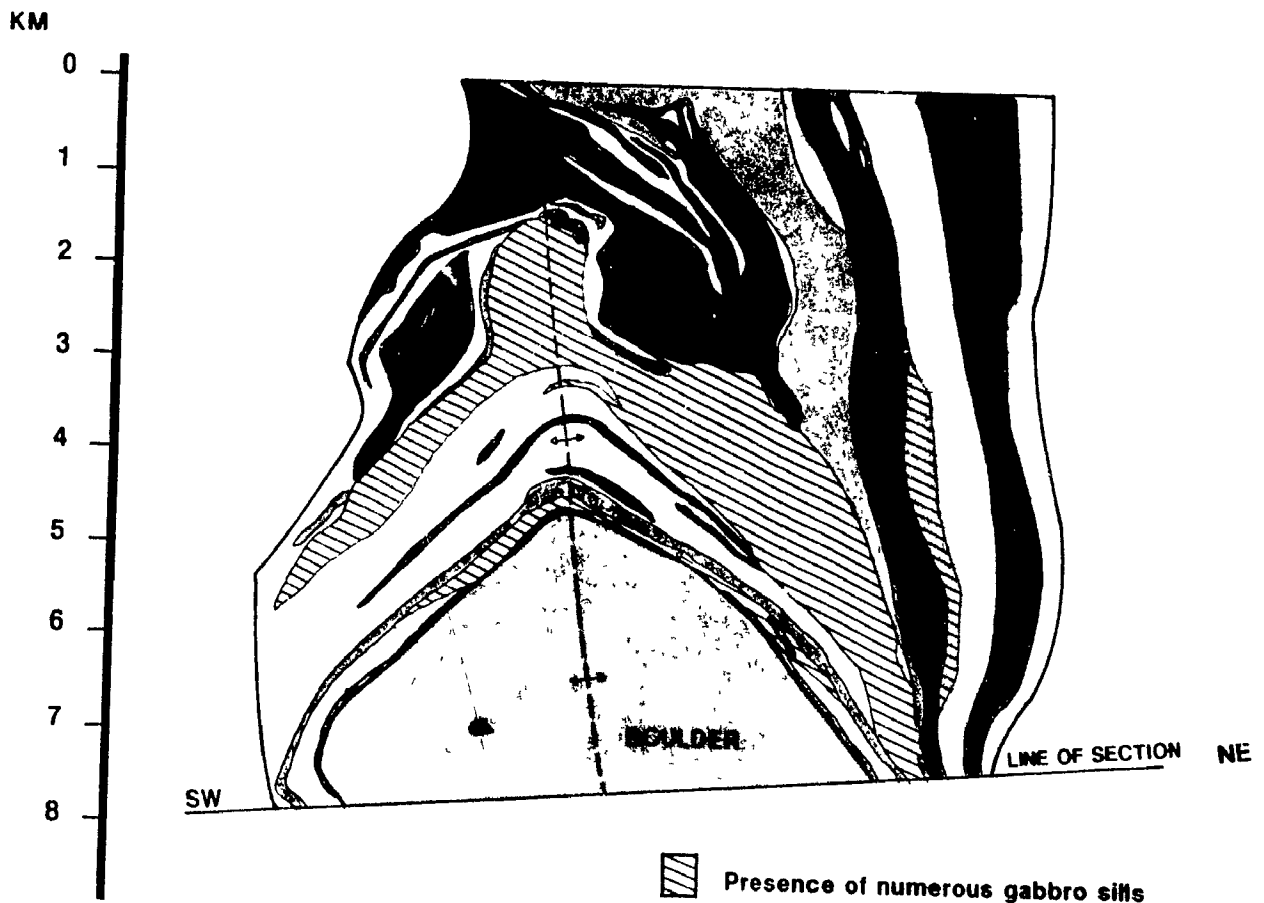


Figure 18: Down plunge projections of the NW closures of the Boulder and Moyer domes. The legend is the same as figure 17.

3.3.3) Origin of the basement gneiss bodies

3.3.3.1) Introduction

The four basement gneiss bodies of the western hinterland zone can be used as a reference point to test any structural model. The gneiss bodies are assumed to have undergone a common tectonic history. Without this assumption specific models could be invoked to explain the formation of each individual gneiss body but not for the four basement gneisses as a whole. The presence of the two basement cored synforms, the Renia and the Scattered, provides the most critical structural feature. These two downward facing folds that bring basement gneisses on top of cover rocks eliminate a priori some of the most common mechanisms that have been put forth to explain basement gneiss exposures in other orogenic belts. These include: 1) Reverse block faulting leading to the uplift of a basement core (or horst) (Brun, 1983), 2) Crustal stretching by normal or detachment faults (Davis & Coney, 1979; Wernicke, 1984; Lister et al., 1986; Lister and Davis, 1989), 3) upright non-cylindric folds (Brun, 1983) and 4) Crustal shortening by interference between two upright fold sets (Steltenpohl & Bartley, 1988; Stel, 1988; King, 1986; St-Onge & King, 1986; Myers & Watkins, 1985; Duncan, 1984; Okulitch, 1984; Platt, 1980; Bickle et al. 1980; Ross, 1968).

In addition reverse block faulting can be discounted as a mode of formation for the basement gneisses in the hinterland of the northern Labrador Trough given the lack of late faults bounding or surrounding the gneissic bodies. Detachment faults are known to be responsible for the exposure of many large basement gneiss bodies in the southwestern United States (Davis, 1983; Lister and Davis, 1989). No extensional fabrics, either brittle or ductile, have been observed in the study area or reported from the hinterland zone of the Labrador Trough. Most structural features are compressional as

are the ones present to the west in the western and central zones (i.e. SW overturned folds and SW directed thrusts). So extension tectonics are probably not responsible for the formation or the unroofing of the basement gneisses of the hinterland of the Labrador Trough.

Thrust faulting is an effective way of emplacing basement gneiss slices on top of supracrustal rocks and is thought to be responsible for the presence of some basement exposures in different orogens, such as the Malton Gneiss in the Canadian Cordillera (Okulitch, 1984) and the Blue Ridge in the central Appalachians (Boyer & Elliot, 1982). A few basement gneiss slices have been reported in the western zone of the north-central trough (Dressler, 1979; Le Gallais & Lavoie, 1982). In the western hinterland zone, however, the cover succession bounding the different basement bodies appears to be continuous and uninterrupted, the same calcareous unit envelops each gneiss body. Unless an unrecognized thrust fault exists between the synformal and antiformal gneiss bodies, the Renia and Scattered Gneisses cannot represent hangingwall basement slices. This does not eliminate the possibility that the four gneiss bodies as a whole are floored by a thrust fault at greater depth. This fault could intersect the surface further west in the central allochthonous zone or be cut off along the late Lac Rachel fault.

Thus the structural scheme of the four gneiss bodies requires either:

- 1) The gneisses rose diapirically, in which case the Renia and the Scattered represent the lobes of a mushroom shaped diapir, the Boulder and the Moyer being either the stem or the upward portions of the diapir.
- 2) They represent sections at different levels through mega-sheath folds, the synformal gneisses being sections at a deeper erosion level than the antiformal ones. This implies that probably most of

the deformation features in and adjacent to the gneisses are part of the same deformation event, most likely D_1 .

3) The Renia and Scattered Gneisses are refolded early Pennine-style nappe structures placed on top of more passively behaving Boulder and Moyer Gneisses.

None of the three possibilities can be discounted offhand. The data for and against each model will now be presented and reviewed.

3.3.3.2) Diapirism

Diapiric upwelling of lighter granitoid crust into metamorphosed denser supracrustal rocks has been invoked in quite a few studies to explain basement gneiss exposures within orogenic belts (Krill, 1985; Rickards, 1985; Brun, 1983, 1981, 1977; Schwerdtner, 1982, 1981; Ramberg, 1981; Schwerdtner *et al.*, 1978; Dixon, 1975; Fletcher, 1972; Reesor & Moore, 1971; Price & Mountjoy, 1970; Thompson *et al.*, 1968).

The basement gneisses of the northern Labrador hinterland have features compatible with a diapiric origin: the presence of portions of a rim syncline along the margins of the Moyer and Renia Gneisses and a high strain zone localized at the basement-cover interface. However, these two structural features are also compatible with a crustal shortening mechanism, the high strain zone being the product of shearing along a basal décollement surface developed during D_1 and the rim synclines belonging to an early folding phase, in this case F_1' folds. To explain the complex structures found on the NW closure of the Renia Gneiss Sauvé & Bergeron (1965) invoked a diapiric origin for the basement gneisses.

The presence of alternating synformal and antiformal basement bodies can not be easily explained by a simple multi-headed tear shaped diapir of

upwelling lower crust. To account for the synform-cored basement bodies (Renia and Scattered Gneisses) a diapiric model would have to produce a mature mushroom shaped diapir (Jackson and Talbot, 1989). In this model the Renia and the Scattered Synforms would represent the downward cascading edges of the rising diapir as in the flanks of the mushroom. If this were the case the Renia and Scattered Synforms should link up presumably with the Moyer Dome which would represent the stem of the mushroom shaped diapir. This does not seem to be the case at the present erosion level. The link between the two synformal Gneisses and the Moyer Dome, if it ever existed, would seem to have been eroded. The apparent link between the Scattered Gneiss and a much larger ill defined gneiss mass to the SE (Clark, in press; Fig. 4) is not easily reconcilable with the Moyer Dome representing the center the rising diapir. This diapir would have to be highly mature with an extremely narrow neck. However this does not disqualify the diapir model.

The basement domes in this area lack some fold features associated with the buoyant rise of a granitoid mass: concentrically arranged shallow plunging, outwardly vergent cascading folds (Platt, 1980; Fig. 19) or radially arranged neutral folds (Brun, 1977, 1983; Fig. 20).

Although no strain study was undertaken, the bulk strain as recorded locally by the stretching lineation fabric is not simply related to the morphology of the Renia Synform, but rather to the local presence of the F_1' folds that wrap around the gneisses. No intense flattening was observed near the basement contact as predicted by the diapiric model (Dixon & Summers, 1983).

As stated by Brun (1983), subsequent deformation may obscure many if not all traces of an original diapiric emplacement of the domes (Dixon, 1975), hence if it is not possible to prove a diapiric origin it may not be possible

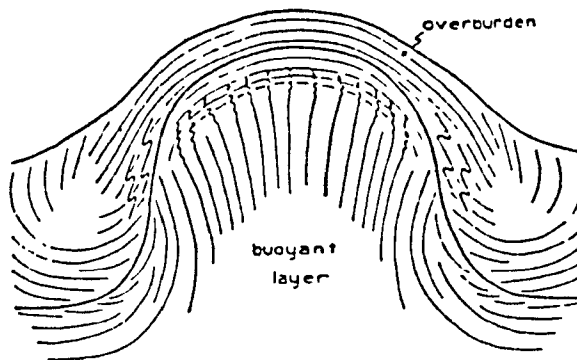


Figure 19: Buoyant uprising of a lighter dome like mass causing outwardly vergent "cascading" folds in the cover sequence, taken from Platt (1980).

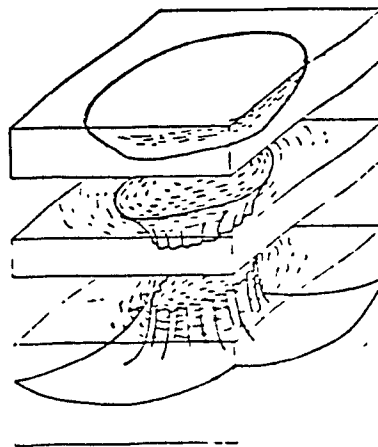


Figure 20: Radially arranged vertical folds around the "neck" of a rising diapir. In this model they are caused by constriction at the base of a mature diapir. The diagram is taken from Brun (1983).

either to discount it completely (Schwerdtner, 1981).

3.3.3.3) Sheath folding

The gneissic domes of the western hinterland zone could be accounted for by the development of large scale basement-cored sheath folds. These would have formed in response to crustal-scale NW directed shearing during D_1 . In this mode of formation the gneiss bodies would develop in a single continuous event. The NW trending F_3 folds coring the gneisses that are ascribed to F_3 (Map I, II & III, Fig. 17 & 18) would not represent F_3 folds similar to those further west but simply be the by-product of the morphology of the sheath folds. In this scheme the folds that wrap around the Moyer and Renia Gneisses (F_1') would also be the product of the NW trending sheath folds and not a distinctive folding phase. The differences between the synformal gneisses (Renia and Scattered) and the antiformal gneisses (Moyer and Boulder) would simply reflect different erosional levels. The synforms representing deeper horizontal sections through the sheath folds than the antiforms. An implication of this is that antiformal gneisses are, in the same fashion as the synformal gneisses, underlain at depth by cover rocks. To respect the sheath fold geometry the basement gneisses of these antiforms would have to eventually curve back on themselves. Some indirect evidence for cover rocks underlying the Boulder Dome can be seen on the 1:250,000 scale aeromagnetic map. The northern third of the Boulder and Renia Gneisses do not have the high relief magnetic pattern that characterizes the basement gneisses of the Superior Province and the southern portions of these domes. This implies that although the Renia and Boulder Gneisses have different configurations at the near surface, the Renia being cored by a synform and the Boulder by an antiform, they may possibly have a roughly similar configuration at greater

depth. The Moyer Dome falls in the northern portion of a much larger magnetic anomaly. This magnetic high zone also underlies the Scattered Gneiss, the granitic body on its SW flank (Clark, 1980; Fig. 4), the large mass of granitoid gneisses to which the Scattered Synform seems to link to the SE (Fahrig, 1965; Fig. 4) and the paragneisses and schists that lie between the SE end of the Renia Gneiss and the Scattered Gneiss.

The Renia Synform seems to end about where its southern extension intersects the Koksoak River. This "isolated" basement cored synform morphology is not readily compatible with either diapiric or fold interference mechanisms. It can however be easily explained as a NW vergent upward facing sheath fold that was subsequently flattened during D_3 . The features of the other three gneiss bodies can also be accounted for by the development of sheath folds, but their characteristics are also compatible with all or some of the other three formation modes.

If sheath folding is responsible for the formation of the basement domes then the NW trending folds coring the domes, ascribed to F_3 , would instead be F_1 folds. In this manner the infolded sediments near the northern closure of the gneiss would represent another F_1 fold incubated on the back of the much larger basement-cored sheath fold (Bell and Hammond, 1984). The later F_3 folding phase would coincidentally lie parallel to the transport direction during D_1 in this portion of the Labrador Trough. F_3 clearly had an effect on the shape of the basement domes. From the down plunge projection the Renia Synform clearly is elongated parallel to the F_3 axial plane. A sheath fold should not have this configuration it should either be subhorizontally oblate or circular shaped in a section perpendicular to the long axis of the fold (Cobbold and Quinquis, 1979; Bell and Hammond, 1984; Vollmer, 1988). Thus if the basement gneisses are really sections through mega sheath folds their

original configurations were highly modified during SW directed homogeneous flattening during the third phase of folding.

Kilometer-scale sheath folds parallel to the early transport direction, as defined by the stretching lineation fabric, have been recognized recently in the internal zones of more recent orogens; the Penninic internal zone of the Swiss Alps (Mattaue, 1981; Lacassin & Mattauer, 1985), the core zone of the Canadian Cordillera (Mattaue et al., 1983) and the Southern Norwegian Caledonides (Bartley, 1982; Steltenpohl & Bartley, 1988; Vollmer, 1988). At lower structural levels these folds commonly deform basement and cover rocks as a coherent unit resulting in geometrically complex Pennine style nappe folds.

The main problem with having these basement-cored, orogen parallel, folds develop as sheath folds is the lack of mesoscopic features that are clearly due to sheath folding. There is a lack of a pervasive or widely distributed stretching lineation fabric as would be expected from the large amounts of non-coaxial shear strains necessary to form the basement-cored sheath folds. No examples of sheath folds or doubly vergent folds have been observed. There are however numerous examples of reclined folds associated the F_1' folding event that wraps around the Moyer and Renia Gneisses.

The F_1' folds are thought to originally trend NNE to NE and to verge between WNW and NW. This folding phase, although lacking some of the characteristics of sheath folds, does have the right trend and vergence to produce NW trending basement-cored sheath folds.

Another shortcoming of the sheath fold model is that the thinnest of the high strain zones at the basement-cover interface does not seem appropriate for a process such as megascopic sheath folding on a kilometric scale that involves large amounts ductile crustal behavior.

3.3.3.4) Interference between early basement cored Pennine style nappes (F_1') and a later more upright folding phase (F_3)

The initial deformation event (D_1) could have been followed by a roughly coaxial deformation event (D_1') that folded basement and cover rocks as a coherent unit into large scale NE to NNE trending, NW to WNW vergent nappe structures. These folds would be followed by the NW trending E to SE plunging upright to SW overturned F_3 folds. The synform-cored gneisses, the Renia and the Scattered, would preserve large parts of the overturned limbs of the Penninic style nappe(s) folded down into the present erosion surface. If this type of model is responsible for the formation of the synformal gneiss bodies, nappe geometry implies that the SE extension of the Renia and Scattered must join up either together or separately with a much larger basement gneiss mass. From the work of Fahrig (1965) and Clark (1980) the Scattered Synform may link up with a larger gneissic mass 50 km SE from its NW termination (Fig. 4).

This refolded Penninic nappe model accounts well for the presence of synform-cored basement bodies. However the antiform-cored gneisses cannot be completely explained by this model; the F_3 fold set explains the long antiformal trace that cores the Boulder and the Moyer Domes but not their elliptical doubly plunging morphology. This trait could be the result of either: 1) a previous open folding event roughly orthogonal to F_3 or 2) the non-cylindrical character of the F_3 folds on a regional scale (whale-back folds).

In the northern Labrador Trough there is a deformation (D_2) event that has the right spatial and morphological characteristics to explain the gently doubly plunging terminations of the antiformal domes. The F_2 folds are E to NE trending shallowly plunging open fold structures that deform both basement and cover rocks into large scale buckles. These folds have been recognized to

the west of our study area (Goulet, 1986, 1987; Wares et al., 1988) and to the east (Bosdachin, 1986; Poirier, 1989). However given the large wavelength of the domes in the NW direction, the possibility of non-cylindrical F_3 folds cannot be discounted.

Interference between basement-cored F_1' nappes and the more upright F_3 folding event is thought to represent the most viable of the three possible models. None of the observed structural features seem to conflict with it.

3.3.3.5) Analogies with some other basement-cover complexes

In the western hinterland zone of the northern Labrador Trough the interaction between the F_1' and F_3 folding events has resulted in the formation of complex basement-cover relationships. Similar if not identical deformation patterns have been described for basement gneiss exposures in the internal portions of other orogens; the Chester gneiss Dome on the eastern flank of the Green Mountain Anticlinorium in the northern Appalachians (Rosenfeld, 1968), the Thor-Odin gneiss Dome of the Shushwap metamorphic complex in the southern Canadian Cordillera (Duncan, 1984) and the eastern area of the western gneiss region on the eastern margin of the Norwegian Caledonides (Krill, 1985; Vollmer, 1988). The following summaries are taken from these authors:

The Chester Dome was deformed by two early events that involved basement cored Pennine type nappe folding. The resulting cover-infolded basement was uplifted by folding about a more upright axial plane with or without a diapiric contribution. Bouyant uplift was latter discounted as a process active in the last deformation event (Nisbet, 1976 taken from Duncan, 1984).

The Thor-Odin Dome comprises three early phases of basement-cored nappes and thrust imbrication. The tectonically thickened basement-cover complex was

then refolded about two late upright fold sets that allowed the earlier structure to be visible in oblique section at the surface.

The basement gneiss bodies of the western gneiss region of Norway have been interpreted to have formed either by early pennine style folding followed by buoyant uprising (Krill, 1985) or by sheath fold nappes during one single crustal shear event (Vollmer, 1988).

The Chester Dome may well have the best constrained 3D geometry since a deep seismic reflection study has been done perpendicular to its length (Ando *et al.*, 1984). Strong moderately E dipping reflectors are clearly visible at depth and are interpreted to bound the lower margins of the Chester Dome and the adjacent much larger Green Mountain basement anticlinorium. They are thought to represent shear zones on which the basement gneisses were carried as hanging wall antiformal structures westwards on to the platform sediments overlying stable basement further west. The authors also interpreted the Aar basement massif of the Swiss alps to be floored by a similar moderately dipping shear zone that translated the allochthonous basement gneisses cratonwards into an allochthonous position. Similar to the basement bodies mentioned above, the upper portion of the Aar massif contains numerous large sets of basement-cored folds. However in a more recent study Laubscher (1988) has no detachment zone underlying the Aar massif leaving it in an essentially para-autochthonous position. He interprets the massif as an upfolded basement mass rather than an upthrust one.

The basement gneiss bodies of the western hinterland zone display many similarities to the Chester Dome. Both involve early recumbent basement cored folds later refolded about a more upright phase, they are both bounded on their lower-grade sides by a reverse faults that are largely responsible for their ultimate exhumation. The main differences lie with the presence of a

first event in the Labrador Trough in which basement behaves passively, and in the steeper dip of the Lac Rachel fault, at least at the surface, than the fault bounding the Chester Dome (Ando *et al.*, 1984).

3.3.4) Deformation events

If the synformal basement gneisses of the western hinterland zone represent refolds of early pennine nappe structures, the following order of structural events is thought to have taken place.

3.3.4.1) The first phase of deformation (D_1)

The study area contains essentially all the D_1 structural features present further west. The only slight difference is that the S_1 schistosity defined by typomorphic minerals is more intensely developed.

3.3.4.1A) F_1 Folds

Although many F_1 folds of various wavelengths and amplitudes (Plate IVb, IVc, IVd) have been recognized in areas to the west (Goulet, 1986, 1987; Wares *et al.*, 1988) few have been recognized in the study area. There is no large scale repetition of the stratigraphy in this area due to F_1 folding, except perhaps one small anticline in the hanging wall of thrust fault b (Map III) in the heart of the N trending (F_1') syncline west of Lac Raymond (Map III). The F_1 anticline is cored by the middle iron member of the Baby Formation intruded by glomeroporphyritic gabbro sills. It is flanked to the south by the thin sheared base of the basalts and to the north by the rest of the basalt sequence. Interference patterns between drag folds associated with this fold and the later set (F_1') are compatible with the presence of an F_1 axial trace coring this iron formation (Plate IVe & IVf). The trace of this fold is

however somewhat conjectural because the iron formation could also cut up section eastwards into the Hellancourt volcanics as suggested by the general eastward thinning of the upper member of the Baby Formation.

Only a few small-scale F_1 folds were observed in the calc-silicate and dolomitic marble units (Plate Va) and the iron formation (Plate Vb). An axial planar schistosity S_1 is commonly intensely developed, and the bedding surfaces are transposed into it, obliterating the fold closures (Plate IVe & Va) or rendering measurements of the fold axes problematical. The few that were measured are typically down the dip of the S_1 schistosity (reclined folds), commonly with steep plunges.

On the outcrop scale, numerous examples of folded quartz veins with S_1 as their axial planar cleavage are visible (Plate Vc). These folds are typically isoclinal with sheared fold closures. There is no compelling reason to believe that these early metamorphic quartz veins were systematically emplaced parallel to the bedding surfaces, hence the fold axes of these veins do not necessarily reflect the true attitude of F_1 folds on the bedding surfaces. Those that were measured plunge vertically or steeply to the east (annex I).

The original trend of the F_1 folds is impossible to determine simply from their orientation on outcrops due to the superposition of two folding events. In the core of the regional-scale F_1' fold, NW of the Renia Gneiss, a coaxial interference (type 3, Ramsay, 1967) pattern was noted (Plate IVe). The F_1' folds in the study area are thought to have been originally NNE to NE trending, westerly overturned folds (see following section dealing with D_1'). This implies that F_1 have roughly similar trends ($\pm 40^\circ$) and possibly vergences. Their fold axes can diverge up to 40° of solid angle and still retain the interference pattern of plate IVe. The vergence of the F_1 folds is

not well constrained. No information can be gleaned from the ones observed in the upper iron formation (Plate IVe & Vb), from the limited number of folds in the dolomitic marbles near the Renia Gneiss (Plate Va) the F_1 folds would be roughly westerly vergent. This sense of vergence for the F_1 folds is in good agreement with the WNW vergence noted by Hynes (1978) for the F_1 folds of the central portion of the hinterland zone. Most of the Labrador Trough displays a WSW vergence approximately perpendicular to the trend of the Orogen, such as in the central Trough (Baragar, 1967; Séguin, 1969; Harrison *et al.*, 1970; Dimroth, 1970, 1972, 1978, 1981; Dimroth *et al.*, 1972; Dressler, 1979) and portions of the central and western zones of the northern Labrador Trough (Goulet, 1987; Hoffman, 1988; Wares *et al.*, 1988; Plate IVc & IVd).

3.3.4.1B) Faults

There are two types of fault associated with D_1 : thrust faults within the metamorphosed cover sequence and a basal décollement surface at the cover-basement interface of the Renia Gneiss.

i) The basal décollement

The strong evidence for shearing at the basement-cover boundary on the Renia Synform (Plate Ib & Va) may be indicative of a basement-cover décollement similar to the one inferred farther west in the trough. The Moyer Dome also displays a zone of high strain at the basement cover-interface (S. Perreault, pers. comm. 1988). The Boulder Dome was studied very briefly; only late brittle features were observed along its southern margin (Plate IIc & IId), but a high strain zone may well be present. The shearing of the topmost portions of the various gneiss bodies is thought to be the product of movement along a basal décollement surface but may also be due to flexural sliding

during the development of the large basement cored F_1' folds and F_3 folds.

Though the three exposures of basement gneisses in this area display contrasting structural morphologies, there is good if not complete evidence for a master décollement surface bounding the Archean basement exposures of the westernmost hinterland zone of the northern Labrador Trough (map I).

ii) Thrust faults

In this area, there are two major thrust faults that repeat the middle and upper portions of the stratigraphic column (map II). The first one (a on Map III) is situated in the NW and N portion of the study area. It is responsible for the thrusting of the lower member of the Baby Formation onto the northwesternmost exposure of the Hellancourt basalts. This fault is cut off to the west by the N trending Lac Rachel Fault. The uppermost portion of the basalts is locally sheared but no clear kinematic indicators were noted.

The second thrust fault (b on Map III) occurs further to the SW in the heart of a large F_2 syncline that wraps around the northern closure of the Renia Gneiss. It places the middle and upper members of the Baby Formation, along with the rest of the overlying rocks, on top of the lower portion of the Thévenet Formation. This creates a structurally repeated band of iron formation and basalt. As in the case of the first thrust fault, local shearing of the footwall and hanging wall units was noticed but no clear kinematic indicators were observed.

From measurements of bedding cutoffs, using the iron formation and the basalts as marker horizons for the first and second thrust faults respectively, the horizontal displacement was a minimum of 15 km for the first thrust and 24 km for the second one.

For the western portion of the hinterland zone as well as the areas to

the west the D_1 deformation event is deemed responsible for: 1) the westward (WSW?) gliding of the cover sequence over the basement gneisses along a thin basal décollement surface, 2) the upward splaying of thrusts that do not involve basement gneisses, 3) the formation of rare fault-associated F_1 folds and 4) the development of a pervasive penetrative bedding parallel schistosity. Basement rocks are thought to have acted passively during this initial westwards telescoping of the supracrustal sequence.

3.3.4.2) The late first phase of deformation (D_1')

3.3.4.2A) Introduction

In addition to the D_1 event the western portion of the hinterland zone displays a post- D_1 deformation event characterized by large westerly vergent basement-cored nappes. These structures are thought to be post- D_1 since their fold morphologies differ markedly from those assigned to the F_1 event. Their fold closures clearly deform the S_1 schistosity and are much more rounded than those of the F_1 folds (Plate IVe, Vd & Ve). Interference patterns between these folds and the F_1 folds have been observed (Plate IVe & IVf). Although interference patterns do not necessarily indicate two distinct folding episodes, their presence along with the morphology differences are thought to be sufficient to invoke two events. However these post- D_1 features may indeed also represent a late stage development in the first phase of deformation.

These post- D_1 folds are pre- D_3 given that they are clearly refolded by the large NNW trending F_3 folds. The morphology and orientation of the nappe structures cannot be correlated to the D_2 event present to the west. Hence the deformation event responsible for the formation of the basement-cored nappes and associated folds has been termed D_1' .

3.3.4.2B) Folds

At this latitude, the westernmost hinterland contains five major isoclinal F_1' folds that involve both cover and basement rocks.

- The Moyer Dome displays two synclines; one on its northern closure and one on its eastern and southern side. The northern one involves only cover rocks (Gélinas, 1958a) while the one on the southern margin clearly folds the basement gneisses of the Moyer Dome (Clark, 1980; Map I & III). The two synclines may be continuous but critical information is missing from the NE margin of the dome (map II & III).

- The northern closure of the Renia Gneiss contains numerous examples at all scales of F_1' folding. There are three major sets of F_1' folds: 1) An upright isoclinal syncline with vertical to moderate plunges that folds most of the cover sequence around the northern end of the Renia Gneiss and 2) A syncline and anticline that folds the lowest units of the cover sequence into the basement gneisses of the northern closure of the Renia Gneiss. The closure angle of the cover-cored syncline is typically sharp while the closure of the basement-cored anticline is slightly more rounded, reflecting the competency contrast of the two rock types. The above mentioned cusped fold morphologies are characteristic of basement-cover folds in other orogens (Rosenfeld, 1968; Ramsay *et al.*, 1983; Duncan, 1984; St-Onge *et al.*, 1986).

On outcrop scale the folds are typically of parallel style (class IB to IC (Ramsay 1967)) deforming both the bedding and the S_1 schistosity (Plate Vd, Ve & VIa). The axial planes to these folds typically lack a parallel cleavage except in the hinge of the F_1' syncline west of the Renia Dome. A poorly developed spaced cleavage was observed in the extrados portions of some fold closures. There are some brittle failure features associated with the megascopic F_1' syncline NW of the the Renia Gneiss (Plate VIb).

A stretching lineation defined by typomorphic minerals, (mostly biotite in sedimentary rocks and plagioclase + hornblende in mafic rocks), or elongated clasts is often parallel to the fold axis (Plate VIc). Although it is not certain that this stretching lineation developed during the F_1' folding event, the observed spatial association between the intensity of the development of the stretching lineation and major F_1' hinge zones in conjunction with the parallelism with F_1' axes indicates that the two fabrics probably were coeval. Stretching lineation fabrics are a rare occurrence outside the hinge zones of F_1' folds.

Interference patterns between F_1' and F_3 folds are quite common. They are most often nearly coaxial, especially at the basement-cover interface, where minor F_1 folds are very common, particularly within the infolded band of sediments (Plate Ve & Vf). This coaxiality decreases slightly to the NW and W away from the contact (Plate VIId & VIe). Rare basin and dome patterns were observed within the heterogeneous amphibolite horizon W of Lac Renia (Plate VIIa & VIIb), near the trace of an F_3 synform which is at an angle to the regional NW trend of F_3 folds. This results in some local variations in the angular relationships between F_1' and F_3 .

In the highly attenuated synclinal keel between the Renia and Boulder Gneisses, F_1' and F_3 folds become indistinguishable. They could only be differentiated using their vergences with respect to larger scale features, such as the F_3 basement-cored gneisses and the F_1' syncline that refolds the mixed volcanic-sedimentary conglomerate horizon north of the Renia Gneiss.

On the SW limb and in the nose of the F_3 synform coring the Renia Gneiss the F_1' fold axes plunge either near vertically or steeply to the NE (annex I, domains 2, 3a & 3b). Further south on the SW margin the F_1' folds plunge to the NNE or the S reflecting interference with the later F_3 folds (Plate VIIa &

VIIb). On the NE margin of the Renia Gneiss the F_1' fold axes show a more scattered pattern with a general southward plunge (annex I, domains 4a & 4b).

The abundance of coaxial interference patterns between F_1' and F_3 folds is due to the steep easterly plunge of many of the F_3 folds along the NW closure of the Renia Gneiss (Annex I). For most of the northern trough and its hinterland the F_3 folds plunge moderately to the SE (Hynes, 1978; Goulet, 1986, 1987; Wares *et al.*, 1988; Poirier, 1989). The E plunge of the F_3 folds in the study area is thought to be due to the overlapping of the F_3 fold trace on the hinge zone of the large basement-cored nappe responsible for placing the Renia gneisses on top of their cover units. This would explain the departure from the more common orientation of the F_3 folds.

3.3.4.3) The second phase of deformation (D_2)

In the hinterland of the northern Labrador Trough, there are a few reported examples of E trending generally open folds that are similar to and have been correlated to the D_2 event (Bosdachin, 1986; Poirier, 1989). In the study area and in the general vicinity of the westernmost hinterland zone the post- D_1 and pre- D_3 folds are either isoclinal or very tight. A strongly developed stretching lineation fabric parallel to their fold axis can be observed near or in the major fold closures. Many but not all of the interference patterns with the subsequent F_3 folds approach coaxiality. This is also corroborated by the small angle between the axes of these folds and F_3 axes in most of the domains surrounding the northern closure of the Renia Gneiss (annex I). All above mentioned features are not readily compatible with the E trending shallowly easterly plunging open cross-folds that characterize the D_2 deformation further W (Goulet, 1987; Wares *et al.*, 1988), SW (Dressler, 1979) and to the NNW (Hardy, 1976; Fig. 11). The second folding

episode in this portion of the hinterland zone is thought to represent a late stage event in D_1 (D_1') and hence to be unrelated to the D_2 event present to the west.

3.3.4.4) The third phase of deformation (D_3)

In the region immediately to the east of Lac Rachel, the most prominent D_3 features are the two large NW trending basement-cored folds; the Renia Synform and the Boulder Antiform. F_3 folds are a common feature on many outcrops; they are by far the most common folds observed. They are usually tight with vertical to steep northeasterly or southwesterly dipping axial planes; most often there is a crenulation cleavage parallel to them. On the SW margin and in the nose of the Renia Synform the F_3 fold axes plunge usually steeply to the E (annex I, domains 2, 3a & 3b). On the NE margin of the dome they plunge moderately to steeply to the SE (annex I, domains 4a & 4b), more in line with the general trend and plunge of F_3 fold axes in the northern Labrador Trough (Goulet, 1986, 1987).

F_3 folds are typically asymmetric with symmetry related to the trace of the Renia Synform. Hence, the southerly flank contains mostly Z folds and the northern flank S folds. This indicates that hinge migration during the growth of the fold was minimal, the axial plane probably nucleated in its present position on the basement-cored synform. Amplitudes and wavelengths vary from millimetric to tens of meters in scale, but usually are from 5 to 50 cm.

On outcrop, F_3 folds can usually be distinguished from the earlier F_1' folds by their sharper fold closures (Plate VIIc), their axial planar cleavage and of course, where applicable (in the hinge of the Renia Synform) their different orientation. The most widespread F_3 feature on outcrops is crenulation (Plate VIId). Locally the F_3 event becomes more pronounced,

developing an axial planar metamorphic layering, that almost completely masks the D_1 event (Plate VIIe). These could be termed D_3 shear bands. Near the contact of the basement and cover rocks, where the deformation and metamorphism are more intense, the different folding episodes become harder to distinguish. This is especially true near and inside the infolded cover sequence at the northern tip of the Renia Synform. In this area, the F_1' and F_3 fold axes typically form coaxial interference patterns (Plate Ve & Vf).

3.3.4.5) Late tectonic features

In addition to the Lac Rachel fault there are two late structural features present within our study area; brittle failure along the southwest margin of the Boulder Dome and small faults within the cover sequence.

3.3.4.5A) Brittle failure on the SW margin of the Boulder Dome

Locally, the southwestern margin of the Boulder Dome exhibits evidence of late stage brittle failure; 1) Aplitic dykes cross-cutting the granitic gneisses are offset left-laterally along regularly spaced (~20 cm) vertical faults, trending 320^0 , parallel to the basement-cover contact (Plate Ic). 2) A 3 m wide by 10 m long (minimum length) tectonic breccia, trending parallel to the basement-cover contact, is composed of gneissic fragments set in a fine-grained material of roughly similar composition (Plate Id).

A tectonic breccia involving only calcareous cover units was observed along the basement cover interface of the Moyer Dome (S. Perreault, pers. comm. 1989).

3.3.4.5B) Transverse faults

In the area bordering the NW closure of the Renia Synform, these faults

are not as well developed. Several sinistral faults oriented at 320° were observed within the metamorphosed equivalents of the Thévenet Formation NW of the tip of the Renia Gneiss (Plate VIIIf). The maximum observed displacement was 1 m. The orientation and sense of movement of these faults is similar to the ones observed along the SW margin of the Boulder Dome (Plate Ic) that are spatially related to a late tectonic breccia (Plate Id). No NE trending faults were observed, so that there is no evidence that the NW oriented ones are part of a conjugate set. The late NW trending sinistral faults in this area could have been developed during either D_3 or as a later feature.

3.4) Summary

Three possible models can be invoked to account for the roughly en échelon sequential disposition of antiformal and synformal basement gneisses of the western hinterland zone: diapirism, sheath folding and refolding of early basement-cored nappe structures.

i) Diapirism

In the diapir model the gneisses would represent sections through mushroom shaped diapirs. However the gneisses lack some of the features that are unique to diapirs such as outwardly vergent cascading folds. The morphology of the four gneiss bodies as a whole cannot be accounted for by one simple mushroom shaped diapir.

ii) Sheath folding

In the sheath fold model the synformal gneisses, Renia and Scattered, would represent deep sections through mega-sheath folds. The antiformal gneisses, Boulder and Moyer, would represent shallower sections through mega-sheath folds. The shortcomings of this model are: the lack of any mesoscopic examples of sheath folding, the lack of a widespread stretching lineation

fabric and the thinnest of the high strain zone at the basement-cover interface. The two last points are not deemed compatible with large scale basement-cored sheath folding.

iii) Upright refolding of earlier basement-cored, Pennine style, nappe structures

In this model a portion of the overthrust cratonic basement was folded along with its overlying para-autochthonous cover succession into large NNE-NE trending WNW-NW vergent nappe structures, designated as F_1' folds. These folds were then uplifted along with the underlying autochthonous basement by large amplitude, NW trending upright to SW overturned, folding related to the third deformation event. The early nappe structures are thus exposed as basement-cored F_3 synforms (Renia and Scattered Gneisses) and the autochthonous basement as F_3 antiforms (Boulder and Moyer).

If the refolded basement-cored nappe model is accepted as the choice model to explain the features of the basement gneisses, five tectonic events are thought to have taken place in the western portion of the hinterland zone. They record a protracted period of crustal shortening in the eastern internal portion of the orogen. One of these events (D_1') appears to be restricted to the hinterland zone; the others can be linked to deformation events in the better studied western part of the trough. The following sequence of events is thought to have taken place:

1) The first phase of deformation (D_1) records: i) the westerly translation of the cover sequence over the Archean basement gneisses along a thin basal décollement plane, ii) the upward splaying of westerly directed thrust faults from the décollement surface; these thrusts do not seem to involve basement rocks, iii) the formation of rare fault associated F_1 folds and iv) the development of a well defined bedding sub-parallel schistosity. Basement rocks are interpreted to have acted passively during this initial

phase of deformation.

2) The overthrust basement gneisses were then folded along with their para-autochthonous cover sequence into large NNE to NE trending, WNW to NW vergent nappe structures.

3) The only evidence in our study area for the presence of the E to NE trending open cross-folds that characterize the second deformation event (D_2) lies in the doubly plunging nature of the basement-cored antiforms (the Boulder and Moyer Domes). This is assuming that the later sets of F_3 folds do not depart from cylindrical. These F_2 would have large wavelengths of up to 40 km. In the central portion of the hinterland, open E trending F_2 folds have been reported (Bosdachin, 1986; Poirier, 1989).

4) The area along with most of the northern trough was then subjected to large amplitude NNW trending, E to SE plunging, upright to SW vergent folds of the third deformation event (D_3). These F_3 folds are responsible for the sequential disposition of synformal and antiformal basement bodies and the large amount of structural thickness visible in oblique section at the surface.

5) the final event includes the unroofing of the imbricated and folded basement-cover complex by the reverse motion on the steeply E dipping Lac Rachel fault. This fault may have a dextral-strike slip component (Goulet, 1987). Small scale longitudinal and transverse brittle faults are also locally developed.

4.0) METAMORPHISM:

4.1) Setting and previous work

The Labrador Trough has been the subject of numerous studies. Most were either regional mapping projects or dealt primarily with structural or stratigraphic aspects. There are only two studies dealing specifically with the metamorphism of the Labrador Trough; Gélinas (1965, unpublished manuscript) and Dimroth & Dressler (1978). The former author studied an area in the northern Labrador Trough (Fig. 5), spanning the upper-greenschist facies up to locally preserved granulite facies. The study area is contained within the lower-grade portion of this area. Dimroth & Dressler (1978) did a comprehensive, larger scale study involving most of the central Labrador Trough. The metamorphic zones within and adjacent to the Labrador Trough are shown in Figure 21. Their study covers the western and central zones and the westernmost portion of the hinterland zone. The following summary is taken from their work.

The first metamorphic episode affected only the Superior craton granitoid gneisses. Conditions attained upper amphibolite to granulite facies during the Kenoran Orogeny (approx. 2700 Ma). In the northernmost Labrador Trough the Archean gneisses are clearly involved in the Hudsonian tectono-metamorphic episode. The basement inliers within the western hinterland zone are strongly retrogressed to the upper-greenschist facies.

The second metamorphic event is local contact metamorphism of sediments, usually fine-grained siltstones and shales, adjacent to mafic-ultramafic intrusives. These intrusives usually occur within the central allochthonous zone. They form the feeder system for the overlying mafic volcanism.

The third and most prevalent episode took place during the compressional

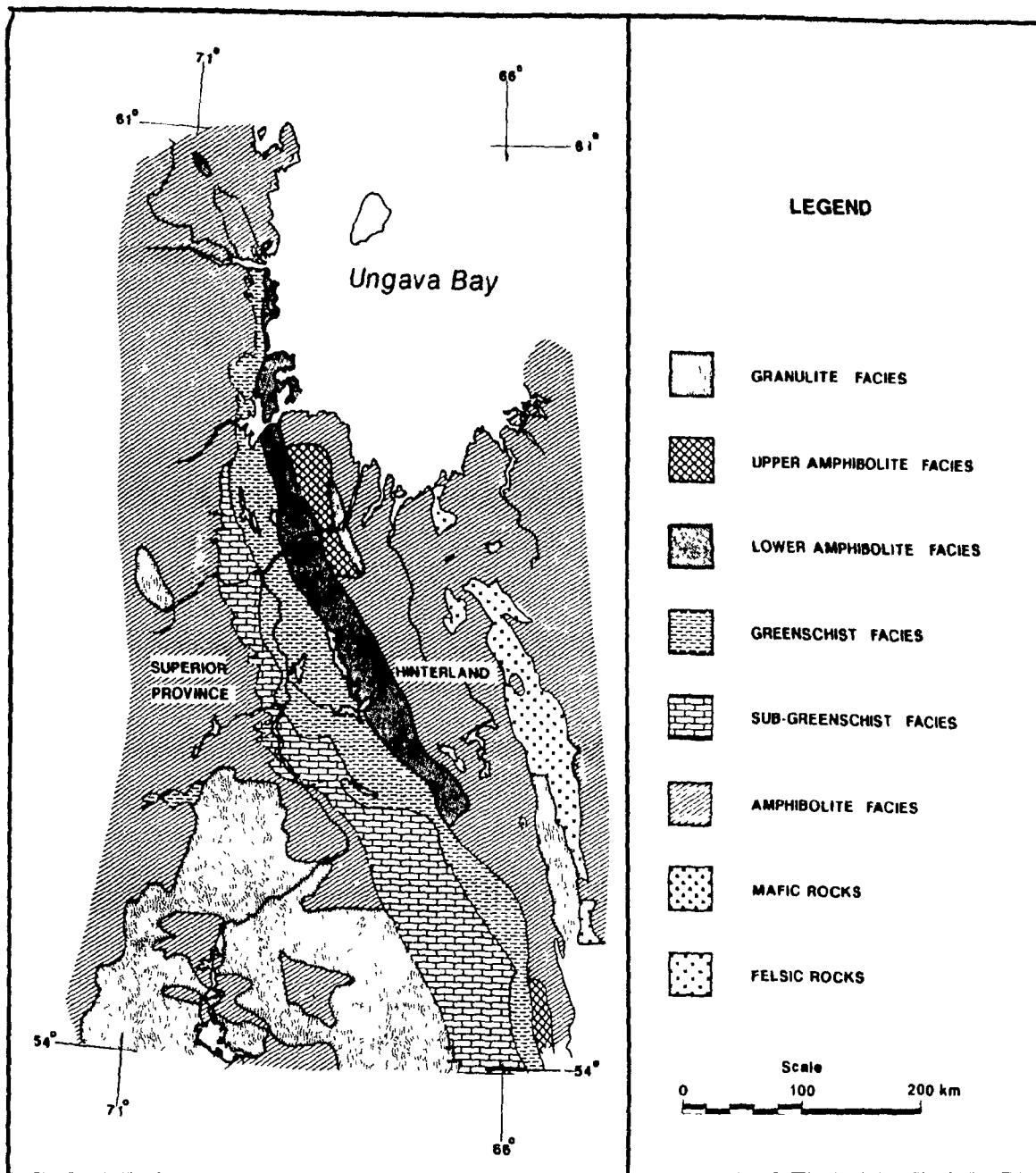


Figure 21: Metamorphic zones of the Labrador Trough, its eastern hinterland zones and the adjacent Superior craton, from Fraser *et al.* (1978).

phase of the Hudsonian Orogeny at 1783-93 Ma (Machado et al., 1988). It affects all the Archean volcano-sedimentary assemblage of the Labrador Trough and the local Archean basement culminations within it. Metamorphic grade increases from west to east and south to north, from sub-greenschist facies in the western autochthonous - para-autochthonous zone to granulite facies in the hinterland zone. The granulite facies are well developed in the hinterland of the central Labrador Trough (Taylor, 1979) but occur only locally and are strongly retrogressed in the hinterland of the northern Labrador Trough (Perreault et al., 1988; Poirier, 1989).

Relations between metamorphism and deformation vary systematically across different zones of the Labrador Trough (Dimroth & Dressler, 1978). In the sub-greenschist facies, the peak metamorphic assemblage predates the main Hudsonian deformation event. Within the greenschist facies the typomorphic minerals, (chlorite & muscovite) are parallel to the main schistosity (S1) indicating peak metamorphic and deformation conditions were attained synchronously. The transition to the amphibolite facies closely parallels the eastern limit of the Labrador Trough (*sensu stricto*). The greenschist-amphibolite boundary corresponds generally to the eastern limit of the basalt sequence within the central allochthonous zone. In the northern Labrador Trough, this transition occurs slightly west of the easternmost exposures of mafic volcanics (Gélinas, 1965; Boone, 1987). Metamorphic index minerals (garnet, staurolite, kyanite, sillimanite) in the lower amphibolite facies vary from syn- to late kinematic. In the upper amphibolite and granulite facies, the peak metamorphic assemblages are post-kinematic.

The traces of isograds trend NNW to NW generally following the main structural grain. However, the trace of the biotite isograd is somewhat more erratic. The dip of the isograd surfaces varies from shallowly W dipping for

the biotite isograd within the greenschist facies to steeply W dipping for the isograds within the amphibolite zone (garnet, sillimanite) (Dimroth & Dressler, 1978). The authors attributed the differences in amount of dip to greater uplift of the hinterland zone versus the central and western zones.

Several isograds were mapped in the northern Labrador Trough by Gélinas (1965) and more recently by Boone (1987), Gélinas and Perreault (1985), Moorhead and Hynes (1986), Perreault *et al.* (1987, 1988) and Poirier (1989), (Map I & III). Our study area is bounded to the west by the albite / oligoclase isograd within the mafic volcanics and to the east by the sillimanite isograd. It contains the garnet, the staurolite, and the kyanite isograds. The garnet isograd follows the western shoreline of Lac Rachel where pin-sized euhedral garnets are visible within micaceous schist belonging to the lower member of the Baby Formation. The staurolite and kyanite isograds are closely associated and nearly overlap each other. The kyanite isograd occurs slightly to the east of the staurolite isograd (Poirier, 1989; Map III). The traces of these two isograds, particularly the kyanite one, cannot be mapped continuously and with as much certainty as the garnet isograd because of the relative scarcity of pelitic horizons within the more abundant semi-pelitic micaceous schist unit. The traces of all three isograds trend to the N, approximately parallel to the Lac Rachel reverse fault; a late tectonic feature. The isograds clearly cut major F_3 folds in the area (Gélinas, 1965; Map III) and have been interpreted as being post-kinematic (Moorhead & Hynes, 1986; Perreault *et al.*, 1987; Poirier, 1989).

Cross-cutting relationships are visible at all scales. In thin section, metamorphic index minerals close to their respective isograds clearly are post F_3 folding. In thin section, staurolite porphyroblasts locally overgrow F_3 fold closures (Plate VIIIa & b) and kyanite has been observed cross-cutting

limbs of F₃ crenulations.

Extensive recent work has been done on the metamorphism of the units to the east of our study area (Perreault & Gélinas, 1985; Perreault *et al.*, 1987, 1988; Poirier, 1989; Poirier *et al.*, in press). The following summary is largely taken from Poirier (1989). Two isograds occur east of the three Archean basement domes; the staurolite-out isograd in the footwall of the Lac Olmstead fault and the muscovite-out isograd in the footwall of the Lac Turcotte fault (map I). Both of these isograds are parallel to the adjacent faults. East of the Lac Turcotte fault, in the arc related suspect terrane, there is evidence for an older granulite grade metamorphic event synchronous with the emplacement of I-type calc-alkaline granitoid intrusives. The metamorphism has been dated at 1833-1829 Ma (Machado *et al.*, 1988).

4.2) GENERAL PETROGRAPHY

Introduction:

Although this study area is not extensive, encompassing approximately 120 km², it contains all the stratigraphic units, or their correlatives, of the northern Labrador Trough. The rocks can be divided into five groups which are, from oldest to youngest:

- (1) Granitic - granodioritic gneisses of the Archean basement.
- (2) Various calcareous rocks that include:
 - Mafic marls or heterogeneous amphibolite that are mineralogically similar to the metabasites but are richer in quartz and calcite.
 - Dolomitic marbles
 - Calc-silicate rocks
 - Calcareous schists
- (3) Micaceous schists that vary between psammitic and pelitic in

composition. The semi-pelites represent by far the most common member.

(4) Meta iron formation

(5) Meta ultramafics

4.3) Mineral petrography

4.3.1) Garnet:

Garnet is a common mineral within pelitic schists, semi-pelitic schists and iron formations. It also occurs locally within the more mafic, hornblende rich calcareous unit, namely the heterogeneous amphibolites. Garnets are usually disseminated within their host lithologies; some are, however, concentrated in 10 to 50 cm thick horizons that contain between 10 and 50 % garnets. These garnet rich horizons are a common feature within pelitic schists and in the garnet amphibolites which are part of the heterogeneous unit of the calcareous rock assemblage. Both of these lithologies are found near the basement gneisses of the Renia Synform. Garnets vary considerably in size from < 1 mm in the semi-pelitic schists close to the isograd in Lac Rachel to up to 35 mm in pelitic horizons adjacent to the Renia gneisses.

In thin section, garnets are usually idiomorphic to subidiomorphic. They are only slightly altered in the pelitic and semi-pelitic schists. In the garnet amphibolite horizons they are, more often than not, highly retrograded to chlorite. Garnets contain numerous and varied internal structures. Quartz and opaques are common inclusions within garnets. They typically are concentrated within the core of the mineral; the rims are often inclusion free. The inclusion trails are aligned most often as straight barrels parallel to the main schistosity in the host rock. Locally the alignment of the inclusion trails is at an angle to the matrix foliation. The angle

between the aligned inclusion trails and the matrix foliation (S_1) usually is small, only rarely were helicitic textures observed. The drag folds defined by the angle between the matrix schistosity and the aligned inclusion trails within the garnets locally reflect mesoscopic F_3 fold sets (Plate VIIIc). This is commonly observed within the infolded sediments at the northern tip of the Renia Synform.

4.3.2) Biotite:

Biotite is a ubiquitous and abundant mineral within the micaceous schist unit. Along with muscovite it most often defines the major schistosity (S_1), and locally forms a stretching lineation fabric. In some instances biotite is retrogressed to chlorite. Biotite is also a common if not abundant constituent of the heterogeneous amphibolite unit. Within these amphibolites it occurs in two distinct habits; as a prograde mineral and as a retrograde phase at the expense of hornblende.

4.3.3) Muscovite:

Muscovite is a common constituent of the micaceous schist where it occurs either as well aligned crystals locally forming solid mats or as larger prismatic crystals overgrowing the main schistosity. Muscovite blades also define the axial planes of some (F_3) crenulations.

4.3.4) Staurolite:

Staurolite is found in pelitic schist horizons typically rich in opaques and is commonly associated with garnet and kyanite. It forms subidiomorphic crystals up to 15 mm long that are sometimes twinned. The crystals are often riddled with quartz inclusions; the concentration of inclusions diminishes

towards the edges. The habit of Staurolite is typically post-kinematic, overgrowing F_3 fold crests (Plate VIIIa & b) and cross-cutting the S_1 schistosity.

4.3.5) Kyanite:

Kyanite occurs in two distinct settings in the study area. The first is as long bluish blades (up to 10 cm long) in quartz rich pegmatitic lenses within the lower micaceous schist unit. The most prevalent occurrence is, however, as prismatic yellowish translucent crystals up to 1 cm long disseminated in garnet rich pelitic horizons. The growth of kyanite is typically post-kinematic, cross-cutting previously developed features such as the S_1 schistosity and limbs of F_3 crenulations.

4.3.6) Chlorite:

Chlorite is another ubiquitous if not abundant phase. It occurs as a prograde phase in micaceous schists up to the staurolite isograd. Above, it was only observed as a retrograde mineral growing at the expense of biotite or garnet. In the metabasites of sedimentary or igneous origin, it was observed pseudomorphing hornblende and garnet.

4.3.7) Hornblende:

Hornblende forms an important constituent of the various amphibolite units and the iron formation. It also is found disseminated in the micaceous schists. It usually forms subidiomorphic crystals, but occurs locally as long, (up to 7 cm), slender feathery crystals within the iron formation and the heterogeneous amphibolite unit.

4.3.8) Tremolite - Actinolite:

These minerals occur as abundant phases within the dolomitic marbles and the calc-silicate rocks respectively. They occur as elongated crystals that are commonly found radiating from a common "nucleus". These nuclei are often aligned parallel to bedding planes forming strings of radiating tremolite-actinolite crystal clusters (Plate Ie).

4.3.9) Plagioclase:

Plagioclase occurs as xenomorphic crystals in amphibolites and micaceous schists. In the latter unit it occurs as disseminated grains within a mosaic of granoblastic quartz.

4.3.10) Epidote:

Epidote forms a small component in the various metabasite units. It occurs typically as xenomorphic aggregated grains.

4.3.11) Accessory Minerals:

i) Tourmaline occurs as subidiomorphic grains in pelitic and semi-pelitic horizons. It is typically zoned with bluish green cores and green rims. Tourmaline is found mostly in the matrix but also occurs locally as inclusions within garnets.

ii) Opaques are a common feature in most rocks. They consist of ilmenite which is locally associated with rutile. They are commonly observed as inclusions within garnets.

iii) Zircons are commonly visible in pelitic horizons where they are present as inclusions within biotite.

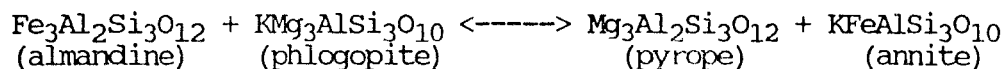
4.4) Quantitative petrology:

4.4.1) Introduction:

The use of various geothermometric and geobarometric calibrations permits the calculation of maximum P & T values that the rocks have undergone. In some cases, portions of the P/T loop that the rocks were subjected to may be unravelled. This allows the characterization of tectonic processes that were operative during the burial & uplift stages of orogens (Spear et al., 1984). Geothermobarometric calculations were undertaken in our study area in order better to constrain temperature and depths of burial the rocks were subjected to. Due to the post kinematic nature of the metamorphism in this area, (Moorhead & Hynes, 1986; Perreault et al., 1987) no information is gained from this type of study on the motions of the early thrust faults. The data however are a good complement to the burial depths required by the down plunge projection of the basement ~~meisses~~ in the previous chapter.

4.4.2) Geothermometry

Temperature calculations are based on the Fe/Mg cation exchange between garnet and biotite. Biotite and garnet are used because of their abundance and widespread occurrence for different bulk compositions of metamorphosed siliciclastic rocks. The Fe/Mg exchange is essentially a function of temperature, pressure having only a very slight effect on the Fe/Mg partitioning. All the geothermometers involving garnet and biotites are based on the following exchange:



Thompson (1976) empirically calibrated the reaction using naturally occurring assemblages and temperatures based on other experimental phase equilibria. Ferry and Spear (1978) experimentally derived the first

calibration of the above mentioned reaction. The bulk composition of the experiments was kept at 0.9 (Fe/Fe + Mg). The Ferry and Spear (1978) calibration is applicable to garnets of restricted composition (>80% almandine + pyrope components). Most garnet rim composition of this study are within/or approach these compositional limits. The limits are generally exceeded for the garnet cores that are typically richer in Ca and particularly Mn. Ferry and Spear (1978) suggested the limit of $0.15 (Al^{Vi} + Ti)/(Al^{Vi} + Ti + Fe + Mg)$ for biotite, this limit is attained or generally slightly exceeded for the biotites of this study area. Perchuk & Lavrent'eva (1983) also experimentally calibrated the reaction but kept the composition of their experiments at 0.6 (Fe/Fe + Mg).

The Ferry and Spear (1978) calibration assumes ideal mixing for the 4 major cations (Fe, Mg, Ca, Mn) within the garnets. The assumption can be justified if the following is true: 1) the deviations from ideality in garnet and biotite are small or 2) The deviations from ideality in garnet and biotite tend to cancel out (Chipera & Perkins, 1988). The study of Hodges and Spear (1982) found that only Ca-Mg mixing in garnet departed significantly from non-ideality over the T^0 and P range of their study, which contains the range present in our study. They compensated for the non-ideality by the introduction of activity coefficients.

4.4.3) Geobarometry

The samples taken along a section perpendicular to the isograds display varying mineralogical assemblages. These variations are not uniquely a function of metamorphic grade but reflect variations in the bulk compositions. The pelitic horizons containing an aluminosilicate phase (kyanite) are widespread only near the contact with the basement gneisses of

the Renia Synform. They occur only sporadically higher in the succession towards the kyanite and staurolite isograd. The most common garnet bearing assemblage found between the staurolite and garnet isograds contains:

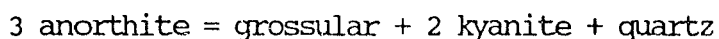
~~quartz-biotite-garnet-muscovite-chlorite-opaques+plagioclase+tourmaline~~

For the samples taken at or near the garnet isograd no plagioclase was observed. In order to be able to assess pressure values for the whole of the study area, in light of the differing assemblages, three main geobarometers were employed.

The reactions used to determine paleopressures values are based on volume dependent cation exchanges between coexisting phases, or changes in coordination site of an element within a phase. These are not completely independent of temperature, so an independent estimate of T must be made in order to constrain the pressure. This is not a major problem since the Fe/Mg exchange between garnet and biotite end members is essentially independent of pressure.

1) ~~Garnet-kyanite-silica-plagioclase (GKSP)~~ (Newton & Haselton, 1981)

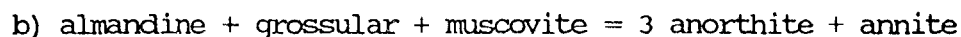
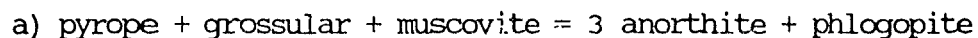
This assemblage has been modeled for the Ca end member equilibrium:



The Ca exchange in this reaction is between a low density and higher density phase and thus is sensitive to ambient pressure changes. Ghent (1976) assumes ideal mixing for the Ca exchange, whereas Newton & Haselton (1981) use activity coefficients for the same exchange.

2) ~~Garnet-plagioclase-biotite-muscovite (GPPM)~~ (Ghent & Stout, 1981)

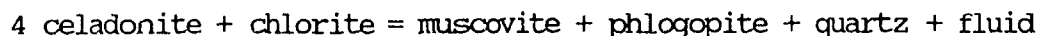
This assemblage can be modeled by the following equilibria:



Equilibria (a) and (b) involve a change in Al coordination from 6 to 4 and change in Fe/mg coordination from 8 to 6 and should be sensitive to pressure. Ghent & Stout (1981) used the garnet-plagioclase-kyanite-quartz geobarometer (Ghent, 1976) in conjunction with the Ferry and Spear (1978) geothermometric calibration to derive an empirical geobarometer.

3) ~~Biotite-muscovite-chlorite-quartz~~ (EMCQ) (Powell & Evans, 1983;
Bucher-Nurminen, 1987)

This mineralogical assemblage can be modelled by the following equilibrium:



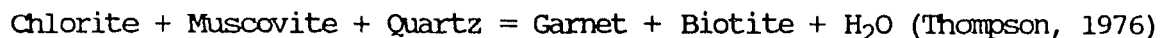
This equilibrium involves a change in the coordination of Al in muscovite from tetrahedral to octahedral with increasing pressure. The fluid dependency of this calibration is an additional handicap that most other geobarometers do not have. This study did not evaluate the composition of the metamorphic fluid, so an assumption is made that it is pure H₂O. This seems to be a reasonable assumption considering that studies of fluid compositions in pelitic rocks often yield almost pure H₂O (Ghent *et al.*, 1979).

The first geobarometer (GKSP) is applicable to the kyanite bearing assemblages that occur in the Lower Baby schists adjacent to the Renia basement gneisses. Given the ubiquitous occurrence of the assemblage garnet-plagioclase-biotite-muscovite the second geobarometer (GPBM) can be applied almost to all of the study area. The third one (EMCQ) is needed because of the lack of plagioclase as a phase in the semi-pelitic schists at the garnet isograd. It can be applied up to the staurolite isograd which also marks the disappearance of prograde chlorite.

4.4.4) Approach and assumptions

The garnets exhibit "normal" or prograde chemical zoning (Hollister,

1966; Tracy et al., 1976) characterized by Ca & Mn rich cores and Fe & Mg rich rims (Fig. 22). The Mg/Fe ratio increases from the core outwards. The prograde zonation is consistent for all the metamorphic zones of the study area. The bell shaped profiles are however much more flattened for the garnets in the kyanite zone than for those in the garnet zone. This chemical zonation is consistent with a trend of garnet compositions involved in the continuous Fe-Mg-Mn reaction:



From the element distributions in the limiting binary systems it is predicted that $T^{\text{O}}_{\text{Mg}} > T^{\text{O}}_{\text{Fe}} > T^{\text{O}}_{\text{Mn}}$, where T^{O}_{Mn} represents the temperature of the reaction in the pure Mn system at constant pressure and H_2O (Tracy et al., 1976.). The above mentioned chemical zonation of garnets reflects its internal diffusion rates being slower than its growth rates under sub-granulite conditions (Woodsworth, 1977). Often the garnets show a reversal of zonation trends at their margins (Fig. 23). These retrograde rims are typically small with respect to the size of the garnets. Textural evidence for the observed reversal in chemical zonation is only present with some of the more pronounced reversals in the zonation patterns at their rims (Fig. 22). This is usually in the form of retrograde chlorite growing at the expense of garnet and/or biotite.

In many studies chemical zonation has been reported also for plagioclase, where typically anorthite content increases with metamorphic grade due to Ca exchange with garnet. In this study area the plagioclase grains displayed only slight, oscillatory and/or contradictory zonation patterns, often within the same sample. The phyllosilicate phases are characterized by high internal diffusion rates and are typically unzoned.

Given the prograde nature of the chemical zonation within the garnets,

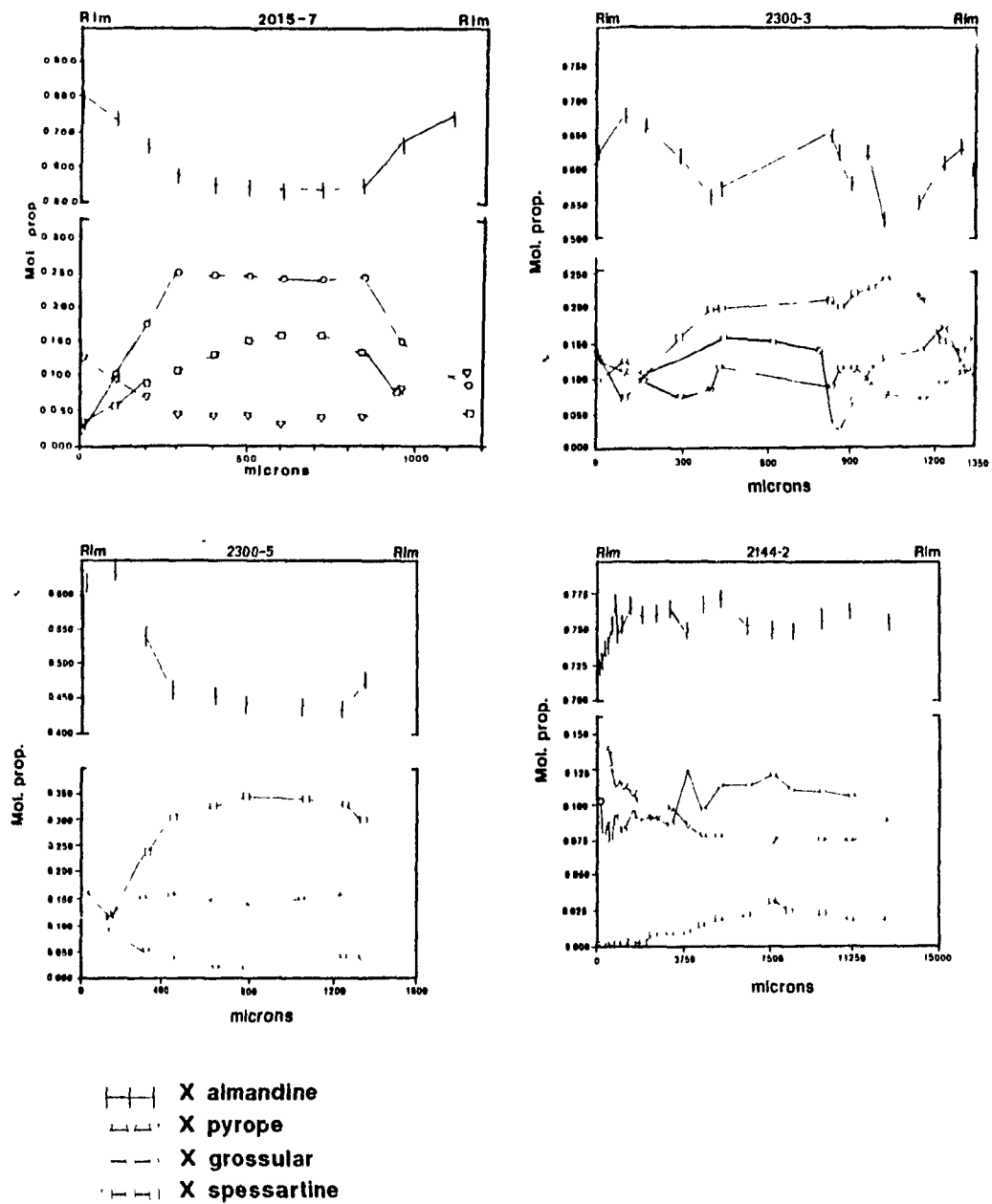


Figure 22: Prograde chemical zonation profiles accross garnets from different metamorphic zones.

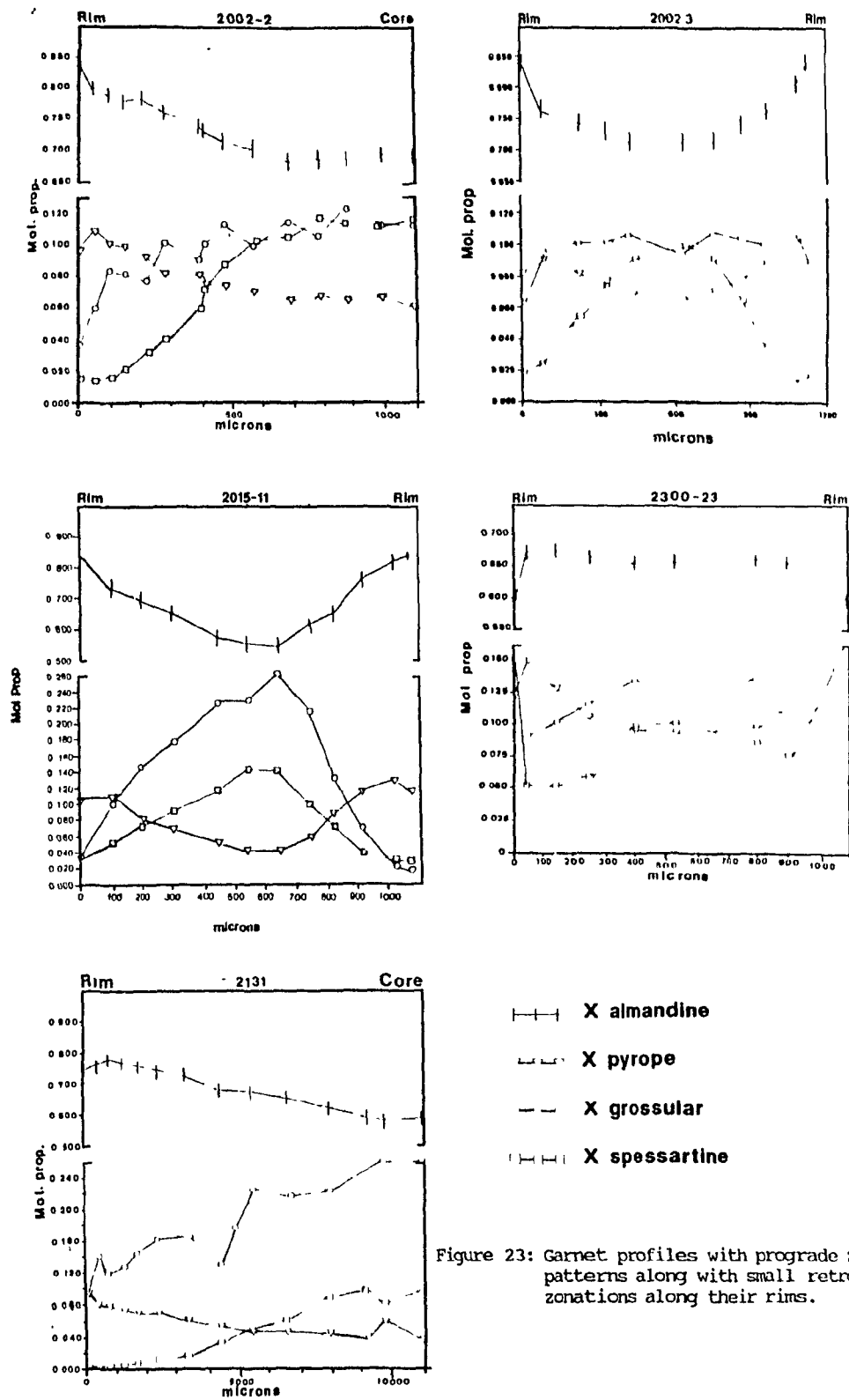


Figure 23: Garnet profiles with prograde zonation patterns along with small retrograde zonations along their rims.

the maximum temperature and pressure values can be obtained using the rim compositions of the garnets and the matrix biotite and plagioclase compositions. This assumes that all the coexisting phases have attained equilibrium. Biotites in contact with the garnet were not used in order to avoid the possibility of post-metamorphic peak cation exchange (Tracy et al. 1976). Where retrograde rims in the garnets were observed a composition point on the inside of the rim was used.

Temperature values can be derived from the core of the garnets if the following assumption is made. In samples where biotite is much more abundant than garnet, the biotite may have acted as an infinite cation reservoir. In this way the bulk amount of garnet is not high enough to change significantly the Fe/Mg ratio of the matrix biotite. Care was taken to choose the largest garnets within the section in order to get a section cut closest to the core of the garnet. The same reservoir assumption cannot be made for plagioclase which is not significantly more abundant than garnet and thus cannot be considered an infinite reservoir of Ca cations. In addition the garnets are zoned with respect to Ca and the plagioclase are either unzoned or erratically zoned, indicating that there is no simple relationship of Ca content with respect to these two phases. This means that the pressures under which the cores of the garnets nucleated and grew cannot readily be quantified. The rims of the garnets are assumed to be in equilibrium with the rims of adjacent plagioclase grains.

4.4.5) Sources of error

Several factors influence the pressure and temperature values determined from cation exchange calibrations between phases. The error brackets reported in various studies are typically ± 50 °C and ± 1 kbar. These bracket include

only the uncertainties related to the positioning of the equilibrium curve in P-T space (Hodges & McKenna, 1987).

One of the main uncertainties regarding thermobarometric studies is the assumption that chemical equilibrium was attained between coexisting phases. In order to better constrain the peak metamorphic conditions sections showing evident signs of retrogression, such as the presence of retrograde phases, were not used. Textural equilibrium was established by the presence of straight sharp contacts between the different phases, this however does not exclude the possibility of chemical disequilibrium (Loomis, 1983). One of the possibilities that leads to such a case is strain induced post-equilibrium dissolution by shearing (Bell, 1985; Duebendorfer & Frost, 1988). This case can be discounted for this study given the post-kinematic nature of the peak metamorphic assemblages and the traces of their respective isograds.

Another type of uncertainty is the choice of solution models (Hodges & McKenna, 1987). Some minerals depart strongly from ideality with respect to certain components, such as Ca in garnet and plagioclase. The calibration of certain elements within some phases is still in debate (e.g. the activity coefficient of anorthite in plagioclase (Kozior & Newton, 1986)).

This study suffers a further uncertainty in that three different geobarometers are used to determine pressure. This leads to uncertainties not only in the absolute pressure values, that are influenced by the above mentioned factors, but also in comparing results from the different geobarometers (relative pressure differences between different metamorphic zones). Still the results presented here are in broad agreement with other petrological data and the results of other studies in the same general area (Perreault et al., 1987; Poirier, 1989).

4.4.6) Results

4.4.6.1) Geothermometry

Four geothermometers based on the Fe/Mg exchange between garnet and biotite were tested; Ferry & Spear, 1978 (FS); Hodges & Spear, 1982 (HS); Thompson, 1976 (T); Perchuk & Lavrent'eva, 1983 (PL). The results of which are summarized in Table I. For samples up to the kyanite zone, the Ferry & Spear (1978) solution model seems to underestimate peak T° values by 30 to 40 $^{\circ}\text{C}$ with respect to the other three solution models (HS, T, PL). In the kyanite zone the (FS) solution model is in closer agreement with the solution models of (T) and (PL). The (HS) solution model gives results close to those of the (T) and (PL) solution models, except for the kyanite zone where it gives T° values 30 to 40 $^{\circ}\text{C}$ higher. The (T) and (PL) solution models nearly always give results within 10 $^{\circ}\text{C}$ of each other of each other. The Hodges & Spear solution model is thought to be the most applicable to this study area, given: i) the importance of the Ca content in several of the garnets and ii) the Fe/Fe + Mg ratios for the garnet rims are all $>.82$ which is much closer to the values used in the experimental study of Ferry & Spear (1978) on which the Hodges & Spear (1982) solution model is based than those of Perchuk & Lavrent'eva (1983).

The peak temperatures (± 50 $^{\circ}\text{C}$) are thought to be:

- i) 510-550 $^{\circ}\text{C}$ at the garnet isograd
- ii) 530-560 $^{\circ}\text{C}$ in the garnet zone
- iii) 480-540 $^{\circ}\text{C}$ at the staurolite isograd
- iv) 520-650 $^{\circ}\text{C}$ in the kyanite zone

The peak temperatures at the staurolite isograd may be underestimated due to the strong amount of retrogression visible on the rims of the garnet and the high amount of retrograde chlorite in the sample.

TABLE 1

ZONE	GARNET SPECIMEN NO	Xgr	Xsp	BIOTITE Specimen no	T° Fs	T° Hs	T° T	T° Pl
Garnet Isograd	2002-2 "0" Retrograde rim	.05	.015	2002-9 AVG	462	481	505	515
	2002-2 "0" Retrograde rim	.05	.015	2002-15 AVG	464	483	507	517
	2002-2 "0" Retrograde rim	.05	.015	2002-10 AVG	465	484	508	517
	2002-2 "50" INNER RIM	.08	.013	2002-9 AVG	508	541	543	544
	2002-2 "50"	.08	.013	2002-15 AVG	511	543	546	545
	2002-2 "50" INNER RIM	.08	.013	2002-10 AVG	512	545	547	546
	2002-2 "885" CORE	.135	.114	2002-9 AVG	412	465	463	483
	2002-2 "885" CORE	.135	.114	2002-15 AVG	414	467	465	485
	2002-2 "885" CORE	.135	.114	2002-10 AVG	415	468	465	485
	2002-3 "0" Retrograde rim	.077	.018	2002-9 AVG	430	460	478	495
	2002-3 "0" Retrograde rim	.077	.018	2002-15 AVG	432	462	480	497
	2002-3 "0" Retrograde rim	.077	.018	2002-10 AVG	433	463	481	497

ZONE	GAPM1 Specimen no	Xgr	Xsp	BIOTITE Specimen no	T° Fs	I° Hs	I° I	I° Pl
Garnet Isograd	2002-3"100" INNER RIM	110	024	2002-9AVG	467	511	509	519
	2002-3"100" INNER RIM	110	024	2002-15AVG	469	514	511	520
	2002-3"100" INNER RIM	.110	.024	2002-10AVG	470	515	512	521
	2002-3"630" CORE	123	098	2002-9AVG	415	463	466	485
	2002-3"630" CORE	123	098	2002-15AVG	417	466	467	487
	2002-3"630" CORE	.123	098	2002-10AVG	418	466	468	487
GARNET ZONE (1/2 WAY TO STABLE ROLITE ISOGRAD)	2015-11"0" RETROGRADE RIM	.035	.031	2015-11AVG	476	489	517	524
	2015-11"1070" RETROGRADE RIM	020	.028	2015-11AVG	501	508	537	539
	2015-11"100" INNER RIM	.103	.049	2015-11AVG	514	556	548	547
	2015-11"1025" INNER RIM	.031	030	2015-11AVG	532	544	563	558
	2015-11"645" CORE	271	.142	2015-11AVG	364	476	421	451

ZONE	GARNET Specimen no	Δg_1	Xsp	BIOTITE Specimen no	T° Fs	T° Hs	T° T	T° Pl
Garnet Zone	2015-7"0" RIM	.039	.031	2015-73AVG	517	533	551	549
	2015-7"0" RIM	.039	.031	2015-71AVG	514	529	548	547
	2015-7"500" CORE	265	150	2015-73AVG	346	453	405	438
	2015-7"500" CORE	265	150	2015-71AVG	344	450	403	436
Stauro- lite Isograd	2300-5"0" RIM	.091	.160	2300-5-3	481	518	521	527
	2300-5"0" RIM	.091	160	2300-5-1M	471	507	513	521
	2300-5"0" RIM	.091	.160	2300-5-2M	476	512	517	524
	2300-5"780" CORE	171	.339	2300-5-3	278	339	343	387
	2300-5"780" CORE	.171	.339	2300-5-1M	273	333	338	383
	2300-5"780" CORE	.171	339	2300-5-2M	276	336	340	385
	2300-23"0" RETROGRADE RIM	118	149	2300-2-3	467	514	509	518
	2300-23"0" RETROGRADE RIM	.118	149	2300-2-3AVG	455	502	499	511

ZONE	GARNET Specimen no	Xgr	λ_{sp}	BIOTITE Specimen no	T° Fs	T° Hs	T° T	T° Pl
STAURO- LITE ISOGRAD	2300-23"50" INNER RIM	.114	.053	2300-2-3	492	539	530	534
	2300-23"50" INNER RIM	.114	.053	2300-23AVG	480	526	520	526
	2300-23"400" CORE	.156	.094	2300-2-3	386	447	440	466
	2300-23"400" CORE	.156	.094	2300-23AVG	377	437	432	459
	2300-3"0" RIM	.122	.132	2300-51AVG	436	484	484	499
	2300-3"0" RIM	.122	.132	2300-5AVG	448	496	493	506
	2300-3"440" CORE	.069	.191	2300-5-1M	431	457	479	496
	2300-3"440" CORE	.069	.191	2300-5-2M	435	462	483	499

ZONE	GARNET Specimen no	Xgr	Xsp	BIOTITE Specimen no	T° Fs	T° Hs	T° I	T° Pl
KYANITE ZONE	2144-4"0" RIM	.132	.001	2144-22AVG	569	626	592	579
	2144-4"0" RIM	.132	.001	2144-4AVG	589	646	607	589
	2144-4"0" RIM	.132	.001	2144-2AVG	561	617	585	574
	2144-4"7540" CORE	.144	.030	2144-22AVG	415	471	465	485
	2144-4"7540" CORE	.144	.030	2144-4AVG	401	457	543	476
	2144-4"7540" CORE	.144	.030	2144-2AVG	384	439	438	464

4.4.6.2) Geobarometry

4.4.6.2A) Chlorite-biotite-muscovite assemblage

Pressure conditions at the garnet isograd were estimated using the Powell & Evans (1983) (PE) and Bucher-Nurminen (1987) (BN) calibrations of the chlorite-biotite-muscovite assemblage. The results are presented in Table II. The range of pressure estimates within a given calibration is mostly due to compositional differences in the muscovites, reflected in their celadonite contents. Since the celadonite values are raised to the fourth power in the equilibrium equation any spread in these values strongly affects the outcome. An attempt to minimize within grain and sample variances was done by taking several points on each mineral grain. For the range of pressure at the garnet isograd the the two calibrations give comparable results, except for the lowest values which have a 1.8 kb difference.

4.4.6.2B) Plagioclase-biotite-garnet-muscovite assemblage

Pressures were determined with the Ghent & Stout (1981) (GS) calibration of the plagioclase-biotite-garnet-muscovite assemblage. The assemblage is present within most of the micaceous schist unit except right at the garnet isograd. The results are summarized in Table III. The pressure values at the staurolite isograd are 5.3 to 6.1 Kb. They are 1 to 2.5 Kb lower than those of the adjacent garnet zone. Given the amount of retrogression visible in the samples at the staurolite isograd the pressure values may have recorded the retrograde conditions and not the peak metamorphic ones. The only sample in the kyanite zone gave pressure results between 8.1 and 8.4 Kb.

4.4.6.2C) Kyanite bearing assemblage

Only one sample chosen for this study contained the assemblage kyanite-

TABLE II

ZONE	SPECIMEN NUMBER	W. SPEC. LITE		D. SPEC. LITE		S. SPEC. LITE		T. SPEC. LITE		A. SPEC. LITE		P. SPEC. LITE		M. SPEC. LITE		L. SPEC. LITE		O. SPEC. LITE		N. SPEC. LITE		U. SPEC. LITE		V. SPEC. LITE		W. SPEC. LITE		X. SPEC. LITE		Y. SPEC. LITE		Z. SPEC. LITE	
		1	2	3	4	5	6	7	8	9	10	11	12	13	14	15	16	17	18	19	20	21	22	23	24	25	26	27	28	29	30	31	32
ISOCORAD	0000-0000	1	1	1	1	1	1	1	1	1	1	1	1	1	1	1	1	1	1	1	1	1	1	1	1	1	1	1	1	1	1	1	1
	0000-0001	1	1	1	1	1	1	1	1	1	1	1	1	1	1	1	1	1	1	1	1	1	1	1	1	1	1	1	1	1	1	1	1
	0000-0002	1	1	1	1	1	1	1	1	1	1	1	1	1	1	1	1	1	1	1	1	1	1	1	1	1	1	1	1	1	1	1	1
	0000-0003	1	1	1	1	1	1	1	1	1	1	1	1	1	1	1	1	1	1	1	1	1	1	1	1	1	1	1	1	1	1	1	1

TABLE III

OVI	Position	PIAGI001ASF	BPT IITF		MUS 0VITF		GAFT				PGRD
	NUMBER	km	oph1	km	NaI	Nmms	Npv	NaI	Ngr	Nsp	
GAFT ZON	2017-11-1	997	416	398	985	994	110	738	103	043	7.5
	2017-11-2	119	410	392	995	994	110	738	103	043	6.6
	2015-11-3	119	410	392	744	423	110	738	103	043	7.9
	2015-7-1	081	410	390	961	624	126	803	039	031	7.1
	2015-7-2	0846	410	390	0.961	624	126	803	039	031	7.0
	2015-7-	096	410	390	961	624	126	803	039	031	6.7
STIMROIT ISO PMP	2300-5.0"	298	521	301	894	605	130	620	091	160	5.3
	2300-3.90"	235	521	301	902	601	121	626	122	132	5.9
	2300-2.4"50"	225	579	306	889	626	111	667	139	084	6.1
FYWITI ZON	2144-4-1	225	420	390	925	722	141	725	133	001	9.2
	2144-4-2	225	420	390	915	737	141	725	133	001	8.3
	2144-4-3	225	420	364	925	722	141	725	133	001	9.2
	2144-6	224	426	364	927	722	141	725	133	001	9.1
	2144-7	224	426	390	915	733	141	725	133	001	9.2

garnet-biotite-muscovite-plagioclase-tourmaline. The presence of an aluminosilicate phase allows for the use of the Newton & Haselton (1981) calibration. The calculated pressure was 8.4 Kb using the peak T^O of 630 °C from the garnet rim. This is in good agreement with the pressure values determined from the Ghent & Stout (1981) geobarometer.

4.5) Burial history

This study lacks some key ingredients for deciphering the complete P-T trajectories of the rocks, such as the presence of biotite and plagioclase inclusions within the garnets and the widespread presence of kyanite (Selverstone et al., 1984; St-Onge & King, 1987). T^O values can be estimated for the cores of the garnets by assuming the matrix biotite acts as an infinite sink of Fe and Mg cations. Pressure values on the other hand cannot be estimated in the same way because: 1) plagioclase is not abundant enough to act as an infinite cation reservoir of Ca and 2) because of the lack of correspondence in the Ca zonation patterns of garnet and plagioclase.

An attempt has been made to constrain qualitatively the P-T trajectory of the retrograde rims. This is done by plotting the pyrope versus the grossular content of the interior and exterior portions of the retrograde rims (Martignole & Nantel, 1982). The variations in Mg content being mostly a function T^O and Ca a function of P. The interior portions of the rims reflect peak metamorphic conditions while the exterior portions reflect the retrograde conditions. The trajectories of the four retrograde garnet rims are shown in Figure 24. Three of the samples (2015-11, 2002-2, 2002-3) display shallow slopes that are indicative of isothermal unloading. Two of the samples (2300-23, 2131-1) show steeper slopes characteristic of unloading and cooling. This data set is very small to draw any conclusions from, nevertheless the flatter

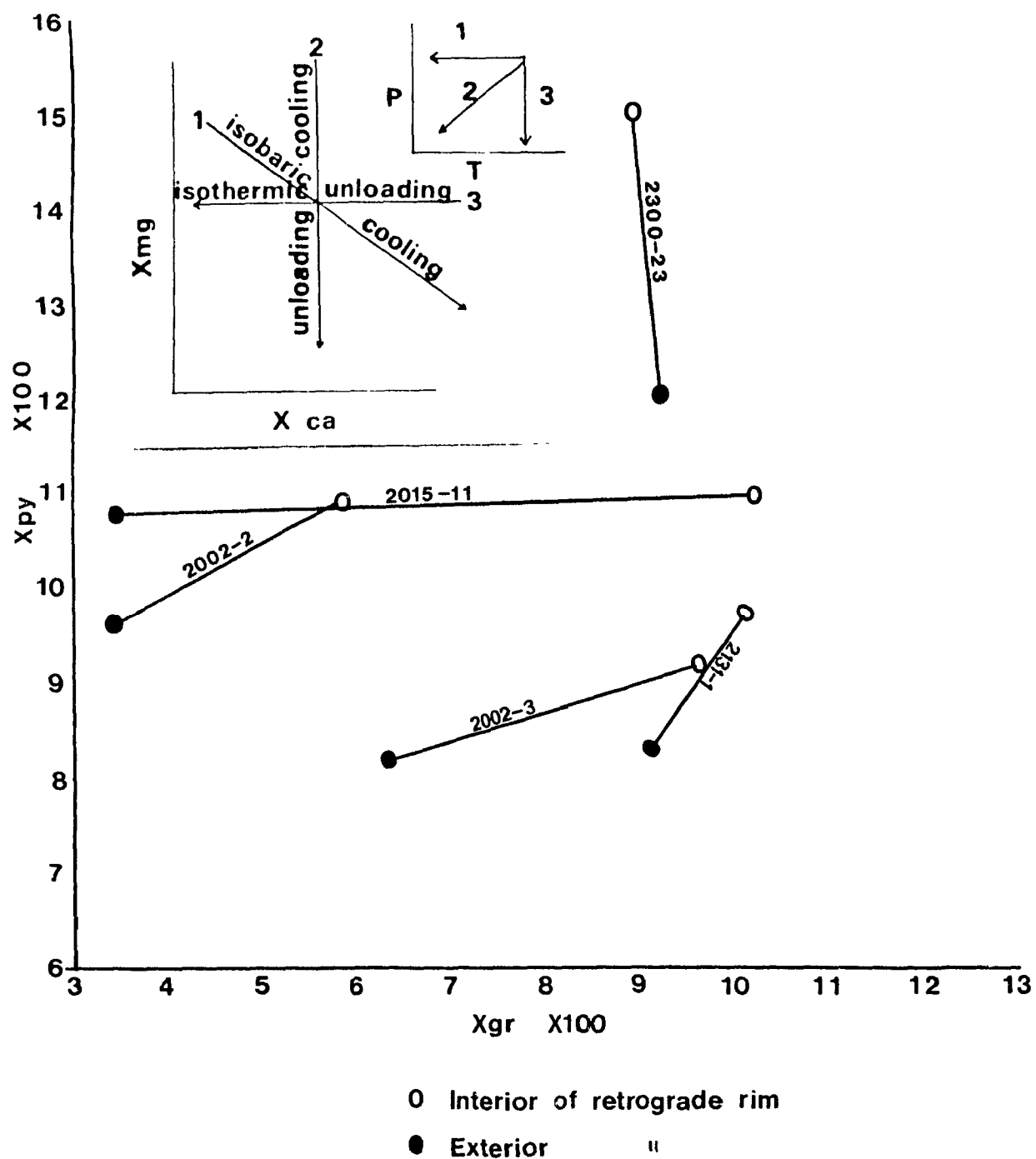


Figure 24: Plot of the pyrope versus grossular content of the retrograde rims in garnets (after Martignole & Nantel, 1982). The interior portion of the rims corresponds to the peak metamorphic conditions while the exterior portion mark the late stage equilibrium reached under retrograde conditions.

slopes in the garnet zone could possibly be due to more rapid uplift near the Lac Rachel fault.

All of the available P-T data are plotted on Figure 25 which includes data from the study of Gélinas & Perreault (1965) from a locality on the sillimanite isograd within the Renia Gneiss body. The two most reliable P-T determinations are thought to be the ones from the garnet zone and the kyanite zone. Given that the samples taken at the garnet isograd (2002-2, -3) are situated only 2 km east of the ones from the garnet zone (2015-7, -11), it seems unlikely that a 2 to 4 Kb difference exist between samples. The chlorite-biotite-muscovite barometer seems to underestimate pressures by 1 to 2.5 Kb with respect to the (GS) geobarometer. The samples taken from the staurolite isograd (2300-23, -3, -5) show strong signs of retrogression that probably resulted in lower P and T⁰ values. Logically, the sample from the staurolite isograd should give results between the garnet and kyanite zones.

The data of this study compare favourably to the peak metamorphic conditions and uplift path of the study of Gélinas & Perreault (1985). The pressures in the kyanite zone are however 1 Kb higher than those recorded from their kyanite-sillimanite assemblage.

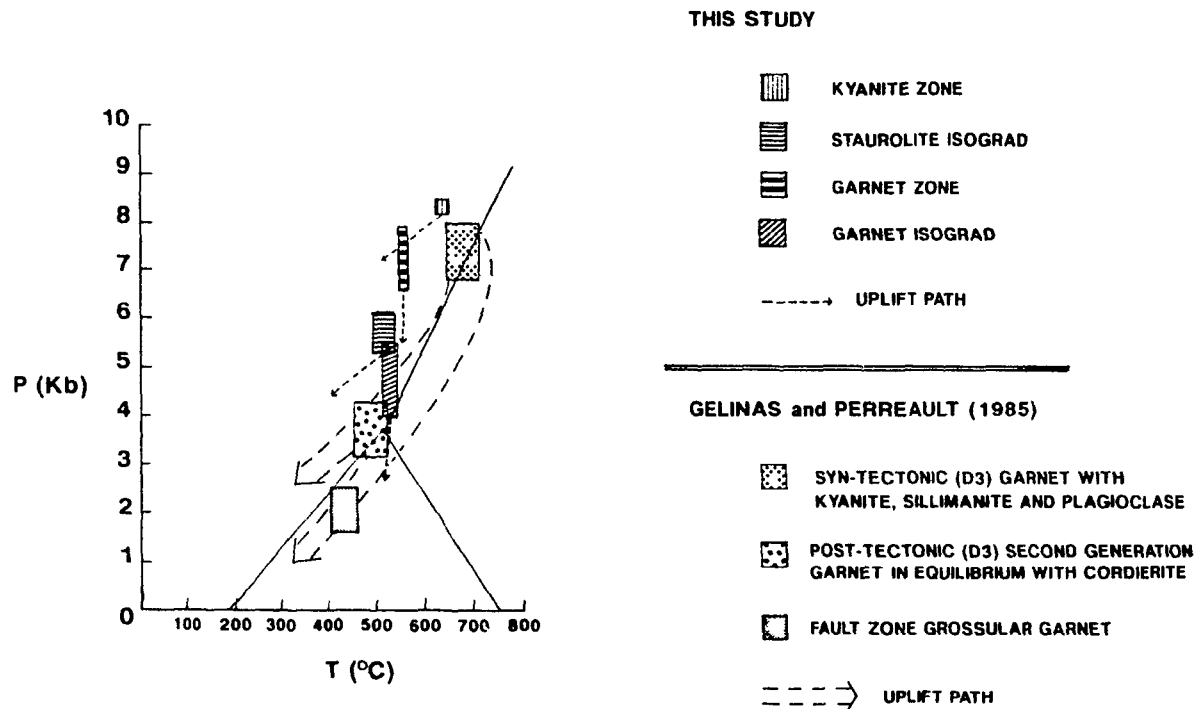


Figure 25: Pressure-temperature diagram with aluminosilicate phase boundaries showing the results of this study in conjunction with results from the work of Gélinais & Perreault (1985). In order to keep the diagram legible the error margins of ± 50 °C and ± 1 kb have not been added to the data of this study.

5.0) SUMMARY

5.1) Stratigraphy

The stratigraphy of the cover succession overlying the Archean basement gneisses of the western hinterland zone has many similarities to that of the Kaniapiskau Supergroup of the central and western zones. From the base upwards the following correlations have been made:

- 1) The various calcareous units at the base of the sequence would correlate with the Harveng Fm.
- 2) The overlying micaceous schist unit would be the equivalent of the Lower Member (L.M) of the Baby Fm.. This unit however coarsens upwards which does not seem to be the case for the L.M. of the Baby Fm. (Sauvé & Bergeron, 1965).
- 3) The iron formation is identical to the iron-rich sediments of the Middle Member of the Baby Fm..
- 4) A thin micaceous schist unit overlying the iron formation would represent a much thinner equivalent to the Upper Member of the Baby Fm..
- 5) The mafic volcanic unit is identical to the Hellancourt Fm. further west, although slightly thinner.

The mafic volcanic unit is overlain by a volcanic conglomerate horizon which grades upwards into a thick and extensive coarse-grained siliciclastic assemblage. A few volcanic-rich conglomerate horizons occur higher up stratigraphically. This assemblage seems to correlate with the fine-grained Thévenet Fm. capping the easternmost exposure of the Hellancourt basalts in the central allochthonous zone. The Thévenet Fm. has no equivalent further west. The Thévenet Fm. and its more extensive correlative in the hinterland zone could represent the northern extension of the Laporte Group metasediments

further south. The Laporte Group forms the bulk of the western hinterland zone of the central Labrador Trough (Dimroth, 1970, 1978; van der Leeden et al., in press).

An important feature of the study area is the eastern provenance of the Thévenet Fm. and probably the upper portion of the micaceous schist unit underlying the iron formation. This source would include uplifted siliciclastic sediments and mafic volcanics along with granitoid crystalline rocks.

5.2) Structure

5.2.1) Basement gneiss bodies

The main striking feature of the western hinterland zone at this latitude is the presence of four large, NW trending, en échelon Archean basement bodies. These are from north to south: the Boulder, the Renia, the Moyer and the Scattered Gneisses. The Boulder and the Moyer are exposed as doubly plunging antiforms whereas the Renia and Scattered are exposed as SW plunging synforms.

Any choice of model that is used to account for the origin of the basement gneisses changes the interpretation of the chronology of the different structural features. The key constraint is the presence of two gneiss bodies overlying cover rocks, the Scattered and Renia Gneisses. This restricts to three the number of models that can account for the presence of basement gneisses overlying cover rocks.

5.2.1.1) Diapirism

In this model the gneisses would have risen buoyantly into the denser metamorphosed cover rocks. The Renia and Scattered Gneisses would represent

sections through the lower portions of the lobes in a mushroom shaped diapir. The Moyer and Boulder would either be higher level sections through the diapir or sections through the stem of the mushroom shaped diapir. The four gneiss bodies cannot simply be related to a single diapir. They also lack some features unique to and diagnostic of diapiric upwelling, such as radially arranged neutral folds (Brun, 1983) and outwardly vergent cascading folds (Platt, 1980).

5.2.1.2) Sheath folding

In this model the gneiss bodies developed as mega-sheath folds during a single NW directed shearing event, presumably D_1 . The Renia and Scattered synformal gneisses would represent deeper sections in the mega-sheath folds than the Moyer and Boulder antiformal gneisses. All of the major folds in and surrounding the gneisses would be part of this single deformation event. Although this model accounts well for the shape and disposition of the gneiss bodies, no deformation event compatible with this style of folding on any scale has been observed in the study area.

5.2.1.3) Refolding of early Pennine type nappe structures

This model involves the folding of the overthrust Superior basement along with its overlying para-autochthonous cover sequence into large NNE to NE trending WNW to NW vergent nappe structures. These were then refolded by large amplitude, NW trending upright folds. This resulted in the early nappe structures being exposed as basement-cored synforms (Renia and Scattered Gneisses) and the underlying autochthonous basement gneisses as antiforms (Boulder and Moyer Gneisses). The model explains most if not all the structural features of the western hinterland and is not in conflict with any

of our observations.

5.2.2) Tectonic history

Assuming the Renia and the Scattered basement gneisses represent refolds of basement-cored nappe structures, the western hinterland zone has undergone four, possibly five, distinct tectonic events.

The first deformation event (D_1) records the westerly translation of the cover sequence over the basement gneisses along a thin basal décollement zone and the local stacking of the cover sequence along two thrust faults that partially repeat the cover stratigraphy. Basement is thought to have remained relatively inactive during this event.

The next event (D_1') resulted in the formation of large NNE to NE trending WNW to NW vergent basement-cored nappe structures that folded large portions of the basement gneisses and the overlying cover sequence onto themselves.

The following deformation event (D_2) produced E to NE trending open cross-folds in the central portion of the hinterland zone (Bosdachin, 1986; Poirier, 1989). In the study area the only evidence for this event lies in the doubly plunging configuration of the antiformal gneiss bodies (Moyer and Boulder Domes). This assumes that the folding phase coring the long axis of these two domes (F_3) does not depart from cylindrical.

The next event (D_3) produced the large amplitude, NW trending, SE plunging upright folds that characterize much of the hinterland and central allochthonous zones of the northern Labrador Trough. The folds are responsible for the large amounts of structural thickness visible in oblique section at the present erosion surface.

The final event includes the unroofing of the imbricated and folded

basement-cover complex by reverse motion on the steeply easterly dipping Lac Rachel fault. This fault may have a dextral strike-slip component (Goulet, 1987).

5.3) Metamorphism

In the study area metamorphic grade increases west to east from lower amphibolite grade near Lac Rachel to mid-amphibolite grade at the cover-basement interface of the Renia Gneiss. Three sub-parallel isograds trending N-S occur in the area. The garnet isograd runs up the center of Lac Rachel and the closely spaced staurolite and kyanite isograds are situated halfway between the lake and the Renia Gneiss (Map III). The isograds cross-cut all major fold structures (Map I & III) indicating that the peak in metamorphism is post-kinematic.

The Hoges & Spear (1982) calibration of the garnet-biotite geothermometer is thought to yield the most consistent results across the different metamorphic zones of the study area. Peak temperatures were evaluated at 510-550 °C at the garnet isograd up to 620-650 °C in the kyanite zone near the basement-cover interface on the NW closure of the Renia Gneiss. The Ghent & Stout (1981) (GS) and Newton & Haselton (1982) (HS) geobarometers give similar results in the kyanite zone (8.1 to 8.4 kb). Given the lack of widespread kyanite in the micaceous schists the (HS) geobarometer has limited use. The (GS) one was used on most samples, in the garnet zone it gives pressures between 6.7 and 7.4 kb. The Powell & Evans (1983) and Bucher-Nurminen (1987) calibrations of the chlorite-biotite-muscovite assemblage were used at the garnet isograd where no plagioclase was observed. They yielded pressures between 4.0 and 5.5 kb which seem to be 1 to 2 kb lower than expected when compared with the (GS) geobarometer.

6.0) CONCLUSIONS AND SUGGESTIONS FOR FURTHER WORK

6.1) Conclusions

The four basement gneiss bodies in the western hinterland zone of the northern Labrador Trough are overlain by an outward facing, upward-coarsening, cover sequence. The lower and middle portion of the sequence correlates with the Kaniapiskau Supergroup further west, whereas the upper portion correlates with the Laporte Group metasediments described in the hinterland zone of the central trough. From the middle portion upwards the cover sequence displays a lithologically varied eastern provenance which contrasts with the predominantly cratonic western source characteristic of much of the Kaniapiskau Supergroup further west (Le Gallais & Lavoie, 1982). The importance of an eastern source for the cover sequence in the hinterland zone provides a new constraint, it does not however lead to any unique solution with respect to tectonic models. If the passive margin model (Wardle & Bailey, 1981; Le Gallais & Lavoie, 1982; Boone, 1987; Poirier, 1989) is accepted an outer high to the E is needed to account for the eastern provenance. An uplifted eastern source region is also compatible with a foredeep model (Hoffman, 1987) and a back arc model. The foredeep model is hampered by the presence of voluminous MORB type volcanism and intrusion in the central portion of the trough (Dimroth *et al.*, 1970; Boone, 1987). The current limited geochronological data base shows no evidence for the back arc model.

The closing of the basin is thought to be somewhat better understood. It involves the westerly translation and imbrication of the cover sequence over the basement gneisses (D_1). The gneisses and the cover sequence were then folded into large westerly vergent Pennine style nappe structures (D_1'). This

was followed by E to NE trending open cross-folding (D_2) and ultimately by large amplitude NW trending, SE plunging, upright folding (D_3). The folded basement-cover complex was then uplifted by reverse motion on the N trending Lac Rachel fault, which marks the western boundary of the hinterland zone.

Diapir and sheath fold models can account for some but not all of the features of the gneiss bodies. No structural data unique to either of these models have been observed. They are thought not to have been important in the development of the gneisses in the western hinterland zone.

The Pennine style nappes seem to be restricted to this portion of the hinterland zone. The recognition of large early basement-cored nappe structures points to the importance of basement involvement during the early deformation stages of the Orogeny. These nappes compare well with similar structures from the internal portion of other orogens, such as the Canadian Cordillera (Duncan, 1984) and the northern Appalachians (Rosenfeld, 1968).

6.2) Suggestions for further work

More data are needed to complete the sparse data set of fold closures from which the composite down plunge projection was constructed. This would include mostly F_3 fold plunge measurements for much of the area present within the section.

Much critical information would be gained by mapping the area S & SW of the Renia Gneiss and E of the Scattered Gneiss. This would constrain the S and SE limit of the Moyer Gneiss. It would also establish if the Renia and the Scattered Gneisses join up at the present erosion surface into one large basement-cored nappe structure as is implied by the down plunge section and the refolded Pennine type model.

There is also a need for a detailed examination of kinematic indicators

along the Lac Rachel fault to assess the history of motion along it.

Dating of the detrital sediments overlying the basement gneisses would provide constraints on the nature and more importantly the age of the uplifted terrane that shed sediments to the west. The ages could possibly distinguish between the outer basement high model, the foredeep model (Hoffman, 1987) or a back arc model for the basin present during the upper portion of the succession overlying the Archean basement bodies of the western hinterland zone.

REFERENCES

- ANDO, C.J., CZUCHRA, B.L., KLEMPERER, S.L., BROWN, L.D., CHEADLE, M.J., COOK, F.A., OLIVER, J.E., KAUFMAN, S., WALSH, T., THOMPSON, J.B., j.r., LYONS, J.B. and ROSENFELD, J.L., 1984. Crustal profile of a mountain belt: COCORP deep seismic profiling in New England Appalachians and implications for architecture of convergent mountain chains. *American Association of Petroleum Geologist Bulletin*, Vol. 68, no.7, p. 819-837.
- AVRAMICHEV, L., 1985. Carte géologique du Québec, échelle 1:1 500 000. Ministère de l'Énergie et des Ressources, Québec, DV 84-02, carte no.2000.
- BALLY, A.W., 1981. Thoughts on the tectonics of folded belts. In *Thrust and Nappe Tectonics*, McClay, K.R. and Price, N.J. (editors). Geological Society of London Special Publication no. 9, p. 13-32.
- BARAGAR, W.R.A., 1974. Volcanic studies in the Cape Smith-Wakeham Bay belt, New Quebec: Geological Survey of Canada, Paper 74-1. p. 155-157.
- _____, 1967. Wakuach map area, Quebec-Labrador (230); Geological Survey of Canada, Memoir 344.
- _____ and SCOATES, R.F.J., 1981. The Circum-Superior belt: a Proterozoic plate margin?. In *Precambrian Plate Tectonics*, edited by A. Kroner, p. 297-330, Elsevier, Amsterdam, 1981.
- BARRETT, T.J., WARES, R.P. and FOX, J.S., 1988. Two-stage hydrothermal formation of a lower Proterozoic sediment-hosted massive sulphide deposit, Northern Labrador Trough, Québec. *Canadian Mineralogist*, Vol. 26, p. 871-888.
- BARTLEY, J.M., 1982. Limited basement involvement in the Caledonian deformation, Hinnoy, North Norway, and tectonics implications. *Tectonophysics*, Vol. 83, p. 185-203.
- BEALL, G.H., HURLEY, P.M., FAIRBAIRN, H.W. and PINSON, W.H., 1963. Comparison of K-Ar and whole-rock Rb-Sr dating in New Quebec and Labrador, *American Journal of Science*, 261: 571-580.
- BÉLANGER, M., 1982. Région du lac Faujas, Nouveau-Québec. Ministère de l'Énergie et des Ressources, Québec; DP 82-06.
- _____ and VAN DER LEEDEN, J., 1987. Le projet de la Rivière Georges: une première évaluation métallogénique. Ministère de l'Énergie et des Ressources, Québec, Exploration au Québec, Études géoscientifiques récentes, Séminaire d'information 1987. DV 87-25.
- BELL, T.H., 1985. Deformation partitioning and porphyroblast rotation in metamorphic rocks: A radical reinterpretation: *Journal of Metamorphic Geology*, Vol. 3, p. 109-118.
- _____ and HAMMOND, R.L., 1984. On the internal geometry of mylonite

- zones. *Journal of Geology*, Vol. 92, p. 667-686.
- BÉRARD, J., 1965. Région du lac Bérard. Ministère des Richesses Naturelles, Québec; RG-111.
- _____, 1956. Région du lac Harveng (moitié ouest), Nouveau-Québec. Ministère des Mines, Québec; RP-320.
- _____, 1955. Région du lac Thévenet (partie ouest), Nouveau-Québec. Ministère des Mines, Québec; RP-311.
- BERG, J.H. and KLEWIN, K.W., 1988. High-MgO lavas from the Keweenawan midcontinent rift near Mamainse Point, Ontario. *Geology*, Vol. 16, no. 11, p. 961-1060.
- BERGERON, R., 1957. Rapport préliminaire sur la région de Brochant- De Bonnard, Nouveau-Québec. Ministère des Mines du Québec, RP-348.
- BICKLE, M.J., BETTENAY, L.F., BOULTER, C.A., GROVES, D.I. and MORANT, P., 1980. Horizontal tectonic interaction of an Archean gneiss belt and greenstones, Pilbara block, Western Australia. *Geology*, Vol. 8, p. 525-529.
- BOONE, E., 1987. Petrology and tectonic implications of the Hellancourt volcanics, Northern Labrador Trough, Quebec. M.Sc. thesis, McGill University, Montréal, Québec.
- _____ and HYNES, A., in press. A structural cross section of the Northern Labrador Trough, New Quebec. Trans-Hudsonian symposium volume, Geological association of Canada.
- BOYER, S.E. and ELLIOT, D., 1982. Thrust Systems. *American Association of Petroleum Geologist Bulletin*. Vol. 66, No. 9, p.1196-1230.
- BOSDACHIN, R., 1986. Structural deformation and metamorphism of the Lac à Foin metasediments, Fort Chimo, Quebec. B.Sc. thesis, McGill University, Montréal.
- BROWN, R.L. and LANE, L.S., 1988. Tectonic interpretation of west-verging folds in the Selkirk Allochthon of the southern Canadian Cordillera. *Canadian Journal of Earth Sciences*, Vol. 25, p. 292-300.
- _____ and READ, P.B., 1983. Shuswap terrane of British Columbia: A mesozoic "core complex". *Geology*, Vol. 11, pp. 164-168.
- BRUN, J.P., 1983. L'origine des domes gneissiques: modèles et tests. *Bull. Soc. géol. France*, tome XXV, n^o 2, p. 219-228.
- _____, 1980. The cluster-ridge pattern of mantled gneiss domes in eastern Finland: Evidence for large scale gravitational instability of the Proterozoic crust. *Earth and Planetary Science Letters*, Vol.47, p. 441-449.
- _____, 1977. La zonation structurale des dômes gneissiques. Un exemple:

le massif de Saint-Malo (Massif armoricain, France). Canadian Journal of Earth Sciences, Vol. 14, p. 1697-1707.

BUCHER-NURMINEN, K., 1987. A recalibration of the chlorite-biotite-muscovite geobarometer. Contributions to Mineralogy and Petrology, Vol. 96, p. 516-522.

BUDKEWITSCH, P., 1986. A structural study of the Chioak-Abner Formation contact, northern part of the Labrador Trough, New Quebec. B.Sc. Thesis, Concordia University, Montréal.

CARD, K.D. and CIESIELKI, A., 1986 - DNAG #1. Subdivisions of the Superior Province of the Canadian Shield. Geoscience Canada Volume 13, number 1.

CARMICHAEL, D.M., 1978. Metamorphic bathozones and bathograds: A measure of the depth of post-metamorphic uplift and erosion on the regional scale. American Journal of Science, Vol. 278, p. 769-797.

CHANDLER, F.W., 1982. The structure of the Richmond Gulf Graben and the geological environments of lead-zinc mineralizations of iron-manganese formation in the Nastapoka Group, Richmond Gulf area, New-Quebec-Northwest Territories. In Current Research part. A, Geological Survey of Canada, paper 82-1A, p. 1-10.

CHEVE, S., 1987. Le complexe carbonatique du lac Castignon, Fosse du Labrador. Ministère de l'Énergie et des Ressources, Québec, DP 87-10.

_____ and MACHADO, N., 1988. Reinvestigation of the Castignon Lake Carbonatite Complex, Labrador Trough, New Quebec. Geological Association of Canada, Program with Abstracts, 13: p. A20.

CHIPERA, S.J., PERKINS, D., 1988. Evaluation of biotite-garnet geothermometers: application to the English River subprovince, Ontario. Contributions to Mineralogy and Petrology, Vol. 98, p. 40-48.

CIESIELSKI, A., 1977. Contact archéen-protérozoïque entre les lacs Forbes et Sénat, Fosse du Labrador. Ministère des Richesses Naturelles; DPV-449.

CLARK, T., (in press). Cartes géologiques de la partie nord de la Fosse du Labrador, échelle 1:250 000. Ministère de l'Énergie et des Ressources, Québec.

_____, 1988. Stratigraphie, pétrographie et pétrochimie de la Formation de Fer de Baby, région du lac Hérodier, Fosse du Labrador. Ministère de l'Énergie Ressources, Québec, ET 87-13.

_____, 1984. Géologie de la région du lac Cambrien, Territoire du Nouveau-Québec. Ministère de l'Énergie et des Ressources, Québec, ET 83-02.

_____, 1980. Région de la rivière Koksoak, Nouveau-Québec. Ministère de l'Énergie et des Ressources, Québec, DPV-781.

- _____, 1979. Région du lac Napier, territoire du Nouveau-Québec. Ministère des Richesses Naturelles, Québec; DPV-663.
- _____, 1978. Région du lac Hérodier, Nouveau-Québec. Ministère des Richesses Naturelles, Québec; DPV-568.
- _____, 1977. Forbes Lake area. Ministère des Richesses Naturelles, Québec; DPV-452.
- _____, THORPE, R.I., (in press). Model lead ages from the Labrador Trough and their stratigraphic implications. Trans-Hudsonian Symposium, Geological Association of Canada.
- COBBOLD, P. and QUINQUIS, H., 1980. Development of sheath folds in shear regimes. *Journal of Structural Geology*, Vol. 2, p. 119-126.
- DAVIS, G.H., 1983, Shear zone model for the origin of metamorphic core complexes, *Geology*, Vol. 11, pp. 342-347.
- _____ and CONEY, P.J. 1979, Geologic development of the Cordilleran metamorphic complexes, *Geology*, Vol. 7, pp. 120-124.
- DE ROMER, H.S., 1956. The geology of the eastern border of the "Labrador Trough", east of Thevenet Lake, New Quebec.
- DEWEY, J.F. and BURKE, K.C., 1973. Tibetan, Variscan and Precambrian basement reactivation: products of continental collision. *Journal of Geology*, Vol. 81, p. 683-692.
- DIMROTH, E., 1985. Depositional Environments and Tectonic Setting of the Cherty Iron-Formations of the Canadian Shield. *Journal Geological Association of India*. Vol. 28, p.239-250.
- _____, 1981. Labrador Geosyncline: type example of early Proterozoic cratonic reactivation. In *Precambrian Plate Tectonics* (A. Kroner, ed.). *Developments in Precambrian Geology* 4, 331-352. Elsevier, Amsterdam.
- _____, 1978. Région de la Fosse du Labrador/Labrador Trough area (54°30' - 56°30'). Ministère des Richesses Naturelles, Québec; RG-193.
- _____, 1977a. Models of physical sedimentation of iron formations. In *Geoscience Canada*; volume 4, number 1, pages 23-30.
- _____, 1977b. Diagenetic facies of iron formation. *Geoscience Canada*; Vol. 4, number 2, pages 83-88.
- _____, 1972. The Labrador Geosyncline revisited. *American Journal of Science*, Vol. 272, 487-506.
- _____, 1971. The Attikamagen-Ferriman transition in the central part of the Labrador Trough: *Canadian Journal of Earth Sciences*, Vol. 8, p.1432-1454.
- _____, 1970. Evolution of the Labrador geosyncline. *Geological Society*

of America Bulletin; Vol. 81, pages 2717-2742.

- _____ and DRESSLER, B., 1978. Metamorphism of the Labrador Trough. In *Metamorphism in the Canadian Shield* (J.A. Fraser & W.W. Heywood, eds.). Geological Survey of Canada, Report 78-10, p. 215-236.
- _____ and CHAUVEL, J.J., 1973. Petrography of the Sokoman iron formation in part of the Central Labrador Trough, Quebec, Canada. *Geological Society of America Bulletin*, Vol. 84, p. 111-134.
- _____, BARAGAR, W.R.A., BERGELSON, R., JACKSON, G.D., 1970. The filling of the Circum-Ungava geosyncline. In *Symposium on basins and geosynclines of the Canadian Shield*, A.J. Baer, editor. Geological Survey of Canada, paper 70-40, p. 45-142.
- DIXON, J.M. and SUMMERS, J.M., 1983. Patterns of total and incremental strain in subsiding troughs: experimental centrifuged models of inter-diapir synclines. *Canadian Journal of Earth Sciences*, Vol. 20, 1843-1861.
- _____, 1975. Finite strain and progressive deformation in models of diapiric structures. *Tectonophysics*, Vol. 28, p. 89-124.
- DOUGLAS, R.J.W., 1973. Geological Provinces Map 27-28, National Atlas of Canada, 4th Edition: Surveys and Mapping Branch, Department of Energy Mines and Resources, Ottawa.
- DRESSLER, B., 1979. Région de la Fosse du Labrador (56°30' - 57°15'). Ministère de l'Énergie et des Ressources, Québec, RG-195.
- _____, 1975. Lamprophyres of the north-central Labrador Trough, Quebec, Canada. *Neues Jahrbuch für Mineralogie, Monatshefte*, 6: 245-290.
- DUEBENDORFER, E.M. and FROST, B.R., 1988. Retrogressive dissolution of garnet: Effect on garnet-biotite geothermometry. *Geology*, Vol. 16, p. 875-877.
- DUNCAN, I.J., 1984. Structural evolution of the Thor-Odin gneiss dome. *Tectonophysics*, Vol. 101, p. 87-130.
- ELLIS, M.A., 1986. Structural morphology and associated strain in the central Cordillera (British Columbia and Washington): Evidence of oblique tectonics. *Geology*, Vol. 14, p. 647-650.
- ENGLAND, P.C. and RICHARSON, S.W., 1977. The influence of erosion upon the mineral facies of rocks from different metamorphic environments. *Journal of the Geological Society of London*, Vol. 134, p. 201-213.
- _____ and THOMPSON, A., 1984. Pressure-temperature - time paths of regional metamorphism I. Heat transfer during the evolution of regions of thickened continental crust. *Journal of Petrology*, Vol. 25, p. 894-928.
- EVANS, J.L., 1978. The geology and geochemistry of the Dyke Lake area (parts of 23J/8, 9), Labrador; Newfoundland Department of Mines and Energy, Mineral Development Division, Report 78-4.

- FAHRIG, W.F., 1967. Shabogamo Lake map area (23G E1/2), Newfoundland, Labrador and Quebec; Geological Survey of Canada, Memoir 354.
- _____, 1965. Lac Hérodier, Québec. Commission géologique du Canada; carte 1146 A.
- _____ and WANLESS, R.K., 1963. Age and significance of diabase dyke swarms of the Canadian Shield: *Nature*, Vol. 200, p. 934-937
- FERRY, J. M. and SPEAR, F.S., 1978. An experimental calibration of partitioning of Fe and Mg between biotite and garnet. *Contributions to Mineralogy and Petrology*, Vol. 66, p. 113-117.
- FLETCHER, R.C., 1972. Applications of a mathematical model to the emplacement of Mantled gneiss domes. *American Journal of Science*, Vol. 272, p. 197-216.
- FOURNIER, D., 1985. Minéralisations de la partie orientale du géosynclinal du Labrador (Groupe de Laporte). Ministère de l'Énergie et des Ressources, Québec; ET 83-23.
- _____, 1982. Gîtes de Cu-Zn et Cu-Ni dans la partie centrale de la Fosse du Labrador. Ministère de l'Énergie et des Ressources, Québec; DPV-929.
- FRANCIS, D., LUDDEN, J. and HYNES, A., 1983. Magma Evolution in a Proterozoic Rifting Environment. *Journal of Petrology*, Vol. 24, part 4, p. 556-582.
- FRAREY, M.J., 1961. Menihek Lakes, Quebec, and Newfoundland; Geological Survey of Canada, Map 1087A.
- FRASER, A.A., HEYWOOD, W.W. and MAZURKI, M.N., 1978. Metamorphic map of the Canadian Shield. Geological Society of Canada, Map No. 1475A.
- FREEDMAN, R.O., 1958. Report on Red Dog Lake area (Ungava). Ministère des Mines, Québec, DP 49.
- FRYER, B.J., 1972. Age determinations in the Circum-Ungava geosyncline and the evolution of Precambrian banded iron-formations. *Canadian Journal of Earth Sciences*, Vol. 9, p. 652-663.
- GÉLINAS, L., 1984. Métamorphisme du secteur est de la Fosse du Labrador. Unpublished Manuscript.
- _____, 1965. Géologie de la région de Fort Chimo et des Lacs Gabriel et Thévenet, Nouveau-Québec. D.Sc. thesis, Université Laval, Québec, 212 p.
- _____, 1960. Région du Fort Chimo (partie est), Nouveau-Québec. Ministère des Mines, Québec, Rapport préliminaire 418.
- _____, 1959. Région du Lac Gabriel (partie est), et la région de Fort Chimo (partie ouest), Nouveau-Québec. Ministère des Mines, Québec, Rapport préliminaire 407.

- _____, 1958a. Thévenet Lake area, (east half) New Québec. Québec Department of Mines, Preliminary report 363.
- _____, 1958b. Rapport préliminaire sur la région du Lac Gabriel (partie ouest), Nouveau-Québec. Ministère des Mines, Québec, Rapport Préliminaire 373.
- _____ and PERREAULT, S., 1985. The metamorphic evolution of the Renia gneissic dome on the eastern flank of the Labrador Trough, Ungava Bay. Geological Association of Canada and Mineralogical Association of Canada, Joint Annual Meeting, Program with Abstracts, p. 20.
- GHEENT, E.D., 1976. Plagioclase, garnet, Al_2SiO_5 , quartz: a potential geothermometer - geobarometer. American Mineralogist, Vol. 61, p. 710-714.
- _____ and STOUT, M.Z., 1981. Geobarometry and geothermometry of plagioclase-biotite-garnet-muscovite assemblages. Contributions to Mineralogy and petrology, Vol. 76, p. 92-97.
- _____, ROBBINS, D.B. and STOUT, M.Z., 1979. Geothermometry, geobarometry, and fluid compositions of metamorphosed calc-silicates and pelites, Mica Creek, British Columbia. American Mineralogist 64, p. 874-885.
- GIBB, R.A., 1983. A model for suturing of Superior and Churchill plates: an example of double indentation tectonics. Geology, Vol. 11, p. 413-417.
- _____ and WALCOTT, R.I., 1971. A Precambrian suture in the Canadian Shield. Earth and Planetary Science Letters, Vol. 10, p. 417-422.
- GIRARD, R., 1989. A new stratigraphic subdivision of the Laporte Group, Labrador Trough. Geological Association of Canada and Mineral Association of Canada, Joint Annual Meeting, Program with Abstracts, p. 38.
- GOLD, D.P., 1962. Rapport préliminaire sur la région de la Baie Hopes Advance, Nouveau Québec. Ministère des Richesses Naturelles, Québec. RP 442.
- GOULET, N., 1987. Étude tectonique de la partie nord de la Fosse du Labrador, Rapport intérimaire. Ministère de l'Énergie et des Ressources, Quebec; MB 87-21.
- _____, 1986. Étude tectonique et stratigraphique de la partie nord de la Fosse du Labrador: région de la baie aux Feuilles et du lac Bérard. Ministère de l'Énergie et des Ressources, Québec; MB 86-27.
- _____, GARIÉPY, L., MARESCHAL, J.-C. and MACHADO, N., 1987. Structure, geochronology, gravity and tectonics of the Northern Labrador Trough. Geological Association of Canada and Mineralogical Association of Canada, Joint Annual Meeting, Program with Abstracts, p.48.
- GROSS, G.A., 1983. Tectonic systems and the deposition of iron-formation. Precambrian Research, Vol. 20, 171-187.
- _____, 1962. Iron Deposits near Ungava Bay, Quebec. Geological Survey of

Canada, Bulletin 82.

- HAMILTON, W., 1981. Crustal evolution by arc magmatism. *Phil. Trans. Roy. Soc. of Lond.*, Vol. 301, p. 279-291.
- HARDY, R., 1976. Région Lac Roberts des Chefs. Ministère des Richesses Naturelles, Rapport géologique 171.
- HARRISON, J.M., HOWELL, J.E. and FAHRIG, W.F., 1970. A geological cross-section of the Labrador miogeosyncline near Schefferville, Quebec, Geological Survey of Canada, Paper 70-37, p. 1-34.
- HELWIG, J., 1976. Shortening of the continental crust in orogenic belts and plate tectonics. *Nature*, Vol. 260, p. 768-770.
- HILDEBRAND, R.S., HOFFMAN, P.F. & BOWRING, S.A., 1986. Tectono-magmatic evolution of the 1.9 Ga Great Bear magmatic zone, Wopmay orogen, Northwestern Canada. *Journal of Volcanology and Geothermal Research*, Vol. 32, p. 99-118.
- HOBBS, B.E., MEANS, W.D. and WILLIAMS, P.F., 1976. An outline of structural geology. John Wiley & Sons, 571 p.
- HODGES, K.V. and MCKENNA, C.V., 1987. Realistic propagation of uncertainties in geologic thermobarometry. *American Mineralogist*, Vol. 72, p. 671-680.
- _____ and CROWLEY, P.D., 1985. Error estimation and empirical geothermobarometry for pelitic systems. *American Mineralogist*, Vol. 70, p. 702-709.
- _____ and SPEAR, F.S., 1982. Geothermometry, geobarometry and the Al_2SiO_5 triple point at Mt. Moosilauke, New Hampshire. *American Mineralogist*, Vol. 67, p. 1118-1134.
- HOFFMAN, P.F., 1988. United plates of America, the birth of a craton: Early Proterozoic assembly and growth of Laurentia. *Annual Review of Earth and Planetary Sciences*, Vol. 16: 543-603.
- _____, 1987. Early Proterozoic foredeeps, foredeep magmatism and Superior-type iron formations of the Canadian Shield. In *Proterozoic Lithospheric Evolution* (A. Kroner, ed.). Amer. Geophys. Union, Geodyn. Ser. 17, 85-98.
- _____, 1985. Is the Cape Smith Belt (northern Quebec) a klippe?. *Canadian Journal of Earth Sciences*. Vol. 67, p. 1118-1134.
- _____, 1980. Wopmay Orogen: a Wilson cycle of early Proterozoic age in the northwest of the Canadian Shield. In *The Continental crust and its mineral deposits*. Edited by D.W. Strangway. Geological Association of Canada, special paper 25, pp. 523-549.
- _____ and GROTZINGER, J.P., 1989. Abner/Denault reef complex (2.1 Ga), Labrador Trough, NE Quebec. Reefs, Canada and adjacent area.

Edited by H.H. Geldsetzer, N.P. James and G.E. Tebbutt. Canadian Society of Petroleum Geologists. Memoir 13, p. 49-54.

- HOLDAWAY, M.J., 1971. Stability of andalusite and the aluminum silicate phase diagram. *American Journal of Science*, Vol. 271, p. 97-131.
- HOLLISTER, L.S., 1966. Garnet zoning: an interpretation based on the Raleigh Fractionation model. *Science*, Vol. 154, p.1647-1651.
- HYNES, A., 1978. Early recumbent folds in the north-eastern part of the northern Labrador Trough. *Canadian Journal of Earth Sciences*, Vol. 15, p. 245-252.
- _____, and FRANCIS, D.M., 1982. A transect of the early Proterozoic Cape Smith foldbelt, New Quebec. *Tectonophysics*, Vol. 88, p. 23-59.
- JACKSON, G.D. and TAYLOR, F.C., 1972. Correlation of major Archean rock units in the Canadian Shield. *Canadian Journal of Earth Sciences*, Vol. 9, p. 1650-1669.
- JACKSON, J.A. and WHITE, N.J., 1989. Normal faulting in the upper continental crust: observations from regions of active extension. *Journal of Structural Geology*, Vol. 11, No. 1/2, p. 15-36.
- JACKSON, M.P.A. and TALBOT, C.J., 1989. Anatomy of mushroom-shaped diapirs. *Journal of Structural Geology*, Vol. 11, No. 1/2, p. 211-230.
- JOURNEAY, M.J., 1983. Progressive deformation and inverted regional metamorphism associated with mesozoic emplacement of the Shuswap-Monashee Complex, S.E. British Columbia. *Geological Society of America, Abstracts with Programs*, p. 606.
- KEAREY, P., 1976. A regional structural model of the Labrador Trough, Quebec from gravity studies, and its relevance to continental collision in the Precambrian. *Earth and Planetary Science Letters*, Vol. 28, p. 371-378.
- KING, J.E., 1986. The metamorphic internal zone of the Wopmay Orogen (Early Proterozoic), Canada: 30 km of structural relief in a composite section based on plunge projection. *Tectonics*, Vol. 5, p. 973-994.
- KLEIN, C. Jr. and FINK, R.P., 1976. Petrology of the Sokoman iron formation in the Howells River area, at the western edge of the Labrador Trough. *Economic Geology*, Vol. 71, p. 453-487.
- KOZIOL, A.M. and NEWTON, R.C., 1988. Redetermination of anorthite breakdown and improvement of the plagioclase-garnet-aluminosilicate-quartz barometer. *American Mineralogist*, Vol. 73, p. 216-224.
- KRILL, A.G., 1985. Relationships between the Western Gneisses Region and the Trondheim region: stockwork-tectonics reconsidered. In: *The Caledonide Orogen - Scandinavia and Related Areas*. Edited by Gee, D.G. & Sturt, B.A., John Wiley, New York.
- KRONER, A., 1981. *Precambrian plate tectonics*. (editor) Elsevier, Amsterdam,

- LACASSIN, D. and MATTAUER, M., 1985. Kilometer sheath fold at Mattamark and implication for transport in the Alps. *Nature*, Vol. 316, p. 739-742.
- LAMOTHE, D., PICARD, C. and MOORHEAD, J., 1984. Bande de Cap Smith-Maricourt, région du Lac Beaugouard. Ministère de l'Energie et des Ressources, Québec. DP 84-39 (carte annotée).
- LASAGA, A.C., RICHARDSON, S.M. and HOLLAND, H.C., 1977. Mathematics of cation diffusion exchange between silicate minerals during retrograde metamorphism. In: *Energetics of geological processes*, Edited by S.K. Saxena and S. Bhattacharji. Springer-Verlag, Berlin, p. 353-388.
- LAUBSCHER, H., 1988. Material balance in Alpine orogeny. *Geological Society of America Bulletin*, Vol. 100, p. 1313-1328.
- LE GALLAIS, C.J. and LAVOIE, S., 1982. Basin evolution of the lower Proterozoic Kaniapiskau Supergroup, central Labrador miogeocline (trough), Quebec. *Bull. Can. Petroleum Geol.* 30, 150-166.
- LEWRY, J.F., 1981. Lower Proterozoic arc-microcontinent collisional tectonics in the western Churchill Province. *Nature*, Vol. 294, p. 69-72.
- _____ and SIBBALD, T.I.I., 1980. Thermotectonic evolution of the Churchill Province in northern Saskatchewan. *Tectonophysics*, Vol. 68, p. 45-82.
- LISTER, G.S. and DAVIS, G.A., 1989. The origin of metamorphic core complexes and detachment faults formed during Tertiary continental extension in the northern Colorado River region, U.S.A.. *Journal of Structural Geology*, Vol. 11, No. 1/2, p. 65-94.
- _____, ETHERIDGE, M.A., SYMONDS, P.A., 1986. Detachment faulting and the evolution of passive continental margins. *Geology*, Vol. 14, p. 246-250.
- LOOMIS, T.P., 1983. Compositional zoning of crystals: a record of growth and reaction history. In: *Kinetics and Equilibria in Mineral Reactions*, Edited by S. K. Saxena, *Advances in Geochemistry*, Vol. 3, p. 1-60.
- LOWDEN, J.A., STOCKWELL, C.H., TIPPER, H.W. and WANLESS, R.K., 1963. Age determinations and geological studies. *Geological Survey of Canada*, Paper 62-17, p. 100-103.
- MACHADO, N., PERREAULT, S. and HYNES, A., 1988. Timing of continental collision in the northern Labrador Trough, Quebec; Evidence from U-Pb geochronology. *Geological Association of Canada and Mineralogical Association of Canada, Joint Annual Meeting, Program with Abstracts*, p.76.
- _____, GOULET, N. and GARIÉPY, C., 1987. Evolution of the northern Labrador Trough basement: evidence from U-Pb geochronology. *Geological Association of Canada and Mineralogical Association of Canada, Joint*

Annual Meeting, Program with Abstracts, p.69.

MADORE, C. and PERREAULT, S., 1987. Behaviour of tourmaline in the prograde metamorphism of pelitic schist, Labrador Trough, KUUVJUAQ, Quebec. Geological Association of Canada and Mineralogical Association of Canada, Joint Annual Meeting, Program with Abstracts, p. 70.

MARTIGNOLE, J. and NANTEL, S., 1982. Geothermobarometry of cordierite-bearing metapelites near the Morin Anorthosite Complex, Grenville Province, Quebec. Canadian Mineralogist, Vol. 20, p. 307-318.

MATTAUER, M., 1981. Plis en fourreau d'échelle pluri-kilométrique dans la zone interne des Alpes Suisses (couverture nord de la Nappe du Mont-Rose). Comptes Rendus de l'Académie des Sciences, Paris. tome 293, p. 929-932.

_____, COLLOT, B. and VAN DEN DRIESSCHE, J., 1983. Alpine model for the internal metamorphic zones of the North American Cordillera. Geology, Vol. 11, p. 11-15.

MCDONOUGH, M.R. and SIMONY, P.S., 1989. Valemount strain zone: A dextral oblique-slip thrust system linking the Rocky Mountain and Omineca belts of the southeastern Canadian Cordillera. Geology, Vol. 17, p. 237-240.

_____, 1988. Structural evolution of basement gneisses and Hadrynian cover, Bulldog Creek area, Rocky Mountains, British Columbia. Canadian Journal of Earth Sciences, Vol. 25, p. 1687-1702.

McKENNA, L.W. and HODGES, K.V., 1988. Accuracy versus precision in reaction boundaries: Implications for the garnet-plagioclase-aluminum silicate-quartz geobarometer. American Mineralogist, Vol. 73, p. 1205-1208.

McSWIGGEN, P.L., MOREY, G.B. and CHANDLER, V.W., 1987. New model for the midcontinent rift in Eastern Minnesota and Western Wisconsin. Tectonics, Vol. 6, no. 6, p. 677-685.

MOORE, J.M., 1977. Orogenic volcanism in the Proterozoic of Canada. In Volcanic Regimes in Canada, Geological Association of Canada Special Paper, no. 16, edited by Baragar, W.R.A., Coleman, L.C. and Hall, J.M.. p. 127-148.

MOORHEAD, J. and HYNES, A., 1986. Structure and metamorphism of the eastern flank of the Renia gneiss dome. Geological Association of Canada and Mineralogical Association of Canada, Joint Annual Meeting, Program with Abstracts, p. 103.

MYERS, J.S. and WATKINS, K.P., 1985. Origin of granite-greenstone patterns, Yilgarn Block, Western Australia. Geology, Vol. 13, p. 778-780.

NEWTON, R.C. and HASELTON, H.T., Jr., 1981. Thermodynamics of the garnet-plagioclase- Al_2SiO_5 geobarometer. In: Thermodynamics of Minerals and Melts, Edited by R.C. Newton, A. Navrotsky and B.J. Wood. Springer-Verlag, New-York, p. 129-145.

NISBET, B.W., 1976. Structural studies in the northern Chester Dome of east-

central Vermont. Unpublished Ph.D. thesis, University State University, Albany, N.Y..

OKULITCH, A.V., 1984. The role of the Shuswap Metamorphic Complex in Cordilleran tectonism: a review. *Canadian Journal of Earth Sciences*, Vol. 21, p. 1171-1193.

PERCHUK, L.L. and LAVRENT'eva, I.V., 1983. Experimental investigation of the exchange equilibria in the system cordeirite-garnet-biotite. In: *Kinetics and equilibria in mineral reactions*, ed. by Saxena, S.K., *Advances in Geochemistry*.

PERREAULT, S. and HYNES, A., 1988. Timing of the tectonic evolution of the NE segment of the Labrador Trough, Kuujuaq, Northern Québec. *Geological Association of Canada and Mineralogical Association of Canada, Joint Annual Meeting, Program with Abstracts*, p. 97.

_____, HYNES, A. and MOORHEAD, J., 1987. Metamorphism of the eastern flank of the Labrador Trough, Kuujuaq, Ungava, Northern Quebec. *Geological Association of Canada and Mineralogical Association of Canada, Joint Annual Meeting, Program with Abstracts*, p. 80.

PIGAGE, L.C. and GREENWOOD, H.J., 1982. Internally consistent estimates of pressure and temperature: The staurolite problem. *American Journal of Science*, Vol. 282, p. 943-969.

PLATT, J.P., 1983. Progressive refolding in ductile shear zones. *Journal of Structural Geology*, Vol. 5, p. 619-622.

_____, 1980. Archean Greenstone belts: A structural test of a tectonic hypotheses. *Tectonophysics*, Vol. 65, p. 127-150.

POIRIER, G., 1989. Structure and metamorphism of the eastern boundary of the Labrador Trough near Kuujuaq, Québec, and its tectonic implications. Unpublished M.Sc. thesis, McGill University, Montréal.

_____, PERREAULT, S. and HYNES, A., 1987. The nature of the eastern boundary of the Labrador Trough near Kuujuaq, Quebec. *Geological Association of Canada and Mineralogical Association of Canada, Joint Annual Meeting, Program with Abstracts*, p. 81

_____, PERREAULT, S. and HYNES, A. (in press). The Nature of the Eastern Boundary of the Labrador Trough Near Kuujuaq, Quebec. *Trans-Hudsonian symposium volume*, Geological Association of Canada.

POWELL, P. and EVANS, J.A., 1983. A new geobarometer for the assemblage biotite-muscovite-chlorite-quartz. *Journal of Metamorphic Geology*, Vol. 1, p. 331-336.

PRICE, R.A. and MOUNTJOY, E.W., 1970. Geologic structure of the Canadian Rocky Mountains between Bow and Athabasca rivers - a progress report. *Geological Association of Canada, Special Paper no. 6*, p. 7-25.

RAMBERG, H., 1981. *Gravity, deformation and the Earth's crust*. Academic Press,

London, 452 p.

RAMSAY, J.G., 1967. Folding and fracturing in rocks. McGraw-Hill, New-York, 568 p.

_____, CASEY, M. and KLIGFIELD, R., 1983. Role of shear in development of the Helvetic fold-thrust belt of Switzerland. *Geology*, Vol. 11, p. 439-442.

_____ and HUBER, M.I., 1987. The techniques of modern structural geology, volume 2: Folds and Fractures. Academic Press, 700 p.

READ, P.B. and BROWN, R.L., 1981. Columbia River fault zone: southeastern margin of the Shuswap and Monashee complexes, southern British Columbia. *Canadian Journal of Earth Sciences*, Vol. 18, 1127-1145.

REESOR, J.E. and MOORE, J.M., 1971. Petrology and structure of the Thor-Odin Gneiss Dome, Shuswap Metamorphic complex, British Columbia. *Geological Survey of Canada, Bulletin* 195.

RICKARD, M.J., 1985. The Surnadal synform and basement gneisses in the Surnadal-Sunndal district of Norway. In: *The Caledonide Orogen - Scandinavia and Related Areas* (edited by Gee, D.G. and Sturt, B.A.) John Wiley & Sons Ltd., New York.

RICKETTS, B.D., DONALDSON, J.A. and WARE, M.J., 1982. Volcaniclastic rocks and volcaniclastic facies in the Middle Precambrian (Aphebian) Belcher Group, Northwest Territories, Canada. *Canadian Journal of Earth Science*. Vol. 19, p.1275-1294.

_____, 1981. Sedimentary history of the Belcher Group of Hudson Bay. In: *Proterozoic Basins of Canada*, Campbell, F.H.A. ed.. Geological Survey of Canada Paper 81-10.

ROSENFELD, J.L., 1968. Garnet rotations due to the major Paleozoic deformations in southeast Vermont. In: *Studies of Appalachian Geology, Northern and Maritime*, eds: Zen, E-an, White, W.S., Hadley, J.B. and Thompson, J.B., p. 185-202.

ROSS, J.V., 1968. Structural relationships at the eastern margin of the Shuswap Metamorphic Complex, near Revelstoke, southeastern British Columbia. *Canadian Journal of Earth Sciences*, Vol. 5, p.831-849.

SAUVÉ, P., 1959. Région de la baie aux Feuilles, Nouveau-Québec. *Ministère des Mines, Québec*; RP-399.

_____, 1957. De Fréneuse Lake Area (East Half) New Quebec. *Quebec Department of Mines, Preliminary Report* 358.

_____, 1956a. Région du lac Léopard (moitié est), Nouveau-Québec. *Ministère des Mines, Québec*; RP-325.

_____, 1956b. Région du lac de Fréneuse (moitié ouest), Nouveau-Québec. *Ministère des Mines, Québec*; RP-332.

- _____, 1955. Région du lac Gerido (moitié est), Nouveau-Québec. Ministère des Mines, Québec; RP-309.
- _____, and BERGERON, R., 1965. Région des lacs Gerido et Thévenet. Ministère des Richesses Naturelles du Québec, RG 104.
- SCHWERTDINER, W.M., 1982. Salt stocks as a natural analogues of Archean gneiss diapirs. *Geology Rundschau*, Vol. 71, p. 370-379.
- _____, 1981. Archean greenstone belts: a structural test of tectonic hypotheses. *Discussion. Tectonophysics*, Vol. 72, p. 159-163.
- _____, SUTCLIFFE, R.H. and TROENG, B., 1978. Patterns of total strain in the crestal region of immature diapirs. *Canadian Journal of Earth Sciences*, Vol. 15, p. 1437-1447.
- SÉGUIN, M., 1969. Configuration et nature du mode tectonique en bordure ouest de la partie centrale de la Fosse du Labrador. *Canadian Journal of Earth Sciences*, Vol. 6, p. 1365-1379.
- SELVERSTONE, J., SPEAR, F.S., GERHARD, F. and MORTEANI, G., 1984. High-pressure metamorphism in the SW Tauern Window, Australia: P-T paths from hornblende-kyanite-staurolite schists. *Journal of Petrology*, Vol. 84, p. 501-531.
- SIMONSON, B.M., 1985. Sedimentological constraints on the origin of Precambrian iron-formations. *Geological Society of America Bulletin*, vol. 96, p. 244-252.
- SIMONY, P.S., GHENT, E.D., CRAW, D., MITCHELL, W. and ROBBINS D.B., 1980. Structural and metamorphic evolution of the northeast flank of the Shuswap complex, southern Canoe River area, British Columbia. *Geological Society of America, Memoir 153*, p. 445-461.
- SIMPSON, C. and SCHMIDT, S.M., 1983. Evaluation of criteria to deduce the sense of movement in sheared rocks. *Geological Society of America Bulletin*, Vol. 94, p. 1281-1288.
- SPEAR, F.S., SELVERSTONE, J., HICKMOTT, D., CROWLEY, P. and HODGES, K.V., 1984. P-T paths from garnet zoning: A new technique for deciphering tectonic processes in crystalline terranes. *Geology*, Vol. 12, p. 87-90.
- _____, 1983. Quantitative P-T paths from zoned minerals: Theory and tectonic applications. *Contributions to Mineralogy and Petrology*, Vol. 83, p. 348-357.
- STAUFFER, M.R., 1988. Fold interference structures and coaption folds. *Tectonophysics*, Vol. 149, p. 339-343.
- STEL, H., 1988. Basement-cover relations at the Grong-Olden culmination, central Norway. *Norrsk Geologisk Tidsskrift*, Vol. 68, p. 135-147.

- STELTENPOHL, M.G. and BARTLEY, J.M., 1988. Cross folds and back folds in the Ofoten-Tysfjord area, north Norway, and their significance for Caledonian tectonics. *Geological Society of America Bulletin*, Vol. 100, p. 140-151.
- STEVENSON, I.M., 1968. A geological reconnaissance of Leaf River map area, New Quebec and Northwest Territories. *Geological Survey of Canada, Memoir 356*.
- STOCKWELL, C.H., 1982. Proposals for time classification and correlation of Precambrian rocks and events in Canada and adjacent areas of the Canadian Shield. Part I: A time classification of Precambrian rocks and events: *Geological Survey of Canada, Paper 80-19*, 135 p.
- _____, 1968. Geochronology of stratified rocks of the Canadian Shield. *Canadian Journal of Earth Sciences*, Vol. 22, 1361-1369.
- _____, 1964. Fourth report on structural provinces, orogenies and time-classification of rocks of the Canadian Precambrian Shield. Part II *Geological Studies: Geological Survey of Canada, Paper 64-17*, p.1-7.
- _____, 1950. The use of plunge in the construction of cross-sections of folds. *Proceedings of the Geological Association of Canada*, Vol. 3, p. 97-121.
- ST-ONGE, M.R., 1984. Geothermometry and geobarometry in pelitic rocks of north-central Wopmay Orogen (early Proterozoic), Northwest Territories, Canada. *Geological Society of America Bulletin*, vol. 95, p. 196-208.
- _____, and KING, J.E., 1987. Evolution and regional metamorphism during back-arc stretching and subsequent crustal shortening in the 1.9 Ga Wopmay Orogen, Canada. In: *Tectonic setting of regional metamorphism* (Oxburgh, E.R., Yardley, B.W.D. and England, P.C., eds.) *Philosophical Transactions of the Royal Society of London, Ser. A*, Vol. 321, p. 199-218.
- _____ and LUCAS, S.B., in press. Evolution of the Cape Smith Belt: Early Proterozoic continental underthrusting, ophiolite obduction and thick skinned folding. In: *Lithotectonic Correlations and Evolution*, edited by J.F. Lewry and M.R. Stauffer, *Geological Association of Canada, Special Paper*, in press.
- _____ and LUCAS, S.B., 1986. Structural and metamorphic evolution of an early Proterozoic thrust-fold belt, eastern Cape Smith belt (Ungava Trough), Quebec. In *Exploration en Ungava, Données recentes sur la géologie et la gîtologie, Séminaire d'information 1986*, Ministère de l'Énergie et des Ressources. DV 86-16, p.31-39.
- _____ SCOTT, D.J., BEGIN, N.J., HELMSTAEDT, H. and CARMICHAEL, D.M., 1988. Thin-skinned imbrication and subsequent thick-skinned folding of rift-fill, transitionnal-crust, and ophiolite suites in the 1.9 Ga Cape Smith Belt, Northern Quebec. In *Current Research, Part C*, *Geological Survey of Canada*.
- _____ 1987. Tectono-stratigraphy and structure of the Lac Watts-Lac Cross-Riviere Deception area, central Cape Smith Belt, Northern Quebec. In *Current Research, Part*

A, Geological Survey of Canada, Paper 87-1A, p. 619-632.

- _____, 1986. Eastern Cape Smith Belt: an early Proterozoic thrust-fold belt and basal shear zone exposed in oblique section, Wakeham Bay and Cratère du Nouveau-Québec map areas, Northern Quebec. In Current Research, Part A, Geological Survey of Canada, Paper 86-1A, p. 1-14.
- _____, LALONDE, A.E. and KING, J.E., 1983. Geology, Redrock and eastern Calder River Map Areas, District of McKenzie: The central Wopmay Orogen (Early Proterozoic), Bear Province, and the western Archan Slave Province. In: Current Research, Part A, Geological Survey of Canada, Paper 83-1a, p. 147-152.
- SUPPE, J., 1985. Principles of Structural Geology. Prentice-Hall, 537 p.
- TAYLOR, F.C., 1979. Reconnaissance geology of a part of the Precambrian Shield, northeastern Quebec, Northern Labrador and Northwest Territories, Geological Survey of Canada, Memoir 393, p. 1-99.
- _____, 1971. A Revision of Precambrian Structural Provinces in Northeastern Quebec and Northern Labrador. Canadian Journal of Earth Sciences, Vol. 8, p. 579-584.
- _____, and LOVERIDGE, W.D., 1981. A Rb-Sr study of a New Quebec Archean granodiorite; in Rb-Sr and U-Pb Isotopic Age Studies, Report 4, in Current Research, part C, Geological Survey of Canada, Paper 81-1C, p. 105-106.
- _____, and SKINNER, R., 1969. Fort Chimo, New Quebec. Geological Survey of Canada, Paper 63-47.
- THOMAS, M.D. and KEAREY, P., 1980. Gravity anomalies, block faulting and Andean-type tectonism in the eastern Churchill Province. Nature, Vol. 282, p. 61-63.
- _____, and GIBB, R.A., 1985. Proterozoic plate subduction and collision: processes for reactivation of Archean crust in the Churchill Province. In Evolution of Archean Supracrustal Sequences, Edited by L.D. Ayres, P.C. Thurston and W. Weber. Geological Association of Canada Special Paper No. 28.
- THOMPSON, A.B., 1976. Mineral reactions in pelitic rocks: II, Calculation of some P-T-X(Fe-Mg) phase relations. American Journal of Science, Vol. 276, p. 425-454.
- THOMPSON, J.B., ROBINSON, P., CLIFFORD, T.N. and TRASK, N.J., 1968. Nappes and gneiss domes in west central New England. In: studies of Appalachian geology (Northern and Maritime), edited by: Zen, E-an, White, W.S., Hadley, J.B. and Thompson, J.B., p. 203-218.
- _____, and ENGLAND, P.C., 1984. Pressure-temperature-time of paths of regional metamorphism. II: Their inference and interpretation using mineral assemblages in metamorphic rocks. Journal of Petrology, Vol. 25, p. 929-955.

- TRACY, R.J., ROBINSON, P., THOMPSON, A.B., 1976. Garnet composition and zoning in the determination of temperature and pressure of metamorphism, central Massachusetts. *American Mineralogist*, Vol. 61, p. 762-775.
- VAN DER LEEDEN, J., BELANGER, M., DANIS, D., GIRARD, R. and MARTELAIN J., in press. Lithotectonic domains in the high grade terrain east of the Labrador Trough (Québec). In: *The early Proterozoic Trans-Hudson Orogen: Lithotectonic Correlations and evolution*, Lewry, J.F. and Stauffer, M.R. eds.. Geological Association of Canada, Special Paper.
- _____, 1987. Lithotectonic domains in the high-grade terrain east of the Labrador Trough (Quebec). GAC-MAC Program with Abstracts, Saskatoon, 12, p. 98.
- VAN DEN DRIESSCHE, J. and MALUSKI, H., 1986. Mise en évidence d'un cisaillement ductile dextre d'âge crétacé moyen dans la région de Tête Jaune Caché (nord-est du complexe métamorphique Shuswap, Colombie-Britannique), *Canadian Journal of Earth Sciences*, Vol. 23, p. 1331-1342.
- VOLLMER, F.W., 1988. A Computer model of sheath-nappes formed during crustal shear in the Western Gneiss Region, central Norwegian Caledonides. *Tectonophysics, Journal of Structural Geology*, Vol. 10, p. 735-743.
- WANLESS, R.K., 1970. Isotopic map of Canada: Geological Survey of Canada, map 1265A.
- _____, STEVENS, R.D., LACHANCE, G.R. and RIMSAITE, J.Y.H., 1966. Age determinations and geological studies, K-Ar isotopic determinations, Report 6. *Geol. Surv. Canada Pap.*, 65-17, 101 p.
- WARDLE, R.J., 1979. Geology of the eastern margin of the Labrador Trough; Newfoundland Department of Mines and Energy, Mineral Development Division, Report 78-9.
- _____, RYAN, B.A. and NUNN, G.A., 1987. Labrador segment of the Trans-Hudson Orogen: Crustal development through oblique convergence and collision. Geological Association of Canada and Mineralogical Association of Canada, Joint Annual Meeting, Program with Abstracts, p. 99.
- _____, and BAILEY, D.G., 1981. Early Proterozoic sequences in Labrador. In *Proterozoic Basins in Canada* (F.H.A. Campbell, ed.). Geological Survey of Canada, Report 81-10.
- WARES, R.P., BERGER, J. and ST-SEYMOUR, K., 1988. Synthèse métallogénique des indices de sulfures au nord du 50^{ème} parallèle, Fosse du Labrador. *Mineral. Richesses Naturelles du Quebec*, MB-88-05.
- WARE, M.J. and WARDLE, R.J., 1979. Geology of the Sims-Evening Lake area, western Labrador, with emphasis on the Helikian Sims Group; Newfoundland Department of Mines and Energy, Mineral Development Division, Report 79-5.
- WERNICKE, B., 1984. Uniform-sense normal simple shear of the continental

lithosphere. Canadian Journal of Earth Sciences, Vol. 22., p. 108-125.

WOODSWORTH, G.J., 1977. Homogenization of zoned garnets from pelitic schists. Canadian Journal of Earth Sciences, Vol. 13, p. 230-242.

WYNNE-EDWARDS, H.R., 1961. Ossokmanuan Lake (west half), Newfoundland; Geological Survey of Canada, Map 17-1961.

_____, 1960. Geology, Michikamau Lake (west half) Quebec-Newfoundland; Geological Survey of Canada, Map 2-1960.

PLATE I

- a : Most common aspect of the Renia Dome, characterized by foliated to banded quartzo-feldspathic gneisses.
- b : Basement-cover contact, with fine-grain highly strained basement in the upper part of the picture and a disrupted semipelite layer (quartz-biotite-muscovite schist) at the base of the picture.
- c : Brittle sinistral faulting of a small aplitic dyke, outlined in black ink, cross-cutting the basement gneisses of the Boulder Dome.
- d : A 3 m wide tectonic breccia on the southern flank of the Boulder Dome.
- e : Folded calc-silicate horizon of the calcareous unit, here actinolite "nodules" are set in a calcite matrix. In less tectonically disrupted horizons, actinolite along with quartz define regular beds within the calcareous rock. This outcrop is from the infolded sediments within the Renia Dome.
- f : Graded turbidite beds of the lower micaceous unit, stratigraphic tops are to the left of the picture. The outcrop is along the eastern shore of Lac Rachel.



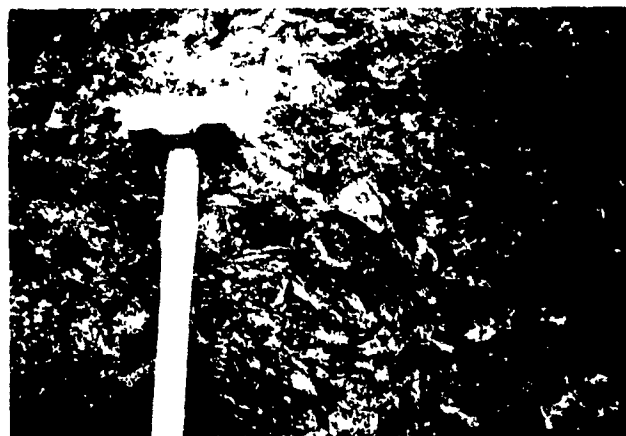
Ia



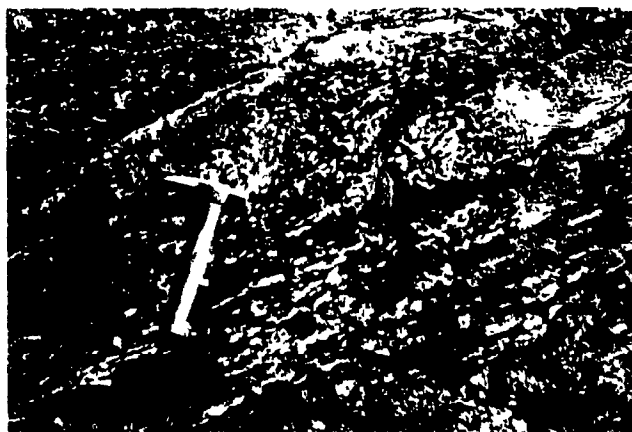
Ib



Ic



Id



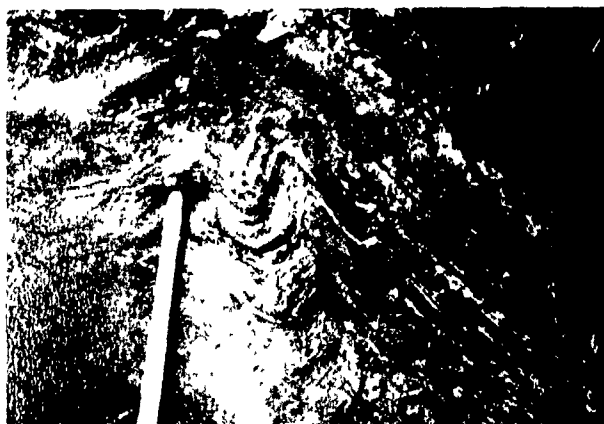
Ie



If

PLATE II

- a : Folded ferruginous shales of the upper iron formation, west of Lac Raymond.
- b : Boudinaged chert layers within the ferruginous shale, same location as previous picture.
- c : Well preserved pillow basalts of the mafic volcanic unit, from an outcrop in the heart of the NW trending Renia Synform, east of Lac Barrie.
- d : The basal volcanic conglomerate overlying the mafic volcanic unit. The lower portion of the basal conglomerate contains angular to sub-rounded basalt and gabbro fragments set in a chlorite-calcite matrix. Outcrop from the hinge zone of the major NW trending Renia Synform, east of Lac Barrie.
- e : The middle portion of the basal volcanic conglomerate overlying the mafic volcanic unit is characterized by more rounded basalt and gabbro clasts mixed in with siltstone fragments. This outcrop is located in the hinge zone of the F_1' syncline west of Lac Raymond, it contains a strong N trending axial planar cleavage parallel to the pencil.
- f : The upper volcanic conglomerate horizon in the siliciclastic assemblage overlying the mafic volcanic unit contains flattened fragments of sandstone, siltstone, quartz, gabbro and basalt set in a hornblende-chlorite-calcite matrix. This outcrop is located NE of Lac Raymond.



IIa



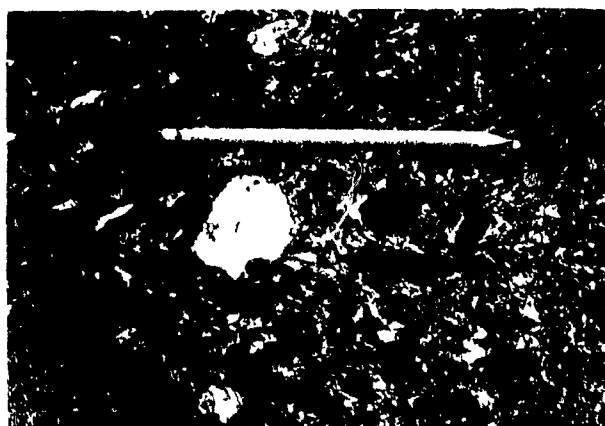
IIb



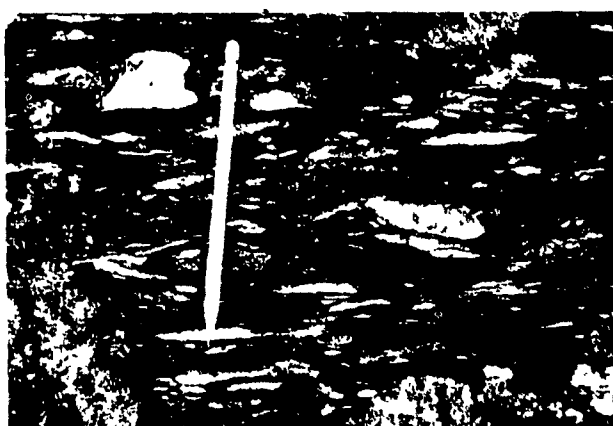
IIc



IId



IIe



IIIf

PLATE III

- a : Trough cross bedding in sandstones of the siliciclastic assemblage overlying the mafic volcanic unit, SE of Lac Barrie.
- b : A small conglomerate bed scouring down the underlying siltstone and sandstone sequence, from the siliciclastic assemblage, SE of Lac Barrie.
- c : Flattened calcareous nodule rimmed by hornblende crystals (indicated by the arrow) from the siliciclastic assemblage north of Lac Raymond. The scale is 5 cm long.
- d : Quartz pebble conglomerate horizon of the siliciclastic assemblage, north of Lac Raymond.
- e : Conglomerate composed of highly flattened siltstone fragments, situated near the upper volcanic conglomerate horizon in the siliciclastic assemblage N of Lac Raymond.
- f : Glomeroporphyritic sill intruding the upper iron formation horizon W of Lac Raymond.



IIIa



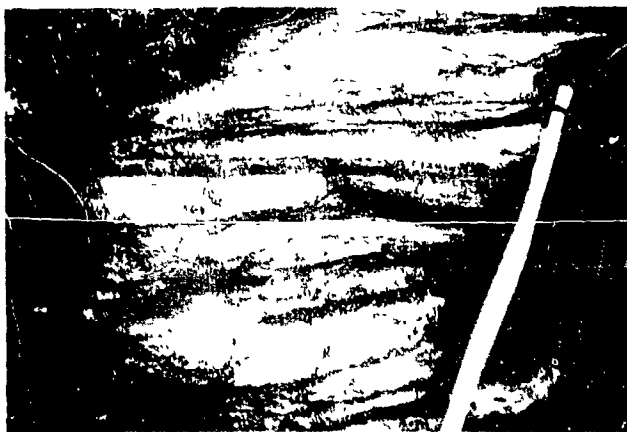
IIIb



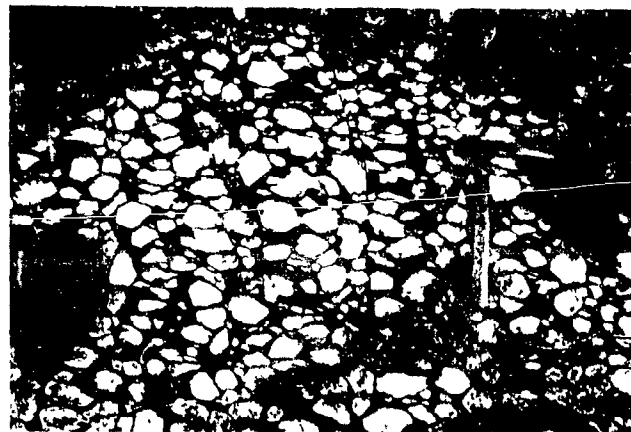
IIIc



IIId



IIIe



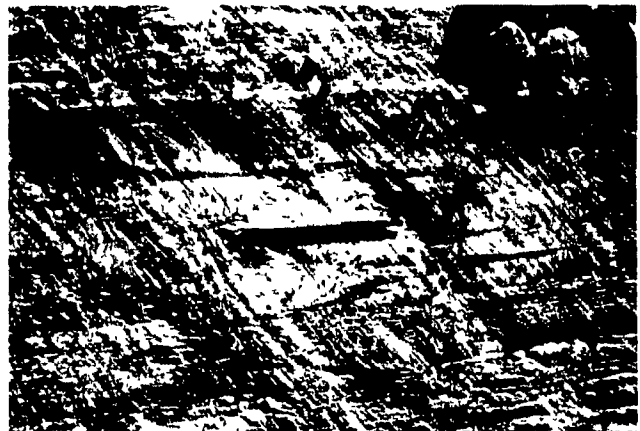
IIIf

PLATE IV

- a : Typical "pitted" appearance of the ultramafic intrusives. The cavities are usually composed of carbonates (ankerite or siderite) and iron oxides.
- b : F_1 isoclinal fold where the finer grained shale layer has flowed into the hinge zone of the fold. The lighter colored rocks are siltstones. Outcrop from the upper member of the Baby Formation central zone of the northern Labrador Trough. (Used by permission of N. Goulet).
- c : Recumbent F_1 fold closure within the middle member iron formation of the Baby Formation, central zone of the northern Labrador Trough. This picture is taken in the hinge zone of a large upright F_3 antiform, small F_3 folds can be seen to the right of the picture. The fold axes of F_1 and F_3 are roughly coaxial. The metal binder is 26 cm wide. (Used by permission of N. Goulet).
- d: Schematic drawing of the main features of plate IVc.
- e: Coaxial interference pattern between the first (F_1) and second (F_1') folding events within the upper iron formation, taken in the closure of F_1' syncline west of Lac Raymond.
- f: Schematic drawing of the main features of plate IVe.



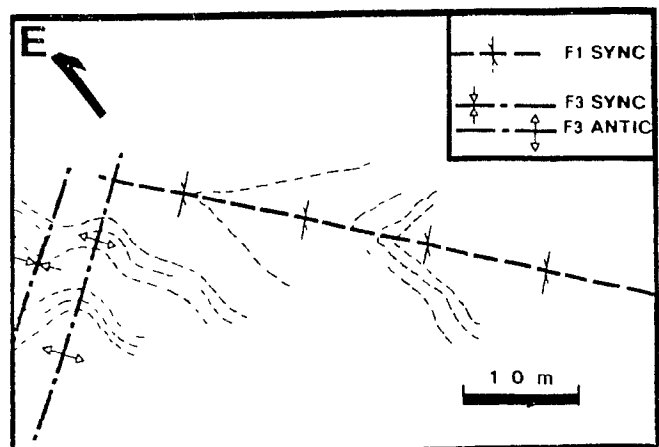
IVa



IVb



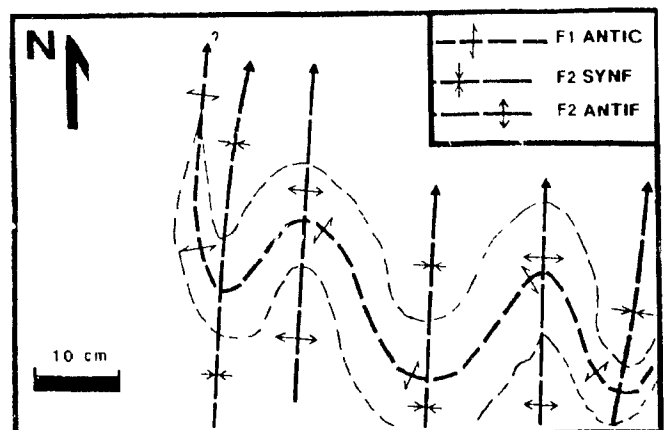
IVc



IVd



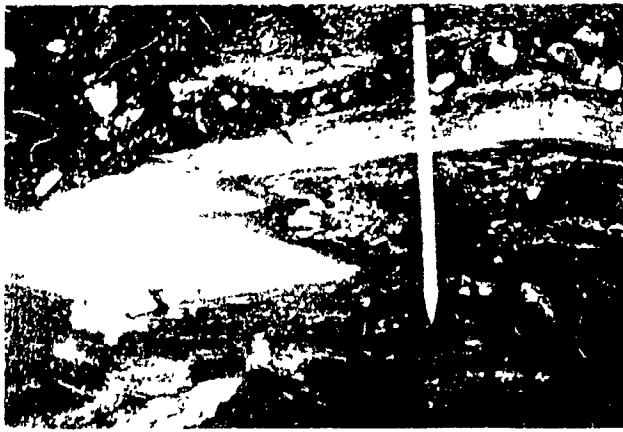
IVe



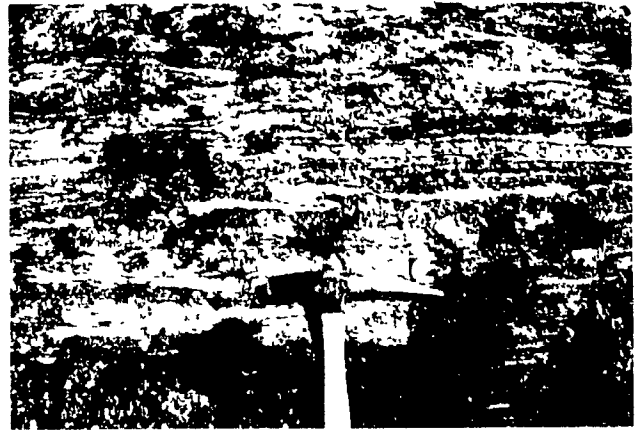
IVf

PLATE V

- a : F_1 fold vergent to west in the tremolite bearing marble horizon directly overlying the NW closure of the Renia Gneiss. The left hand side of the picture contains relatively pure marble whereas the right hand side is rich in tremolite.
- b : A small F_1 S fold deforms a small chert horizon within the upper iron formation west of Lac Raymond. The iron formation is composed mostly of hornblende and garnet.
- c : F_1 isoclinal fold defined by a quartz vein in the siliciclastic assemblage overlying the mafic volcanic unit north of Lac Raymond.
- d : Typical F_1' fold morphology from a sandstone layer in the upper portion of the lower micaceous schist unit. Bed thickness is almost maintained on the limbs, approaching concentric folding. This outcrop is situated east of Lac Raymond.
- e : Minor F_1' fold from the hinge zone of the refolded basement-cored F_1' antiform at the northern closure of the Renia Gneiss. Cross-cutting F_3 folds are visible next to the pencil.
- f: Schematic drawing of the main features of plate Ve.



Va



Vb



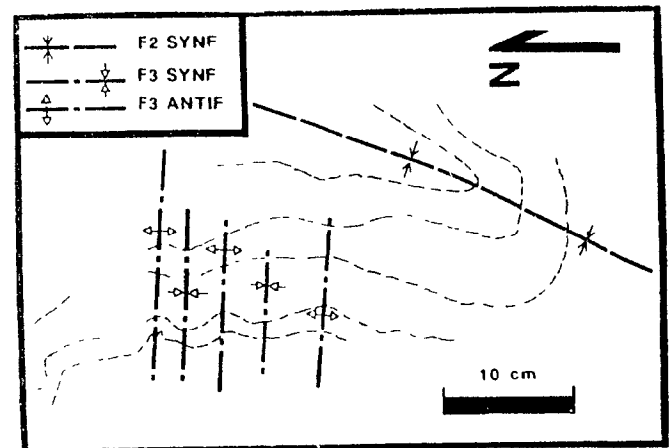
Vc



Vd



Ve



Vf

PLATE VI

- a : Sheared out remnants of F_1' folds defined by competent quartzo-feldspathic layers within a biotite rich horizon in the Renia gneisses, from same location as previous figure.
- b : En echelon quartz veins in a massive sandstone horizon with asymmetric tails indicating sinistral shearing. This is compatible with the sense of vergence of minor F_1' folds, taken on the eastern limb of the large F_1' syncline, south of Lac Raymond.
- c : Stretching lineation fabric defined by elongated quartz rich siltstone fragments set in a hornblende rich volcanoclastic matrix. This outcrop is from the mixed volcanic-sedimentary conglomerate within the upper portion of the siliciclastic assemblage overlying the mafic volcanic unit, north of Lac Raymond.
- d : A close to coaxial interference pattern between F_1' and F_3 . F_1' folds are defined by the crescent shaped calcareous boudins. Open F_3 Z folds can be seen at the base of the picture. This outcrop is located in a fine-grained portion of the siliciclastic assemblage found between the 2 bands of mafic volcanics, in the core of the large F_1' syncline west of Lac Raymond.
- e : Schematic drawing of the main features of plate VI d.



Vla



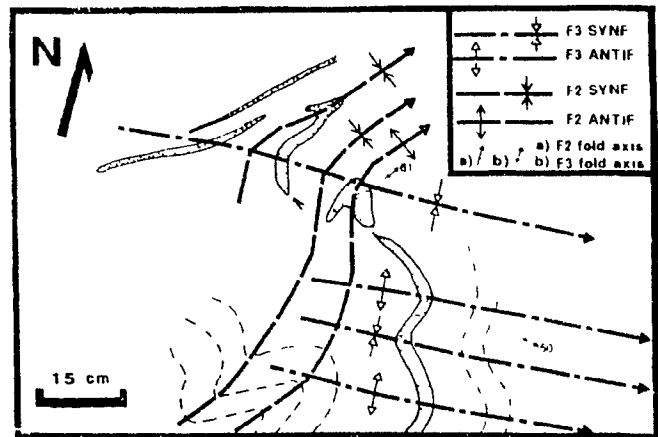
Vlb



Vlc



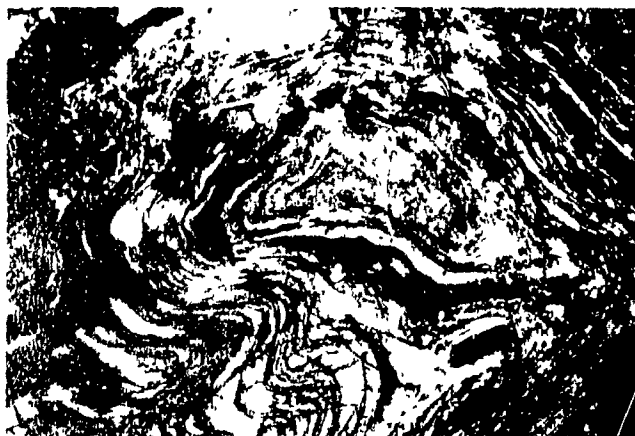
Vld



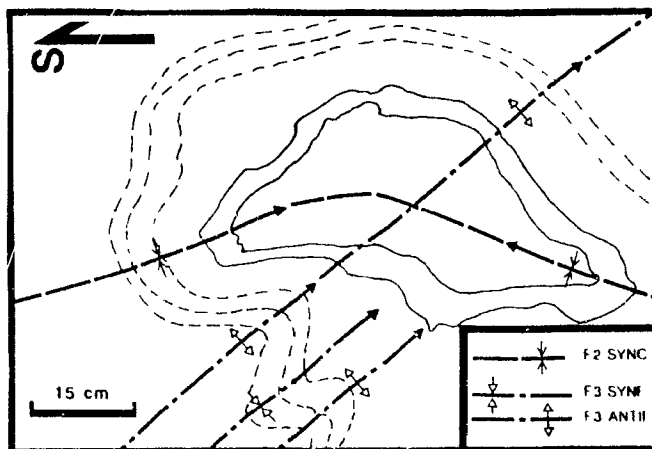
Vle

PLATE VII

- a : Dome and basin interference pattern between the F_1' and F_3 folding phases in a heterogeneous amphibolite horizon from the calcareous unit. This example is composed of hornblende and quartz rich layers. This outcrop is from the SW flank of the Renia Gneiss, west of the northern end of Lac Renia.
- b : Schematic drawing of plate VIIa.
- c : Well developed Z folds related to F_3 , developed in the siliciclastic assemblage overlying the mafic volcanic unit.
- d : F_3 crenulations at a high angle to the main schistosity plane, strongly developed at the base of the mafic volcanic unit, south of Lac Raymond.
- e : Millimeter scale metamorphic layering related to D_3 cross-cutting the bedding surfaces (S_0), eastern shore of Lac Rachel.
- f : Small senestral fault offsetting a quartz rich horizon within a siltstone sequence of the siliciclastic assemblage overlying the mafic volcanic unit. This outcrop is situated in the heart of the Renia Synform, N of Lac Raymond.



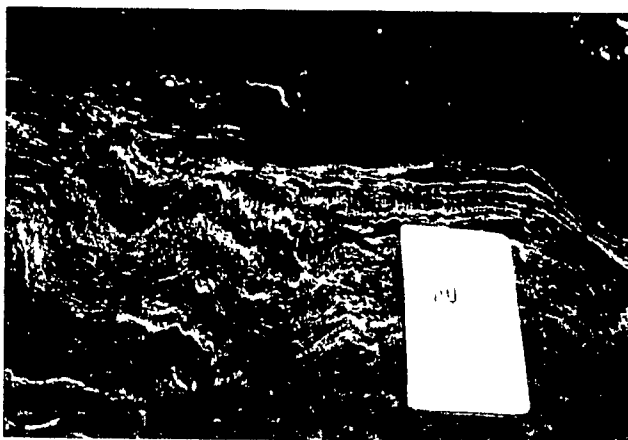
VIIa



VIIb



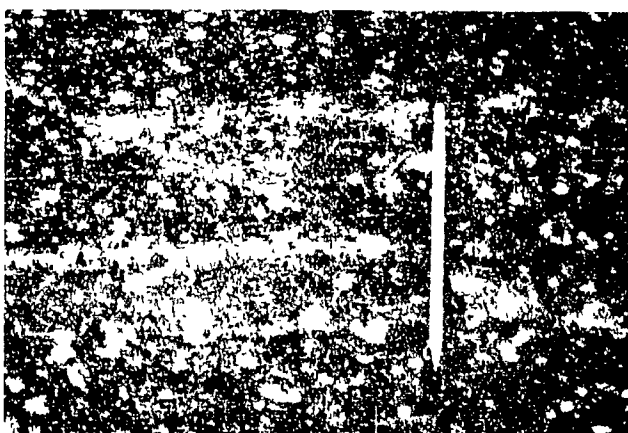
VIIc



VIIId



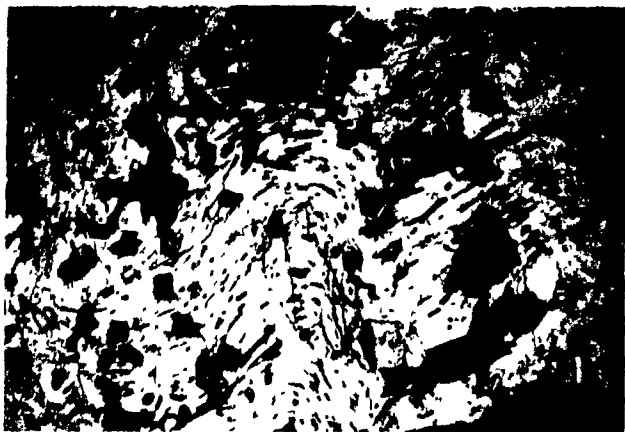
VIIe



VIIIf

PLATE VIII

- a :Staurolite grain overgrowing the hinge zone of an F_3 crenulation fold. The sample is from an outcrop defining the staurolite isograd west of the Renia Gneiss. The scale on the microphotograph is 1 mm.
- b :Staurolite grain overgrowing an F_3 crenulation. The scale is 1 mm.
- c :Garnets with aligned inclusion trails of quartz that define S folds with the matrix schistosity. The folds are related to an S_3 crenulation cleavage. The outcrop is located within the infolded tongue of metasediments at the NW closure of the Renia Gneiss.



VIIIa



VIIIb



VIIIc

APPENDIX I: PROBE ANALYSES OF MINERALS

CHLORITE

	2002-7AVG	2002-9AVG	2002-10AVG
SiO2	24.99	24.75	24.73
TiO2	0.12	0.09	0.09
Al2O3	24.10	23.59	23.61
Cr2O3	0.00	0.00	0.00
FeO	24.93	24.86	24.76
MnO	0.03	0.01	0.05
MgO	14.68	14.54	14.57
BaO	0.00	0.00	0.00
CaO	0.00	0.00	0.01
Na2O	0.01	0.00	0.01
K2O	0.02	0.03	0.01
TOTAL	88.90	87.87	87.86

CHLORITE STOICHIOMETRYS BASED ON 28 OXYGENS

Si	5.161	5.178	5.173
Aliv	2.839	2.822	2.827
Alvi	3.022	2.989	2.989
Ti	0.019	0.015	0.015
Fe	4.305	4.349	4.331
Mn	0.006	0.002	0.010
Mg	4.520	4.535	4.544
Ca	0.001	0.000	0.003
Na	0.006	0.000	0.004
K	0.007	0.008	0.003
Aclin	0.0245	0.0249	0.0251

MUSCOVITE

	2002-7	2002-9	2002-10	2015-11-1	2015-11-3	2015-71
SiO2	47.78	45.52	48.19	49.28	46.19	46.65
TiO2	0.26	0.23	0.29	0.04	0.42	0.33
Al2O3	36.25	35.93	35.80	40.63	36.84	36.78
Cr2O3	0.00	0.00	0.00	0.00	0.00	0.00
FeO	0.71	0.73	0.80	0.37	0.77	0.49
MnO	0.01	0.01	0.00	0.01	0.02	0.01
MgO	0.50	0.42	0.56	0.09	0.43	0.37
BaO	0.00	0.00	0.00	0.00	0.00	0.00
CaO	0.01	0.01	0.01	0.34	0.00	0.01
Na2O	1.33	1.52	1.25	5.77	1.55	2.17
K2O	7.82	9.29	7.97	0.00	7.64	6.92
TOTAL	94.68	93.65	94.88	97.52	93.87	93.73

MUSCOVITE STOICHIOMETRYS BASED ON 22 OXYGENS

Si	6.269	6.123	6.313	6.108	6.128	6.171
Aliv	1.731	1.877	1.687	1.892	1.872	1.829
Alvi	3.869	3.813	3.836	4.037	3.882	3.900
Ti	0.026	0.024	0.028	0.004	0.042	0.032
Mg	0.001	0.001	0.001	0.001	0.003	0.001
Fe	0.078	0.082	0.088	0.039	0.086	0.054
Mn	0.098	0.083	0.109	0.018	0.085	0.072
K	1.309	1.594	1.332	0.154	1.293	1.168
Na	0.339	0.386	0.317	1.387	0.399	0.557
Ca	0.001	0.001	0.002	0.046	0.000	0.001
AMusc	0.577	0.705	0.577	0.074	0.571	0.530
AFeCel	0.011	0.018	0.015	0.001	0.008	0.006

MUSCOVITE

	2300-3	2300-23	2300-5	2144-4-1	2144-4-2
SiO2	48.44	48.93	46.89	47.94	46.18
TiO2	0.34	0.63	0.56	0.51	0.53
Al2O3	35.11	36.30	35.84	35.33	35.05
Cr2O3	0.00	0.00	0.00	0.00	0.00
FeO	2.52	2.55	2.31	0.95	1.22
MnO	0.04	0.02	0.04	0.02	0.01
MgO	0.48	0.68	0.72	0.77	0.66
BaO	0.00	0.00	0.00	0.00	0.00
CaO	0.01	0.00	0.00	0.00	0.00
Na2O	1.14	1.24	1.30	0.81	0.98
K2O	7.51	7.16	7.05	6.65	10.32
TOTAL	95.60	97.51	96.71	93.00	94.95

MUSCOVITE STOICHIOMETRYS BASED ON 22 OXYGENS

Si	6.334	6.262	6.298	6.351	6.170
Aliv	1.666	1.738	1.702	1.649	1.830
Alvi	3.741	3.731	3.734	3.860	3.684
Ti	0.034	0.061	0.054	0.051	0.053
Mg	0.004	0.002	0.004	0.003	0.001
Fe	0.276	0.273	0.294	0.106	0.136
Mn	0.093	0.130	0.138	0.154	0.131
K	1.254	1.169	1.159	1.116	1.759
Na	0.289	0.308	0.325	0.207	0.236
Ca	0.001	0.000	0.000	0.000	0.000
AMusc	0.492	0.448	0.447	0.470	0.726
AFcCel	0.035	0.026	0.025	0.013	0.035

PLAGIOCLASE

	2015-11-1	2015-11-2	2015-7-1	2015-7-2	2015-7-3	2300-5
SiO2	67.65	66.49	67.63	67.73	67.56	60.76
TiO2	0.01	0.00	0.02	0.06	0.06	0.02
Al2O3	21.10	21.44	20.59	21.00	21.48	24.39
Cr2O3	0.00	0.00	0.00	0.00	0.00	0.00
FeO	0.05	0.10	0.02	0.01	0.08	0.11
MnO	0.01	0.00	0.01	0.01	0.00	0.01
MgO	0.01	0.00	0.00	0.00	0.02	0.00
BaO	0.00	0.00	0.00	0.00	0.00	0.00
CaO	1.67	2.42	1.69	1.78	1.94	6.20
Na2O	9.68	9.84	10.46	10.61	10.14	8.05
K2O	0.03	0.04	0.02	0.04	0.00	0.04
TOTAL	100.21	100.33	100.45	101.20	101.28	99.59

NUMBER OF CATIONS BASED ON 32 OXIGENS

Si	11.772	11.619	11.782	11.725	11.674	10.846
Ti	0.001	0.000	0.002	0.003	0.008	0.003
Al	4.324	4.411	4.223	4.280	4.370	5.127
Cr	0.000	0.000	0.000	0.000	0.000	0.000
Fe	0.007	0.015	0.003	0.001	0.012	0.017
Mn	0.001	0.000	0.002	0.001	0.000	0.002
Mg	0.002	0.000	0.001	0.000	0.005	0.000
Ba	0.000	0.000	0.000	0.000	0.000	0.000
Ca	0.313	0.453	0.315	0.330	0.359	1.186
Na	3.270	3.334	3.534	3.561	3.397	2.787
K	0.007	0.009	0.004	0.009	0.000	0.009
Xor	0.002	0.002	0.001	0.002	0.000	0.002
Xab	0.908	0.875	0.916	0.912	0.900	0.697
Xan	0.090	0.123	0.083	0.085	0.100	0.301

PLAGIOCLASE

	2300-3"90"	2300-23"50"	2144-1	2144-6
SiO2	61.00	62.28	62.89	62.89
TiO2	0.04	0.02	0.00	0.02
Al2O3	24.47	24.05	23.02	23.23
Fe2O3	0.00	0.00	0.00	0.00
Cr2O3	0.00	0.00	0.00	0.00
FeO	0.18	0.10	0.05	0.04
MnO	0.03	0.01	0.01	0.00
MgO	0.00	0.00	0.00	0.00
BaO	0.00	0.00	0.00	0.00
CaO	6.08	5.56	4.70	4.89
Na2O	7.98	8.00	8.88	8.77
K2O	0.07	0.07	0.09	0.08
TOTAL	99.85	100.08	99.65	100.01

NUMBER OF CATIONS BASED ON 32 OXIGENS

Si	10.857	11.013	11.165	11.141
Ti	0.005	0.002	0.001	0.002
Al	5.128	5.007	4.813	4.839
Cr	0.000	0.000	0.000	0.000
Fe	0.026	0.015	0.007	0.006
Mn	0.004	0.002	0.002	0.001
Mg	0.000	0.000	0.000	0.000
Ba	0.000	0.000	0.000	0.000
Ca	1.161	1.054	0.894	0.926
Na	2.755	2.742	3.058	3.009
K	0.016	0.015	0.020	0.019
Xor	0.004	0.004	0.005	0.005
Xab	0.701	0.714	0.768	0.760
Xan	0.295	0.281	0.227	0.235

GARNET

	2002-2"0"	2002-2"50"	2002-2"885"	2002-3"0"	2002-3"100"	2002-3"630"
SiO2	37.14	37.72	37.25	36.94	37.29	37.21
TiO2	0.06	0.16	0.14	0.06	0.17	0.16
Al2O3	20.69	20.79	20.73	20.49	20.63	20.30
Cr2O3	0.00	0.05	0.06	0.00	0.05	0.05
FeO	37.58	36.19	30.68	36.23	34.29	31.86
MnO	0.64	0.58	5.00	0.79	1.04	4.33
MgO	2.39	2.74	1.58	2.02	2.23	1.66
CaO	1.74	2.83	4.68	2.65	3.79	4.30
TOTAL	100.24	101.06	100.12	99.18	99.49	99.87

RESULTS NORMALIZED TO 8 CATIONS

Si	3.002	3.010	3.007	3.017	3.022	3.016
Ti	0.004	0.010	0.008	0.004	0.010	0.010
AlIV	0.000	0.000	0.000	0.000	0.000	0.000
AlVI	1.969	1.953	1.970	1.970	1.969	1.938
Cr	0.000	0.003	0.004	0.000	0.003	0.003
Fe	2.540	2.415	2.071	2.475	2.324	2.159
Mn	0.044	0.039	0.342	0.055	0.071	0.297
Mg	0.288	0.326	0.190	0.246	0.269	0.201
Ca	0.151	0.242	0.405	0.232	0.329	0.373
Xal	0.840	0.799	0.689	0.823	0.777	0.713
Xsp	0.015	0.013	0.114	0.018	0.024	0.098
Xpy	0.095	0.108	0.063	0.082	0.090	0.066
Xgr	0.050	0.080	0.135	0.077	0.110	0.123

GARNETS

	2015-11"0"	2015-11"100"	2015-11"545"	2015-11"1025"	2015-11"1070"
SiO2	37.37	37.46	37.45	37.58	37.43
TiO2	0.00	0.00	0.14	0.04	0.00
Al2O3	20.93	20.91	20.86	20.90	20.83
Cr2O3	0.09	0.05	0.00	0.01	0.04
FeO	35.67	32.19	23.80	35.55	36.12
MnO	1.33	2.11	6.13	1.29	1.22
MgO	2.60	2.70	1.05	3.17	2.89
CaO	1.18	3.52	9.26	1.06	0.66
TOTAL	99.17	98.94	98.69	99.06	99.19

RESULTS NORMALIZED TO 8 CATIONS

Si	3.044	3.038	3.035	3.039	3.047
Ti	0.000	0.000	0.009	0.002	0.000
AlIV	0.000	0.000	0.000	0.000	0.000
AlVI	2.008	1.997	1.990	1.990	1.997
Cr	0.006	0.003	0.000	0.001	0.003
Fe	2.430	2.183	1.613	2.404	2.459
Mn	0.092	0.145	0.421	0.088	0.084
Mg	0.216	0.326	0.127	0.382	0.351
Ca	0.103	0.306	0.804	0.092	0.058
Xal	0.826	0.737	0.544	0.811	0.833
Xsp	0.031	0.049	0.142	0.030	0.029
Xpy	0.107	0.110	0.043	0.129	0.119
Xgr	0.035	0.103	0.271	0.031	0.020

GARNETS

	2015-7"0"	2015-7"500"	2300-5"0"	2300-5"780"	2300-23"0"	2300-23"400"
SiO2	37.67	37.69	37.41	36.74	37.26	37.42
TiO2	0.00	0.29	0.02	0.10	0.01	0.11
Al2O3	20.52	20.65	20.75	20.12	21.03	20.64
Cr2O3	0.02	0.02	0.01	0.00	0.00	0.01
FeO	35.27	23.93	27.53	20.37	28.10	29.94
MnO	1.35	6.49	7.01	14.94	6.75	4.19
MgO	3.11	1.00	3.22	0.84	3.06	2.29
CaO	1.35	9.07	3.17	5.95	4.24	5.51
TOTAL	99.29	99.14	99.12	99.06	100.45	100.11

RESULTS NORMALIZED TO 8 CATIONS

Si	3.057	3.046	3.022	3.004	2.970	3.001
Ti	0.000	0.018	0.001	0.006	0.001	0.007
AlIV	0.000	0.000	0.000	0.000	0.030	0.000
AlVI	1.960	1.965	1.973	1.937	1.943	1.946
Cr	0.001	0.001	0.001	0.000	0.000	0.001
Fe	2.355	1.602	1.835	1.336	1.817	1.965
Mn	0.093	0.444	0.480	1.035	0.456	0.285
Mg	0.376	0.120	0.388	0.102	0.364	0.274
Ca	0.117	0.618	0.274	0.521	0.362	0.474
Xal	0.803	0.578	0.620	0.457	0.613	0.662
Xsp	0.031	0.159	0.160	0.339	0.149	0.093
Xpy	0.126	0.043	0.130	0.033	0.119	0.089
Xgr	0.039	0.221	0.091	0.171	0.119	0.156

GARNETS

	2300-3"440"	2144-4"0"	2144-4"7540"
SiO2	37.15	37.87	36.99
TiO2	0.03	0.09	0.04
Al2O3	20.59	20.88	20.37
Cr2O3	0.02	0.03	0.01
FeO	28.53	33.34	33.65
MnO	8.55	0.05	1.32
MgO	2.83	3.64	1.84
CaO	2.44	4.79	5.00
TOTAL	100.14	100.69	99.22

RESULTS NORMALIZED TO 8 CATIONS

Si	2.990	2.998	3.007
Ti	0.002	0.005	0.002
AlIV	0.010	0.002	0.000
AlVI	1.942	1.944	1.950
Cr	0.001	0.002	0.001
Fe	1.920	2.207	2.288
Mn	0.583	0.003	0.091
Mg	0.340	0.430	0.223
Ca	0.210	0.406	0.436
Xal	0.629	0.725	0.753
Xsp	0.191	0.001	0.030
Xpy	0.111	0.141	0.073
Xgr	0.069	0.133	0.144

BIOTITE

	2002-9 AVG	2002-15 AVG	2002-10 AVG	2015-11 AVG	2015-73 AVG
SiO2	35.42	35.27	35.95	36.52	36.86
TiO2	1.82	1.65	1.98	1.90	1.78
Al2O3	19.61	19.25	19.41	19.62	19.19
FeO	18.41	18.85	18.95	18.20	17.73
MnO	0.00	0.01	0.01	0.01	0.02
MgO	9.75	9.88	9.90	10.46	10.59
BaO	0.00	0.00	0.00	0.00	0.00
CaO	0.01	0.01	0.00	0.00	0.00
Na2O	0.30	0.27	0.27	0.22	0.22
K2O	8.97	9.02	8.80	8.82	8.44
TOTAL	94.29	94.51	95.27	95.75	94.83

BIOTITE STOICHIOMETRYS BASED ON 22 OXYGENS

Si	5.404	5.428	5.429	5.456	5.553
AlIV	2.596	2.572	2.571	2.544	2.467
AlVI	0.931	0.890	0.884	0.912	0.929
Ti	0.209	0.189	0.225	0.213	0.200
Mg	2.216	2.247	2.228	2.330	2.371
Fe	2.348	2.405	2.393	2.274	2.226
Mn	0.000	0.002	0.001	0.001	0.003
Na	0.088	0.079	0.079	0.063	0.065
K	1.746	1.756	1.696	1.681	1.617
Ca	0.001	0.001	0.000	0.000	0.000
Aphlog	0.041	0.043	0.040	0.046	0.047

BIOTITE

	2015-71 AVG	2300-5-3	2300-51M	2300-52M	2300-2-3	2300-2-3AVG
SiO2	36.28	37.39	36.96	36.51	37.55	37.16
TiO2	2.36	1.54	1.57	1.86	1.26	1.70
Al2O3	19.51	18.95	19.06	18.73	18.87	19.29
FeO	17.77	14.78	14.51	14.47	14.94	14.75
MnO	0.01	0.13	0.08	0.08	0.08	0.14
MgO	10.75	13.36	13.62	13.34	13.30	13.76
CaO	0.00	0.00	0.00	0.00	0.00	0.01
Na2O	0.22	0.29	0.02	0.30	0.26	0.28
K2O	9.43	9.22	9.58	9.04	9.04	9.12
TOTAL	96.21	95.66	95.68	94.33	96.43	96.21

BIOTITE STOICHIOMETRYS BASED ON 22 OXIGENS

Si	5.410	5.515	5.461	5.463	5.523	5.449
AlIV	2.590	2.485	2.539	2.537	2.477	2.551
AlVI	0.839	0.810	0.781	0.766	0.892	0.782
Ti	0.250	0.171	0.174	0.209	0.134	0.187
Mg	2.389	2.937	3.000	2.975	2.897	3.008
Fe	2.217	1.823	1.793	1.811	1.802	1.808
Mn	0.001	0.016	0.010	0.010	0.012	0.017
Na	0.065	0.083	0.080	0.087	0.088	0.080
K	1.794	1.735	1.806	1.725	1.754	1.705
Ca	0.000	0.000	0.003	0.000	0.000	0.002
Aphlog		0.095	0.105	0.098	0.093	

BIOTITE

	2300-51AVG	2300-5AVG	2300-5-1M	2300-5-2M	2144-22AVG
SiO2	37.38	36.95	36.96	36.51	36.28
TiO2	1.68	1.70	1.57	1.86	1.75
Al2O3	18.89	18.89	19.06	18.73	19.69
FeO	13.66	14.21	14.51	14.47	17.02
MnO	0.08	0.08	0.08	0.08	0.01
MgO	13.65	13.54	13.62	13.34	10.67
CaO	0.02	0.01	0.02	0.00	0.00
Na2O	0.27	0.28	0.28	0.30	0.19
K2O	9.25	9.29	9.58	9.04	9.44
TOTAL	94.88	94.96	95.68	94.33	95.05

BIOTITE STOICHIOMETRYS BASED ON 22 OXIGENS

Si	5.530	5.485	5.461	5.463	5.454
AlIV	2.470	2.515	2.539	2.537	2.546
AlVI	0.824	0.790	0.781	0.766	0.942
Ti	0.187	0.190	0.174	0.209	0.198
Mg	3.010	2.995	3.000	2.975	2.391
Fe	1.690	1.765	1.793	1.811	2.140
Mn	0.010	0.010	0.010	0.010	0.001
Na	0.077	0.082	0.080	0.087	0.055
K	1.746	1.759	1.806	1.725	1.810
Ca	0.003	0.002	0.003	0.000	0.000
Aphlog	0.104	0.102	0.105	0.098	0.053

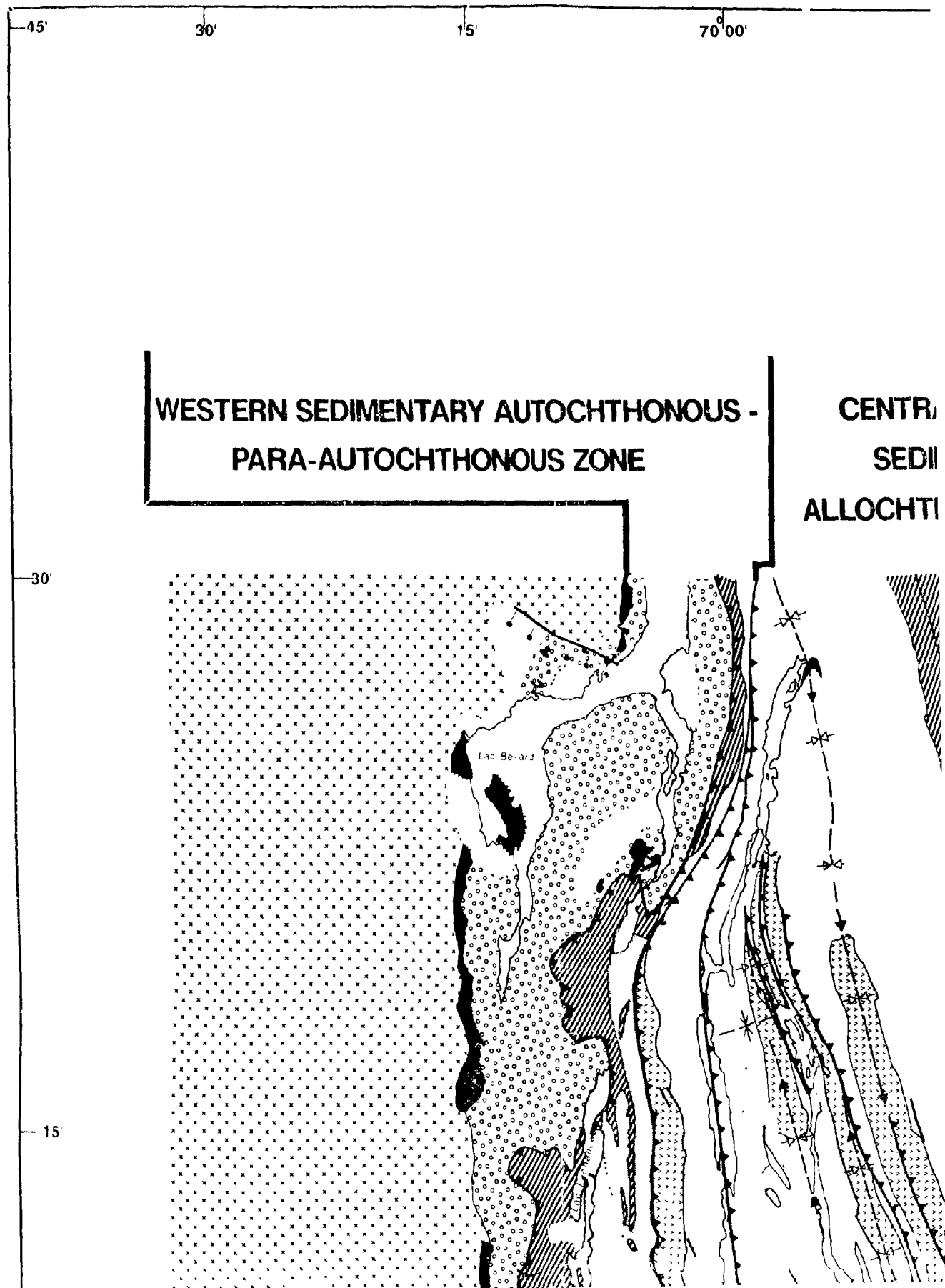
BIOTITE

	2144-4AVG	2144-2AVG
SiO2	35.64	36.34
TiO2	1.97	1.68
Al2O3	18.80	19.91
FeO	17.47	16.61
MnO	0.00	0.03
MgO	10.34	10.69
CaO	0.00	0.00
Na2O	0.18	0.19
K2O	9.66	9.54

TOTAL	94.07	95.02
-------	-------	-------

BIOTITE STOICHIOMETRYS BASED ON 22 OXIGENS

Si	5.451	5.456
AlIV	2.549	2.544
AlVI	0.840	0.979
Ti	0.227	0.190
Mg	2.357	2.392
Fe	2.235	2.085
Mn	0.000	0.004
Na	0.053	0.057
K	1.885	1.828
Ca	0.000	0.001
Aphlog	0.054	0.054



45'

30'

15'

69°00'

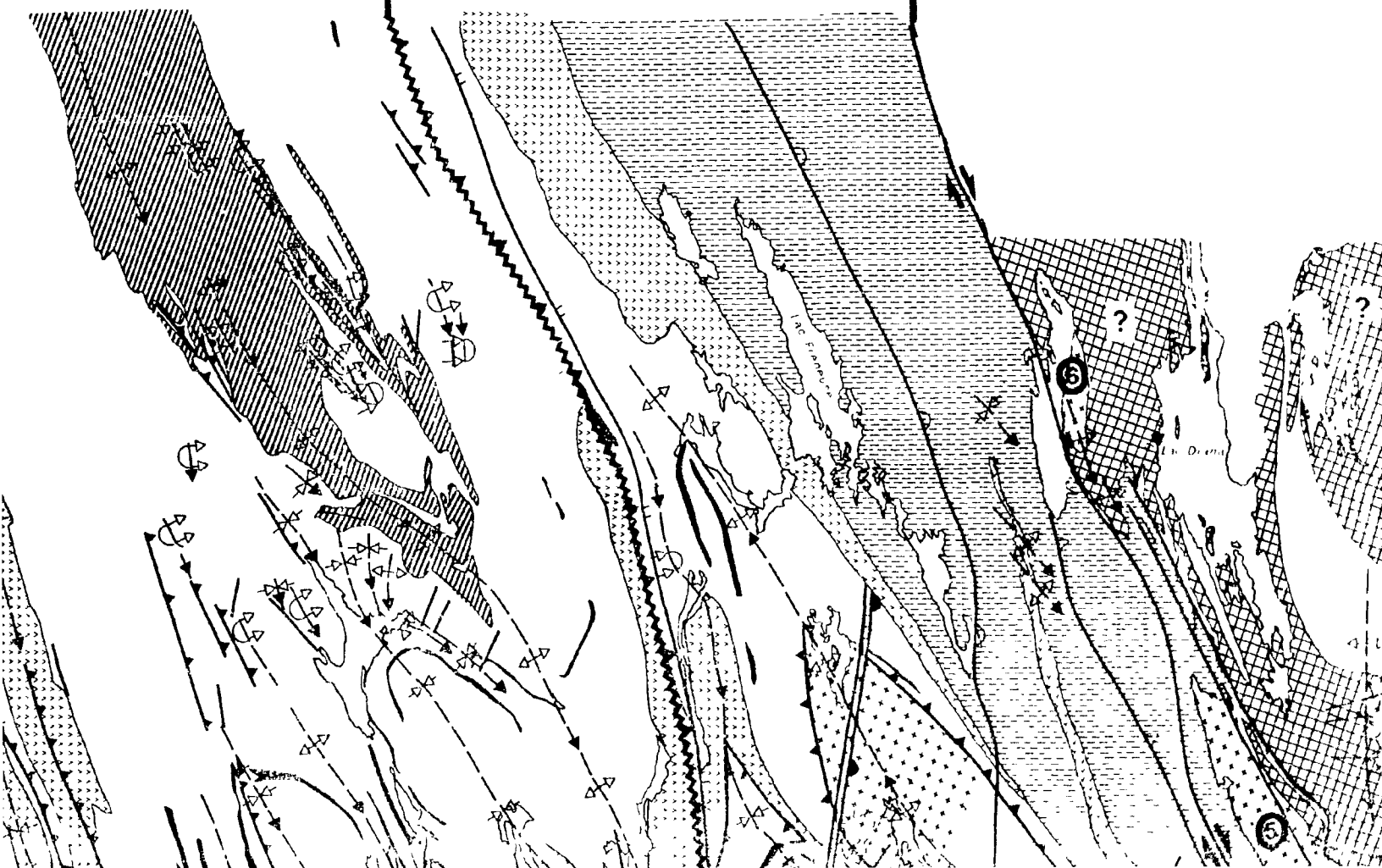
LAC RACHEL FAULT

LAC OLMSTEAD FAULT

CENTRAL IGNEOUS -
SEDIMENTARY
AUTOCHTHONOUS ZONE

WESTERN HINTERLAND ZONE
(LAC RACHEL - LAC MURRAY
BLOCK OF POIRIER, 1989)

LAC GABRIEL BLOCK
[ARC RELATED SUSPECT
TERRANE, POIRIER (1989)]



15'

69°00'

45'

30'

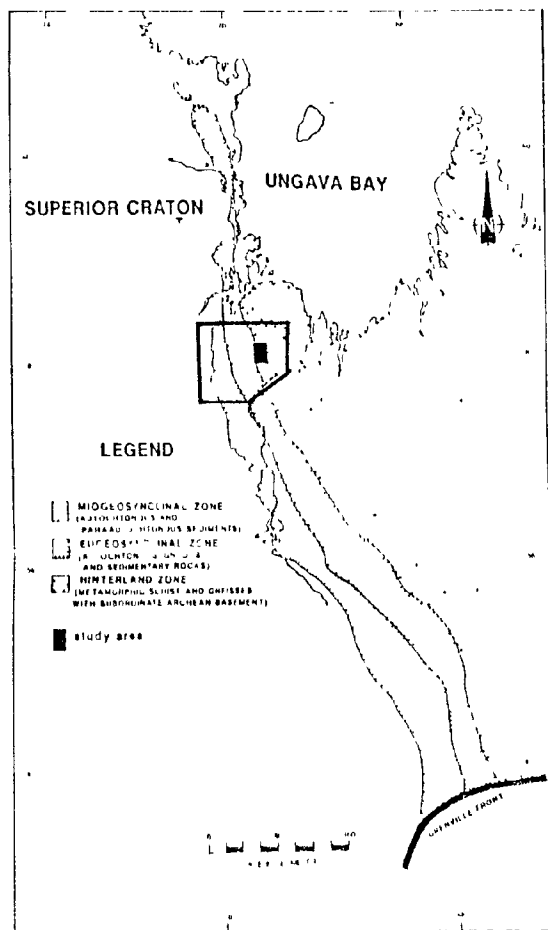
LAC OLMSTEAD FAULT

HINTERLAND ZONE
CHÉL - LAC MURRAY
OF POIRIER, 1989)

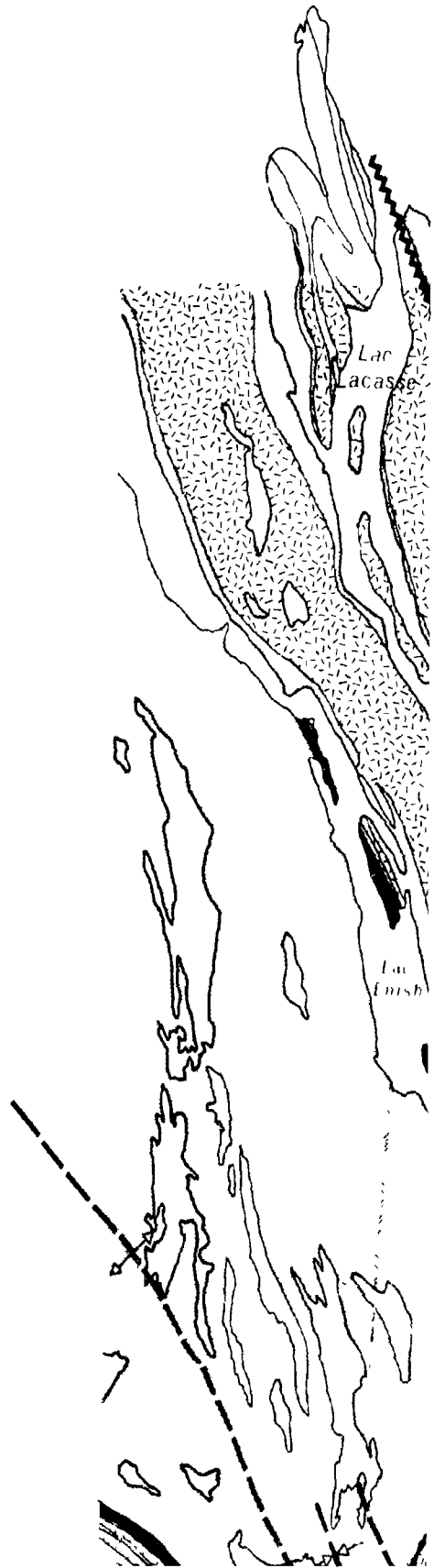
LAC GABRIEL BLOCK
[ARC RELATED SUSPECT
TERRANE, POIRIER (1989)]



MAP I



69° 30'



69° 15'

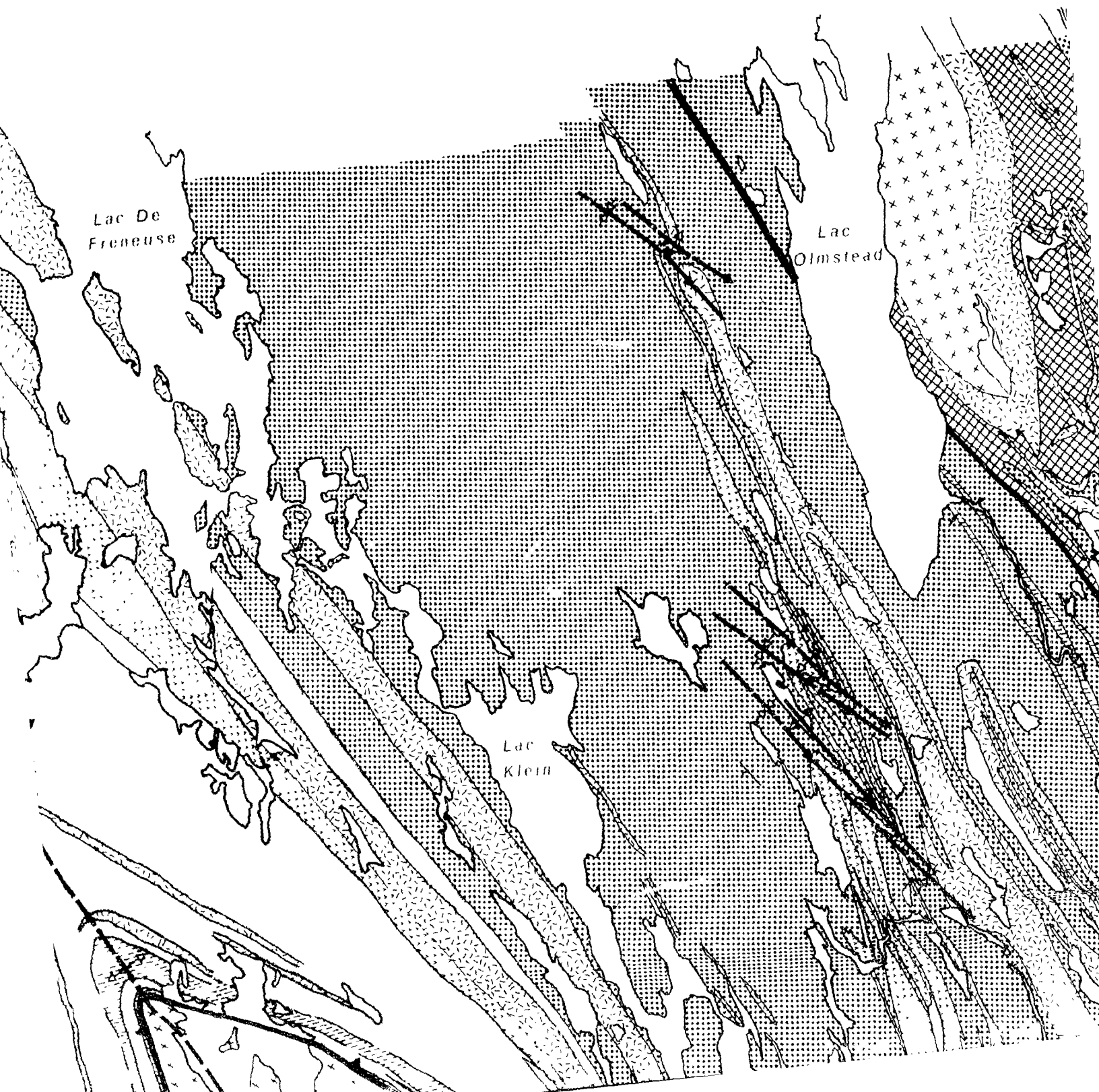


69° 15'

Lac De
Freneuse

Lac
Olmstead

Lac
Klein



69° 00'

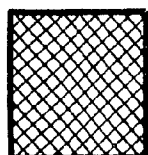
MAP II

LEGEND

STRATIGRAPHY

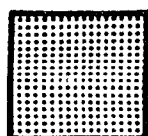
HINTERLAND

LAC GABRIEL BLOCK
(ARC RELATED SUSPECT TERRANE ; POIRIER , 1989)

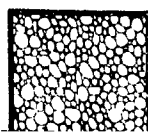


GNEISSIC METASANDSTONE

(THEVENET FM. / LAPORTE GR. ?)



SHALES , SILTSTONES AND SANDSTONES AND
METAMORPHOSED EQUIVALENTS NW OF THE



MIXED VOLCANIC & SEDIMENTARY CONGLOMERATE
(SEDIMENTARY + VOLCANIC FRAGMENTS IN A

MAP II

LEGEND

HINTERLAND

E ; POIRIER , 1989)

ONE

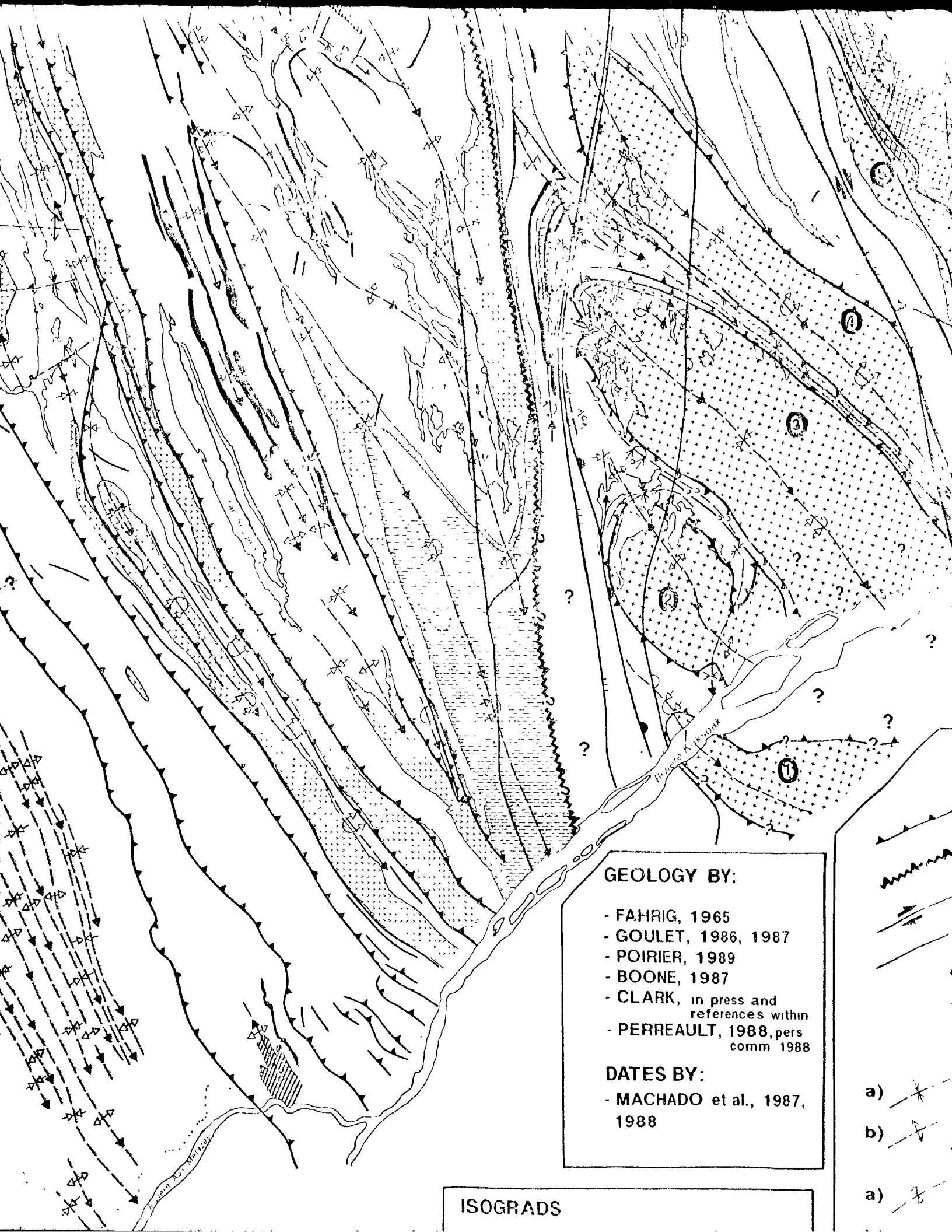
AND SANDSTONES AND THEIR
VALENTS NW OF THE BOULDER DOME

IMENTARY CONGLOMERATE
ANIC FRAGMENTS IN A VOLCANIC MATRIX)

58°00'

45'





GEOLOGY BY:

- FAHRIG, 1965
- GOULET, 1986, 1987
- POIRIER, 1989
- BOONE, 1987
- CLARK, in press and references within
- PERREAU, 1988, pers comm 1988

DATES BY:

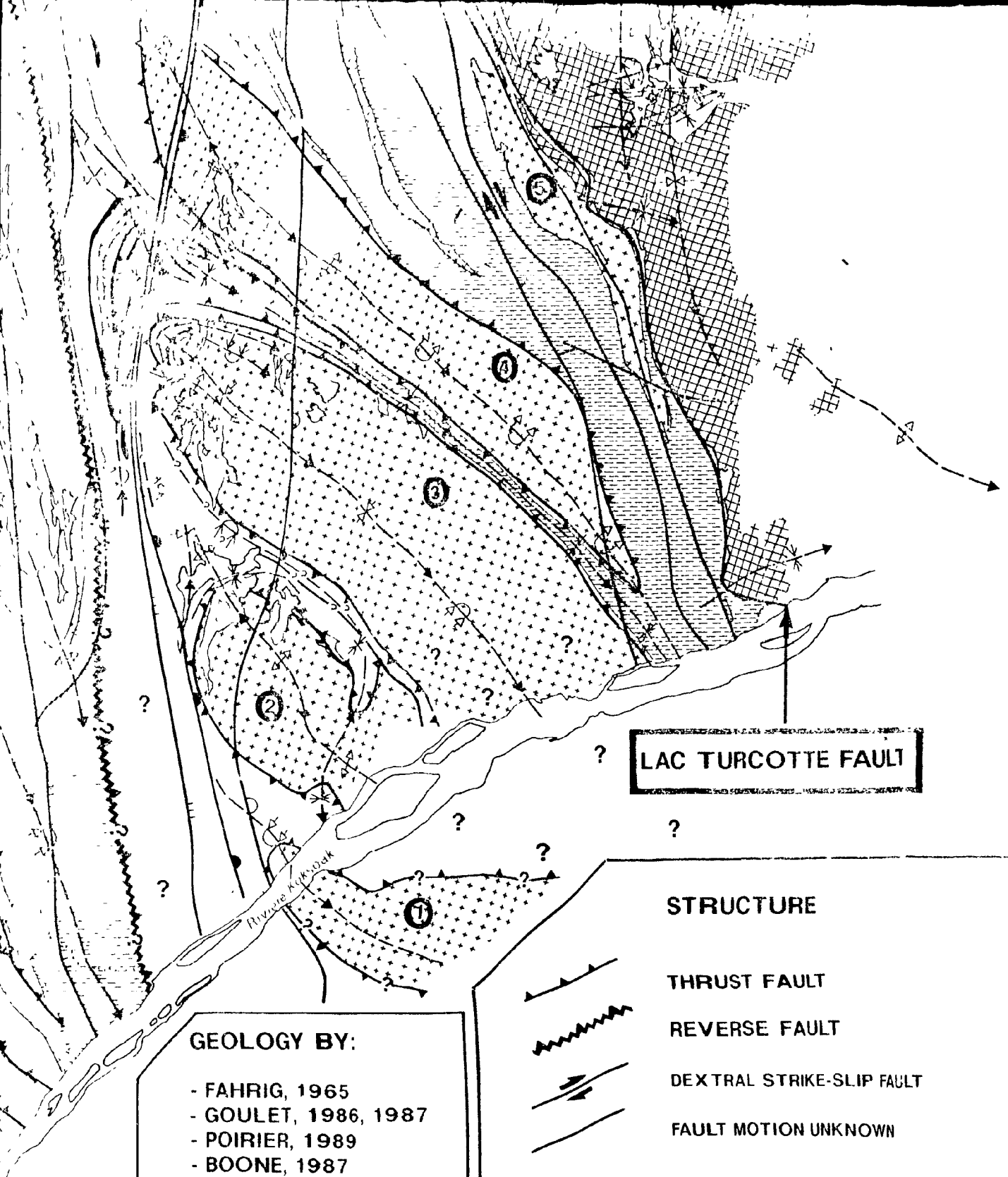
- MACHADO et al., 1987, 1988

ISOGRADS

a)

b)

a)



LAC TURCOTTE FAULT

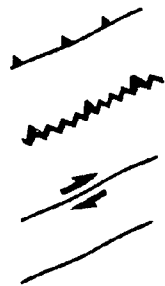
GEOLOGY BY:

- FAHRIG, 1965
- GOULET, 1986, 1987
- POIRIER, 1989
- BOONE, 1987
- CLARK, in press and references within
- PERREAU, 1988, pers. comm. 1988

DATES BY:

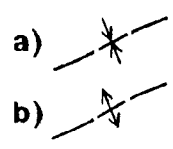
- MACHADO et al., 1987, 1988

STRUCTURE

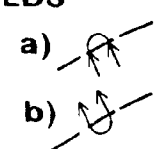


- THRUST FAULT
- REVERSE FAULT
- DEXTRAL STRIKE-SLIP FAULT
- FAULT MOTION UNKNOWN

F2 FOLDS

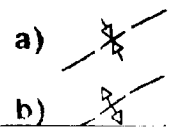


- a) syncline
- b) anticline



- a) overturned syncline
- b) overturned anticline

F3 FOLDS



- a) synform
- b) antiform

STRATIGRAPHY



LAC KANIAFA



CYCLE II

CYCLE I



① SCA

②

ISOGRADS

LEGEND

TIGRAPHY

HINTERLAND

GNEISSIC METASANDSTONE

SEMIPELITIC SCHIST with minor coarse-grained, calc-silicate and amphibolite horizons (THE VENET FM. / LAPORTE GR. ?)

ABRADOR TROUGH (Sensu Stricto)
APISKAU SUPERGROUP (2142 - 1880 Ma.)

58° 00'

BASALT
(WILLBOB / HELLANCOURT FM.)

SANDSTONE / CONGLOMERATE
(CHIOAK FM.)

SILTSTONE
(MENIHEK FM.)

SILTSTONE / SHALE / IRON FORMATION
(BABY FM.) + GABBRO / DIORITE / PERIDOTITE
(MONTAGNAIS GR.)

SILTSTONE
(LARCH RIVER FM.)

IRON FORMATION

45'

+ SHALE (RUTH FM.)
QUARTZITE (WISHART / ALISON FM.) } Only with the Sokoman/
Fenimore iron formation
onlapping the Superior craton
DOLOMITE (ABNER FM.)
+ DOLOMITIC SILTSTONE (HARVENG FM.)

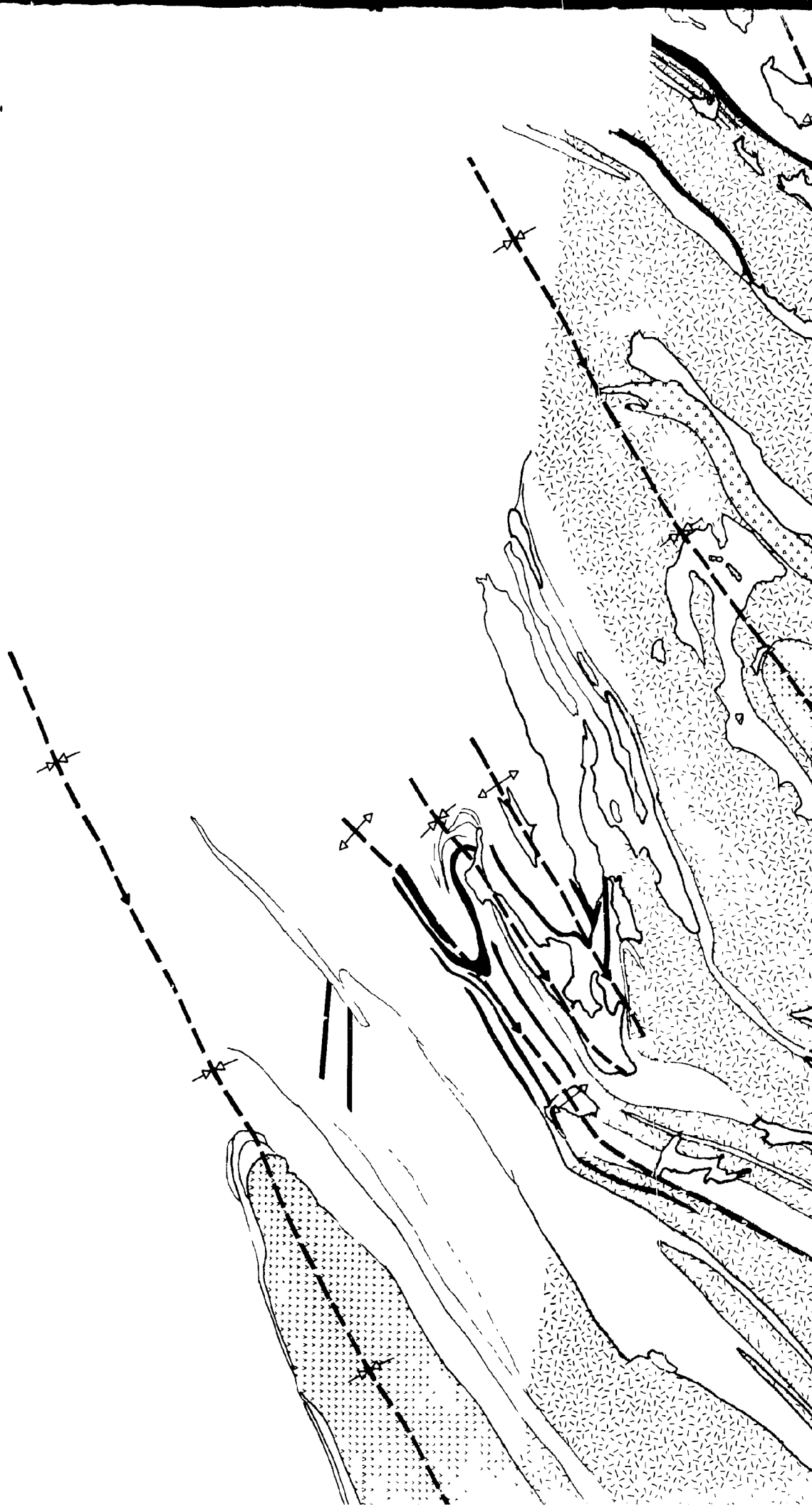
SUPERIOR CRATON (2721 Ma.)

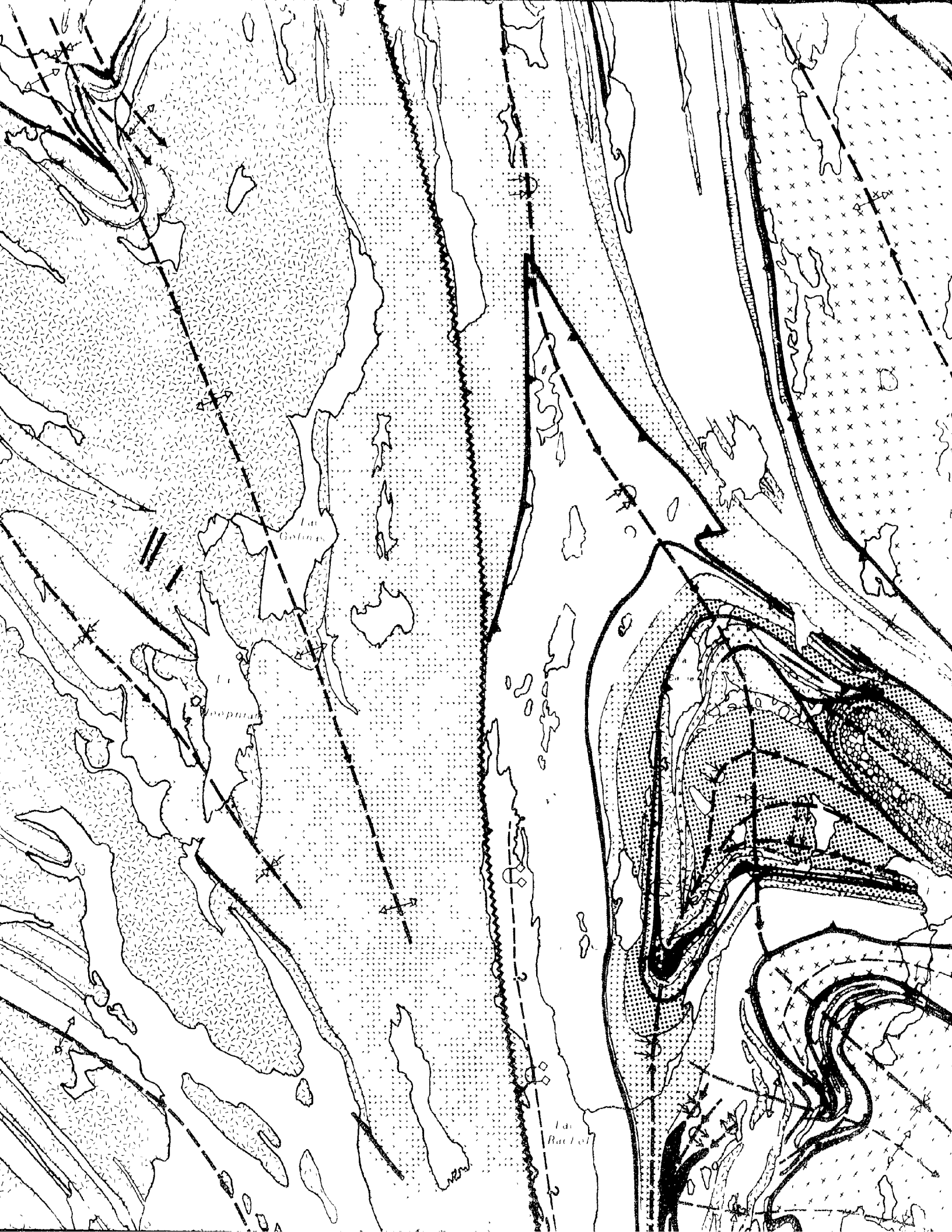
GRANITOID GNEISSES

SCATTERED SYNFORM

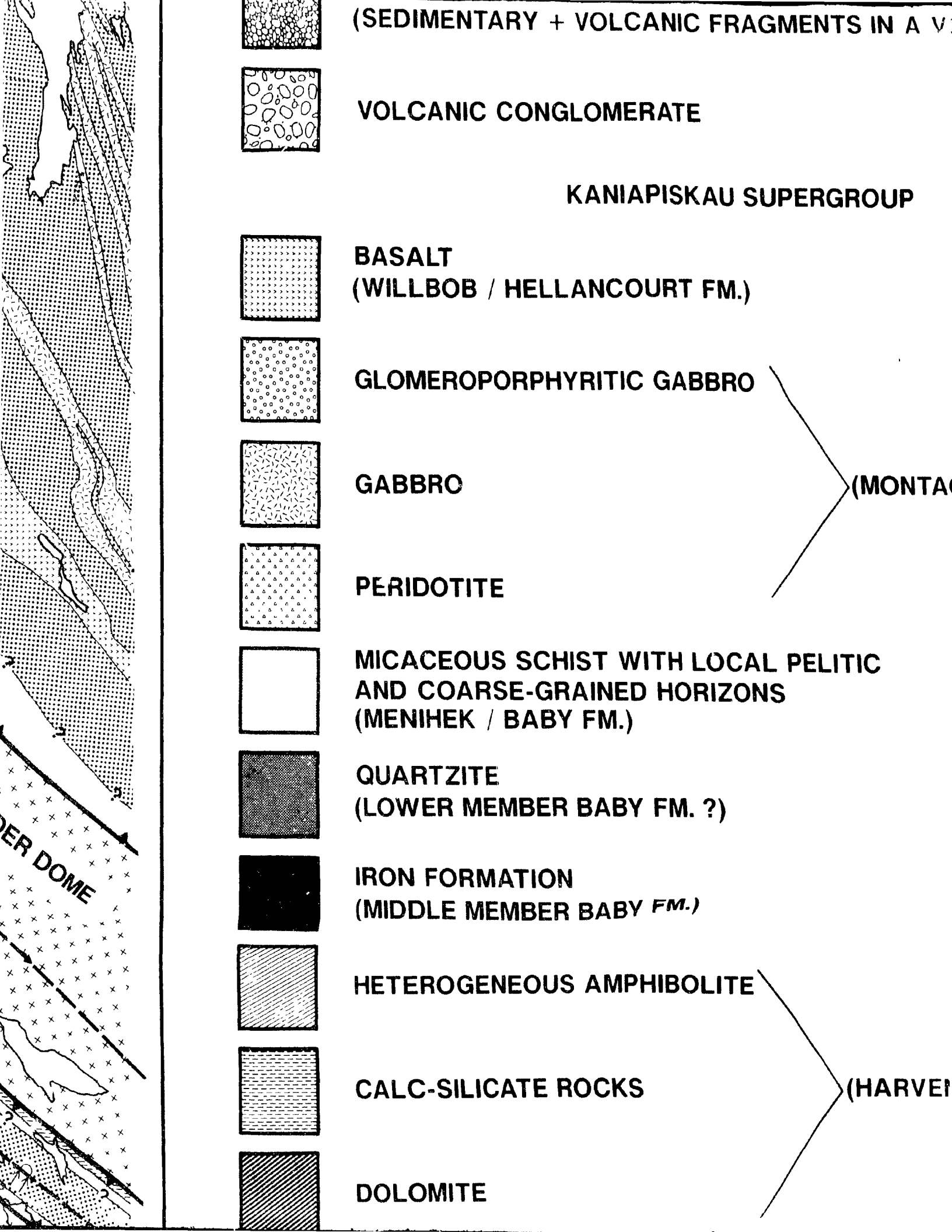
OVERBONE (2870 Ma.)

58°15'









VOLCANIC FRAGMENTS IN A VOLCANIC MATRIX)

58° 15'

ERATE

APISKAU SUPERGROUP

COURT FM.)

TIC GABBRO

(MONTAGNAIS GR.)

WITH LOCAL PELITIC
ED HORIZONS

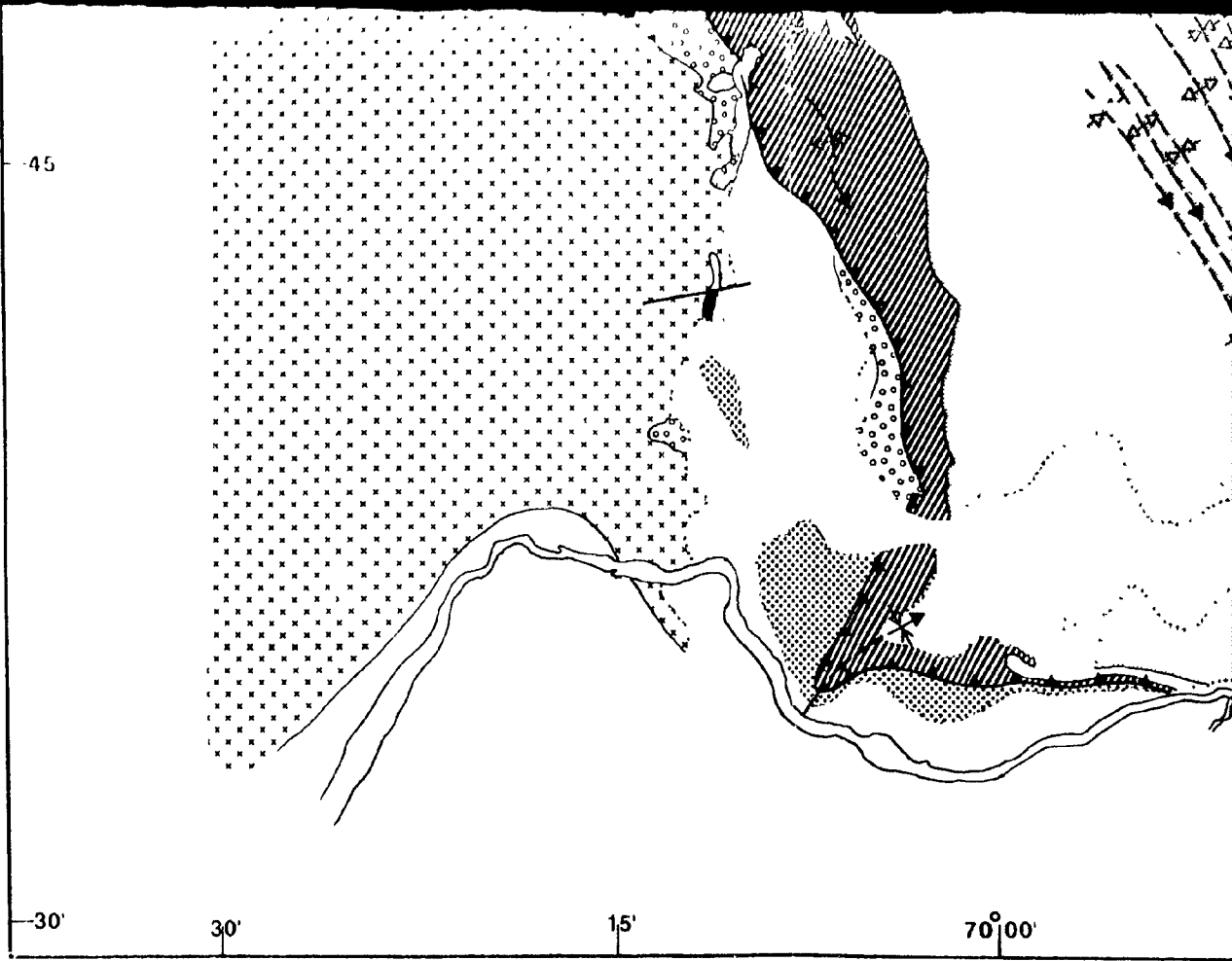
BY FM. ?)

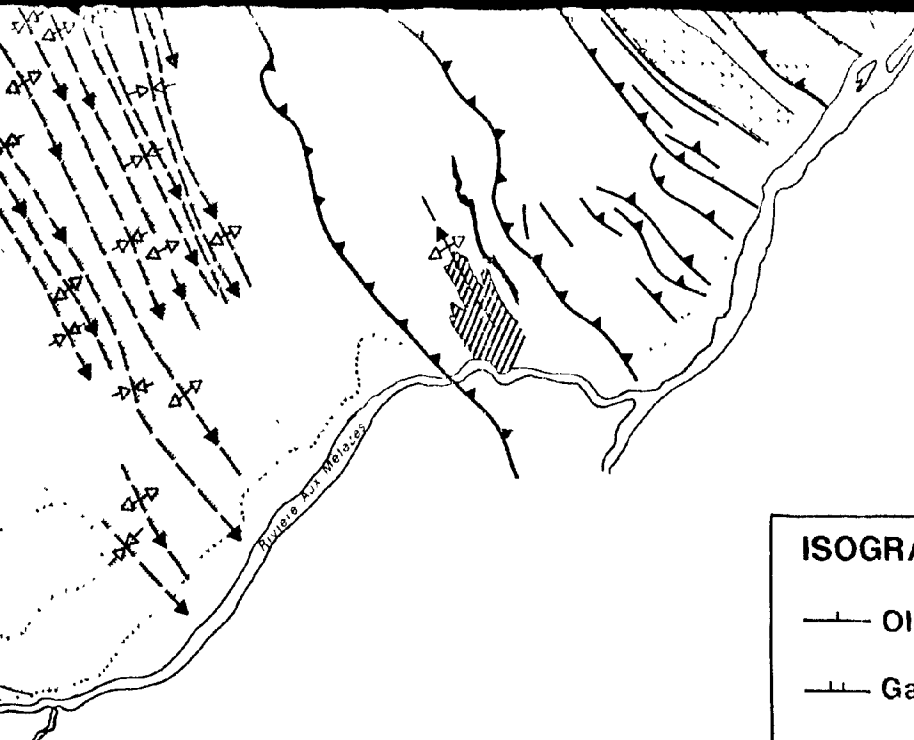
BY FM.)

MPHIBOLITE

CKS

(HARVENG FM. CORRELATIVES)





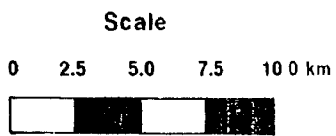
- FAHRIG, 1965
- GOULET, 1986, 1987
- POIRIER, 1989
- BOONE, 1987
- CLARK, in press and references within
- PERREAULT, 1988, pers. comm 1988

DATES BY:

- MACHADO et al., 1987, 1988

ISOGRADS

- | | |
|---------------------|--------------------|
| — — Oligoclase-in | —∩— Sillimanite-in |
| — — Garnet-in | —△— Staurolite-out |
| — — Staurolite-in | —▭— Muscovite-out |
| —●— Kyanite-in | |



- a)
- b)
- c)
- d)

- FAHRIG, 1965
- GOULET, 1986, 1987
- POIRIER, 1989
- BOONE, 1987
- CLARK, in press and references within
- PERREAULT, 1988, pers. comm. 1988

DATES BY:

- MACHADO et al., 1987, 1988





ISOGRADS

- Oligoclase-in — Sillimanite-in
- Garnet-in — Staurolite-out
- Staurolite-in — Muscovite-out
- Kyanite-in

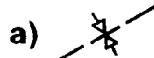
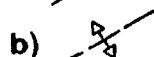


DEXTRAL STRIKE SLIP

FAULT MOTION UNKNOWN

F2 FOLDS

- | | | | |
|--|-----------|--|----------------------|
| a)  | syncline | a)  | overturned syncline |
| b)  | anticline | b)  | overturned anticline |

F3 FOLDS

- | | |
|--|---------------------|
| a)  | synform |
| b)  | antiform |
| c)  | overturned synform |
| d)  | overturned antiform |

CYCLE I



①

SCATT

②

MOYE

③

RENIA

④

BOULD

⑤

TURCO

⑥

OLMS

15'

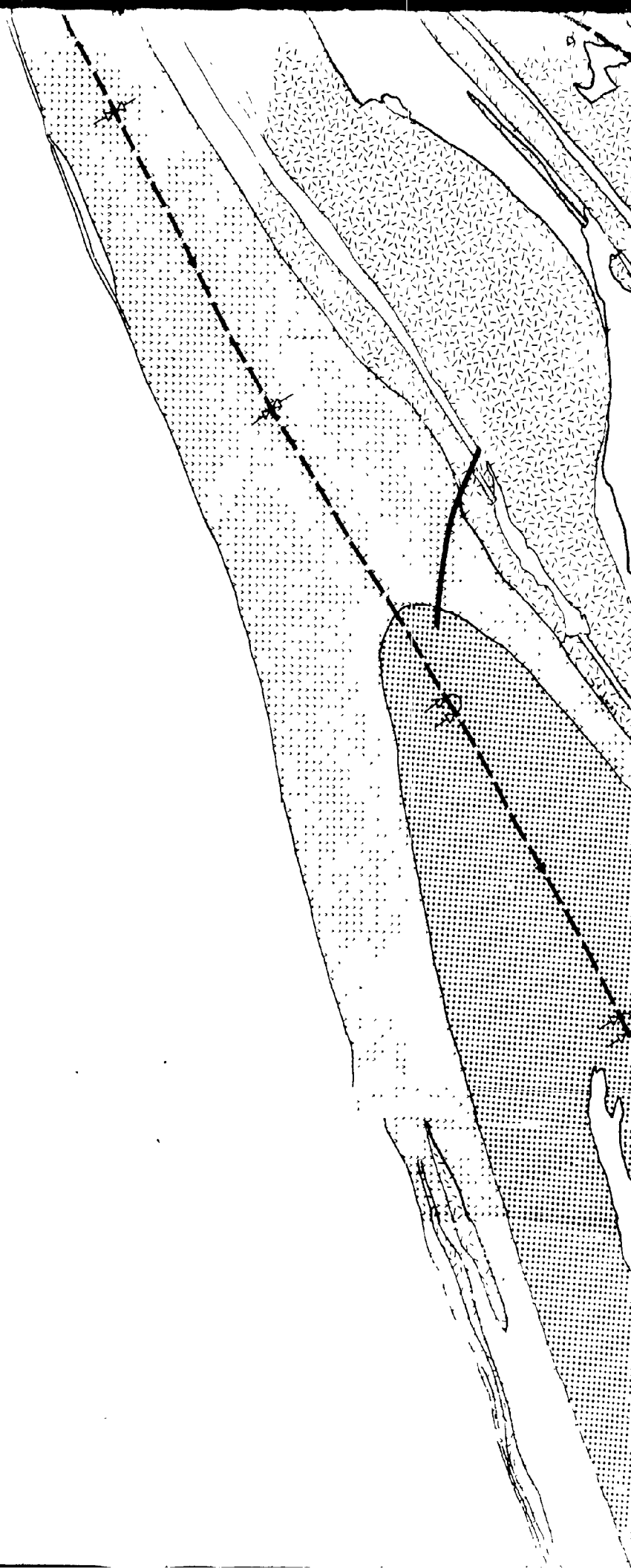
69°00'

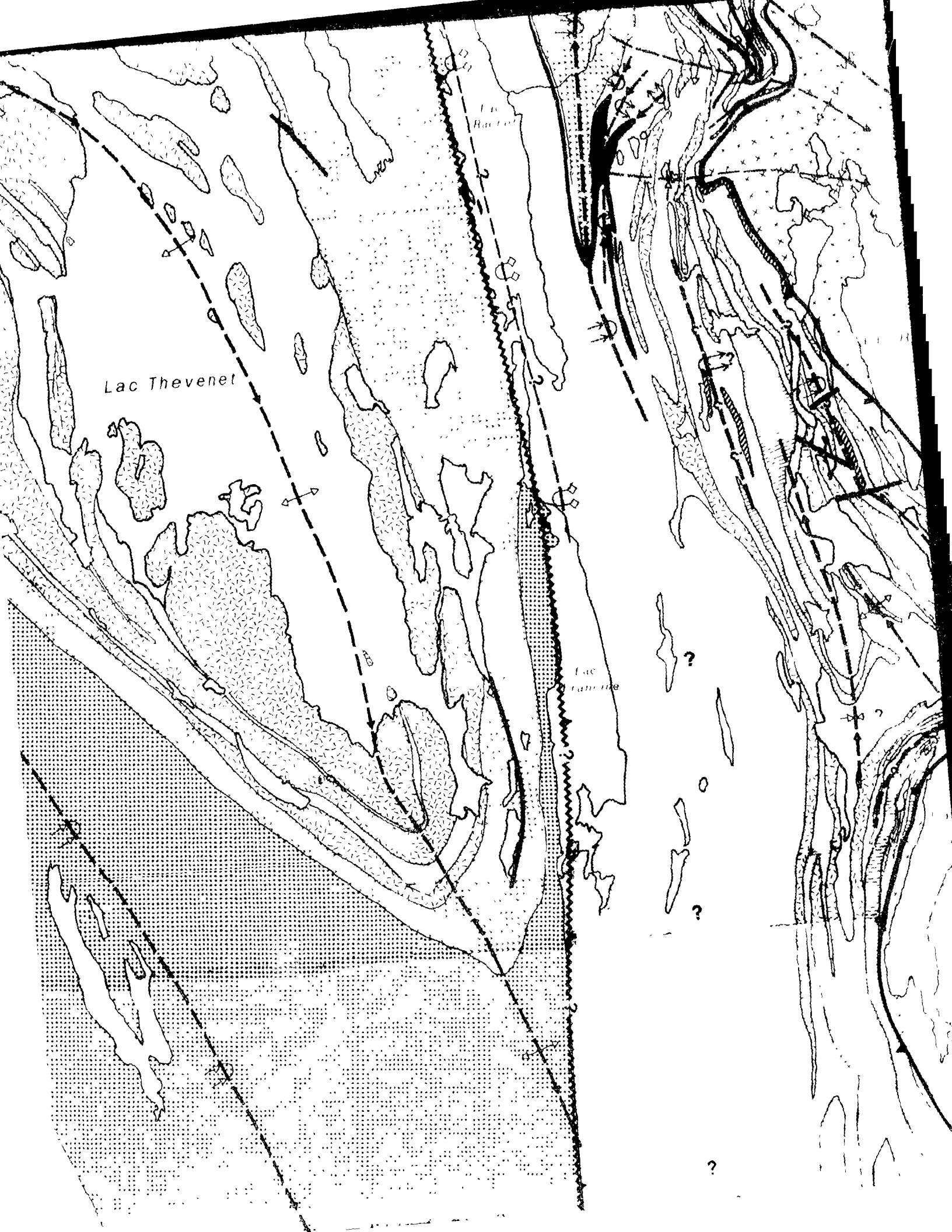
45'

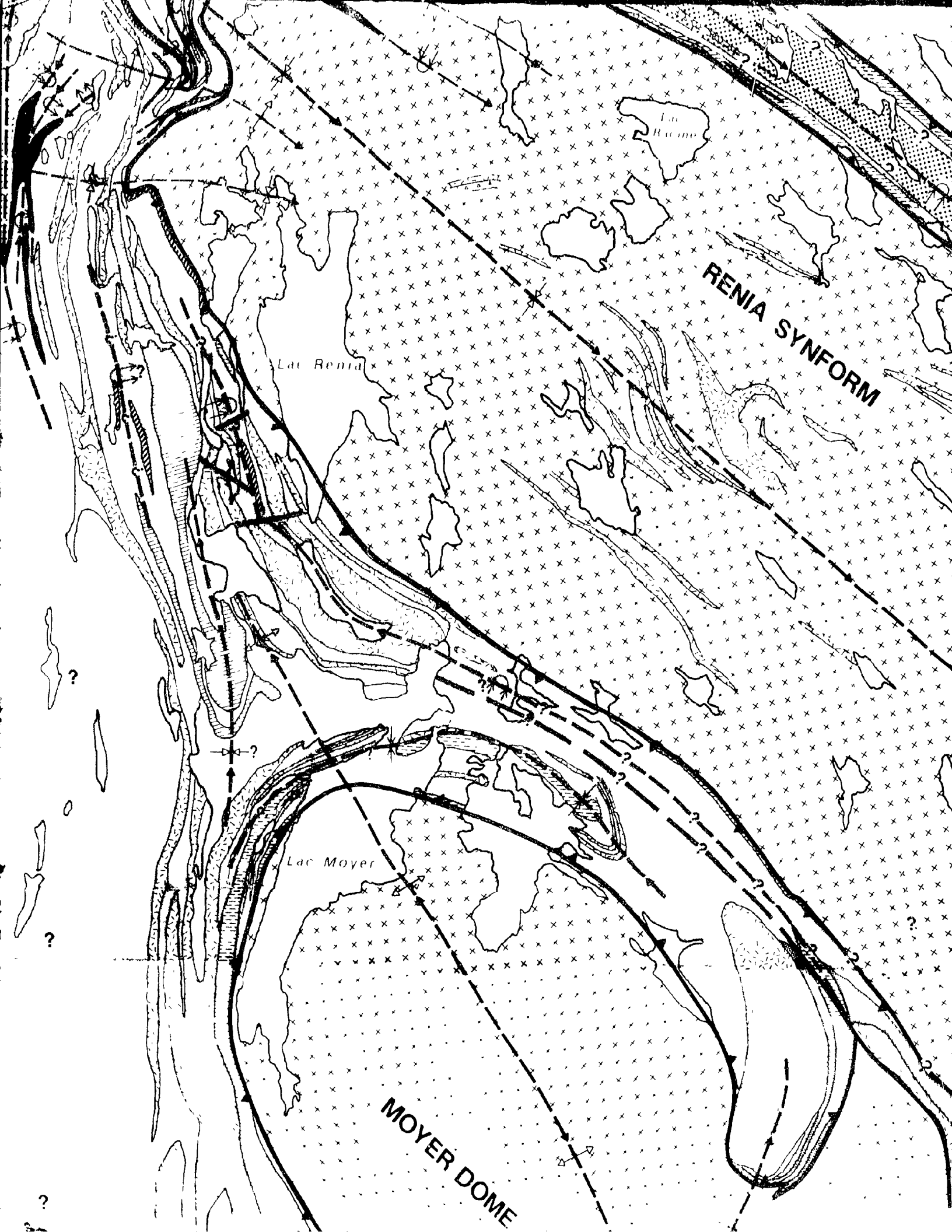
30'

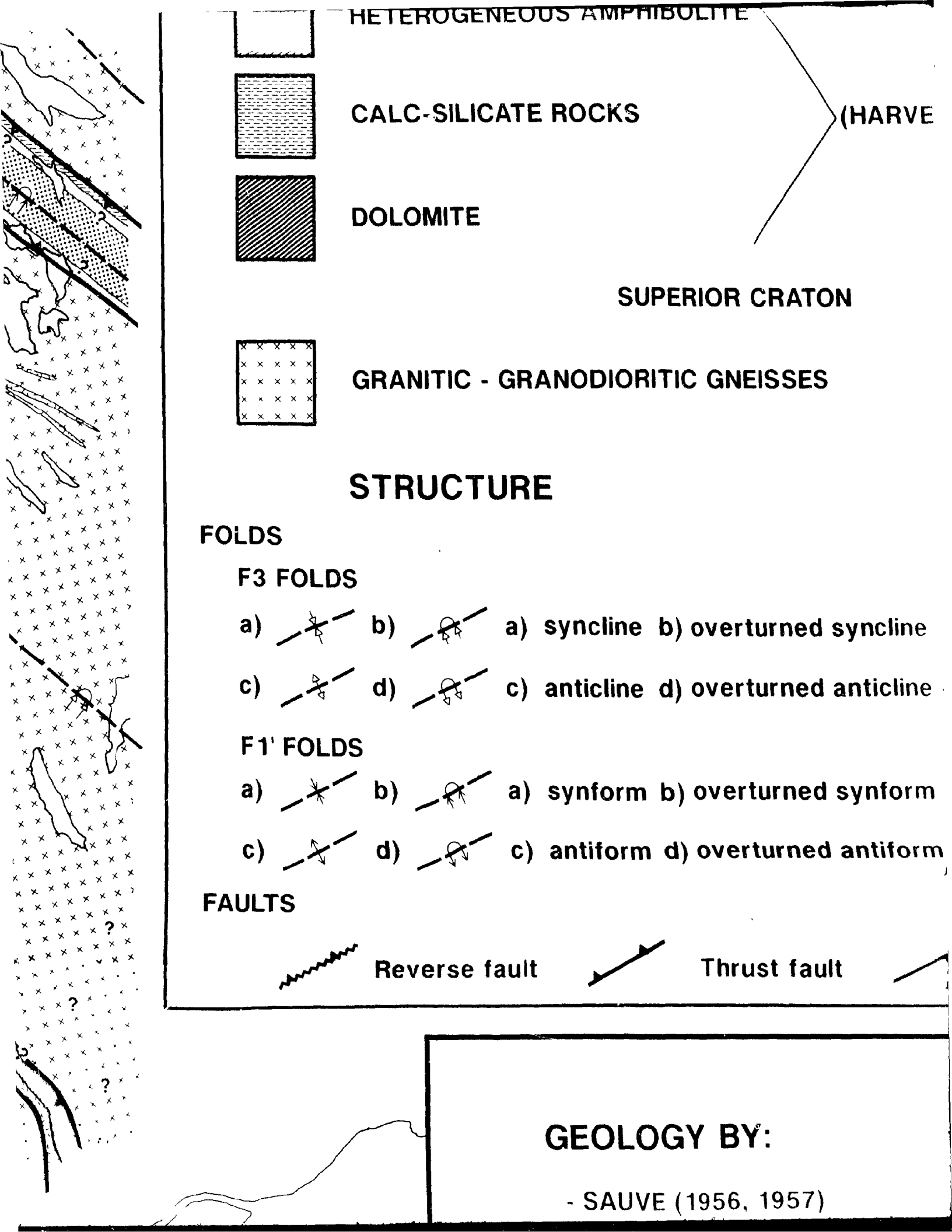
30'

— 58° 00'









HETEROGENEOUS AMPHIBOLITE

CALC-SILICATE ROCKS

DOLOMITE

GRANITIC - GRANODIORITIC GNEISSES

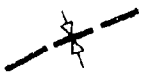

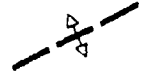

SUPERIOR CRATON

(HARVE



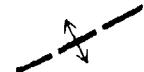
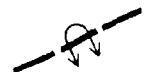
STRUCTURE

FOLDS

F3 FOLDS

- a)  b)  a) syncline b) overturned syncline
c)  d)  c) anticline d) overturned anticline

F1' FOLDS

- a)  b)  a) synform b) overturned synform
c)  d)  c) antiform d) overturned antiform

FAULTS



Reverse fault



Thrust fault

GEOLOGY BY:

- SAUVE (1956, 1957)

IBOLITE

(HARVENG FM. CORRELATIVES)

UPERIOR CRATON

CRITIC GNEISSES

CONJECTURAL FOLDS

F4 FOLDS

b) overturned syncline

a)



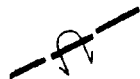
overturned
anticline

d) overturned anticline

F1 FOLDS

b) overturned synform

a)



overturned
anticline

d) overturned antiform

Thrust fault

Motion unknown

58°00'

DY BY:

E (1956, 1957)





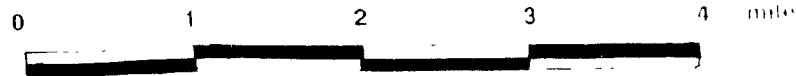
Reverse fault

Thrust fault

GEOLOGY BY:

- SAUVE (1956, 1957)
- GELINAS (1958a, 1965)
- SAUVE AND BERGERON (1965)
- CLARK (1980)
- GOULET (1986, 1987)
- POIRIER (1989)
- PERREAULT (pers. com. 1988)

SCALE



Thrust fault

Motion unknown

LOGY BY:

UVE (1956, 1957)

LINAS (1958a, 1965)

UVE AND BERGERON (1965)

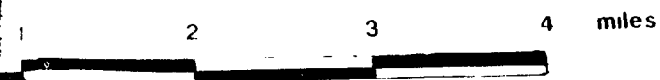
ARK (1980)

ULET (1986, 1987)

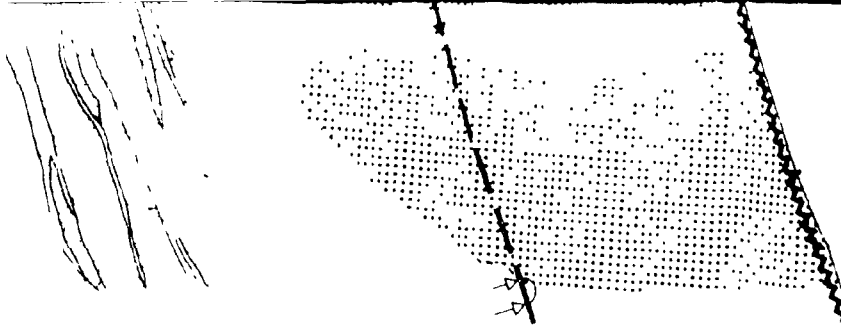
RIER (1989)

RREAULT (pers. com. 1988)

SCALE



69° 30'

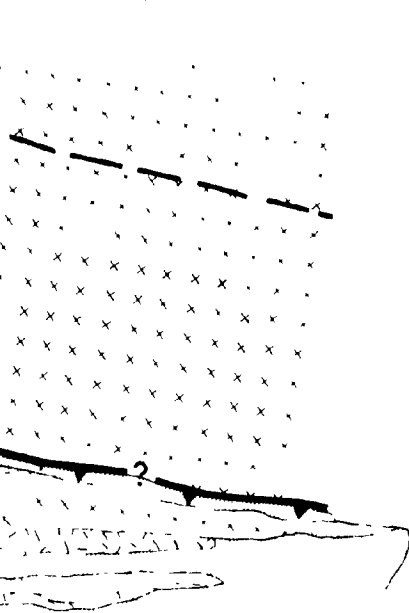


2

69°15'



69° 15'



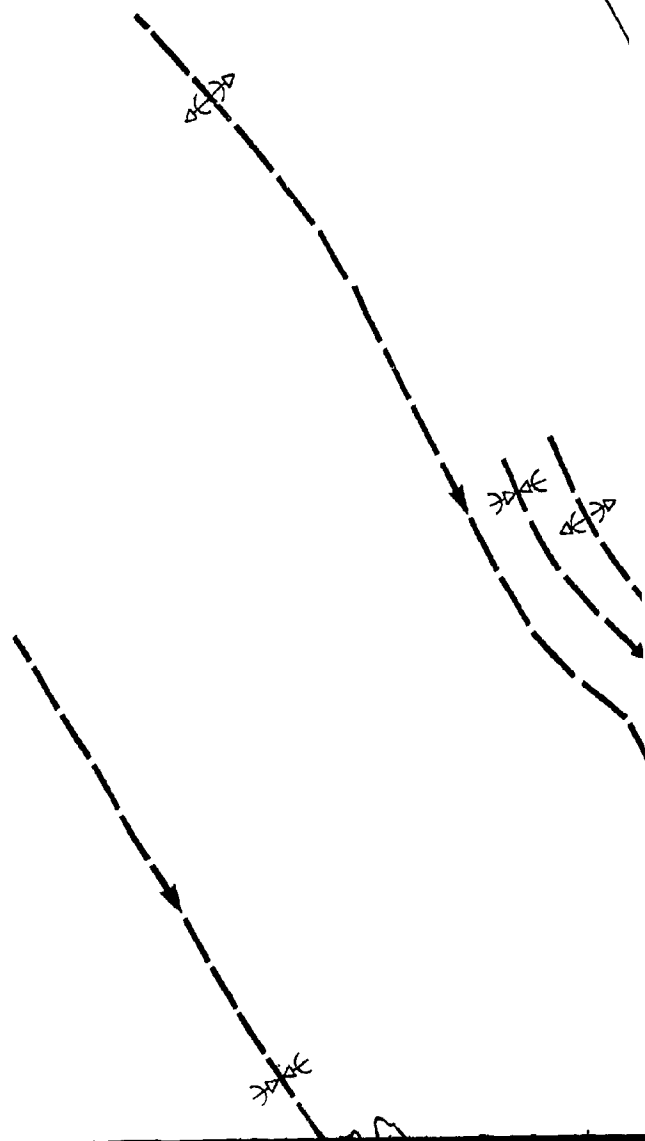
69°00'

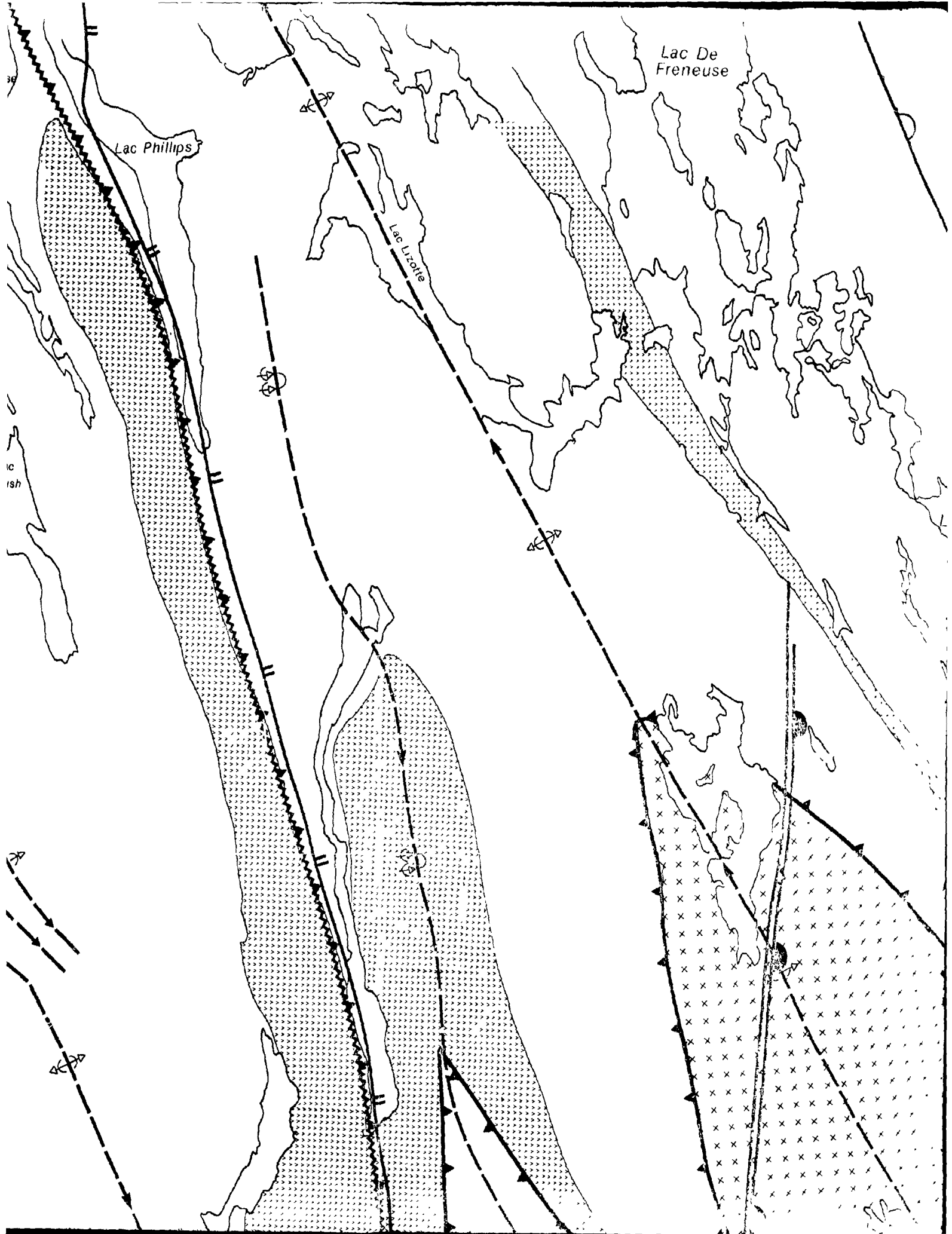
69°30'

Lac
Lacasse

Lac
Enish

—58°15'





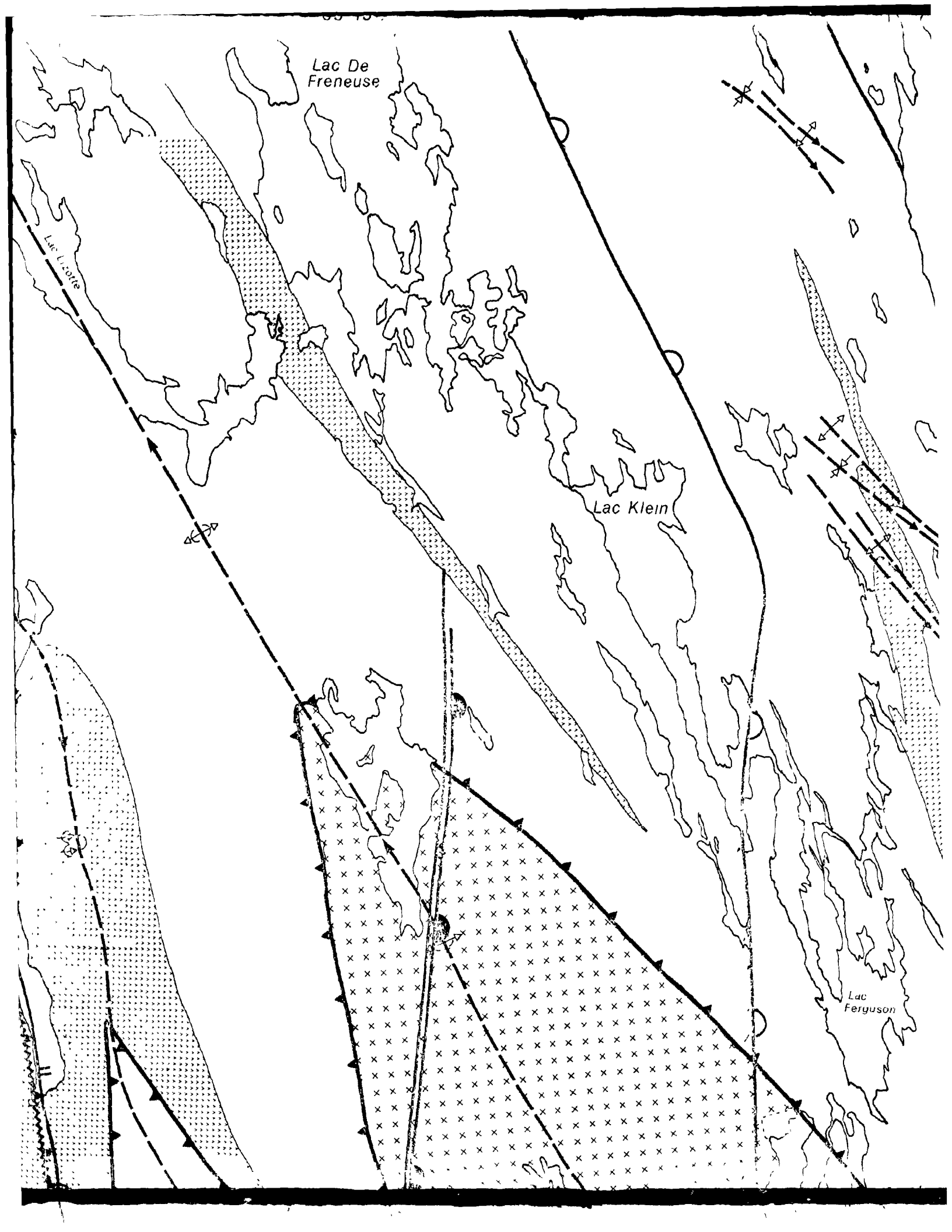
65 10

Lac De
Freneuse

Lac Lizotte

Lac Klein

Lac
Ferguson

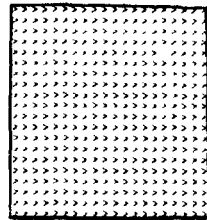


MAP III

LEGEND

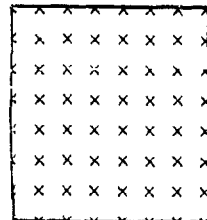
STRATIGRAPHY

KANIAPISKAU SUPERGROUP (2nd CYCLE)



BASALT
(WILLBOB / HELLANCOURT FM.)

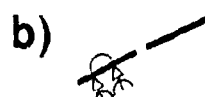
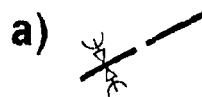
SUPERIOR CRATON



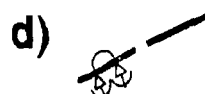
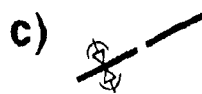
GRANITOID GNEISSES

STRUCTURE

F3 FOLDS



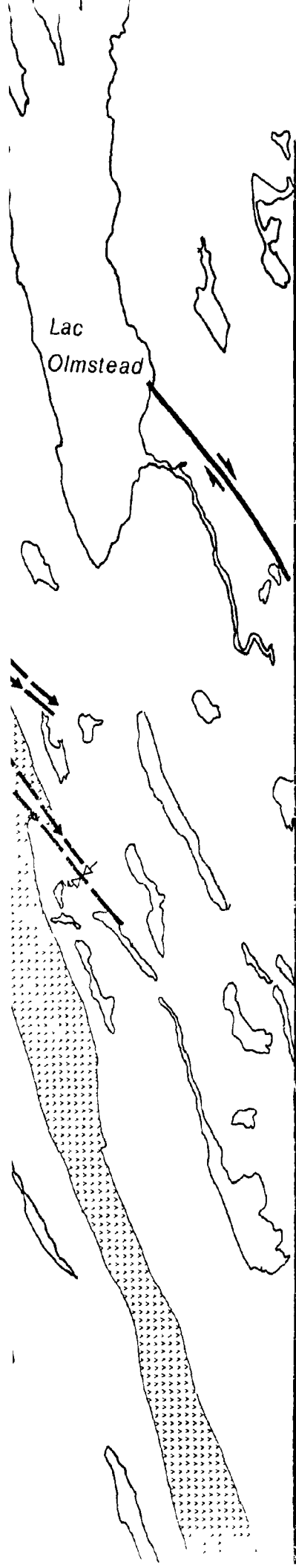
a) synformal syncline b) c



c) synformal anticline d) c



e) antiformal anticline f) c



MAP III

LEGEND

GROUP (2nd CYCLE)

/ HELLANCOURT FM.)

D GNEISSES

58°15'

- | | |
|-------------------------|------------------------------------|
| a) synformal syncline | b) overturned synformal syncline |
| c) synformal anticline | d) overturned synformal anticline |
| e) antiformal anticline | f) overturned antiformal anticline |

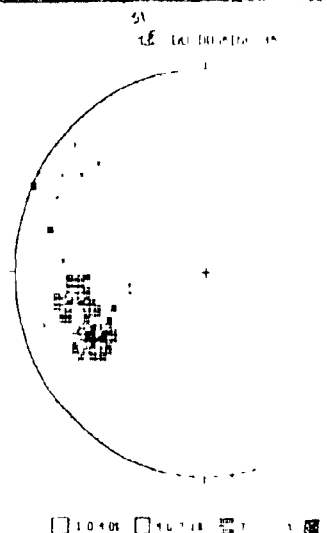
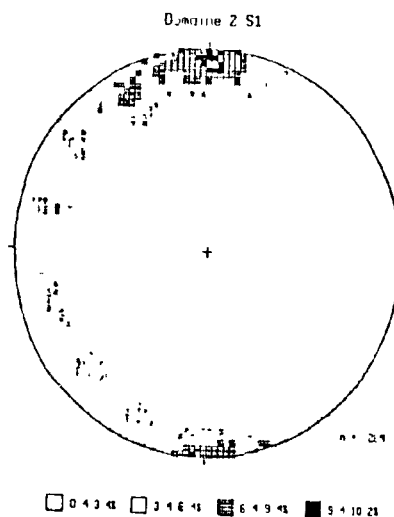
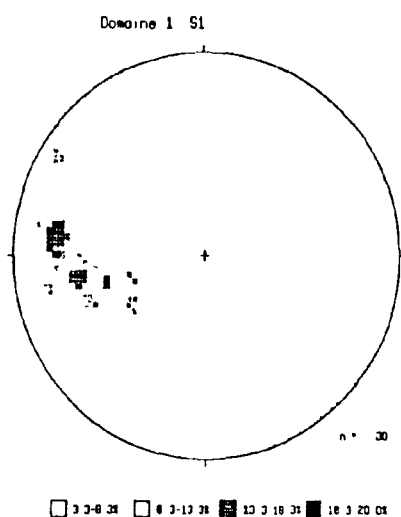
STRUCTURAL
FEATURE

DOMAINE 1

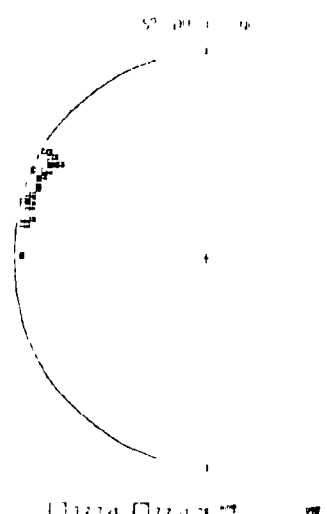
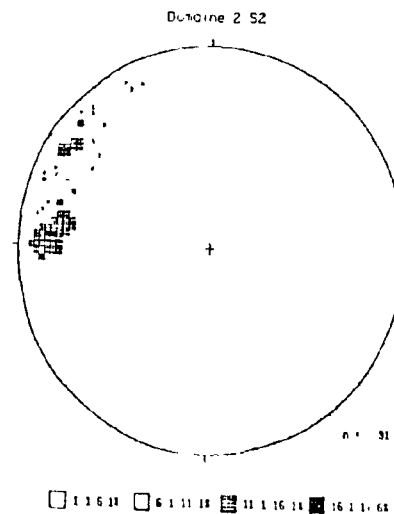
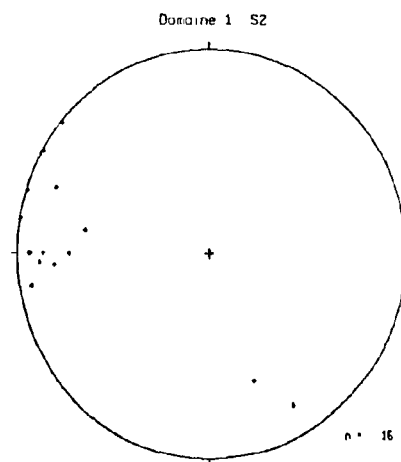
DOMAINE 2

DOMAINE 3A

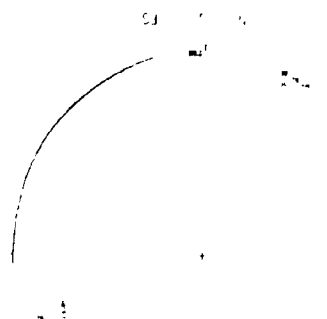
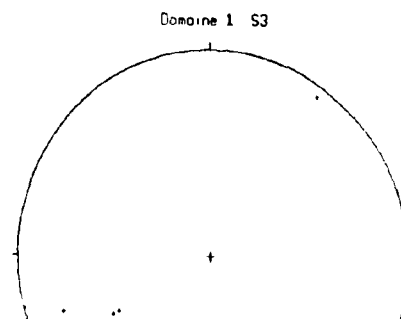
S0/S1



S2

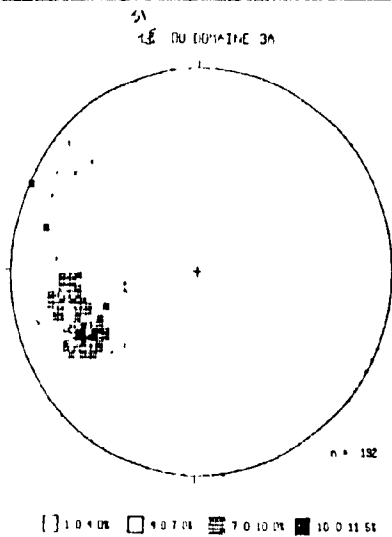


S3

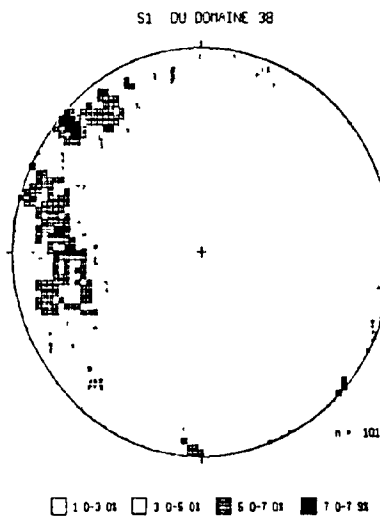


ANNEX I

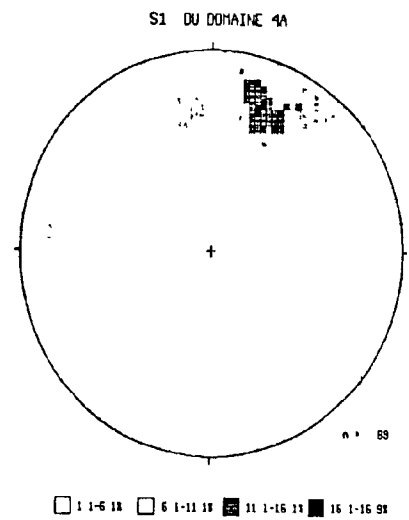
DOMAINE 3A



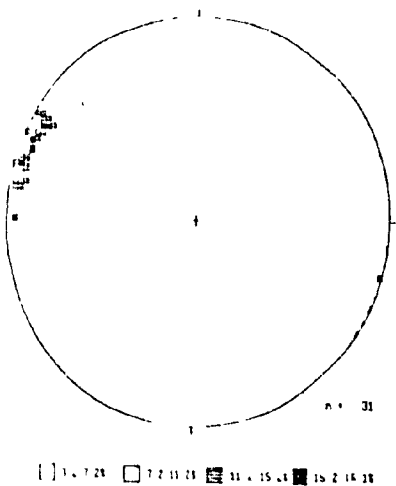
DOMAINE 3B



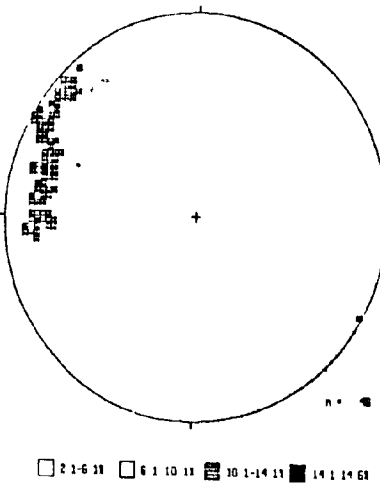
DOMAINE 4A



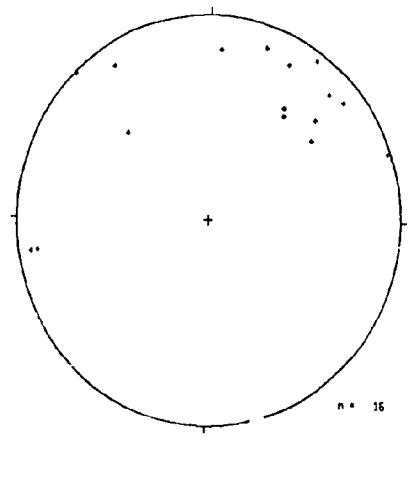
S2 DU DOMAINE 3A



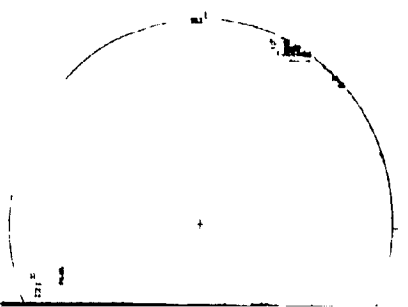
S2 DU DOMAINE 3B



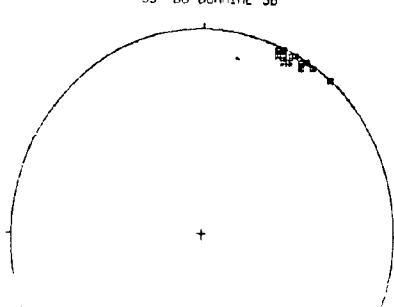
S2 DU DOMAINE 4A



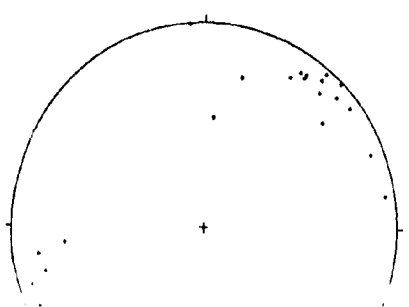
S3 DU DOMAINE 3A



S3 DU DOMAINE 3B

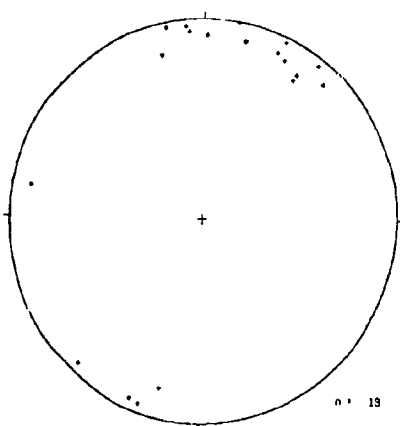


S3 DU DOMAINE 4A



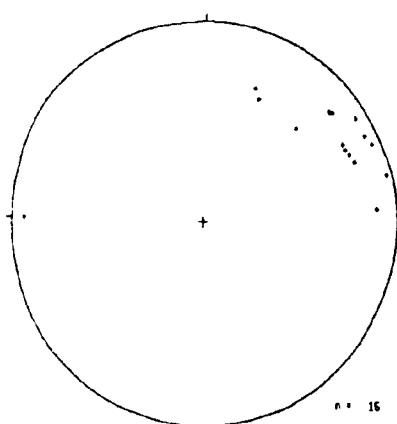
DOMAINE 4B

S1 DU DOMAINE 4B



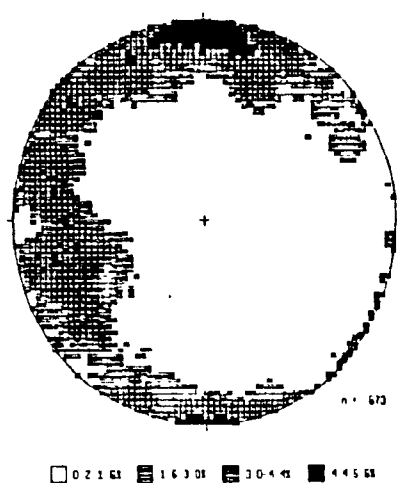
DOMAINE 5

S1 DU DOMAINE 5

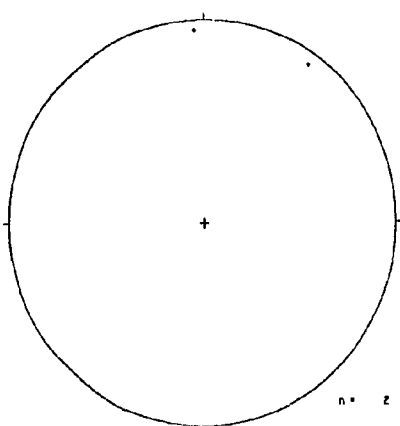


SYNOPTIC

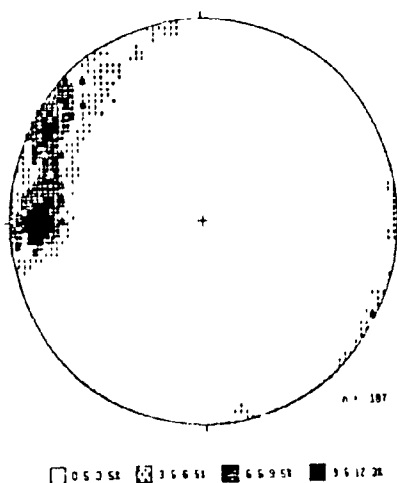
S1 de STRUCT1



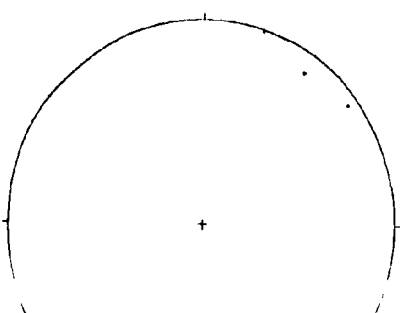
s2 du domaine 4b



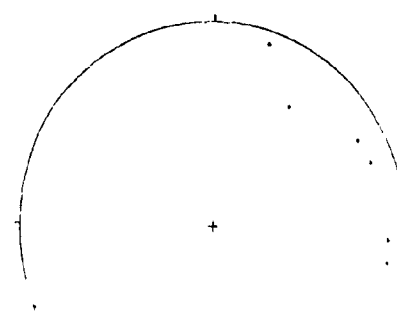
2P DE STRUCT1



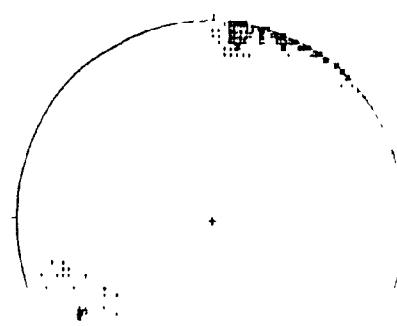
S3 DU DOMAINE 4B

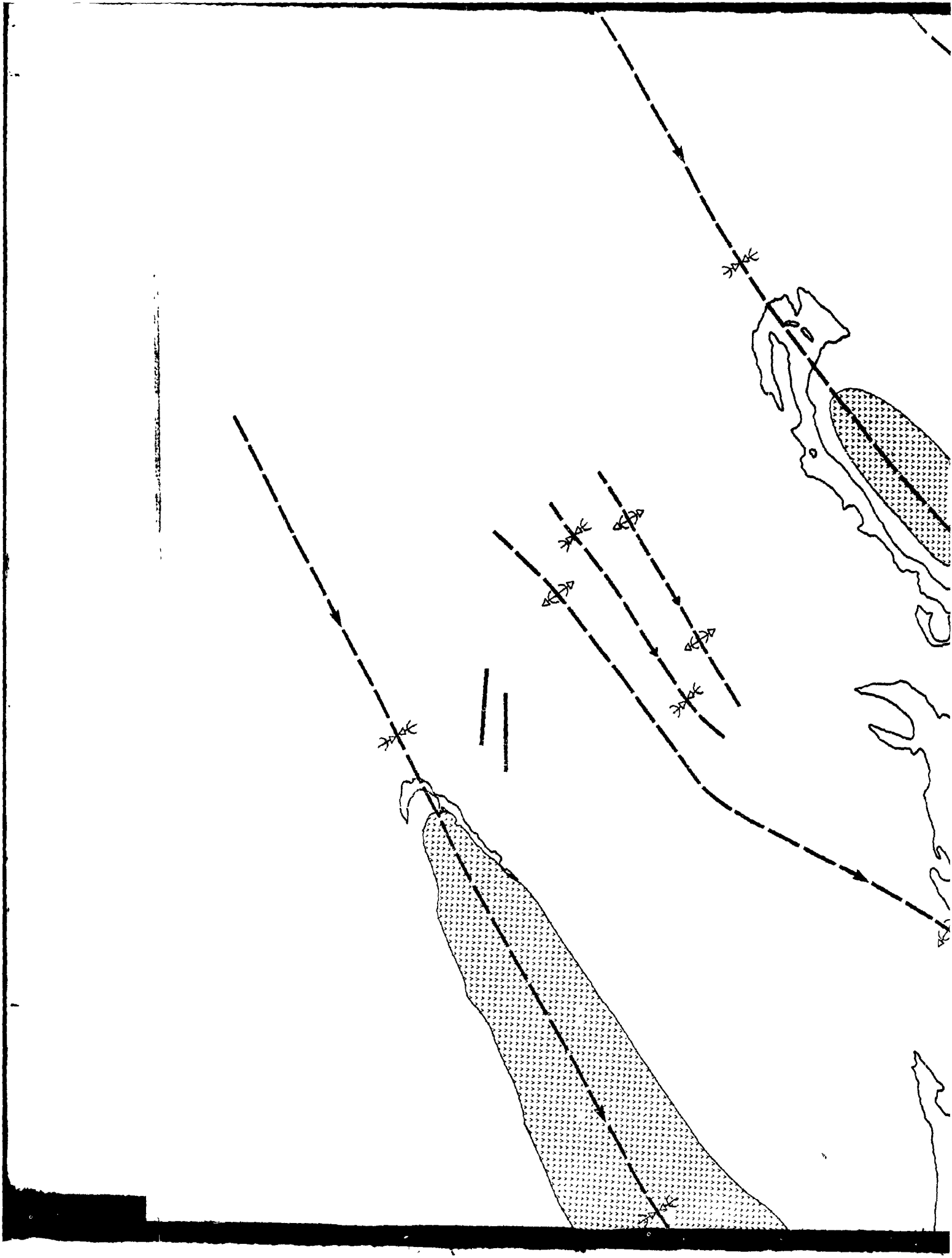


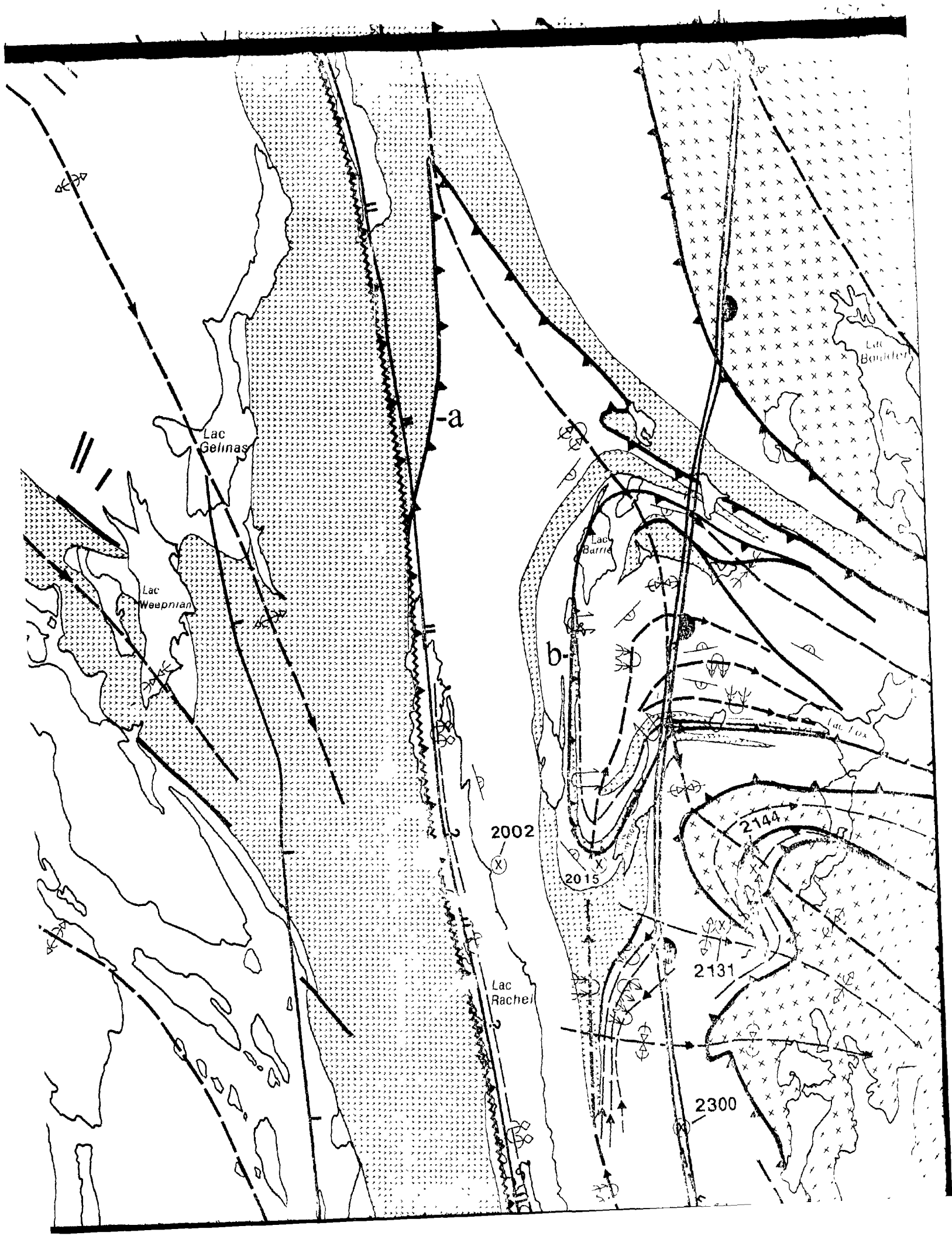
S3 DU DOMAINE 5

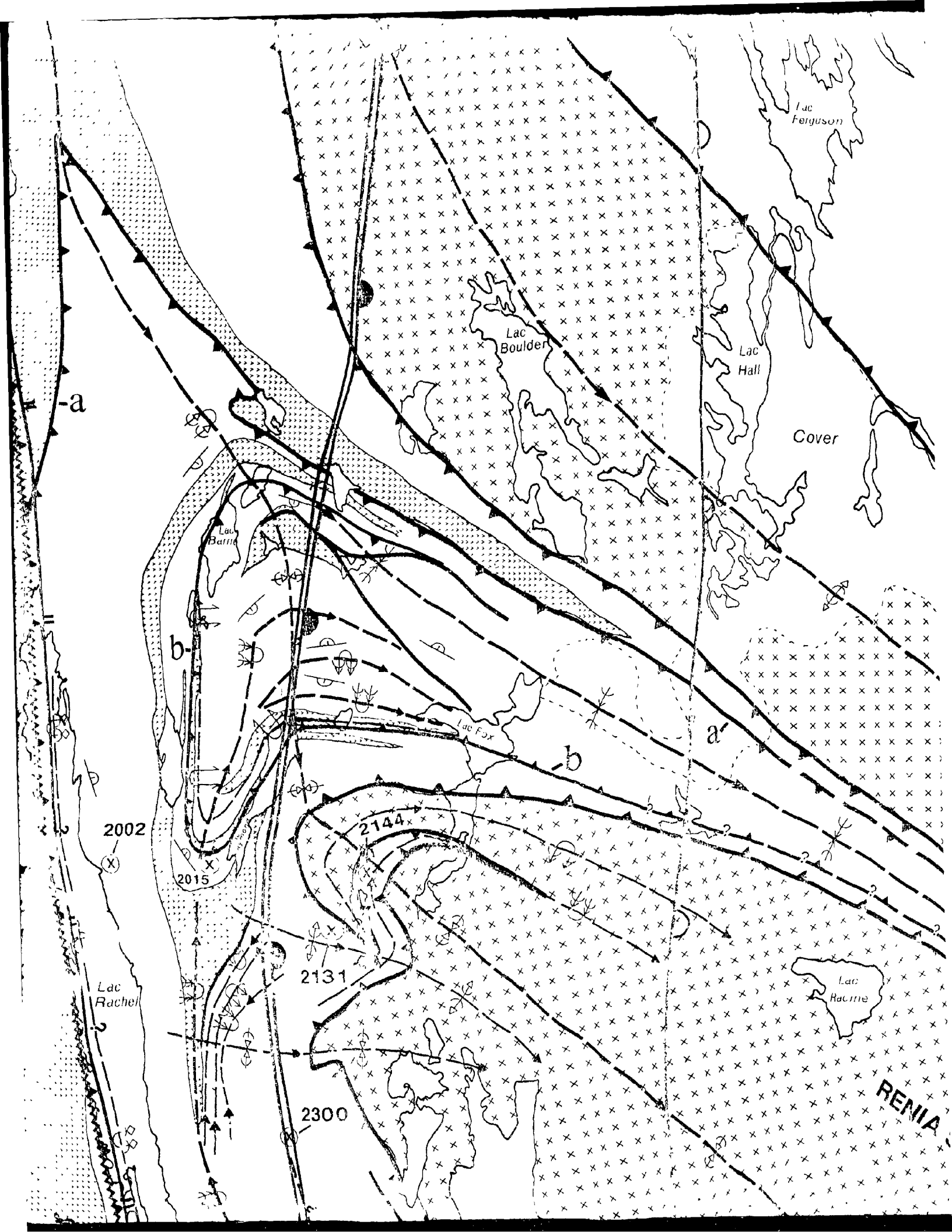


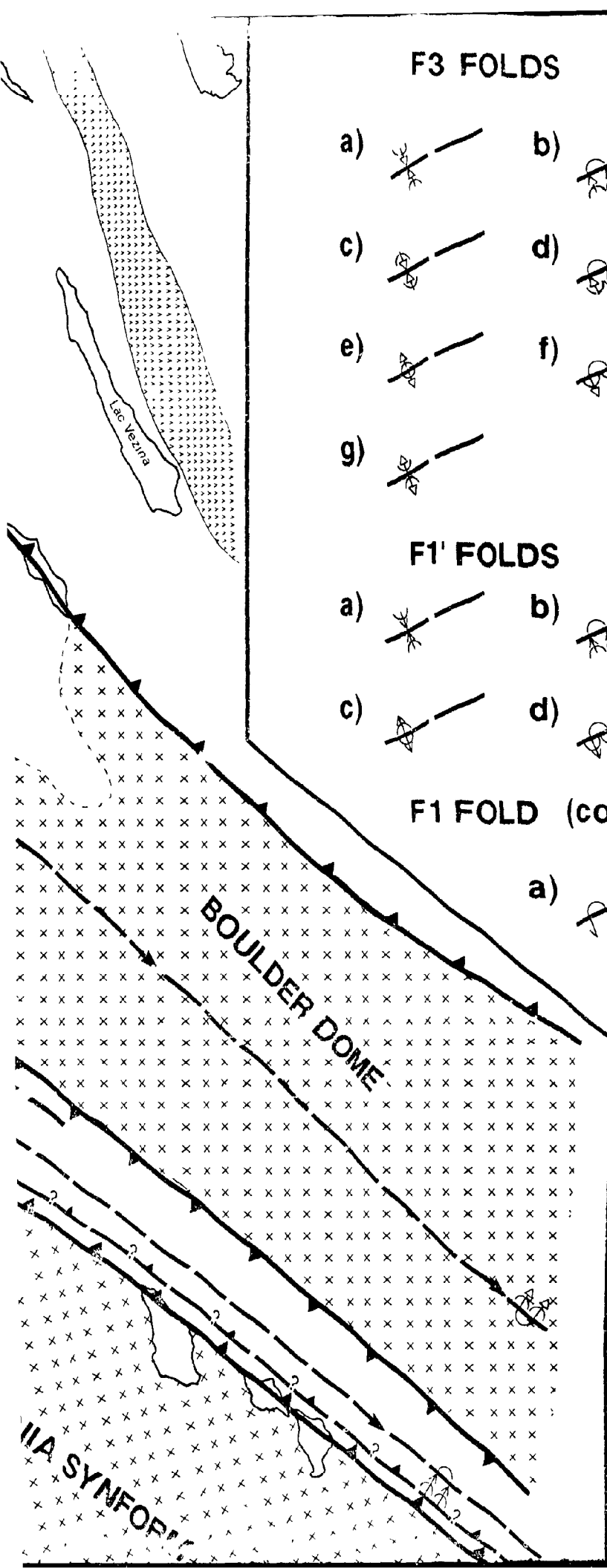
3P DE STRUCT1











F3 FOLDS

- | | | | |
|----|----|------------------------|------------------|
| a) | b) | a) synformal syncline | b) over
sync |
| c) | d) | c) synformal anticline | d) over
antic |
| e) | f) | e) antiform anticline | f) over
antic |
| g) | | g) antiform syncline | |

F1' FOLDS

- | | | | |
|----|----|--------------|---------|
| a) | b) | a) syncline | b) over |
| c) | d) | c) anticline | d) over |

F1 FOLD (conjectural)

- | | |
|----|-------------------------|
| a) | a) overturned anticline |
|----|-------------------------|

F4 FOLD (conjectural)

- | | |
|----|-------------------------|
| a) | a) overturned anticline |
|----|-------------------------|

FAULTS

- | | | | |
|----|----|--------|--------|
| a) | b) | a) Thr | b) Thr |
| c) | d) | c) Rev | d) Pos |
| e) | | e) Mo | |

a) synformal syncline b) overturned synformal syncline

c) synformal anticline d) overturned synformal anticline

e) antiformal anticline f) overturned antiformal anticline

g) antiformal syncline

h) syncline i) overturned syncline

j) anticline k) overturned anticline

l) overturned anticline

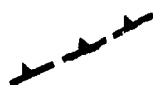
m) (conjectural)



a) overturned anticline



b)



a) Thrust fault

b) Thrust fault
uncertain position



d)



c) Reverse fault

d) Possible dextral
component



e) Motion unknown

- ☐ SHALES, ARGILLITES AND SANDSTONES (SILT CLAY)
- ☐ METASANDSTONES EQUIVALENTS HW OF THE B. POLYCLINE
- ☐ MIXED VOLCANIC & SEDIMENTARY CONGLOMERATE
(SEDIMENTARY & VOLCANIC ELEMENTS IN A VOLCANIC MATRIX)
- ☐ VOLCANIC CONGLOMERATE

KANABISKAN SUPERGROUP

- ☐ BASALT
(WELLS, MELLANCOURT FM)
- ☐ ALKALI-SPORPHYRIC GABBRO
- ☐ GABBRO
- ☐ PERidotite

(MOUNTAIN GR)

- ☐ QUARTZITE
- ☐ GRANITE
- ☐ GNEISS

STRUCTURE

FOLDS

F1 FOLDS

a) b) a) synform b) overturned synform

c) d) c) antiform d) overturned antiform

F2 FOLDS

a) b) a) synform b) overturned synform

c) d) c) antiform d) overturned antiform

FAULTS

Reverse fault Thrust fault Normal fault

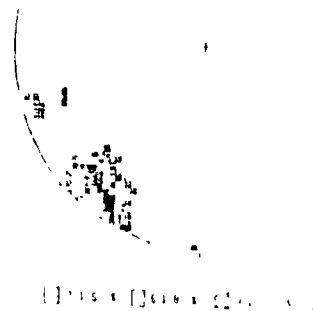
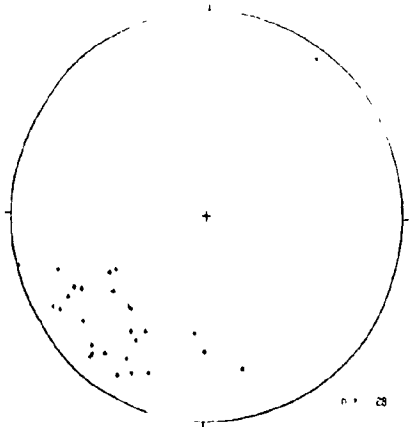
CORRELATION FOLDS

F4 FOLDS

a) b) a) synform b) overturned synform

c) d) c) antiform d) overturned antiform

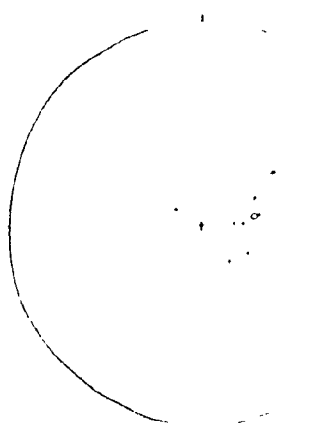
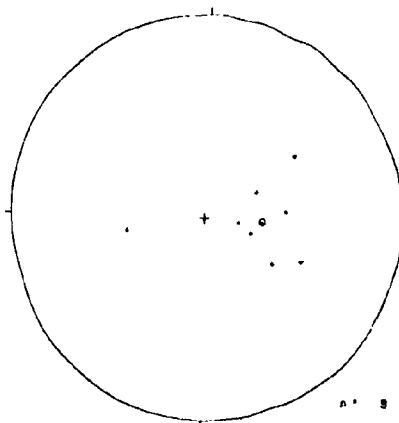
S3



L1-0

Ls

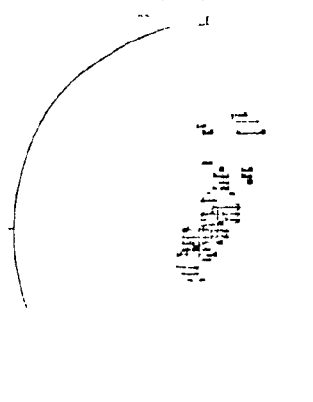
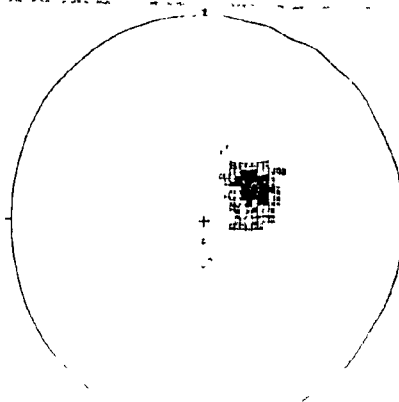
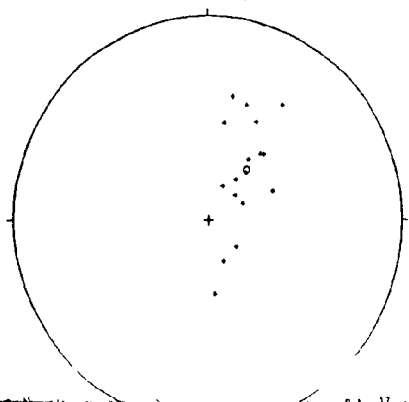
Domaine 2 LE

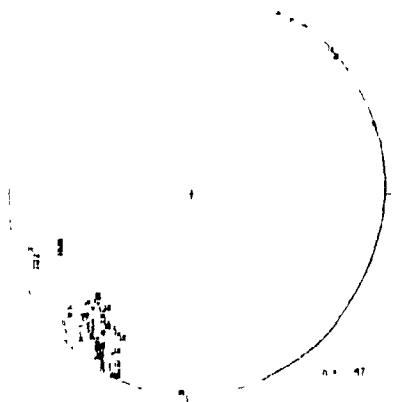


Domaine 1 L21

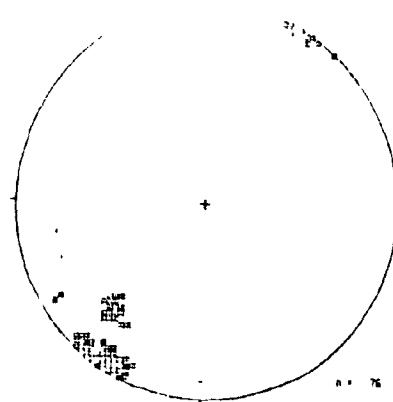
Domaine 2 L21

L2-1

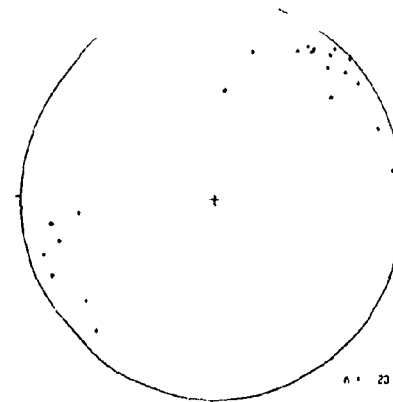




n = 47



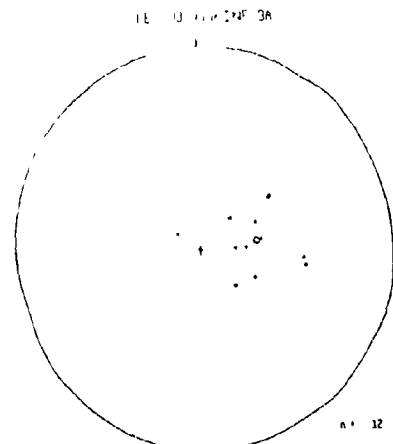
n = 76



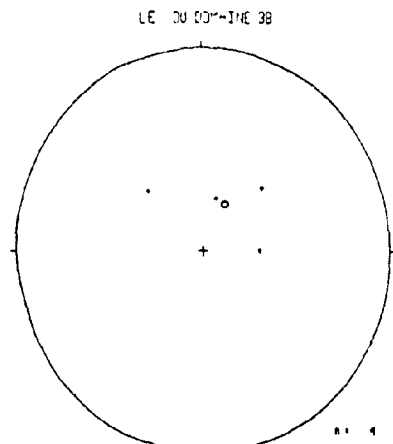
n = 23

1 2 3 4 5 6 7 8 9 10 11 12 13 14 15 16 17 18 19 20 21 22 23 24 25 26 27 28 29 30 31 32 33 34 35 36 37 38 39 40 41 42 43 44 45 46 47 48 49 50 51 52 53 54 55 56 57 58 59 60 61 62 63 64 65 66 67 68 69 70 71 72 73 74 75 76 77 78 79 80 81 82 83 84 85 86 87 88 89 90 91 92 93 94 95 96 97 98 99 100

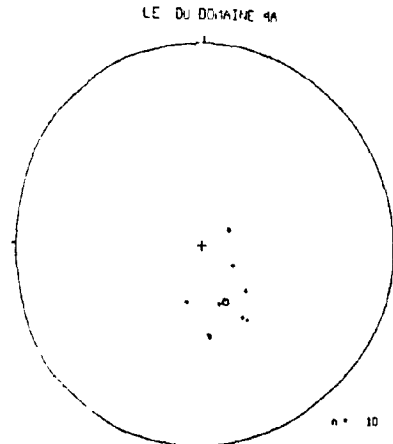
1 2 3 4 5 6 7 8 9 10 11 12 13 14 15 16 17 18 19 20 21 22 23 24 25 26 27 28 29 30 31 32 33 34 35 36 37 38 39 40 41 42 43 44 45 46 47 48 49 50 51 52 53 54 55 56 57 58 59 60 61 62 63 64 65 66 67 68 69 70 71 72 73 74 75 76 77 78 79 80 81 82 83 84 85 86 87 88 89 90 91 92 93 94 95 96 97 98 99 100



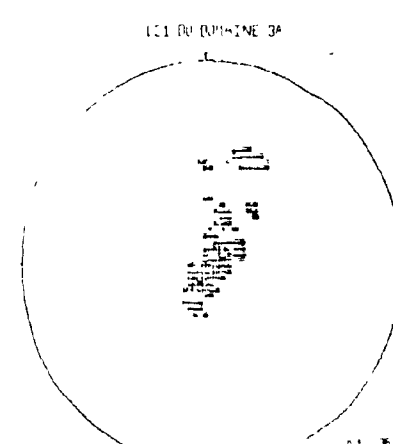
n = 32



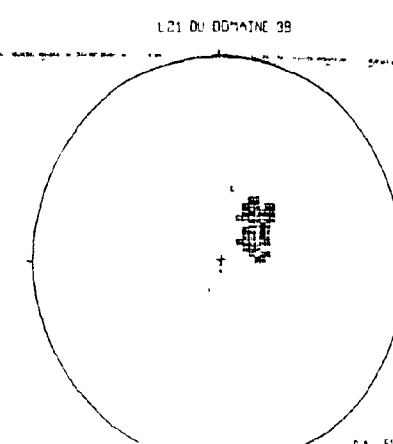
n = 4



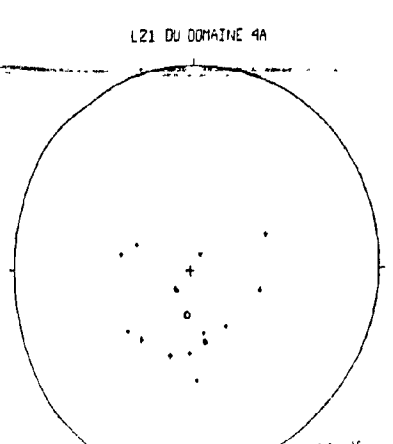
n = 10



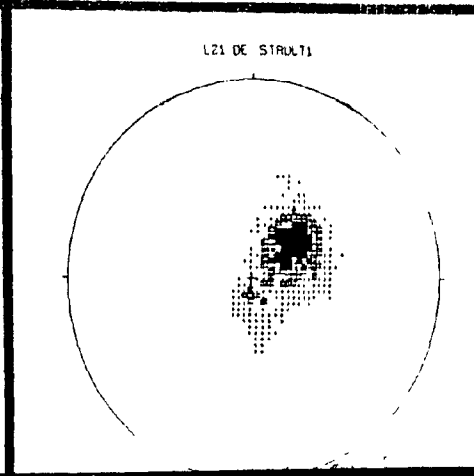
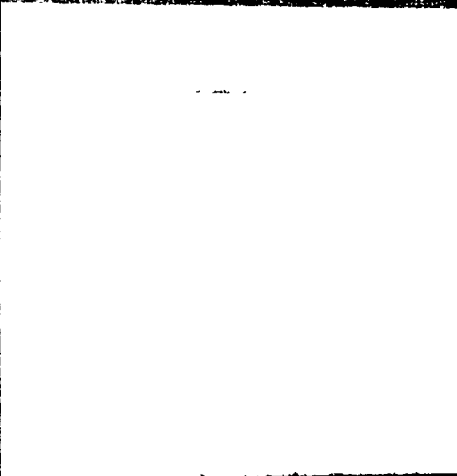
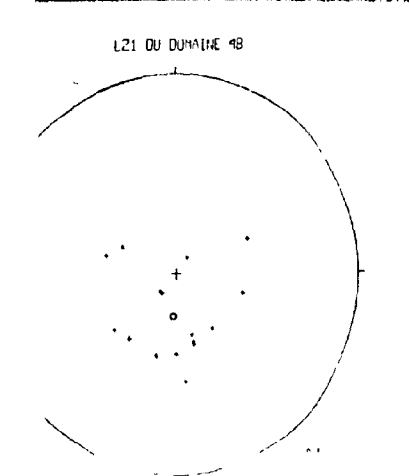
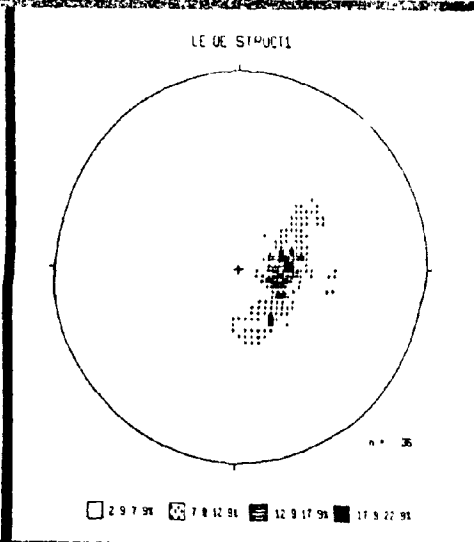
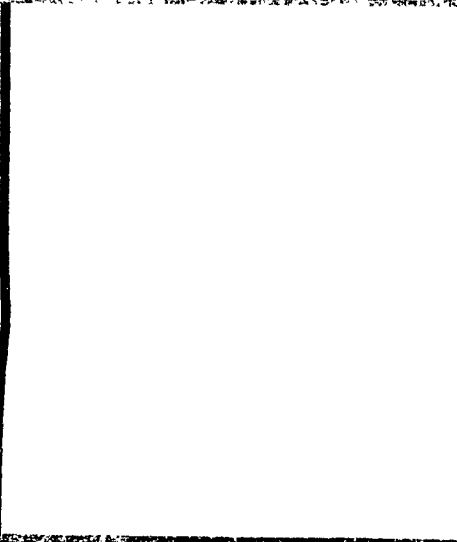
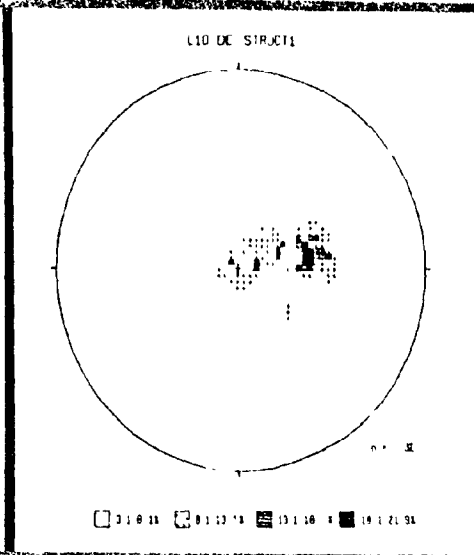
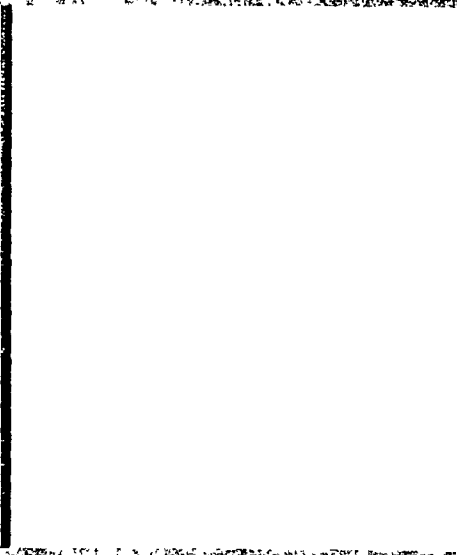
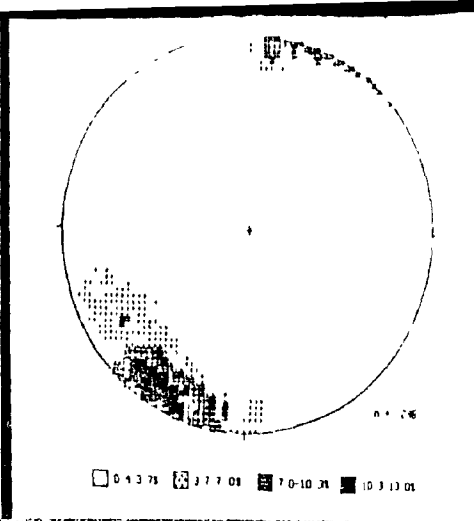
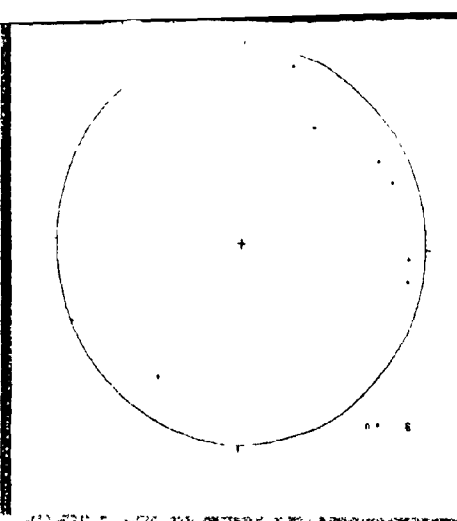
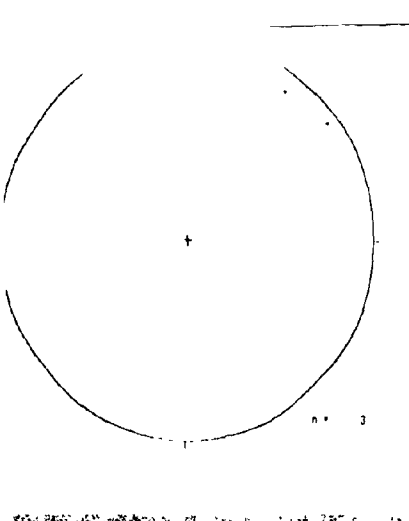
n = 36

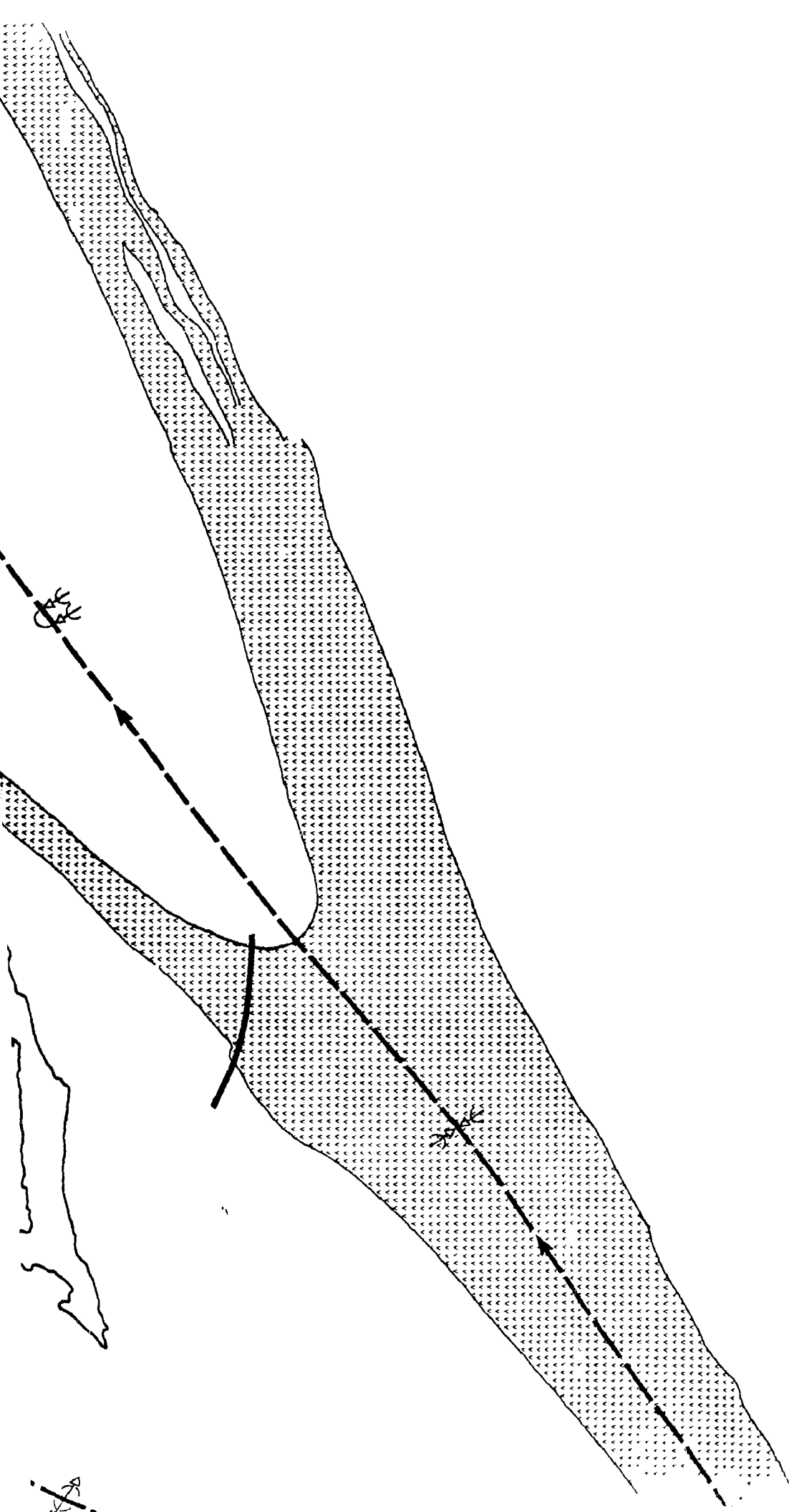


n = 51

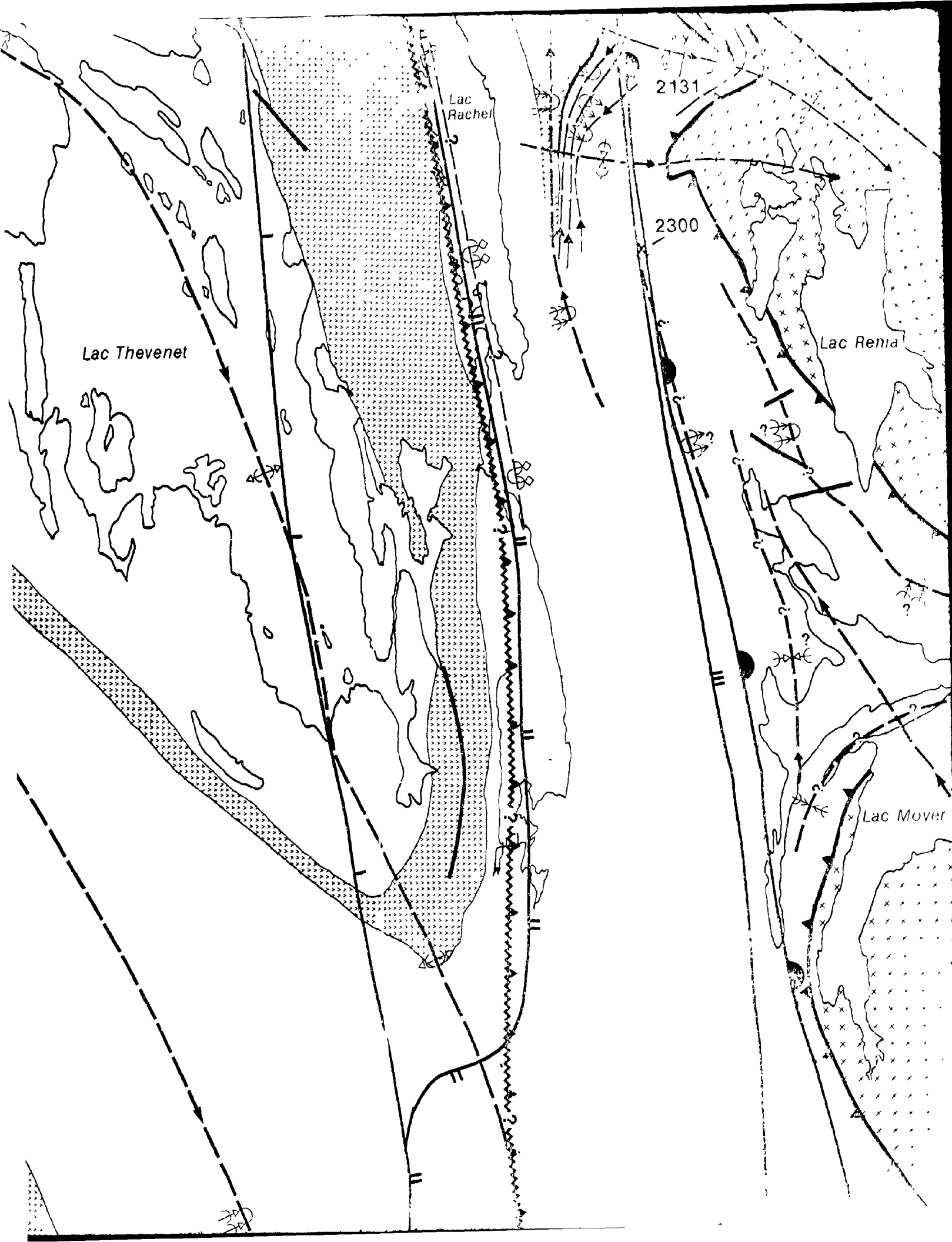


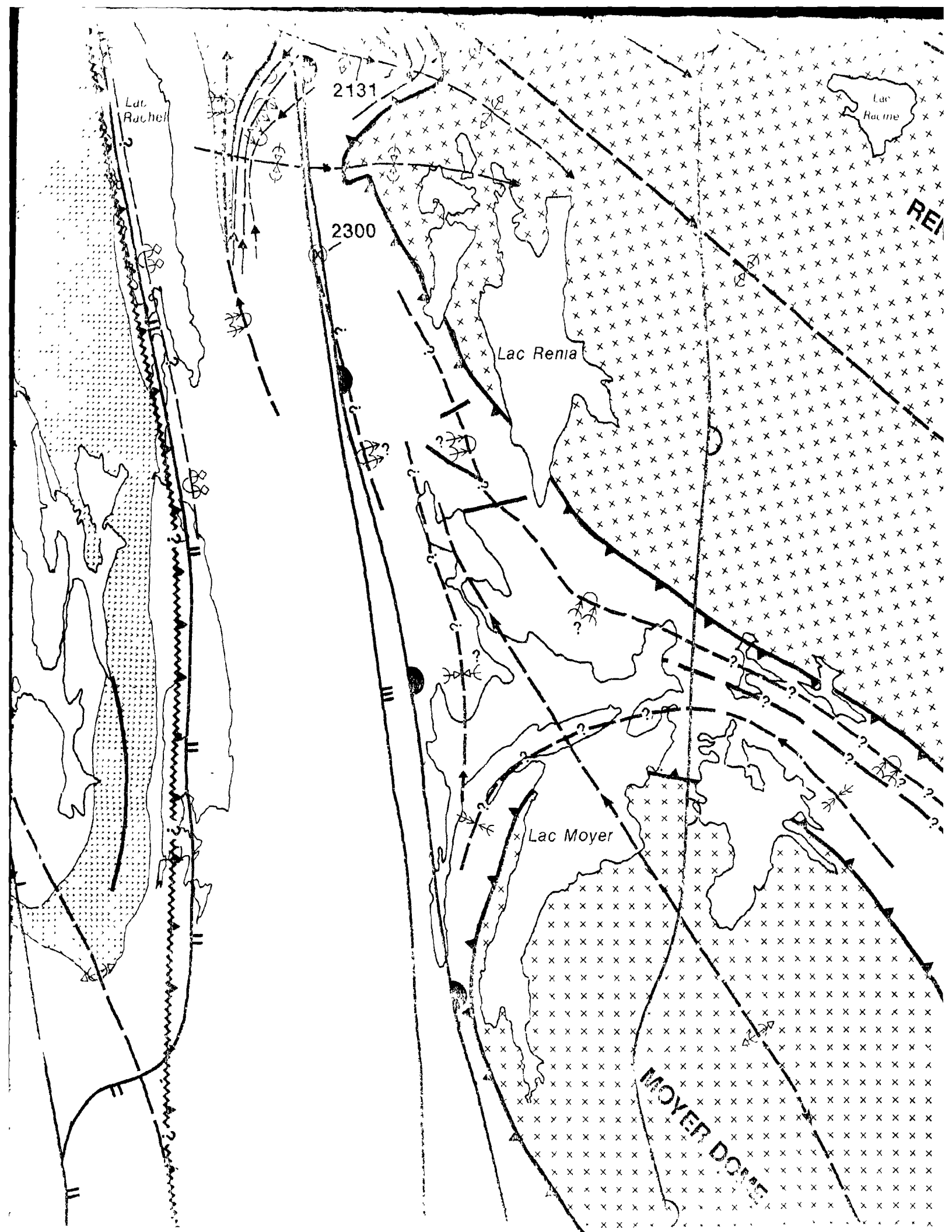
n = 16

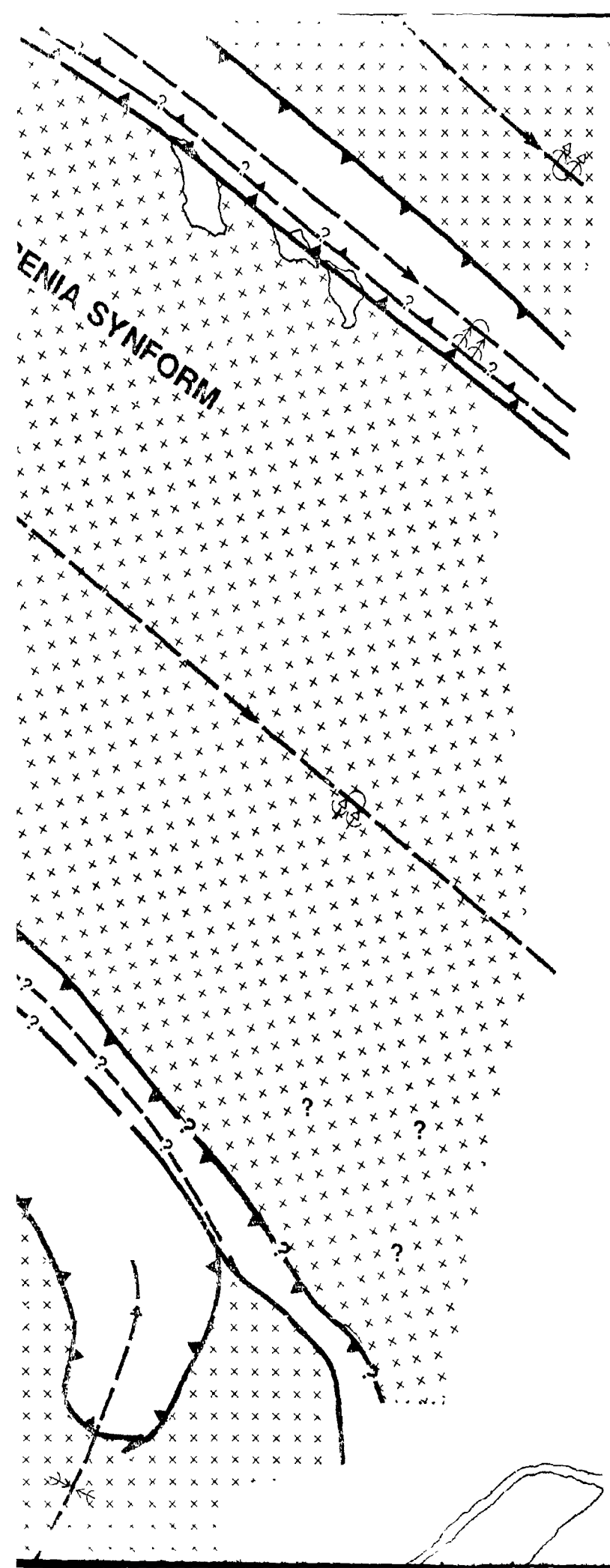




— 89.00







a)

b)

a) ?

b) ?

c)

d)

c) ?

d) ?

e)

e) ?

Bedding with facing direction

METAMORPHISM

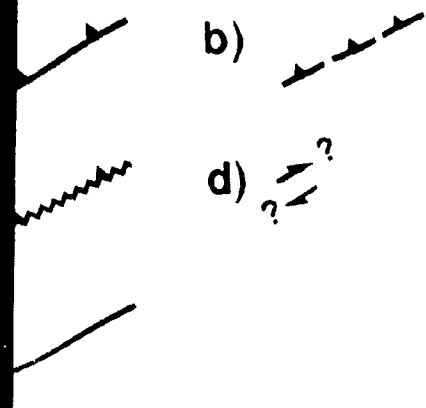
⊗ Samples for geothermobarometry

ISOGRADS

OLIGOCLASE-IN

GARNET-IN

STAUROLITE-IN



- a) Thrust fault
- b) Thrust fault
uncertain position
- c) Reverse fault
- d) Possible dextral
component
- e) Motion unknown

bedding with facing direction

AMORPHISM

Samples for geothermobarometric study

GRADS

OLIGOCLASE-IN



KYANITE-IN

GARNET-IN



SILLIMANITE-IN

STAUROLITE-IN

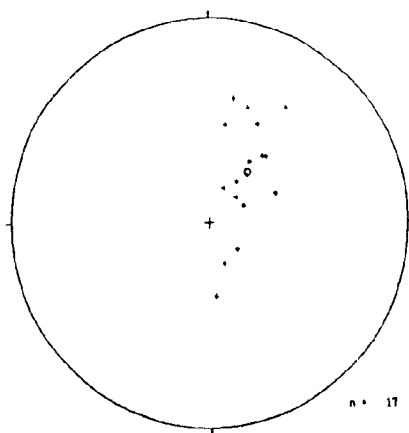
58° 00'

L2-1

L3-1

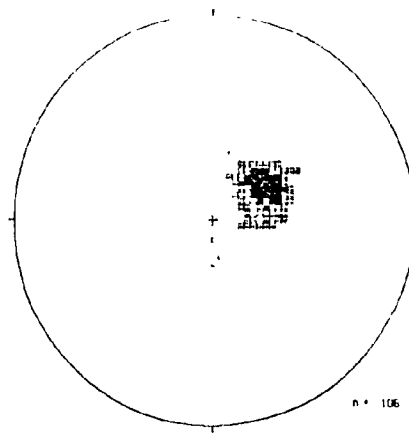
2-1

Domaine 1 L21



n = 17

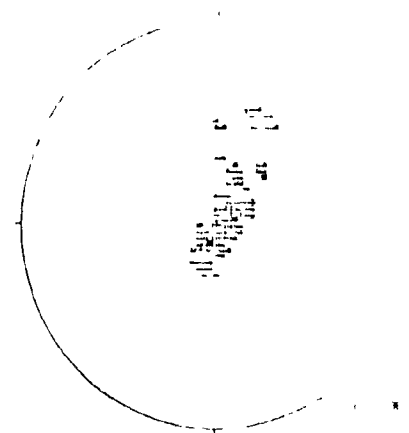
Domaine 2 L21



n = 106

0 9 6 11 6 1 11 31 11 3 16 51 16 5 20 61

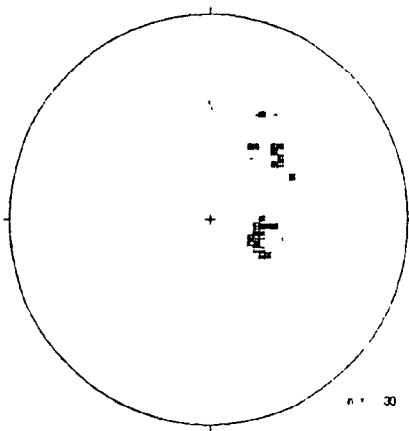
Domaine 3 L21



2 9 7 31 7 5 12 51 12 5 1 1

3-1

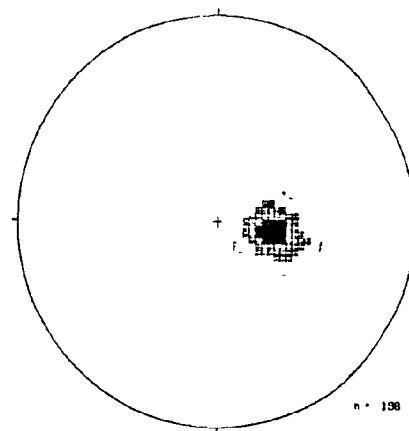
Les Modèles, domaine 1 L21



n = 30

3 3-7 31 7 3 11 31 11 3 16 51 15 3 16 71

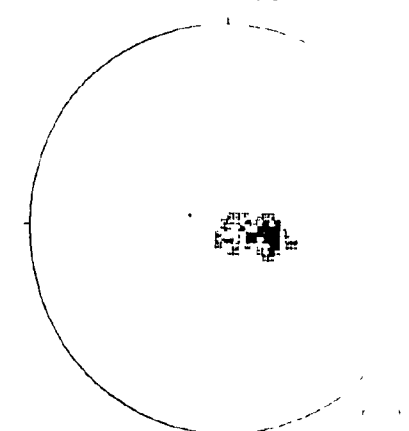
Domaine 2 L31



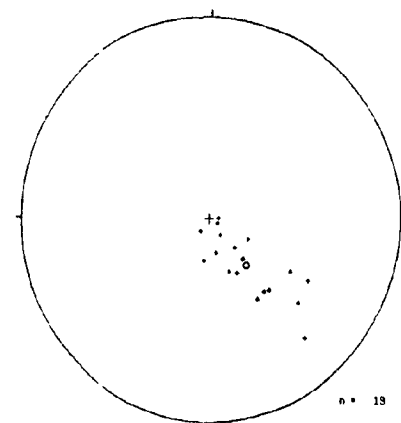
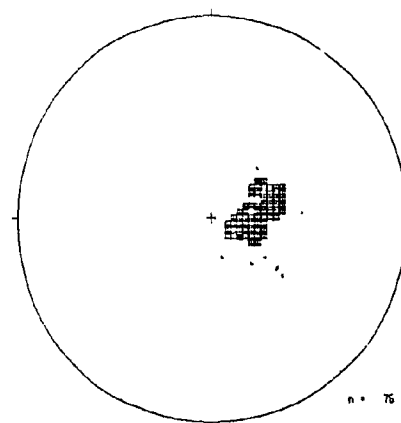
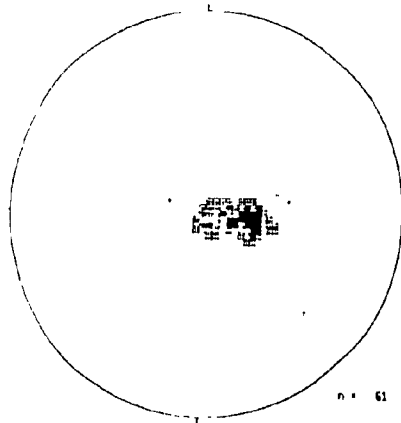
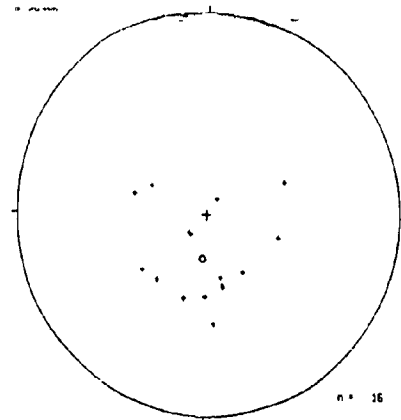
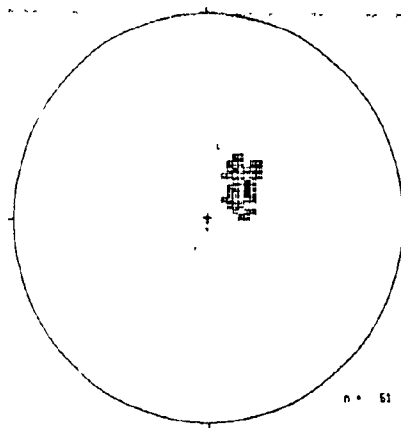
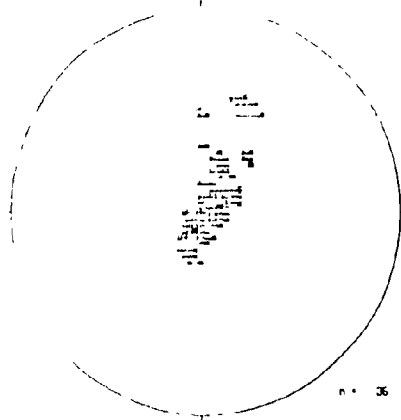
n = 106

0 5-8 61 6 5 16 51 16 5 24 51 24 5 29 31

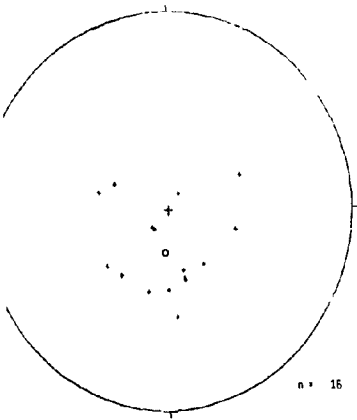
L31 DU DOMAINE 1



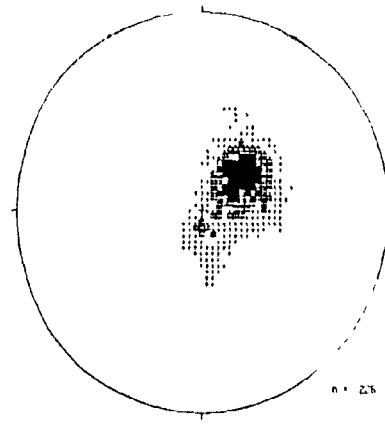
1 6 6 61 6 6 11 61 11 6 1 1



L21 DU DOMAINE 4B

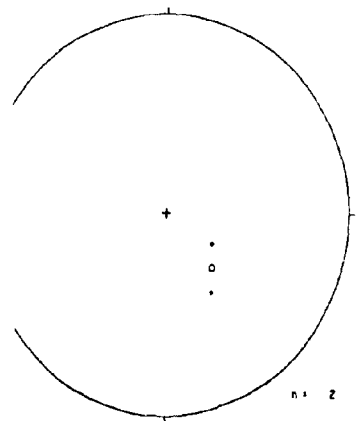


L21 DE STRAITS

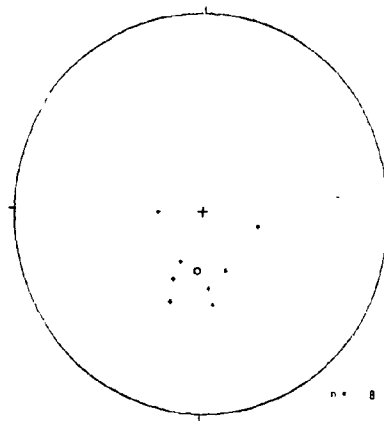


0 1 2 3 4 5 6 7 8 9 10 11 12 13 14 15 16 17 18 19 20 21 22 23 24 25 26 27 28 29 30 31 32 33 34 35 36 37 38 39 40 41 42 43 44 45 46 47 48 49 50 51 52 53 54 55 56 57 58 59 60 61 62 63 64 65 66 67 68 69 70 71 72 73 74 75 76 77 78 79 80 81 82 83 84 85 86 87 88 89 90 91 92 93 94 95 96 97 98 99 100

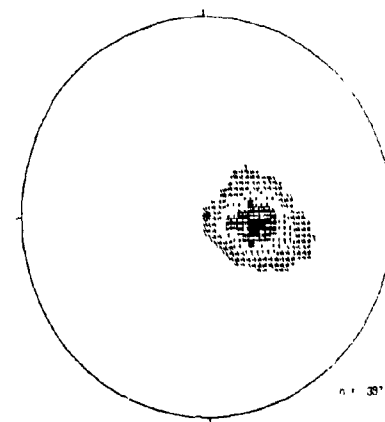
L31 DU DOMAINE 4B



L31 DU DOMAINE 5



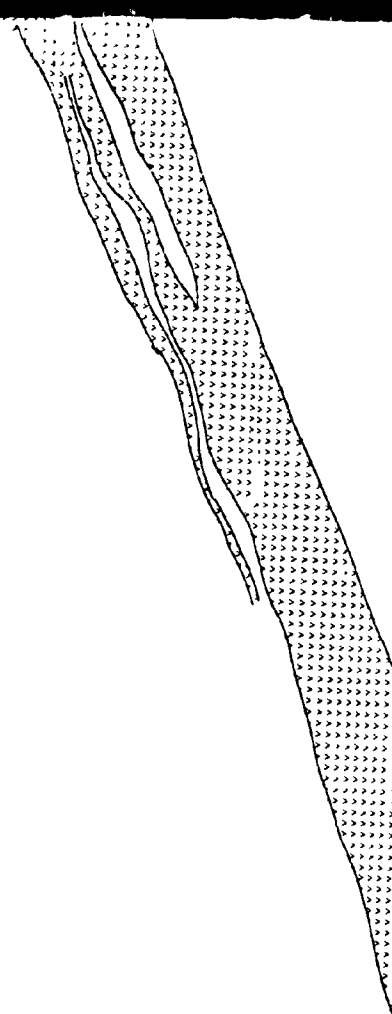
L31 DE STRAITS



0 1 2 3 4 5 6 7 8 9 10 11 12 13 14 15 16 17 18 19 20 21 22 23 24 25 26 27 28 29 30 31 32 33 34 35 36 37 38 39 40 41 42 43 44 45 46 47 48 49 50 51 52 53 54 55 56 57 58 59 60 61 62 63 64 65 66 67 68 69 70 71 72 73 74 75 76 77 78 79 80 81 82 83 84 85 86 87 88 89 90 91 92 93 94 95 96 97 98 99 100

--52'00'

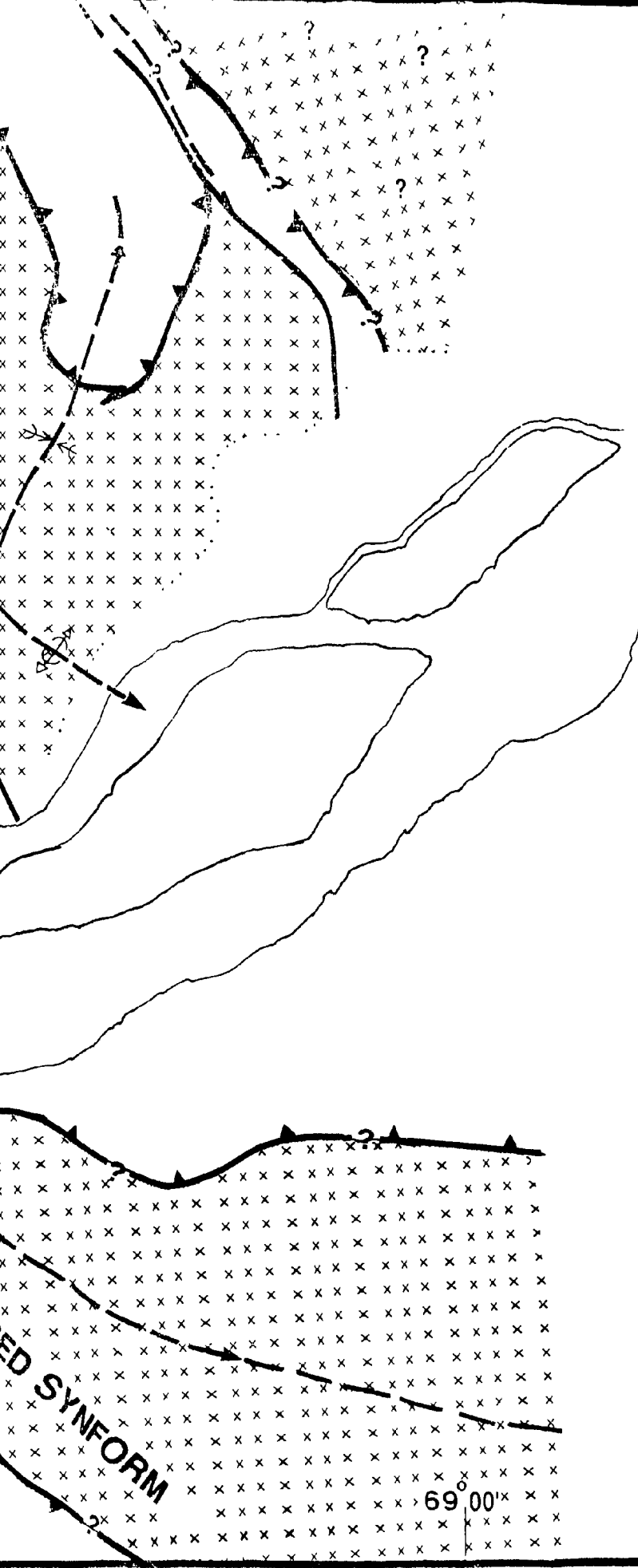
69°30'





69° 15'





SCAL

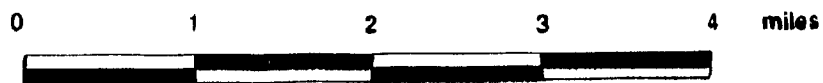
0 1 2



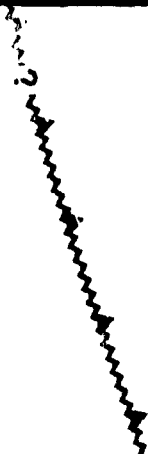
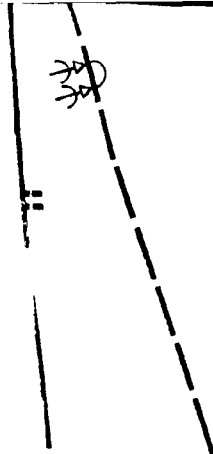
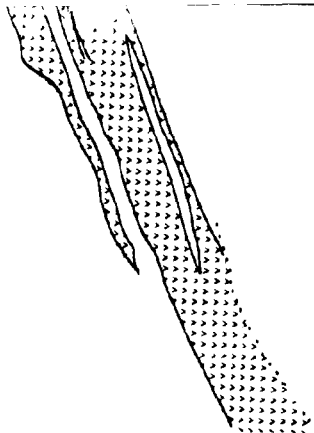
0 1 2 3



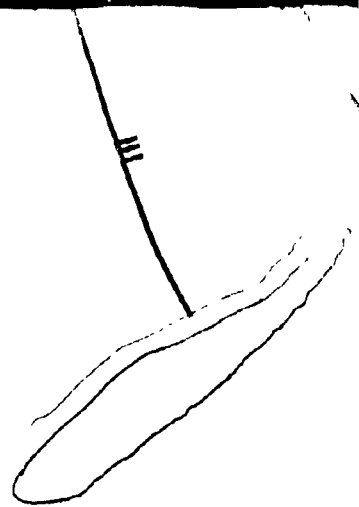
SCALE

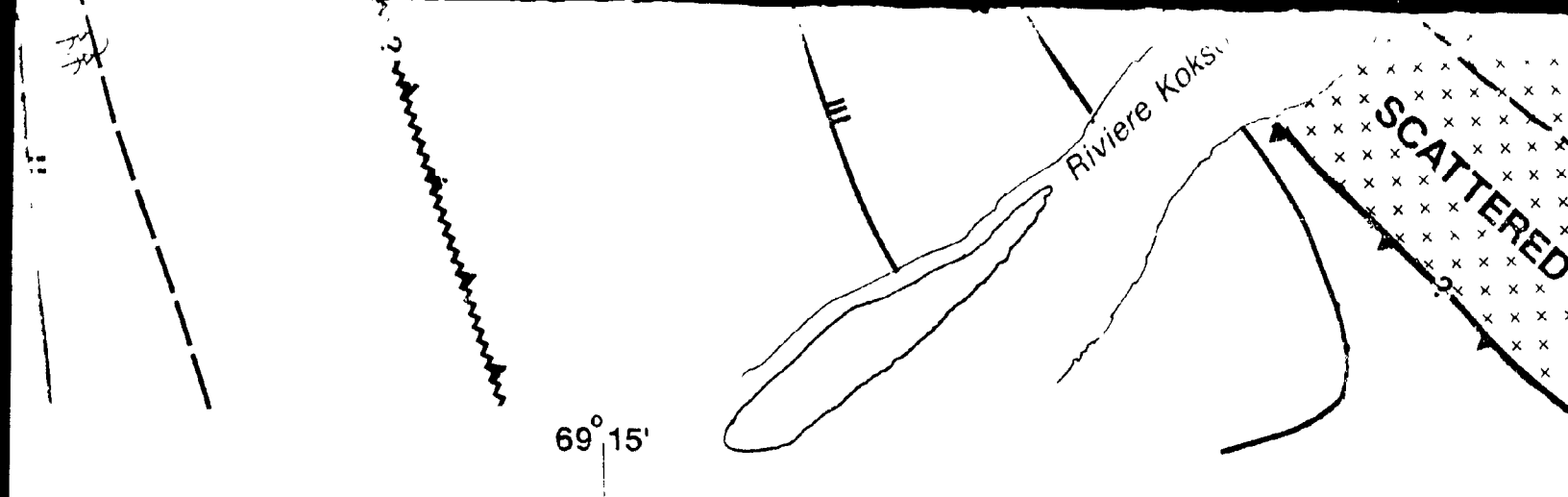


69°30'



69° 15'





0 1 2

RED SYNFORM

69°00'

0 1 2 3 4 5 6 kilometers

